LEVEL III
AFWL-TR-
78-158
Pt. 1

AD A071521

DDC FILE COPY

SIMULATION DEVELOPMENT FOR TARGET ASSESSMENT

Part 1 of 3

J. A. Earickson

Eric H. Wang Civil Engineering Research Facility
University of New Mexico
Albuquerque, NM 87131

March 1979

Final Report

Approved for public release; distribution unlimited.

AIR FORCE WEAPONS LABORATORY
Air Force Systems Command
Kirtland Air Force Base, NM 87117

DDC
RECEIVED
JUL 23 1979
E

This final report was prepared by the Eric H. Wang Civil Engineering Research Facility, under Contract F29601-76-C-0015, Job Order 88091523 with the Air Force Weapons Laboratory, Kirtland Air Force Base, New Mexico. Lt Williams (DED) was the Laboratory Project Officer-in-Charge.

When US Government drawings, specifications, or other data are used for any purpose other than a definitely related Government procurement operation, the Government thereby incurs no responsibility nor any obligation whatsoever, and the fact that the Government may have formulated, furnished, or in any way supplied the said drawings, specifications, or other data is not to be regarded by implication or otherwise as in any manner licensing the holder or any other person or corporation or conveying any rights or permission to manufacture, use, or sell any patented invention that may in any way be related thereto.

This report has been authored by a contractor of the United States Government. Accordingly, the United States Government retains a nonexclusive, royalty-free license to publish or reproduce the material contained herein, or allow others to do so, for the United States Government purposes.

This report has been reviewed by the Information Office (OI) and is releasable to the National Technical Information Service (NTIS). At NTIS, it will be available to the general public, including foreign nations.

This technical report has been reviewed and is approved for publication.

JACK D. WILLIAMS
Lt, USAF
Project Officer

FOR THE COMMANDER

RUDOLPH V. MATALUCCI
Lt Colonel, USAF
Chief, Simulation Branch

STEWART W. JOHNSON
Lt Colonel, USAF
Chief, Civil Engineering Research Division

UNCLASSIFIED

SECURITY CLASSIFICATION OF THIS PAGE (When Data Entered)

REPORT DOCUMENTATION PAGE		READ INSTRUCTIONS BEFORE COMPLETING FORM
1. REPORT NUMBER: AFWL-TR-78-158, Pt. 1	2. GOVT ACCESSION NO.	3. RECIPIENT'S CATALOG NUMBER
4. TITLE (and Subtitle): SIMULATION DEVELOPMENT FOR TARGET ASSESSMENT		5. TYPE OF REPORT & PERIOD COVERED: Final Report 6. PERFORMING ORG. REPORT NUMBER
7. AUTHOR(s): J. A. Earickson		8. CONTRACT OR GRANT NUMBER(s): F29601-76-C-0015
9. PERFORMING ORGANIZATION NAME AND ADDRESS: Eric H. Wang Civil Engineering Research Facility University of New Mexico Albuquerque, NM 87117		10. PROGRAM ELEMENT, PROJECT, TASK AREA & WORK UNIT NUMBERS: 62601F 88091323
11. CONTROLLING OFFICE NAME AND ADDRESS: Air Force Weapons Laboratory (DED) Kirtland Air Force Base, NM 87117		12. REPORT DATE: March 1979 13. NUMBER OF PAGES: 178
14. MONITORING AGENCY NAME & ADDRESS (if different from Controlling Office)		15. SECURITY CLASS. (of this report): UNCLASSIFIED 15a. DECLASSIFICATION/DOWNGRADING SCHEDULE

16. DISTRIBUTION STATEMENT (of this Report)

Approved for public release; distribution unlimited.

17. DISTRIBUTION STATEMENT (of the abstract entered in Block 20, if different from Report)

18. SUPPLEMENTARY NOTES

This report consists of 3 parts. Part 1 contains the front matter and pages 1 to 178. Part 2 contains pages 179 to 364. Part 3 contains pages 365 to 530.

19. KEY WORDS (Continue on reverse side if necessary and identify by block number)

Simulator
HEST (High Explosive Simulation Technique)
Target Assessment
Air Shock

20. ABSTRACT (Continue on reverse side if necessary and identify by block number)

This effort produced design information and experimental data for improving high explosive simulation of nuclear airblasts. Specifically, a peak pressure versus charge density relationship for Ireamite in 100 percent foam cavities was obtained for pressure up to 68 MPa. The results of this effort were transmitted to USAE Waterways Experiment Station. WES is conducting tests on generic silos as part of a DNA targeting research and test program.

DD FORM 1 JAN 73 1473 EDITION OF 1 NOV 65 IS OBSOLETE

UNCLASSIFIED

SECURITY CLASSIFICATION OF THIS PAGE (When Data Entered)

CONTENTS

Section		Page
I	INTRODUCTION	3
II	TEST DESIGNS	5
	General	5
	TA HEST 1	5
	TA HEST 2	6
	TA HEST 3	11
III	CONSTRUCTION METHODS	23
	TA HESTs 1 and 2	23
	TA HEST 3	27
IV	TEST RESULTS	29
	TA HEST 1	29
	TA HEST 2	32
	TA HEST 3	37
V	CONCLUSIONS	47
	APPENDIX A: PRESSURE VERSUS TIME PLOTS	49
	APPENDIX B: DOUBLE-EXPONENTIAL PEAK PRESSURE OVERLAY PLOTS AND CALCULATED RESIDUALS VERSUS X-COORDINATE PLOTS	365
	APPENDIX C: PLOTTED PHOTOPOLE DATA	507
	APPENDIX D: TEST INSTRUMENTATION DETAILS	523
	APPENDIX E: HEST LOCKUP CODE DESCRIPTION	530

Accession For
NTIS GRA&I [X]
DDC TAB [ ]
Unannounced [ ]
Justification
By
Distribution/
Availability Codes
Dist | Avail and/or special
A

ILLUSTRATIONS

Figure		Page
1	TA HEST 1 - Cavity Layout	7
2	TA HEST 1 - Test Bed Plan and Elevation	8
3	TA HEST 2 - Cavity Layout	10
4	TA HEST 2 - Test Bed Plan and Elevation	12
5	TA HEST 1 - View of Test Bed Posttest Showing Effects of Explosive Jetting	13
6	TA HEST 3 - Pressure Versus Range Design Curve	14
7	TA HEST 3 - Shock Velocity Versus Range	15
8	Peak Overpressure Versus Charge Density for Iremite	17
9	TA HEST 3 - Cord Width Spacing Versus Range for Two Layers of Iremite Cord	19
10	TA HEST 3 - Cavity Layout	21
11	TA HEST 3 - Test Bed Plan and Elevation	22
12	TA HEST 1 - View of Concrete Gage Canister Placement and Alignment	24
13	TA HEST 2 - Gage Mount Deformation (Measurement 1)	34
14	TA HEST 2 - Time of Arrival Versus Range	36
15	TA HEST 3 - Pressure Versus Range: Test Results and Design Curve	41
16	TA HEST 3 - Time of Arrival Versus Range	43
17	TA HEST 3 - Shock Velocity Versus Range: Test Results for Weave and Design Curve	45

TABLES

Table		Page
1	Weave Velocity Calculation	44

SECTION I
INTRODUCTION

Interest in studying and verifying the theoretical analysis of strategic protective structures has created a demand for a testing procedure to simulate the high levels of airblast and ground shock emanating from a nuclear surface burst. Efforts in this Target Assessment (TA) test series centered on higher pressures, up to 10,000 psi, a level of airblast which would be expected to inflict severe damage to a strategic structure. Specifically the TA High Explosive Simulation Technique (HEST) series was designed to obtain data on the performance of a HEST for high overpressures, to demonstrate an ability to record these pressures, and generally to expand the data base for Iremite foam HESTs.

BACKGROUND

In the past the techniques for predicting the hardness of strategic structures have been tied to the structure's design. Component tests indicated that these critical damage predictions tend to be low due to the conservative nature of design codes. The Defense Nuclear Agency (DNA) is spearheading efforts to improve hardness predictions with a testing program on target structures. Part of this effort involves gathering more data on the failure modes of the structures, and a program also has been developed to study silo structures. The Waterways Experiment Station (WES) at Vicksburg, Mississippi, will perform the actual silo tests, but the Air Force Weapons Laboratory (AFWL) and the University of New Mexico's Civil Engineering Research Facility (CERF) will develop a simulation technique for WES to use. The purpose of the TA HEST series is to develop the nuclear simulator needed by WES for their tests.

Three TA HEST tests were conducted to study the pressure range of interest, from 5,000 psi to 10,000 psi. The first two tests were small 12- by 12-ft HESTs designed to deliver peak overpressures of 5,000 psi and 10,000 psi respectively. The third test was developed to be a running HEST which would deliver overpressures ranging from 10,000 psi to 3,700 psi along a 70-ft test

bed. An analysis of the pressure data from the first test (TA HEST 1) showed that the explosive charge density needed to deliver 5,000 psi had been overestimated. TA HEST 1 actually produced in the range of 7,500 psi, which caused a reassessment of the data from previous Iremite-foam HESTs. The charge density for TA HEST 1 had been chosen on the basis of data from only three other tests, so a careful study of these four tests produced a vastly improved peak-pressure-versus-charge-density curve on which to base TA HEST 2. It was also decided after TA HEST 1 to aim for a 5,000-psi overpressure in TA HEST 2, and to let TA HEST 1 fix the high end of pressures desired in this test series. With the improved peak-pressure-versus-charge-density relationship, TA HEST 2 did deliver a 5,000-psi overpressure.

The ideal pressure-versus-range curve desired for TA HEST 3 was approximated with 10 pressure steps along the 70-ft length of the test bed. Because TA HEST 2's peak pressure had added to the credibility of the Iremite peak-pressure-versus-charge-density curve, the charge densities of the 10 steps were determined from this function. Whereas the two smaller tests had been fired with a constant speed detonating cord (detcord) driver, a varying speed weave initiated TA HEST 3. This driver was designed to burn at the speed of the detcord (estimated at 22,500 ft/s) for the first 40 percent of the cavity, and then to simulate the ideal nuclear shock velocity over the remainder of the cavity.

SECTION II
TEST DESIGNS

GENERAL

Several design parameters were held constant throughout the test series to ensure a meaningful data relationship from test to test. The proposed design for the 70- by 70-ft HEST for WES's actual silo test, using a 15.625-kt yield, gave an overburden height of 3 ft and a HEST cavity thickness of 7 in. Since the major objective of the TA HEST test series involved calibration of this design for WES, these parameters were used throughout the series. Other parameters remained the same in every test, such as the thickness of the foam layers in each HEST and the types of explosives used in each test. Unnecessary changes from test to test were avoided. However, where methods proved to be lacking (mostly in the instrumentation), improvements were made in each of the three tests.

The parameters to be calibrated for WES concerned the peak pressures and shock velocities generated in the HESTs. Each change made in the detcord driver or Iremite charge density was an attempt to narrow the bounds of error for WES's tests. While the design of the first test originated from a small and scattered set of background information, the two succeeding tests were built on expanded and more carefully studied data bases.

TA HEST 1

By using the pressure data from three previous Iremite HEST tests (Micro Foam HEST 2, Iremite 1, and Foam HEST 1), a crude peak-pressure-versus-charge-density relationship was determined. The peak pressures for this curve were picked by an eyeball fit of the data from these three earlier tests. Since the peak pressures picked for this curve were all lower than the 5,000 psi desired for TA HEST 1, a straight-line extrapolation was used to pick the charge density for the first test. The number arrived at was 4.0 lb/ft^3 of Iremite. After construction the actual charge density was 4.06 lb/ft^3.

A shock velocity of 18,000 ft/s was desired in TA HEST 1, so the 100-grain detcord driver was designed to deliver this velocity. Assuming that 100-grain detcord burned at approximately 21,650 ft/s, the driver was laid out as shown in Figure 1. To document the burn speed, time-of-arrival gages were placed in both detcord layers.

The locations of the pressure gages were chosen not only to determine the HEST peak pressure, but also to determine some of the fine characteristics of the Iremite layout. Four Kulite gages were placed around the test bed for a general sampling of the cavity pressures (measurements 1 through 4), and four bar gages (measurements 5 through 8) were placed in a straight line (Fig. 2) to record the possible jetting of adjacent Iremite cords. Measurement 5 lay directly under an Iremite cord in the bottom layer, while measurements 6, 7, and 8 lay at small increments in distance from this cord. All eight gages were located within the diamonds of the detcord driver so as not to be along any diamond's long diagonal. There was major concern (later substantiated) that shock fronts would slap together as they burned toward the long diagonals of the diamonds, thereby creating very high pressure explosive jets which would destroy any gage nearby. These hot spots were avoided in the gage placements.

TA HEST 2

The design of this test depended heavily on results from the first test. Pressures from TA HEST 1, which were well over the 5,000 psi expected, forced a reevaluation of the old Iremite peak-pressure-versus-charge-density relationship. The eyeball fit technique used for creating this function was really little more than educated guessing; so the restudy of the first four Iremite tests used a proper method for picking peak pressures. To assure a consistent and statistically accurate method of picking peak pressures, Mr. Howard Wampler's double-exponential, peak-pressure computer program* was used. The program best-fits an empirical double-exponential equation, of the form

$$I = A0 + A1e^{B1t} + A2e^{B2t} \qquad (1)$$

*Wampler, Howard W., and Earickson, Jeff A., *High-Pressure and Foam HEST Analyses*, CERF AST-10, Civil Engineering Research Facility, University of New Mexico, Albuquerque, New Mexico, publication pending.

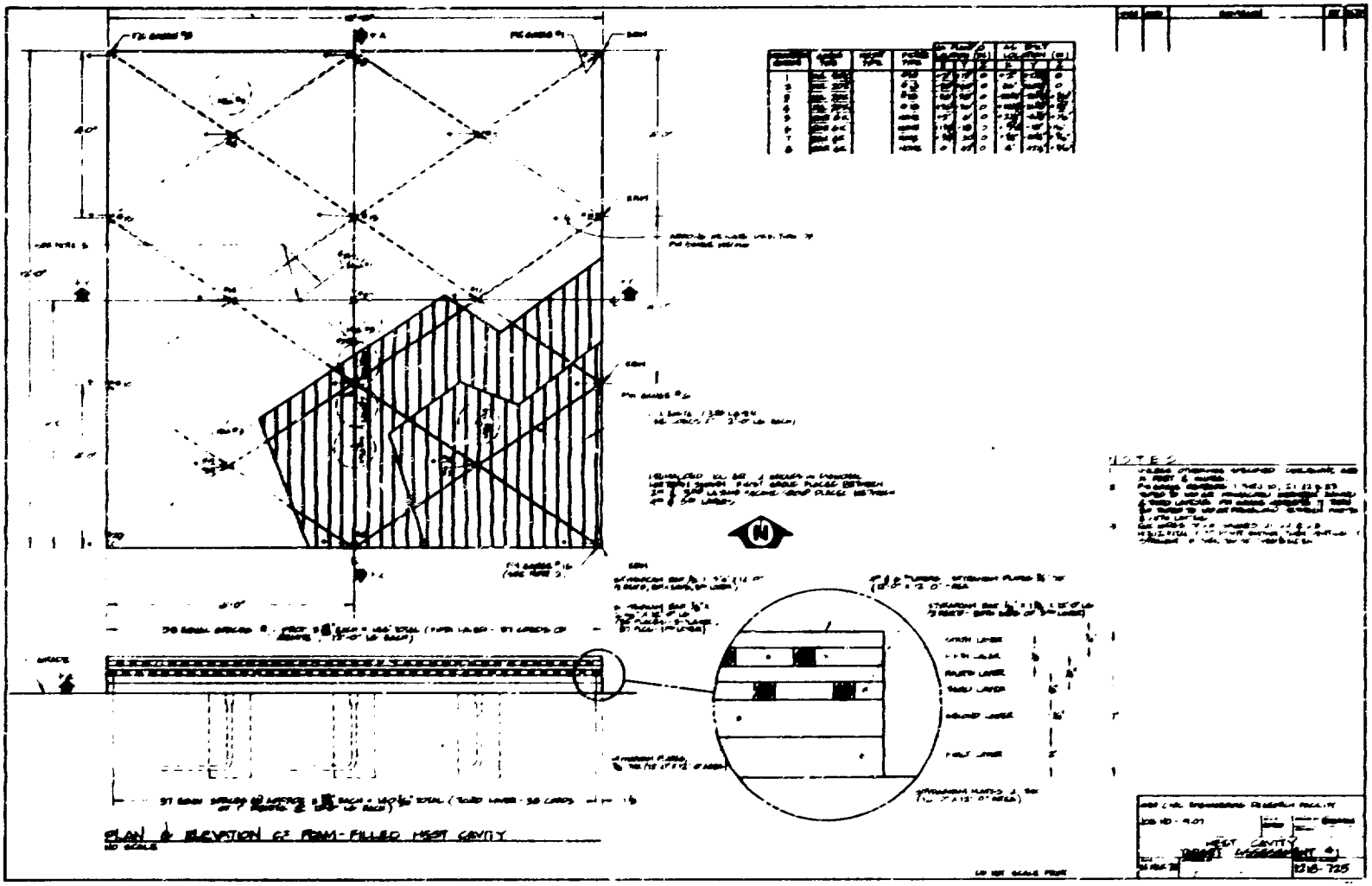

Figure 1. TA HEST 1 - Cavity Layout

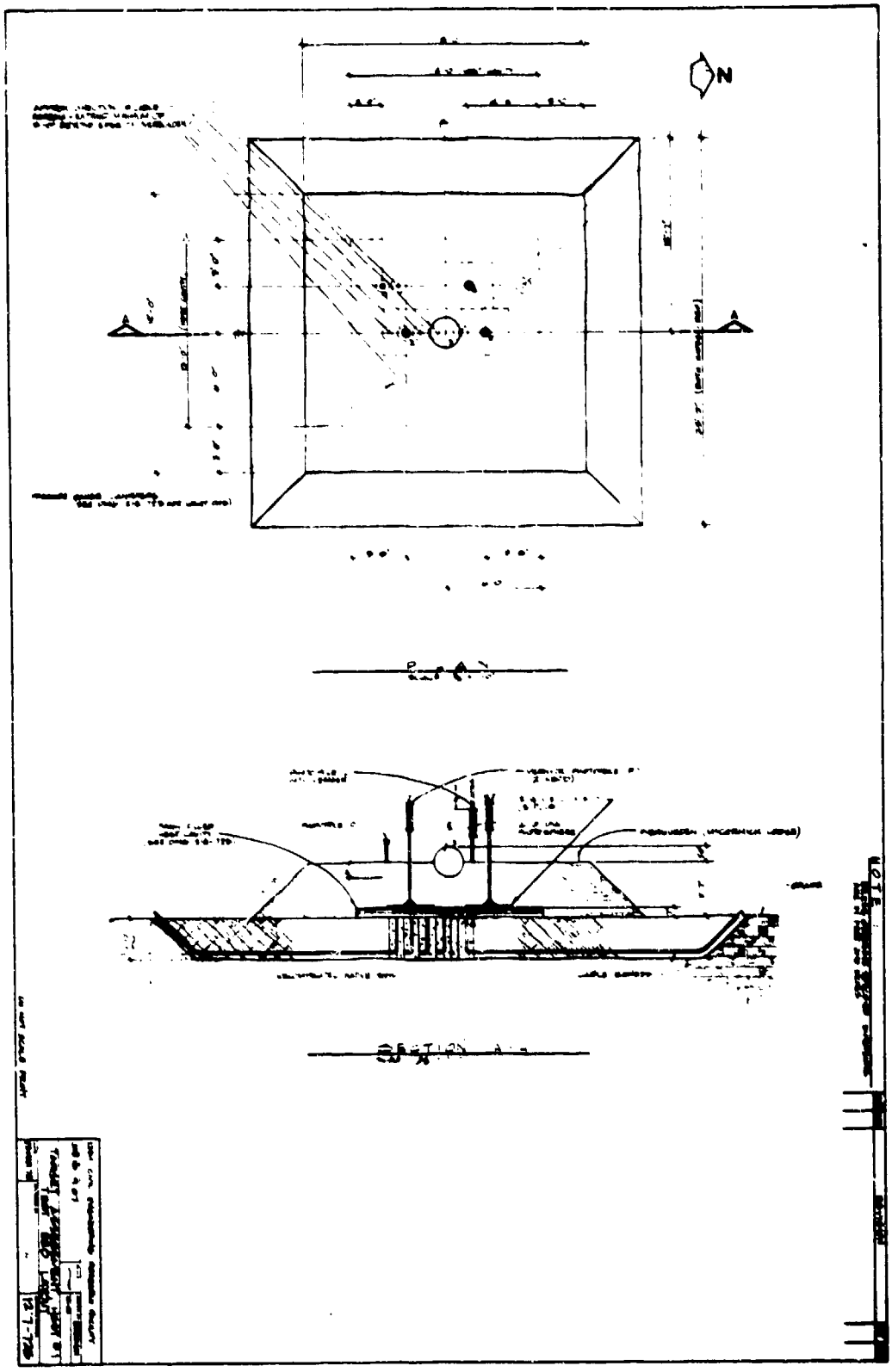

Figure 2. TA HEST 1 - Test Bed Plan and Elevation

to digitized points from an impulse-time curve, by finding optimal values for AØ, A1, B1, A2, and B2. These five values are then used in a differentiated form of Equation 1:

$$P\emptyset = A1(B1)e^{B1t} + A2(B2)e^{B2t} \qquad (2)$$

to solve for the peak pressure, using time, t_0, for t. While this computer program is much more complex than described here, these two equations form its mathematical backbone; and through extensive use it has proven reliable. All of the good pressure traces from the four Iremite tests were analyzed with the program, and a new peak-pressure-versus-charge-density plot was created. The new plot exhibited less scatter, and it estimated a charge density of 2.55 lb/ft^3, for a peak pressure of 5,000 psi, which was considerably lower than the charge density used in TA HEST 1.

After deciding to let TA HEST 1 define the high end of the pressure range in the test series, the search continued for a 5,000-psi overpressure. With TA HEST 2 now chosen as the 5,000 psi test, debate centered on the charge density needed. Several people interested in this test series felt that 2.55 was too low a charge density, and that it would only deliver about 3,300 psi. After more study, 2.65 was chosen with the feeling that if the old plot were right, then the pressure would fall too low; and if the new plot were right, the pressure would be a bit too high. So the HEST cavity was designed with this charge density.

The detcord driver for TA HEST 2 (Fig. 3) remained the same as for the first test. Due to a pin box failure in TA HEST 1, no time-of-arrival data for the driver was obtained. However, a crude analysis of times of arrival from the TA HEST 1 pressure pulses indicated that the shock velocity had been close to the desired 18,000 ft/s. With no reason or changing the driver design, it remained the same. Even the pin gage layout remained the same, and a special effort was made to recover pin data in the second test.

The pressure traces from TA HEST 1 told more about the types of gages used than the characteristics of the explosive. The four Kulite gages gave good results, while the four bar gages gave unusable data.

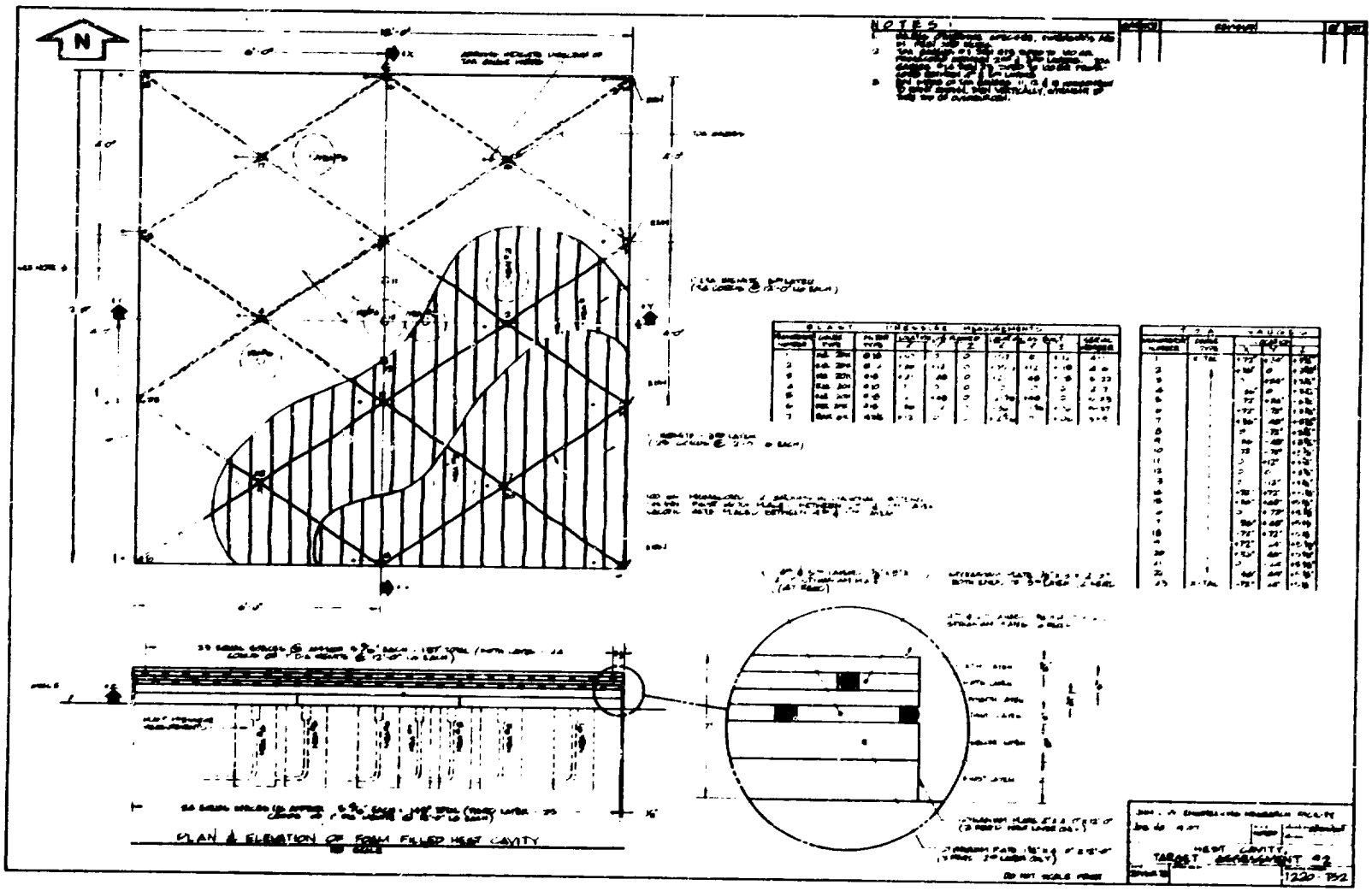

Figure 3. TA HEST 2 - Cavity Layout

Because of the failure of the bar gages in TA HEST 1 the gage choice for the second test was weighted in favor of the Kulites, since time and effort could not be expended in experimentation with the bar gages. Six Kulite gages and one bar gage were used in TA HEST 2. The gages were arranged in a much broader pattern in the second test in order to get a more realistic view of the HEST pressure. As shown in Figure 4, the gages were also placed in different relative locations within the detcord driver diamonds. Some of the gages were placed so as to discover whether or not there were gross jets within the diamonds, since it was believed that shock fronts would slap together as the Iremite burned toward the long diagonals of the detcord diamonds. Even though few results came out of the bar gage arrangement in the first test, there were indications that the lack of data occured due to the nature of the gages. A visual study of the TA HEST 1 test bed posttest (Fig. 5) indicated that gross jetting of the Iremite in the diamonds could be a much larger problem than jetting between Iremite cords. The TA HEST 1 had cuts across the test bed indicating jetting along what had been the diagonals of the diamonds. Therefore this problem was considered in the TA HEST 2 gage arrangement.

TA HEST 3

Analysis of TA HEST 2's pressure traces with the Wampler fitting program gave data which agreed well with the peak-pressure-versus-charge-density plot created by analyzing earlier tests with the Wampler routine. The relationship derived from this plot was used to establish the charge densities needed for TA HEST 3. However, other methods for determining peak overpressures exist beside the Wampler routine, and they can also be successfully used to create a peak pressure-charge density relationship. One procedure, which is related to the HEST design process and is not an empirical fitting to the data as in the Wampler routine, is described in Appendix E. The main complications in the design of TA HEST 3 involved approximating the nuclear-overpressure-versus-range curve (Fig. 6) and the nuclear-shock-velocity-versus-range curve (Fig. 7). Figures 6 and 7 derive from H. L. Brode's approximation of a 1-kt free-air blast (Ref. 1), which gives rather complex functions for pressure versus range and shock velocity versus range:

1. Brode, Harold L., *Review of Nuclear Weapons Effects*, Annual Review of Nuclear Science, Vol. 18, 1968.

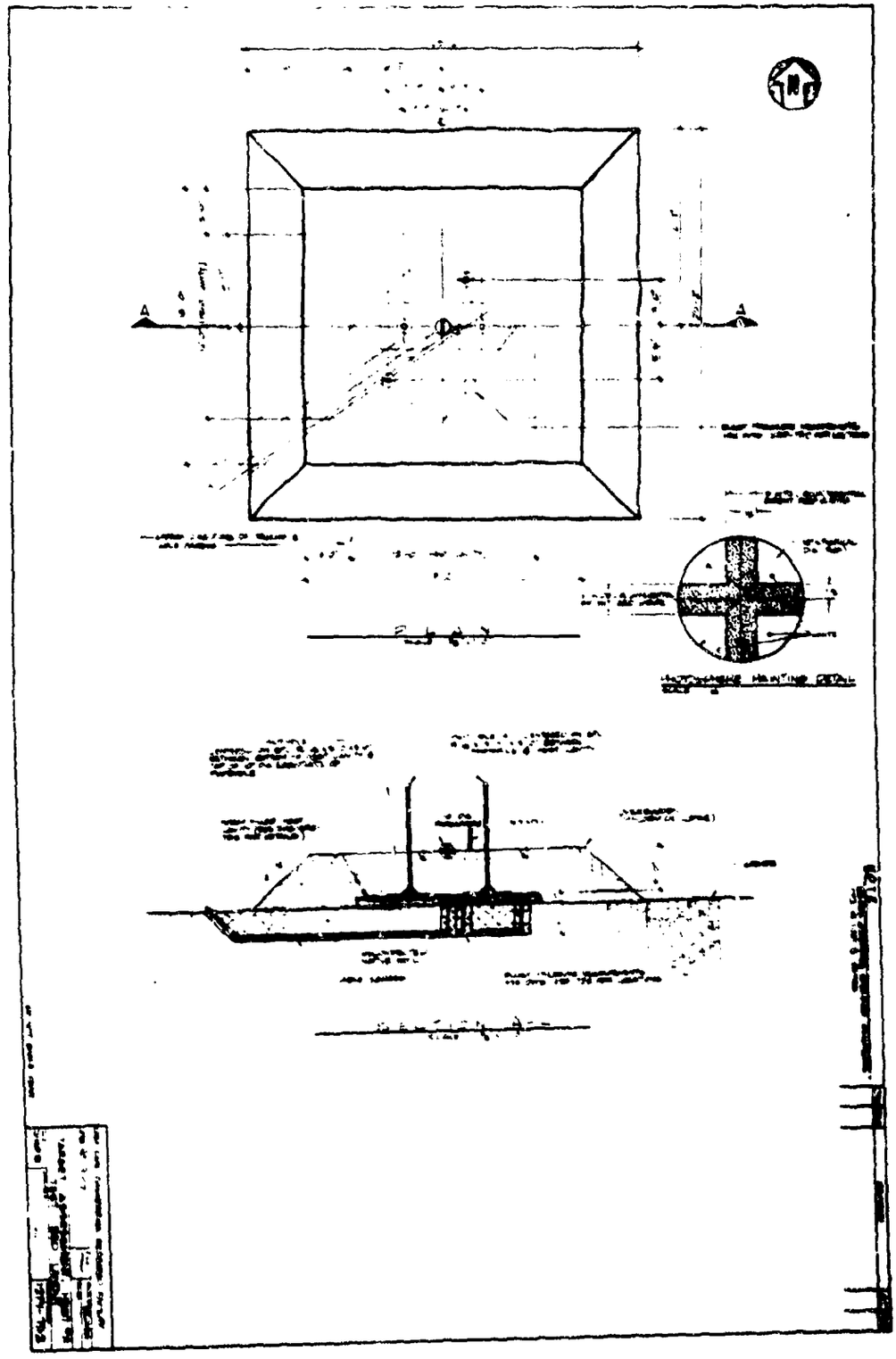

Figure 4. TA HEST 2 - Test Bed Plan and Elevation

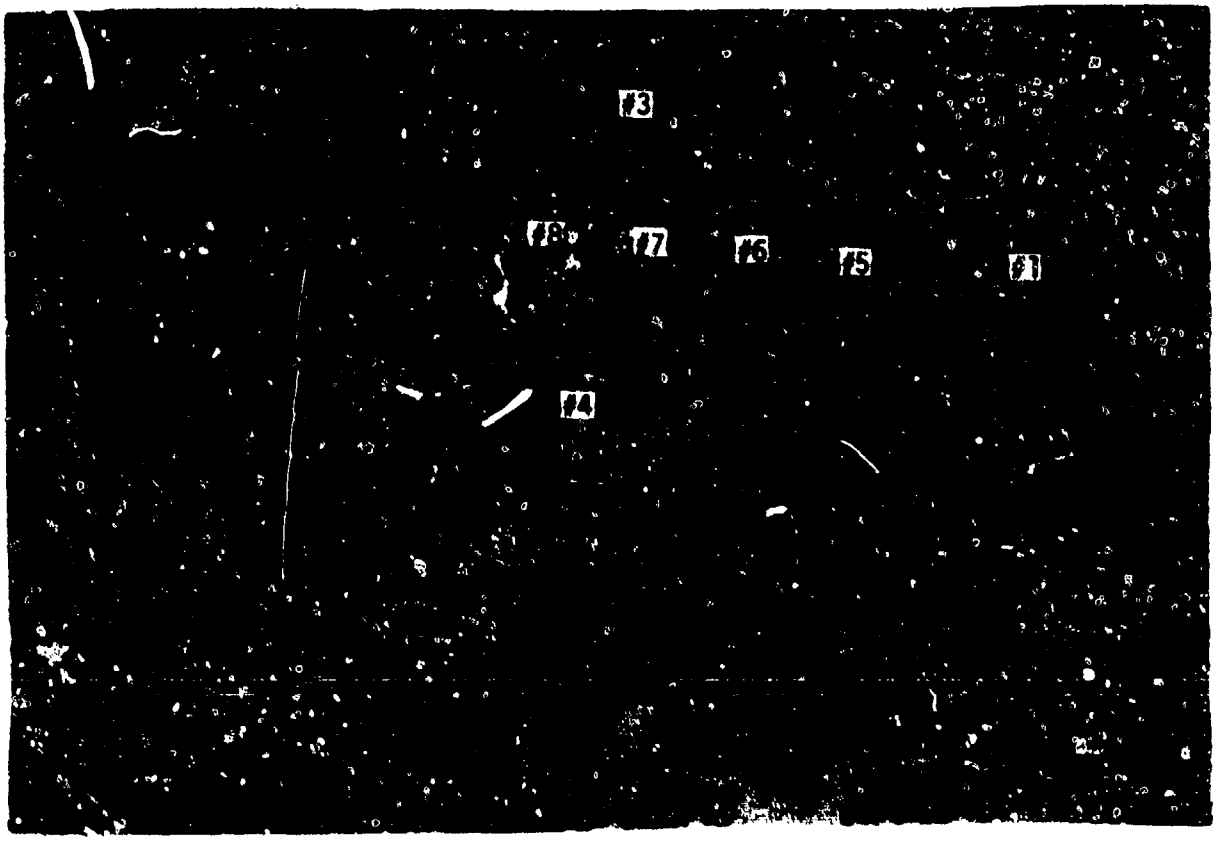

Figure 5. TA HEST 1 - View of Test Bed Posttest Showing Effects of Explosive Jetting

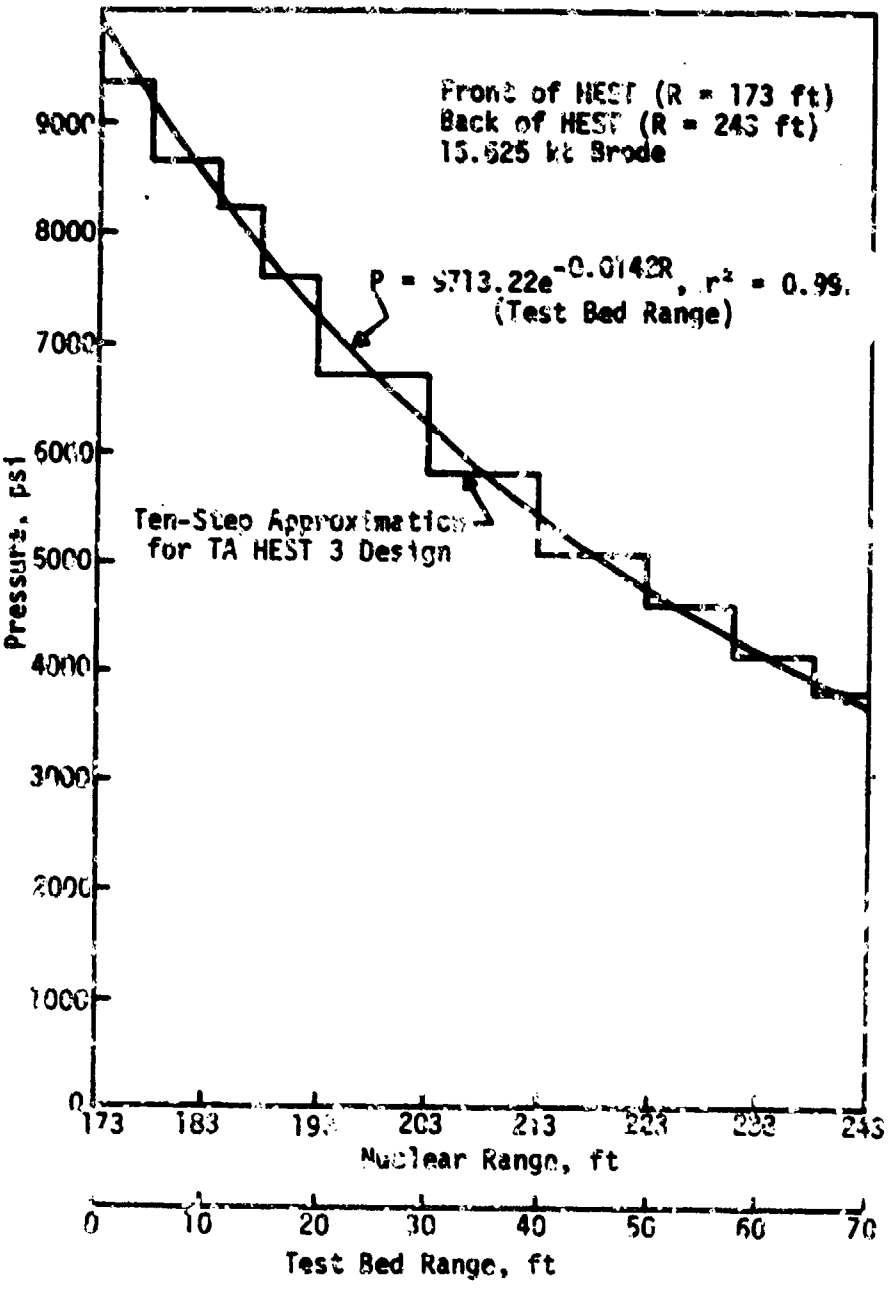

Figure 6. TA HEST 3 - Pressure Versus Range Design Curve

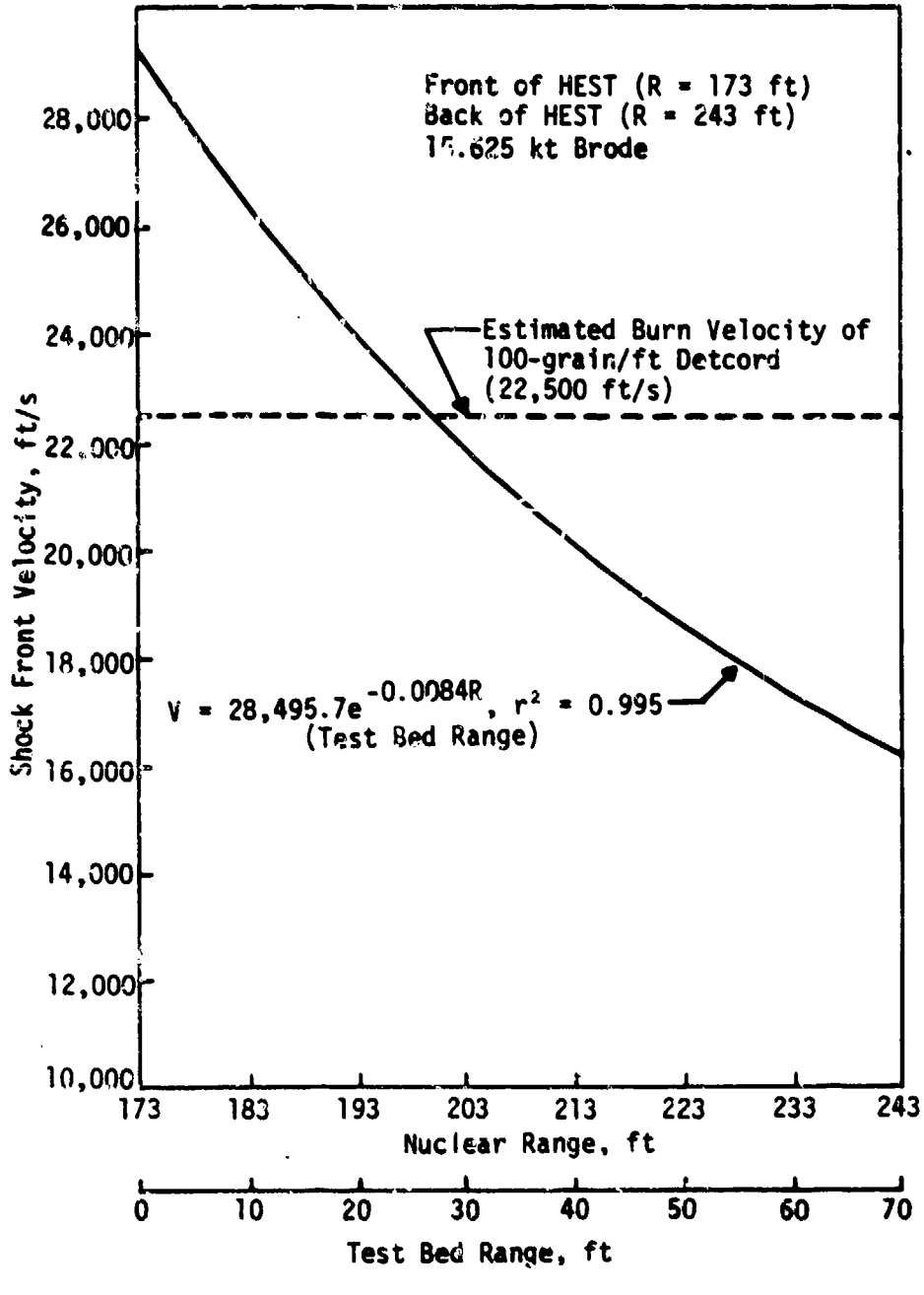

Figure 7. TA HEST 3 - Shock Velocity Versus Range

$$P(R,w) = \frac{1.58w}{R^3} + \frac{5.4w^{1/2}}{R^{3/2}} + 0.0215 \quad (3)$$

and

$$V(R,w) = \frac{1{,}128\left[\left(R/w^{1/3}\right)^2 + 0.7622\left(R/w^{1/3}\right) + 0.3722\right]^2}{\left(\frac{R}{w^{1/3}}\right)^4 + 1.524\left(\frac{R}{w^{1/3}}\right)^3 + 1.241\left(\frac{R}{w^{1/3}}\right)^2 + 0.1126\left(\frac{R}{w^{1/3}}\right) - 0.003483} \quad (4)$$

In Equations 3 and 4, R is the nuclear range in kilofeet; V is the shock velocity in feet per second; P is the peak overpressure in pounds per square inch; and w is the nuclear yield in kilotons. TA HEST 3 was designed to simulate a one-fourth-scale 1-Mt burst, or a 15.625-kt burst. For a surface burst one uses 2w or 31.25 kt in Equations 3 and 4.

These two quantities are unwieldy for the design of a HEST cavity, so they were approximated quite accurately in the range of interest with the following exponential forms:

$$P = 9{,}713.22e^{-0.0142R} \quad (5)$$

with a coefficient of determination (r^2) of 0.997, and

$$V = 28{,}495.7e^{-0.0084R}, \; r^2 = 0.995 \quad (6)$$

In these two equations, R is the test bed range in feet.

In the actual design of the explosives spacing along the HEST cavity for TA HEST 3, several more mathematical steps needed to occur. First, the pressure-range function was related to the pressure-charge density function known at that time. The peak-pressure-versus-charge-density graph (Fig. 8) had a best-fit line to the data of

$$P = 1{,}957.6\, C_D, \; r^2 = 0.997 \quad (7)$$

Charge densities in Figure 8 were obtained by counting Iremite bars in a volume between two ranges, not from Equation 9. The difference in charge density values is as great as 2.4 percent.

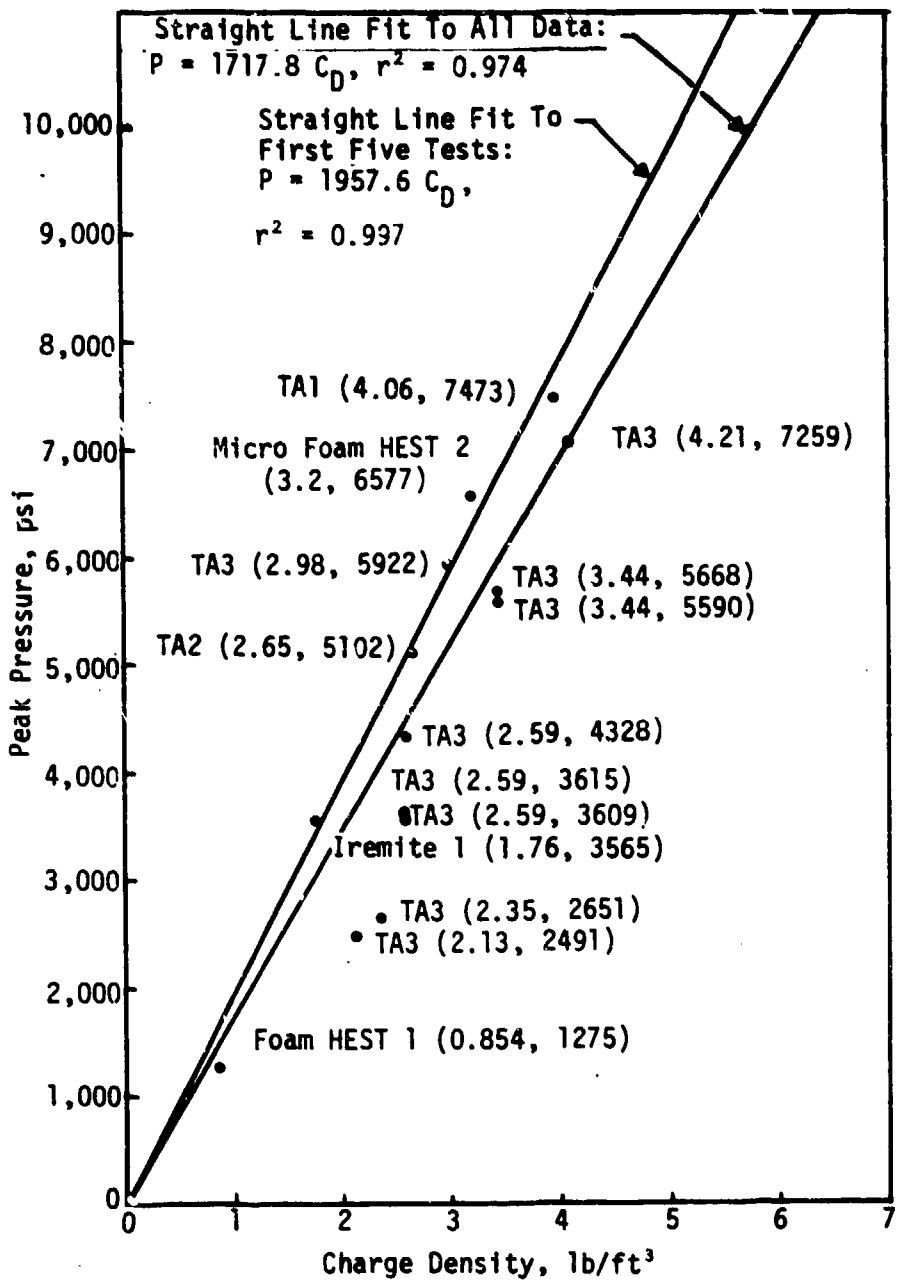

Note: Peak pressures found using the Wampler double-exponential peak pressure rountine.
(TA1 = TA HEST 1; TA2 = TA HEST 2; TA3 = TA HEST 3)

Figure 8. Peak Overpressure Versus Charge Density for Iremite

Combining Equations 5 and 7, a charge-density-versus-range equation can be defined:

$$C_D = 4.95e^{-0.0142R} \tag{8}$$

Next a relationship between charge density and center-to-center cord spacewidth was needed so a function of spacewidth versus range could be created. For one layer of Iremite cords laid across the width of the HEST, the volume around one cord (and the charge density) can be related to the spacewidth by

$$C_D = \frac{144w}{DS_c} \tag{9}$$

where w is the weight of Iremite per foot of cord (0.37867 lb/ft), D is the depth of the HEST cavity in inches (7 in for TA HEST 3), and S_c is the cord spacewidth in inches. From Equations 8 and 9 a function of spacewidth versus test bed range can be created for actual design:

$$S_c = \frac{144we^{0.0142R}}{4.95D} = 1.57e^{0.0142R} \tag{10}$$

Since this equation is for one layer of Iremite, two layers can be put into the cavity by doubling the cord spacewidth:

$$S_c = 3.14e^{0.0142R} \tag{11}$$

This function is plotted in Figure 9, along with the 10-step approximation fitted to it for the design of TA HEST 3. The 10-step approximation was used to limit the number of different sized foam spacers needed to construct the HEST. Stepping the spacewidth (hence the charge density) along the cavity affects the modeling of the pressure-versus-range curve; Figure 6 shows the pressure steps along the HEST caused by stepping the cord spacewidth. For construction purposes, stairstepping the spacewidth of the Iremite cords is far easier, and the pressure curve is modeled well.

Modeling the nuclear-shock-velocity-versus-range curve (Fig. 7) for TA HEST 3 involved the design of an explosives driver to approximate it. The velocity-range curve called for a shock velocity in excess of the 22,500 ft/s burn

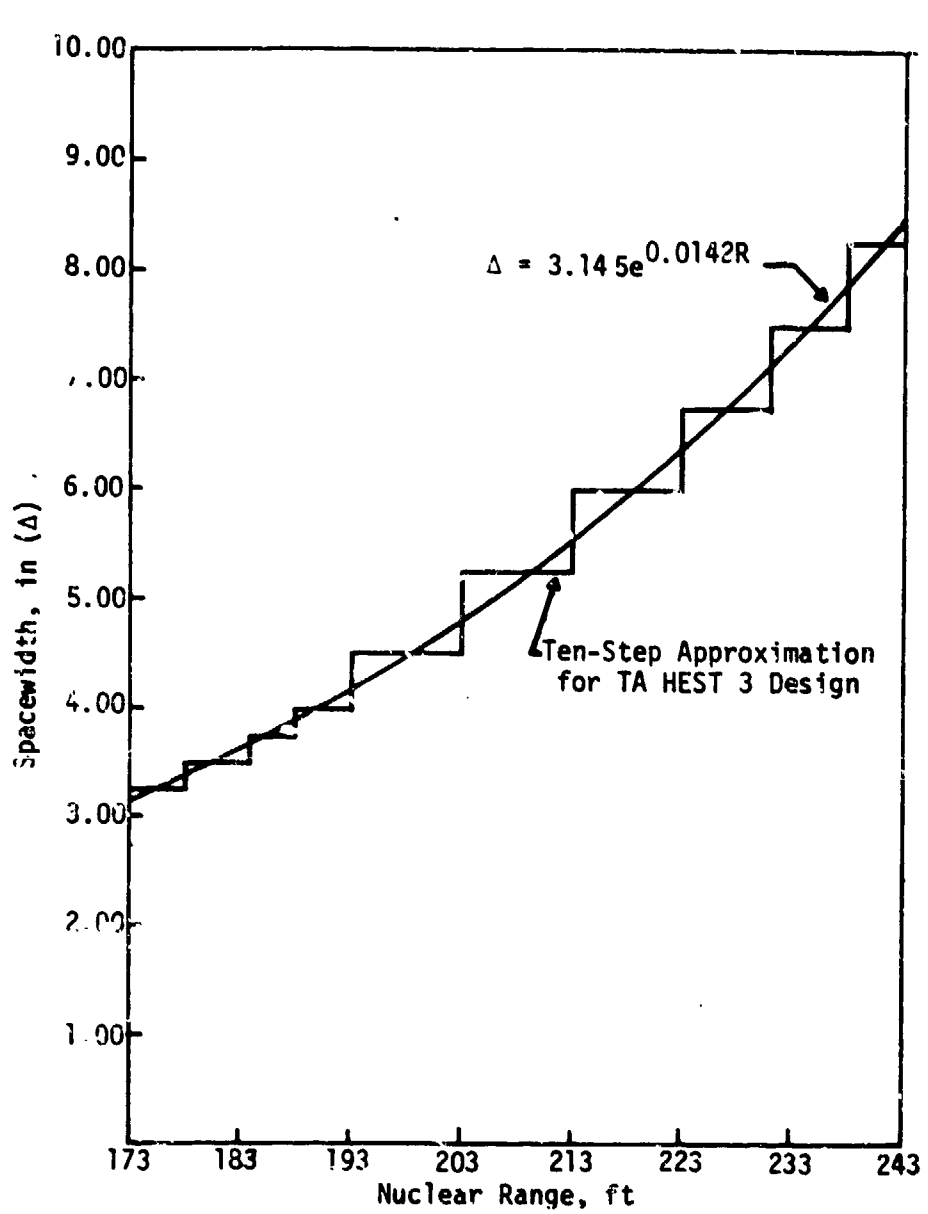

Figure 9. TA HEST 3 - Cord Width Spacing Versus Range for Two Layers of Iremite Cord

speed of 100-grain detcord for the first 27.9 ft of the cavity; therefore this section of the curve was approximated with straight detcord along the cavity. Past the 27.9-ft range the shock velocity curve was approximated by a changing weave pattern of detcord (Fig. 10) along the cavity to slow down the shock velocity as it approached the end of the cavity. The weave pattern was designed by modifying the HEST lockup code of Mr. Ed Seusy at AFWL and letting an HP 9820A computer iterate to a solution. One-hundred grain detcord was used for the driver because it served as an effective initiator for the Iremite, yet the entire amount of cord used in the cavity (about 11 lb) remained negligible compared to the total charge. Time-of-arrival gages were placed along the cavity.

The gage canisters were arranged along the length of the cavity in nine pairs (Fig. 11) in order to obtain a complete sample of the pressures in TA HEST 3. Two additional gages were placed at ranges of 24.5 ft and 45.5 ft (measurements 19 and 20) to give additional readings in the areas of the cavity where pressures of approximately 7,500 psi and 5,000 psi were expected. All of the canisters were placed fairly close to the centerline of the HEST in order to keep pairs of gages close enough together for a good comparison of readings, and to keep the gages away from hot spots in the weave pattern. Results of the gage placement in TA HEST 2 had been quite convincing; any pressure gage placed under an Iremite jet would have no chance of surviving. (Section IV discusses these results in more detail.) Because good data recovery was crucial in TA HEST 3, and because gage problems were expected in the high pressure end of the test, these trouble regions were avoided. All of the cable egress pipes ran southwestward from the canisters to give earthmoving equipment free access to the HEST from the north and east.

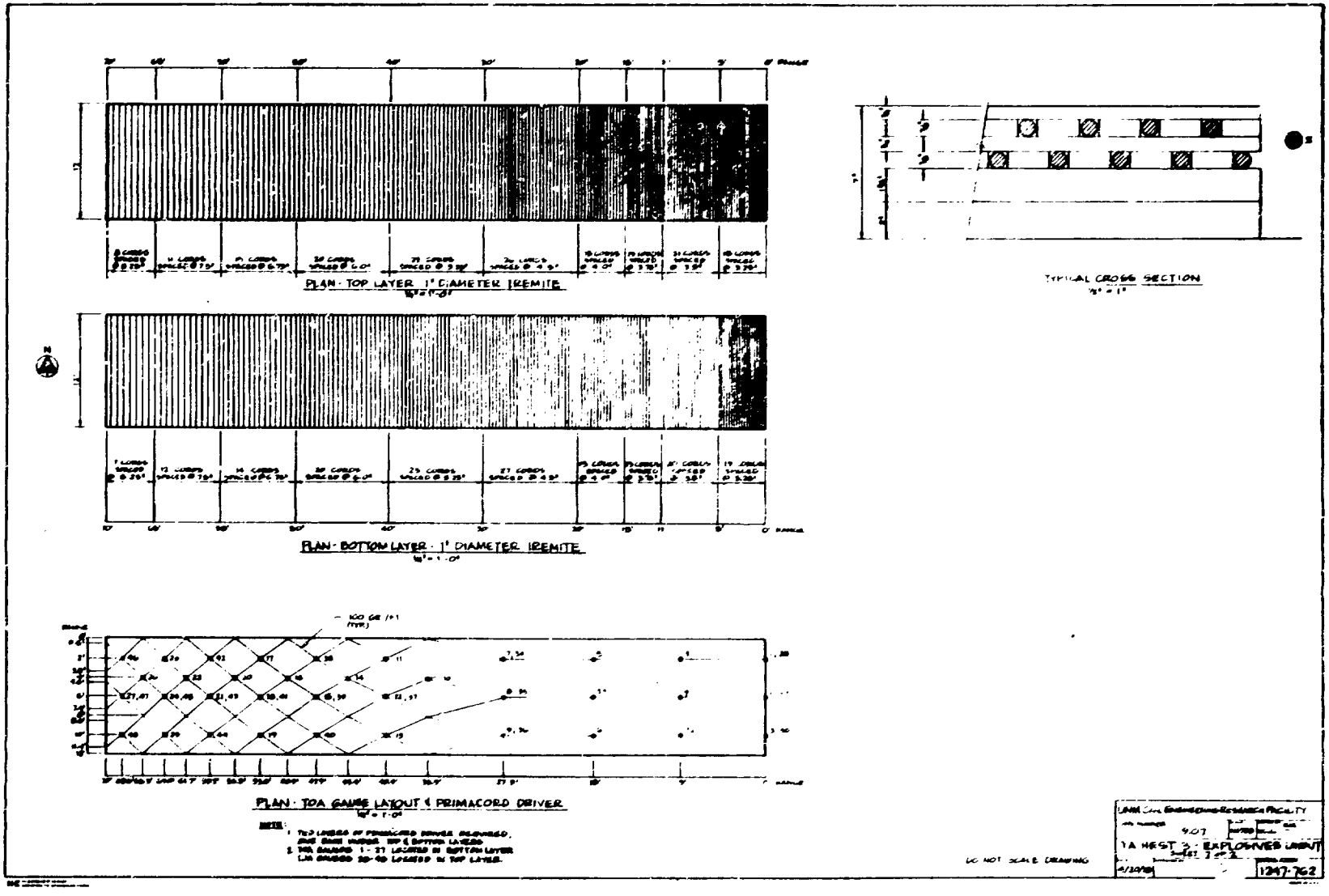

Figure 10. TA HEST 3 - Cavity Layout

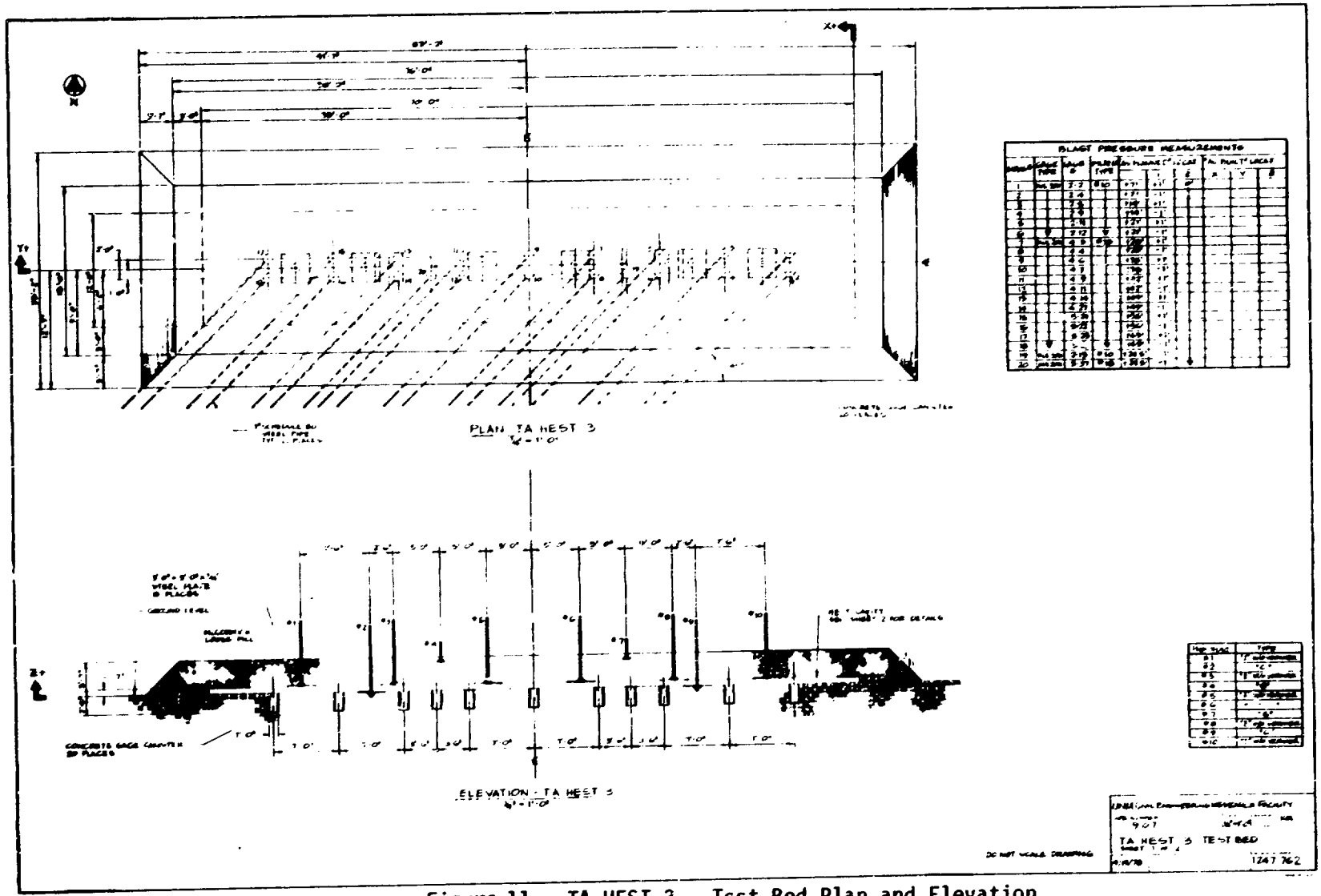

Figure 11. TA HEST 3 - Test Bed Plan and Elevation

SECTION III
CONSTRUCTION METHODS

TA HESTs 1 AND 2

Both of these tests used the same construction techniques, and both used the same sized HEST. The only major differences between these two tests involved the charge densities of the HEST cavities and the arrangement of pressure gages within the area of the test bed. There were also some differences in the types of pressure gages used between the two tests, as well as the placement of photopoles. However, these details do not bear on construction methods, and the following discussion applies to both tests.

After initially grading and leveling the test bed area, a 12- by 12-ft frame was built out of 2- by 4-in boards and fixed to the test bed with wooden stakes. By using string lines across the frame, the desired locations of the pressure gages were generally located. The frame was then removed (without removing the stakes), and trenches dug for the concrete gage canisters and egress pipes. These trenches were dug with a backhoe and needed to be about 2 ft wide and 27 in deep. The trenches for the egress pipes always ran away from the initiating end of the HEST cavity to prevent cable damage before the pressure gage recorded a pulse. Each concrete canister had a long piece of anglebar bolted to its top face at the location where the gage would be located; and each canister was suspended in its hole by resting the angle bar on the edges of the hole. The frame was then replaced and the gage canisters adjusted to match the gage locations defined by the string lines (Fig. 12). In this process the top surfaces of the canisters were also leveled to the same elevation with a transit. Once adjusted, a piece of 16-in-diameter Burke-Tube 4 in high was placed around each canister at the bottom of the trench. Grout was then poured into these forms to anchor the canisters to the ground. Egress pipes were welded (using a sleeve) to the pipes exiting from the canisters, and the trenches were backfilled and tamped.

After the final leveling and test bed recompaction (to a soil density of about 120 lb/ft^3), the photopoles were placed in the test bed. Since these poles had small fins under their baseplates, a small hole had to be dug to accomodate the

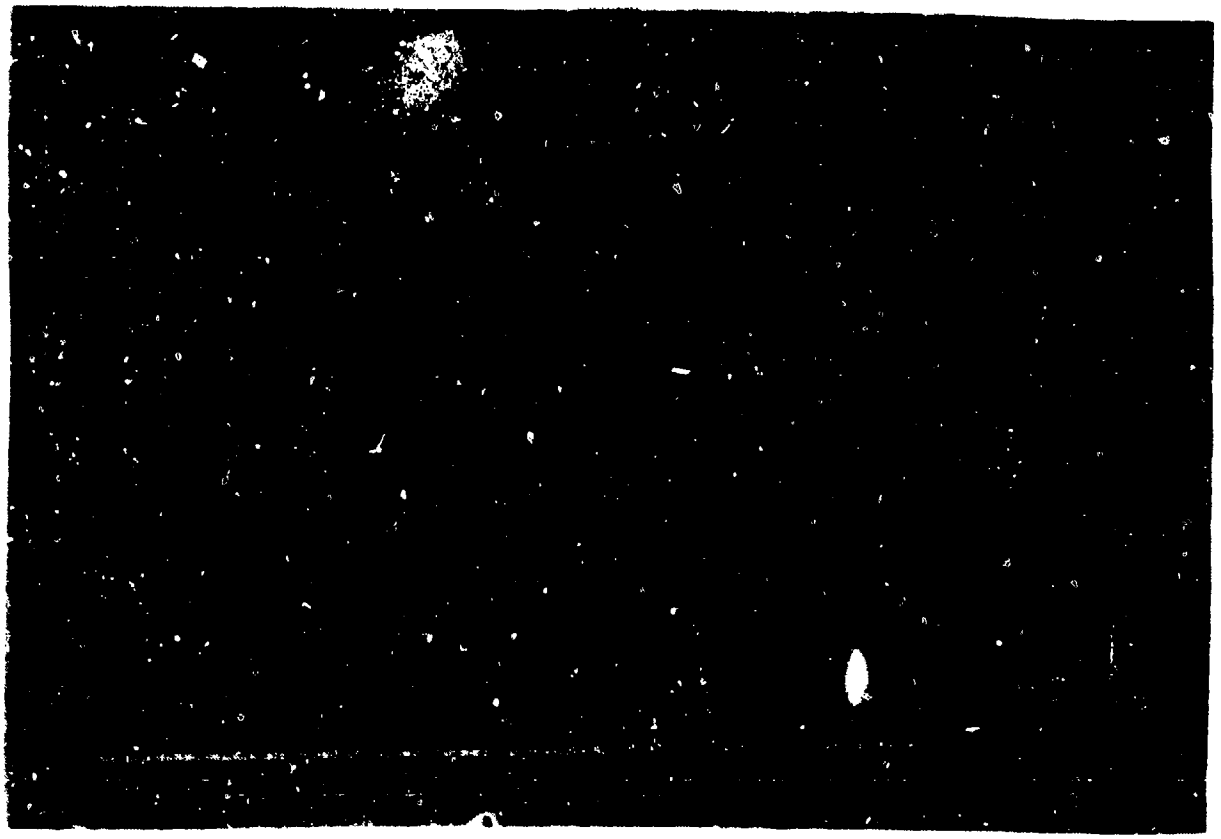

Figure 12. TA HEST 1 - View of Concrete Gage Canister Placement and Alignment

poles. A 3-ft by 3-ft by 1/4-in steel plate with a hole in the middle was placed over the pole to rest like a large washer against the pole's baseplate and the test bed. These poles were checked for vertical alignment with a level. All of the construction up to this point could reasonably be accomplished by one to two workers in one week. With moderate care the gages could be easily placed within 1/4 in of their planned locations.

In the next construction steps the pressure gages were installed in the canisters, wired to the instrumentation van, and checked out. The instrumentation cables were pulled through their egress pipes with baling wire. Because baling wire could not be placed in the pipes before welding due to the problem of potentially welding the wire to the pipe, the baling wire was pulled through the pipes with string. To thread the string through the buried pipe, a small piece of foam was tied to the end of the string and then blown through the pipe with compressed air. Not only did the foam pull the string through the pipe, but the compressed air also cleaned any dirt from the pipe. After the instrumentation cables had been strung through the pipes with the string and baling wire, the pressure gages were connected to the van and their condition checked. If a gage did not respond to the checkout as desired, it was replaced.

After the instrumentation checked out properly the HEST cavity was constructed. For TA HEST 1 and 2, HEST construction began on the morning of the test day. Construction of the cavity and berm took about 4 hours to complete, so a test time could be scheduled for early afternoon. The 12- by 12-ft frame was left in place to serve as a retaining wall for the foam cavity. As shown in Figures 1 and 3, the HESTs for these tests used expanded polystyrene foam, 1-in-diameter Iremite cord for the main explosive charge, and 100-grain detcord for the explosive drivers. The bottom 3-3/4 in of the cavity consisted of two layers of 4- by 8-ft foam sheets 2 in thick and 1-3/4 in thick respectively. In the thin (7-in) cavities of these tests this separation held the explosives away from the gage faces as far as was practical. A major concern with the thin cavities of this test series was the possible breaking of the pressure gages because the explosive would be too close to them. The two bottom layers of foam happened to stick up 1/4 in beyond the top of the frame, which was ideal for the first layer of explosive.

A 100-grain detcord initiator was laid down next. For the first two tests a

simple diamond weave pattern was used. The intersections of this weave with the frame were marked with dowel rods, so the cord could be stretched from rod to rod and attached with plastic ties. The repeating weave pattern was designed for a constant 18,000 ft/s burn velocity. As noted in Figures 1 and 3, time-of-arrival gages were placed at weave intersections to measure the burn velocity of the detcord. The Iremite cords and foam spacers were placed over the detcord for the main explosive charge. The width of the spacers and the number of Iremite cords were determined by the charge density desired for the test. Even though the Iremite was 1 in in diameter, the spacers were only 7/8 in high, which would flatten the Iremite into the 1- by 7/8-in cross-sectional area designed for it. Following the first layer of Iremite came 3/4-in thick foam sheets, followed by another detcord weave, Iremite layer, and the final layer of 3/4-in foam sheets. Then the HEST roof photopoles (and their plates) were placed and the berm built.

In future practice a few items can make a HEST cavity construction easier. The most important item needed is wide duct or mastic tape, since the foam and explosives can be taped into place during construction. Running long pieces of tape across the Iremite and spacers will keep them from shifting out of place; and the top sheets of foam can be taped together to keep soil from sifting into the cavity. If even a slight breeze is blowing, the foam will tend to fly away, so tape can also be used to hold down the HEST during construction. The long angle bars used to support the concrete canisters also served as useful weights to hold down foam. The CERF construction crew had to build both TA HEST 2 and 3 in 20- to 30- mi/h winds, so the angle bars (and sandbags) kept the HEST on the ground. To mark locations for explosives on the foam, a chalkline proved invaluable. Black felt-tip marking pens could also be used for easy marking on the foam.

After building the berm the heavy construction was complete. The CERF crew sprayed the berm with diesel fuel to settle the dust and to change the color of the berm so it would contrast with its background in the photography. The photopoles were cleaned and flashbulbs were placed on the berm just before shot time. Several bulbs were used, and they served different functions. Two or three bulbs were taped to small stakes driven into the berm and then wired to the high voltage detonator. These bulbs illuminated at t_0 to indicate the beginning of the test event on the film. Using a system developed by Mr. Peter Lloyd

of CERF, several other bulbs illuminated on the berm at various later times during the test. These bulbs marked the occurrence of events in order to mark times for data purposes. Mr. Lloyd has Sylvania flashcubes dissected, and the four small bulbs within removed. These bulbs have a short metal pin at one end which, when snapped off, fires the bulb. Small holes were drilled in the photopoles above berm height and a bulb pin placed in each hole. When the explosive shock wave travels up the pole during the event (even before the pole moves perceptibly), the bulb's pin is snapped, and so the bulb ignites when the shock first reaches the top of the HEST. These bulbs can also be used on HEST floor poles to indicate shock arrival at the bottom of the cavity. To indicate when the shock wave reaches the top of the berm, several flashcubes were placed with mechanical firing devices on top of the berm. These devices fire the bulbs with pins which push into the cube, triggering internal springs which snap the flashbulb firing pins. By counting the number of film frames, and by knowing the camera speeds, one can determine shock arrival times with these bulbs from the high speed film made of these events.

TA HEST 3

The construction of the last test used many of the same methods described above but on a larger scale. The test bed grading and leveling was the same as in the earlier tests, but the locations of the concrete gage canisters had to be marked by using standard surveying practices. The concrete canisters were installed in the same manner as in the previous tests, and, as shown in Figure 11, the cable egress pipes ran generally away from the initiating end of the cavity. All of the cable pipes ran southward from the test bed because the instrumentation van was south of the site, and this placement aided in gage hookup. With the north side of the test bed free of cables, heavy earthmoving equipment could be operated on that side without damaging the instrumentation.

A 12- by 70-ft frame built from 2- by 4-in boards was also used for this test, even though it was not used to spot the canister locations. It was used solely to fix the location of the HEST over the pressure gages. The six-piece frame was bolted together on-site after the test bed had been recompacted and relaveled; the frame was staked to the ground after lining it up around the gage locations. Since construction grade 2 by 4's are normally warped, a string line

had to be set up along both of the 70-ft sides. These sides of the frame were then straightened according to the lines by using numerous stakes to force the frame square. With the frame in place, range locations were marked for the Iremite explosive and detcord drivers along the tops of the 2 by 4's.

As shown in Figure 10, both the Iremite arrangement and the detcord driver exhibited the complications of a variable charge HEST. As in the first two tests, all intersections of the driver with the edge of the HEST were marked with wooden dowel rods. Since the 100-grain detcord weave did not run in straight lines from dowel to dowel, the cord had to be fixed to the HEST at internal points. These points were marked with a chalkline and marking pens, and then intersecting cords were fixed to their underlying foam layer with large upholstery staples. Starting from three dowels pushed through the foam at the 27.9-ft range the weave was held together with the staples. These were the only dowels introduced into the middle of the HEST, and the three long strands of detcord running from the zero range were attached to the weave at these dowels. With these three internal points, and all of the exterior intersections of the frame marked with dowels, both layers of the detcord driver were laid out the same.

The 10-step charge density layout along the test bed represented a potential construction problem. To prevent confusion, a list was made up of range locations for all of the Iremite cords in the cavity. On the day before the HEST construction began, CERF technicians laid a 100-ft steel tape along the top of the frame and marked the location of each Iremite cord in the bottom layer of explosives on top of the 2 by 4's. The next day the technicians had only to line up the Iremite cords with the black marks along the frame. For the top layer of Iremite, the technicians were instructed to make each cord lie in between the two cords underneath it, in the bottom layer. In this fashion all of the Iremite was placed quickly and accurately. To ensure that the right width of foam spacer was being used in the right place, a list was also prepared of how many of each width spacers would be needed in each layer. Using this list a technician deployed the spacers as they were needed. Construction of TA HEST 3, which was carried out in strong winds, was facilitated by the use of duct tape and angle bars used for weights. Even so, extra spacers and foam boards were required due to wind damage to the foam. Despite the wind problems the TA HEST 3 cavity was completed in about 6 or 7 hours.

SECTION IV
TEST RESULTS

TA HEST 1

Both the recovered data and the problems encountered in this test indicate what to do in the succeeding tests of this series. Most of the data recovery and interpretation problems arose from the instrumentation used in this test. The instrumentation was new and unfamiliar to the field technicians. Unlike most previous tests where the pressure gage signals were amplified in the instrumentation van after hundreds of feet of cable had filtered the high frequency noise (> 1 MHz), this test used signal conditioning amplifiers near the test bed. This system was designed to amplify the signals before the cables effected any unknown filtrations on them, and then send the signals on to the van. At its best this system should have resulted in a truer record of what the pressure gage detected. However, in this test the signal conditioning amplifiers were apparently miswired to the van power supply, which would have resulted in cross-talk in these channels. The amplifiers were also improperly shielded from high frequency radiation emitting from the test bed. This noise, plus the noise from the gages, was amplified and sent down the cables to the van.

Despite the noise the four Kulite pressure gages performed well. Since unprotected Kulite gages usually fail when exposed to very high pressure microsecond-duration pressure spikes, these gages were all protected with CERF eight-hole debris shields*. The properties of these shields are known; the number 10 shield used on the one 30K Kulite gage (measurement 1) gives the gage a rise time from ambient to the first peak of 30 μs and a pressure overshoot of about 20 percent when it is exposed to a step function of pressure in a shock tube. The number 18 shields used on the 20K gages (measurements 2, 3, and 4) have a

*Palmer, Darwin, *Evaluation of "Eight-Hole" Debris Shields*, CERF FI-12, Task Report, Civil Engineering Research Facility, University of New Mexico, Albuquerque, New Mexico, April 1978.

rise time of 230 μs and an overshoot of 19 percent. The number 18 shields, which are considerably slower, were used to protect the more sensitive 20K gages. A closer look at the results from these four gages reveals anomalies which affect the data analysis. Measurement 1 had major problems with noise which showed up on the impulse curve. The instrumentation noise prior to shock arrival (especially a large spike at 0.1 ms) offset the impulse, and a slow noise burst at 5.5 ms introduced a bump in the impulse curve. Measurement 4 suffered from a massive negative noise spike at shock arrival, which effectively obliterated the first 0.1 ms of the pressure trace. This spike smeared the very beginning of the impulse curve. Since the data from the Target Assessment test series was initially analyzed with the Wampler exponential program (which uses the impulse curve in a peak pressure determination), these two measurements were discounted in peak pressure determinations.

Also disregarded in the analysis were the pressure traces from the four bar gages (measurements 5 through 8). At first glance it seems that despite massive instrumentation problems, these traces might contain usable data. As shown in Appendix A each of these measurements had spikes deleted, and then they were inverted and baseline corrected. These manipulations yielded traces which nominally look like plausible data. The baseline corrections can properly be applied, since these gages were purposely offset 50 percent negative to bandedge in order to give the recording system a wider range in which to catch the high frequency spikes detected by the gage. However, with a posttest analysis of the bar gages, these manipulations proved to have no basis in fact. Each of the gages had the surface plastics forced into the interior of the gage casing, indicating that the surface of the gage failed after the first peak of pressure and the overpressure filled the interior of the gage. Therefore the traces produced give a picture of the gage interior under stress, and not a pressure profile of the HEST. Measurement 7 failed due to the cable breaking.

Measurements 2 and 3 remain to be studied. Both the 20-ms and the 40-ms pressure traces were scrutinized with the peak pressure routine, but the 40-ms numbers were accepted as more realistic for this fitting procedure. While the 20-ms plots give better resolution of the impulse curve at the beginning, the shorter traces do not supply the routine with late time data. The later points control what the program determines as an asymtotic impulse (AØ), and so the

40-ms plots can produce a more realistic fit to the data. The peak pressure routine had some trouble handling the 40-ms plots from measurement 2, as shown by the poor fits it produced (Appendix B). The values of sigma 20 percent and sigma 100 percent [two measures of the fit to the data (a perfect fit gives sigma = 0)] were rather high: 6.73 percent and 4.42 percent for plot 2; 6.90 percent and 4.27 percent for the redundant recording. The routine had better results with measurement 3. The primary recording produced sigmas of 5.60 percent and 3.65 percent, while the redundant channel gave 6.47 percent and 3.71 percent for the two sigmas. The calculated peak pressures from these two plots gave a 7,599 psi and 7,347 psi, for an average of 7,473 psi. Considering the qualities of the recordings, this number is the best estimate of the peak pressure in TA HEST 1 with the peak pressure routine.

A comparison of the impulse curves from the photopoles to the impulse curves of the pressure gages reveals slight differences. Because the view of the photopoles was obscured by the berm within the first 25 ms, the photopole impulse curves (Appendix C) are still rising at their ends. However, a comparison of the impulse curves at 20 ms shows only slight differences between the pressure readings and the photopoles. The photopoles give an impulse of about 13 psi-s here, while measurement 3 shows about 15 psi-s. This difference can be accounted for in the inertia of the photopoles and their consequent lag in take off from the berm. So the photopole data correlate well with the best pressure measurements of TA HEST 1.

The time-of-arrival data for the detcord driver was totally lost in this test, since the pin box failed to function at test time. The box had been thoroughly checked out prior to the test, so this failure came as a surprise. It is conjectured that the box was not turned on prior to the test. However, in an effort to obtain a rough estimate of the HEST shock velocity, the times of arrival at the pressure gages were studied. While this substitute for good data did not produce a clearly defined shock velocity, it indicated that the velocity had been in the range of 18,000 ft/s to 20,000 ft/s. This ballpark figure indicated that the same driver could be used in TA HEST 2 without much fear that it would deviate too far from the desired velocity of 18,000 ft/s.

The soil density measurements from TA HEST 1 resulted in an in situ test bed density of 118.4 lb/ft^3 (an average of two measurements) and a dry density of 104.0 lb/ft^3, with an average moisture content of 12.5 percent. These two measurements were made with CERF's Troxler soil density measuring machine, with the probe set 2 in below the test bed surface. The high moisture content was probably the result of the winter weather at the time of the first test. The overburden had an average in situ density of 78.8 lb/ft^3 (from an average of four measurements), a dry density of 72.5 lb/ft^3, and an average moisture content of 8.7 percent. These four measurements came from soil samples removed from the test site and analyzed in CERF's soils laboratory.

TA HEST 2

The results of TA HEST 1 pointed out some pitfalls to avoid in the next test. Because of the noise problems associated with the signal conditioning amplifiers, they were removed from the second test. Also, due to the poor performance of the bar gages in TA HEST 1, only one was used in TA HEST 2. This measurement (7) was considered an experimental gage, and the surface elements of the gage were improved to prevent the problems which had occurred in TA HEST 1. All of the gage surfaces in the first test had 0.006 in of scotch tape placed across them to prevent the explosive gases from rushing into the 0.003-in gap between the bar and its case. However, the temperatures produced in TA HEST 1 melted the tape and the tape was pushed into the gage interior, allowing the gases to follow. These high pressure gases destroyed the gage's ability to record the HEST pressure correctly. To prevent the tape from melting in TA HEST 2, a 0.002-in steel foil was placed on top of the tape (now only 0.002 in thick), and then a second layer of 0.002-in tape was placed over the foil. This multiple diaphram was designed to solve the thermal problems and keep gases out of the gage interior.

Unfortunately this gage, along with a 20K and the 30K Kulite gages (measurements 1 and 4), failed instantly at shock arrival. It is not known what happened to the surface elements of measurement 7, because the entire gage was blown apart. The back of the bar was blown off, and not enough of the gage was found afterward to determine what failed. These three gages had been located along the diagonals of the detcord drivers (Fig. 3) to study the effects of gross Iremite

jetting; the remains of the three gages gave perhaps a more graphic indication of the peak pressure than data records would have. Figure 13 shows deformation contours mapped from the face of measurement 1's gage mount, and also a possible jet axis. The eight-hole debris shield's face was also severely deformed, and the back of the gage mount showed coining marks from the metal piece which was bolted to it. Such plastic deformations could only occur at pressures above 36,000 psi (for mild steel) inflicted for significant lengths of time. This evidence clearly indicated that gages placed at jetting foci would have little chance of surviving.

The four surviving pressure gages in this test were all 20K Kulite gages. Measurements 3, 5, and 6 all used number 18 debris shields, while measurement 2 used a faster number 12 shield. The number 12 shield has a rise time from ambient to first peak of 140 μs, with an overshoot of 15 percent. Measurements 3 and 5 had been placed along diamond diagonals (Fig. 3), but they were apparently missed by Iremite jets due to minor misalignments in the HEST construction. All four gages exhibited several similarities. They all had the same general waveform, and they all had varying baseline shifts in late time.

Submitting the 20-ms and 40-ms pressure plots for these four measurements to the peak pressure routine yields different results. Scrutiny of the peak pressure overlays and the related residuals plots (Appendix B) shows that the impulse curves for measurements 2 and 3 simply do not fit the double-exponential approximation well. While some of the sigma values do not seem that far off, a glance at the overplots shows that the double-exponential overlays fit very poorly in the area of maximum change in the impulse, and in the late times. The routine also had trouble fitting to the steep early portion of the impulse curves. Measurement 5 fit better generally, but the routine still deviated significantly from the impulse curve in the early time and at the curve's maximum curvature. A study of the residuals plots for measurement 6 shows that these impulse curve data points deviate the least from the fitted curve for any of the plots analyzed. The curves fit well in late time, with only the 40-ms plot for the redundant recording wandering away at the end. By this analysis of the waveforms and the peak pressure fits, measurement 6 gave the best results from the peak pressure routine for TA HEST 2. Excepting the 40-ms plot of the redundant channel, measurement 6 gave an average peak pressure of 5,102 psi with the Wampler fitting procedure.

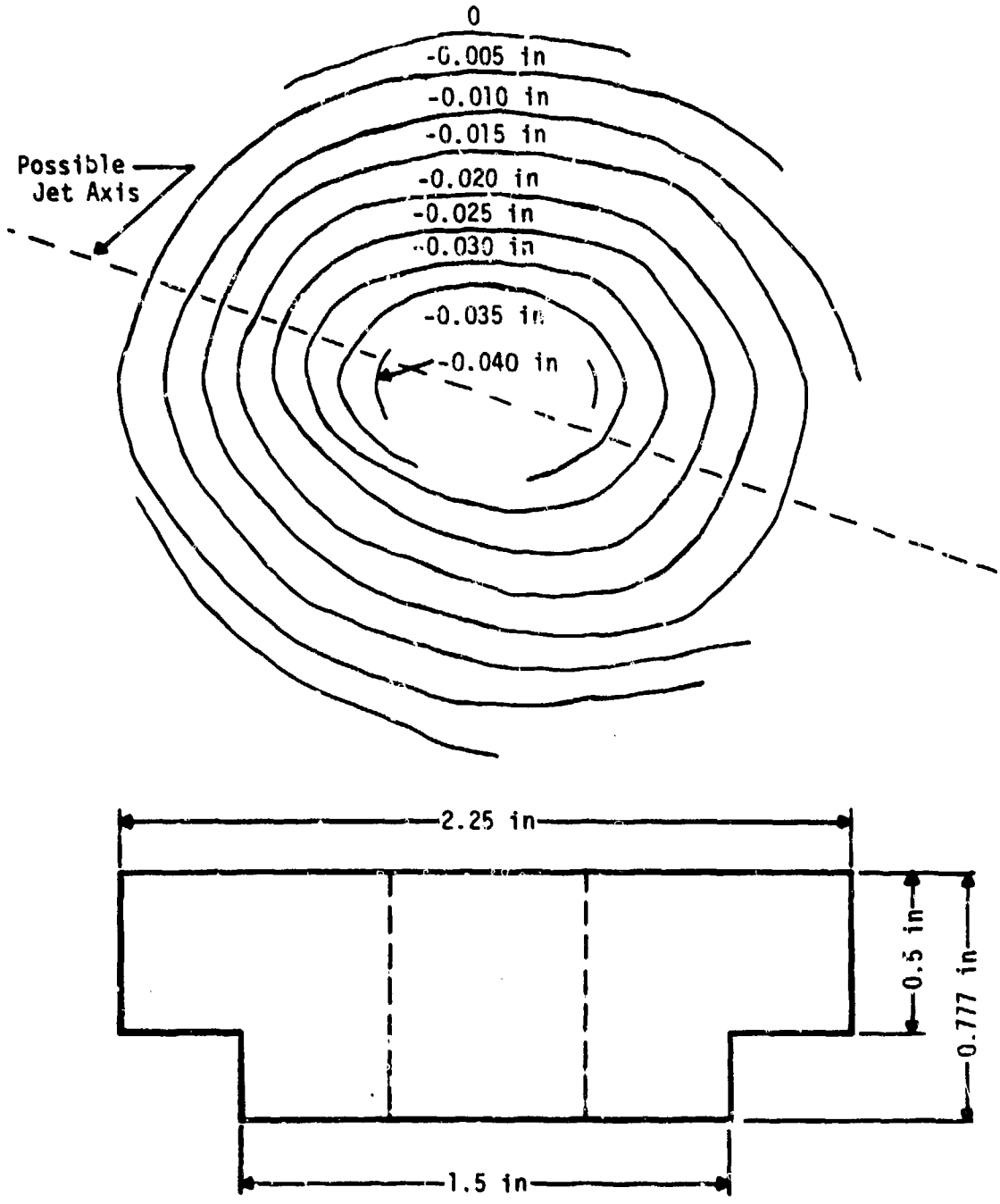

Material - Steel
Shape - Round Diaphragm
Thickness - Center 0.777 in x 1.5 in Diameter,
Rim 0.500 in x 2.25 in o.d.

Figure 13. TA HEST 2 - Gage Mount Deformation (Measurement 1)

The detcord driver design from TA HEST 1 was used again in TA HEST 2, with the same TOA gage layout. This time there were no problems with the pin box, and 21 of the 23 time-of-arrival crystals worked. Figure 14 plots the arrival times of all the crystals attached to the detcord weave against range along the detonation direction of the HEST. With the exception of one point (pin 16 which lay at the cavity edge), the results of the crystals line up well. Best-fitting a straight line to the points by the least-squares method gives an equation

$$t = 0.0534R + 0.5269,\ r^2 = 0.999 \qquad (12)$$

The derivitive of this equation (dR/dt) would be the velocity of the shock wave across the HEST, and this number works out to be 18,702 ft/s. This is slightly faster than the desired 18,000 ft/s, but still within 4 percent. The actual burn speed of the detcord can be quickly estimated by using trigonometry and the detcord weave angle of 33.69°. By dividing the shock velocity by the cosine of this angle (the arc tangent of 4/6), the detcord velocity can be calculated as 22,477 ft/s. So the time-of-arrival data from TA HEST 2 show that the driver design for the first two tests worked as desired.

The photopole impulse curves (Appendix C) compare well with the total impulses from all of the surviving pressure gages, since most of the gages gave total impulses in the range from 10 psi-s to 13.5 psi-s. At 40 ms the photopoles yielded an impulse of 11.8 psi-s, which compares well with the three pressure plots determined as the best representation of this test. Measurement 6 had an impulse of 12.5 psi-s at this time, so the two impulse curves agree within the error bounds created by the analysis of the high speed films.

From 12 measurements made with the Troxler soil density measuring machine, the average in situ soil density of the test bed turned out to be 121 lb/ft^3. The average dry density was figured as 106 lb/ft^3, with an average moisture content of 14 percent. The Troxler machine gave an average in situ berm density of 91 lb/ft^3, an average dry berm density of 88 lb/ft^3, and an average moisture content of 4.2 percent. The berm was tested 4 in below the surface, while the test bed was measured at depths between 2 in and 12 in. Surface can samples from the berm gave an average in situ density of 83.5 lb/ft^3, an average dry density of 77.9 lb/ft^3, and an average moisture content of 7.1 percent. Three can samples

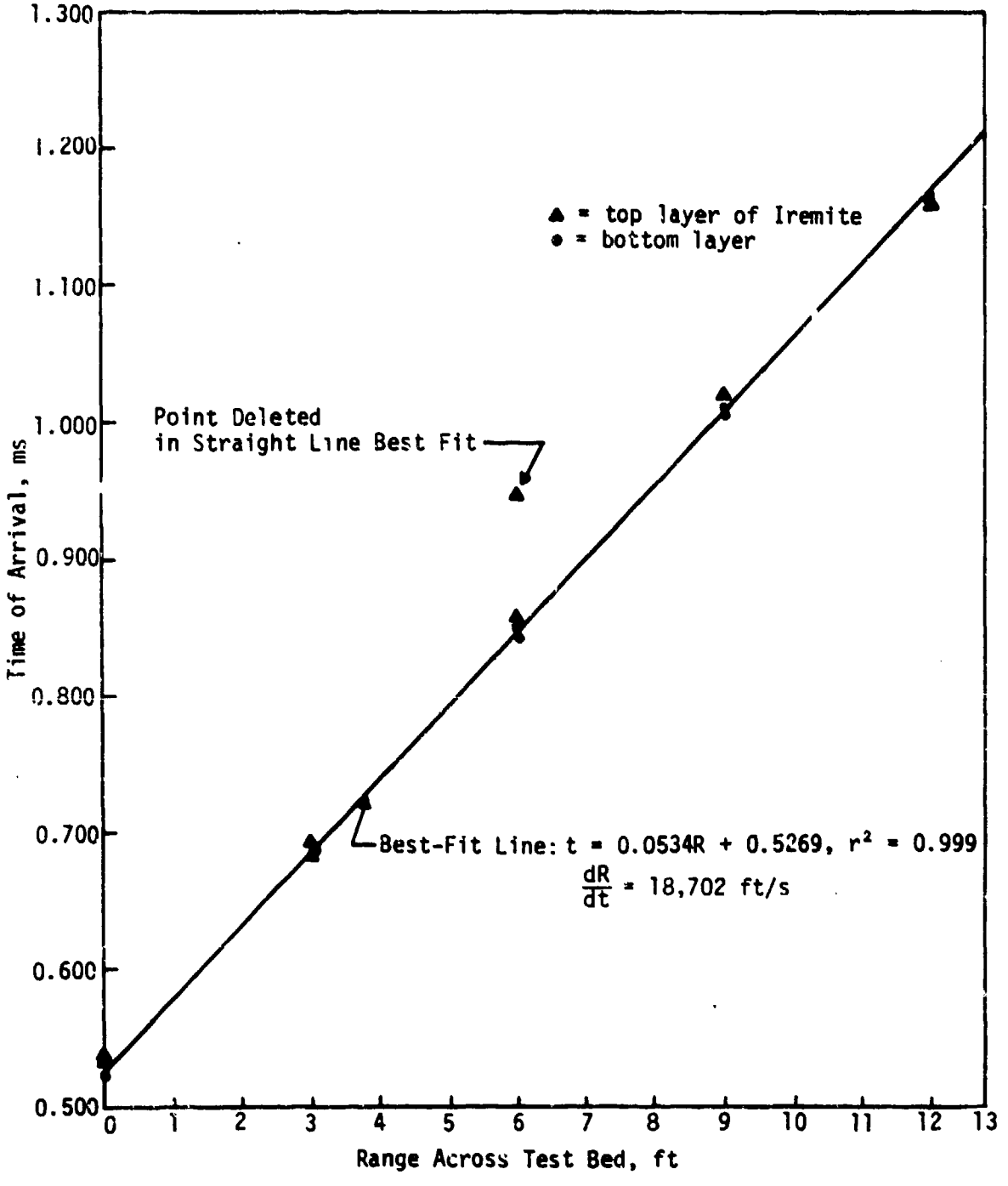

Figure 14. TA HEST 2—Time of Arrival Versus Range

were taken and tested in CERF's soils laboratory. The Troxler measurements are probably higher than the can samples because they were subsurface measurements, where the soil specimens would have been compacted by the earth above it.

TA HEST 3

Results from the first two tests agreed well and made the design of TA HEST 3 straightforward. On the basis of the noise-free pressure traces from the second test, the use of the remote signal conditioning amplifiers was eliminated in TA HEST 3, and all of the gages were Kulite gages. With the pressure and time-of-arrival gages arranged as shown in Figures 10 and 11, the survival rate for instrumentation was very good for a test of such a high pressure range. Fifteen of the twenty pressure gages gave results (the other five failed instantly), and 46 of the 48 time-of-arrival gages worked. All of the gages that failed were in the high pressure end of the HEST. As shown in Appendix A, measurements 1, 2, 6, 7, and 19 failed; significantly all of these except measurement 7 were 30K gages. All of the 30K Kulite gages in TA HEST 3 used the faster number 10 debris shields, with the thought that these gages could withstand the faster rise time allowed by this shield. Only measurements 3 and 4 survived from this group of gages and measurement 4 took a massive offset; therefore slower debris shields probably should have been used on the 30K gages. Measurement 7 was the only 20K gage which developed problems; not even major baseline shifts were encountered in the other twelve 20K gages. All of the 20K Kulite gages used number 18 debris shields.

A study of the pressure waveforms indicates the relative quality of the surviving measurements. The most obvious problems were with measurement 4 which had a baseline shift of -315 psi, but the trace did exhibit a good rise time and a clean waveform. The worst problems, which were not easily correctable, were with measurements 5 and 15. An approximately 750-Hz signal is superimposed on measurement 5. Also, the gage suffered a baseline offset, which can be corrected for. However, the distortion of the actual waveform cannot be easily corrected, nor can the poor rise at shock arrival. Measurement 15 had a large negative spike (probably a noise-burst) 0.5 ms after shock arrival which degraded the impulse curve. This bump in the impulse is hard to deal with in

the Wampler computer routine. The rise time and pressure trace in the first 1/2 ms also indicate that all of the first peak may not be present, but this is not certain. A few other measurements seem to have weak front ends, with slower rise times and late first peaks, such as measurements 8, 12, 14, 16, and 20. Due to their sharp rise and clean waveform with no baseline shifts in late time, the best waveforms are measurements 9, 10, and 18.

The quantitative analysis given here of the peak pressures from this test rests solely upon the results of the double-exponential peak pressure routine and judgment based on qualitative points. Referring to Appendix B, more than 30 calculations were run on the 20-ms and 40-ms plots from TA HEST 3 in order to have a good statistical base to study. By analyzing the plots according to their test bed range rather than strictly by measurement, more confidence could be gained in obtaining credible pressures from the routine. The most needed pressure, at the 7-ft range, cannot be determined because all the gages failed here. At the 14-ft range both measurements 3 and 4 gave pressure traces. For the best pressure determination here, measurement 4 was disregarded due to its baseline shifts and very poor fits by the routine. Of the two fits to measurement 3, neither agrees with the data exceptionally well. The residuals plots show that while the 40-ms plot fits slightly better in the late time, the fit to the initial points is nonsymmetric. Even though not good, the 20-ms plot has a better fit at the front end, so this fit represents the better of the two. Its calculated peak pressure of 7,529 psi can be considered as the best double-exponential fit pressure at the 14-ft range. Since measurement 6 failed, the pressure determination for the 21-ft range comes solely from measurement 5. The failure of measurement 6 was unfortunate due to the problems with measurement 5, and because the best pressure given by measurement 5 is not that credible. Baseline-correcting the 40-ms plot for the gage offset does not improve the residuals over those of the 20-ms fit, and it badly skews the fit to the early points. The calculated peak pressure of 5,668 psi from the fit of the 20-ms plot can be considered the best effort of the peak pressure routine for this range. This pressure is believed to be too low due to the poor quality of the measurement.

At the 28-ft range only one gage survived--measurement 8. Of the two plots fitted by the peak pressure routine, the 20-ms trace exhibited a better general

fit. Both its sigma 20 percent and its sigma 100 percent show better agreement, as do the graphs of the residuals. This fit yielded a peak pressure of 5,590 psi. All of the gages beyond the 28-ft range survived to give two measurements per range location. The double-exponential fits to measurements 9 and 10 at the 35-ft range are not the best, despite the relatively good sigmas. All of the fits to measurement 9 fit poorly about the points of greatest impulse curvature and the late time points. While there are problems in these same areas with the fit to the 40-ms plot of measurement 10, the 20-ms plot fits well. The double-exponential routine produces the best residuals plot here, with only moderate skewness about the first few points. The peak pressure calculated here is 5,922 psi. The fits generated for measurements 11 and 12, at 42 ft, improve over those of the 35-ft range. The routine has few problems with the late points and the area of maximum curvature in the impulses due to their gentler curves. A glance at the residuals plots shows that the 20-ms plot of measurement 11 has the best sigmas because the routine fits very well for most of the curve. The lack of fit to the first data points is about the same for all of these plots, so the pressure of 3,615 psi is the best result from the routine for this range.

With the redundant recording of measurement 14, the peak pressure routine produced a whole group of fits to consider at 49 ft. Unfortunately the fits to the redundant recording were poorer, as indicated by the larger values of sigma, and pressures suggested by them were disregarded. The waveform comparison of measurements 13 and 14 favors measurement 13 because of its sharper rise time and cleaner initial pulse. The sigmas also favor measurement 13, even though the late time data for measurement 14 fits slightly better. Judging by the residuals plots and the waveform quality, measurement 13's peak pressure of 4,328 psi is the routine's best-fit pressure at this range. At the 56-ft range, measurement 15 could not be realisticly analyzed with the peak pressure routine, because of the noise-burst bump in the impulse curve. Only measurement 16 was carefully studied. The fits from measurement 16's traces match the data well, and because of its excellent residuals the 40-ms plot's peak pressure of 2,651 psi was chosen. Since all of the fits to measurement 17 and 18 are very close, and the waveforms are good, the peak pressure at 63 ft can be chosen on the basis of the sigmas. The best-fit peak pressure here is 2,[illegible] psi. With measurement 20, at the 45.5-ft range, a study of the residual plots gives a best-fit peak pressure of 3,609 psi.

The results of these peak pressure studies are summarized in Figure 15. This graph shows not only the best-fit pressures mentioned above, but also all of the calculated peak pressures found by the Wampler double-exponential computer program. The design curve mentioned in Section II is drawn for reference. The result of an exponential fit to the best pressures is the equation

$$P = 9{,}981.17e^{-0.0211R}, \; r^2 = 0.825 \qquad (13)$$

This line is also drawn in Figure 15 and falls below the design curve. By integrating the areas under the two curves across the 70-ft range, and comparing the answers, it can be seen that about 15 percent less energy was expended in TA HEST 3 than desired, according to the pressures determined in the double-exponential fitting routine. It must be noted that while the design curve and the best-fit curves in Figure 15 are skewed relative to each other (they intersect), there is no large reason to believe that the rate of change of pressure over the first portion of the test bed range dropped as dramatically as the best-fit curve indicates. The coefficient of determination for the best-fit curve (0.825) is not that good for an exponential form, and this fit used very few data points in the first 30 feet of the test bed. The best-fit curve is most believable in the larger ranges.

The best peak pressures in this test can be plotted on the peak-pressure-versus-charge-density curve (Fig. 8), with the charge densities figured according to the amount of explosives in the step the pressure gage lay under. TA HEST 3 adds nine more data points to the older information of five data points (excluding the origin), and a straight line fit to all of the data yields a new peak-pressure-versus-charge-density function of

$$P = 1{,}717.8 \, C_D, \; r^2 = 0.974 \qquad (14)$$

with the fit of this line heavily weighted on the origin. This new fit reflects the fact that the pressures in TA HEST 3 fell below the expected results, for the new slope is about 12 percent smaller than the old slope of 1,957.6.

For time-of-arrival data, 46 of the 48 time-of-arrival crystals operated. Because the detcord driver was built in two sections--a constant velocity section

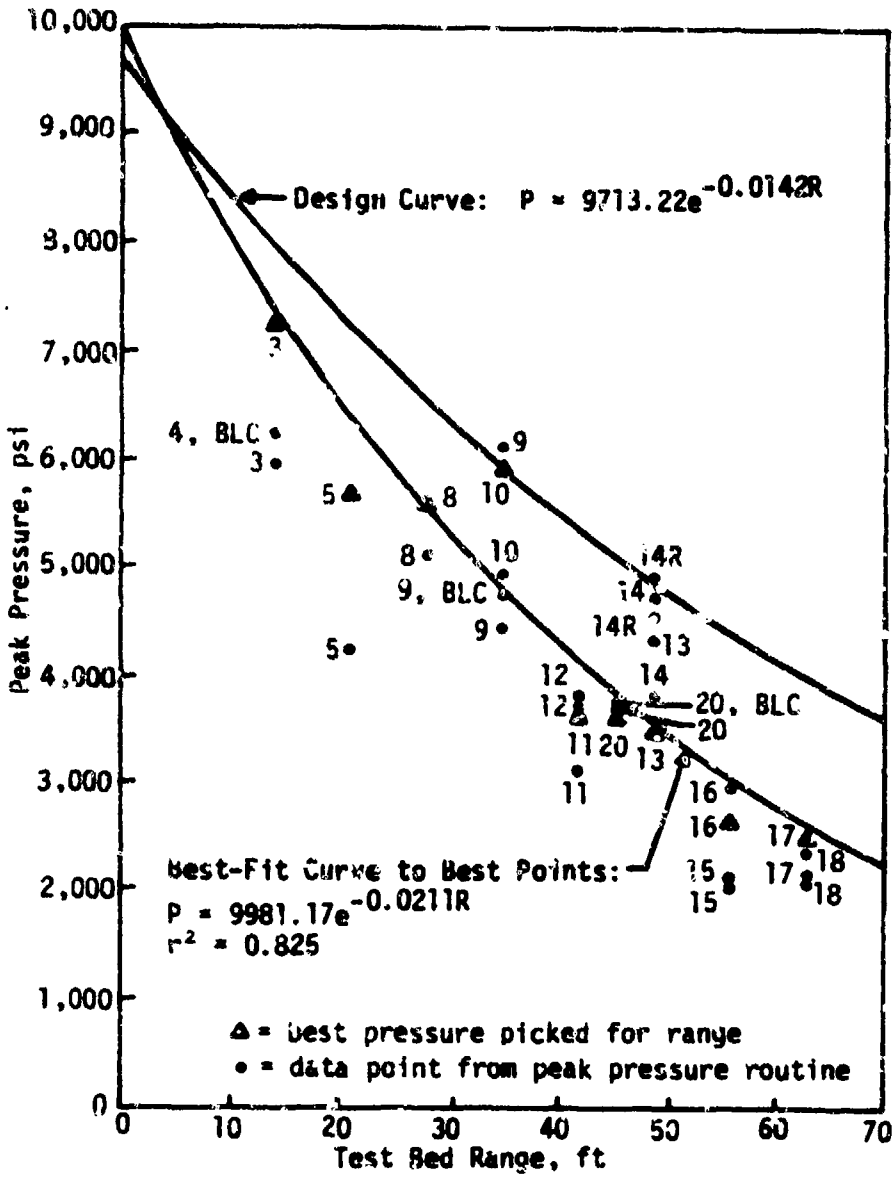

Figure 15. TA HEST 3 - Pressure Versus Range Test Results and Design Curve

for the first 27.9 ft and a variable speed weave for the remainder of the cavity--the data can be studied in two parts. A plot of time of arrivals versus range (Fig. 16) for the first 27.9 ft shows the data to lie nicely on a straight line. A straight line fit to these data points yields

$$R = 22.421t - 10.49, \quad r^2 = 0.998 \tag{15}$$

Taking the derivative dR/dt, and changing the units, gives the velocity of the straight detcord section of the driver as 22,421 ft/s. This velocity matches well with the design detcord speed of 22,500 ft/s. The data from the variable weave section of the driver can also be best fit exponentially, for the time-of-arrival-versus-range plot, and a good fit obtained:

$$t = 1.0155e^{0.0197R}, \quad r^2 = 0.994 \tag{16}$$

However, the velocities of the detcord at 27.9 ft, obtained from differentiated forms of Equations 15 and 16, exhibit an unacceptable discontinuity. A more realistic method of determining the velocity of the weave involved calculating differences in distance over differences in time. Referring to the time-of-arrival data in Appendix D, one can generate the velocities in Table 1 for plotting purposes.

Figure 17 shows the velocities in Table 1 plotted with their median ranges, as well as the HEST driver design curve; an exponential fit of the velocity data gives

$$V = 28,285e^{-0.0079R}, \quad r^2 = 0.831 \tag{17}$$

While the coefficient of determination is not excellent, this fit to the velocities is much more realistic than a derived velocity function from Equation 16. Equation 17 is drawn on Figure 17 and indicates that the detcord weave in TA HEST 3 burned about 2 percent faster than desired.

Certain problems arose in the photopole analysis from TA HEST 3, so the impulse curves of Appendix C do not match well with the pressure gage impulses. The two color cameras tracking the photopoles did not have a timing light generator attached, so neither of the resulting films have precisely known film speeds.

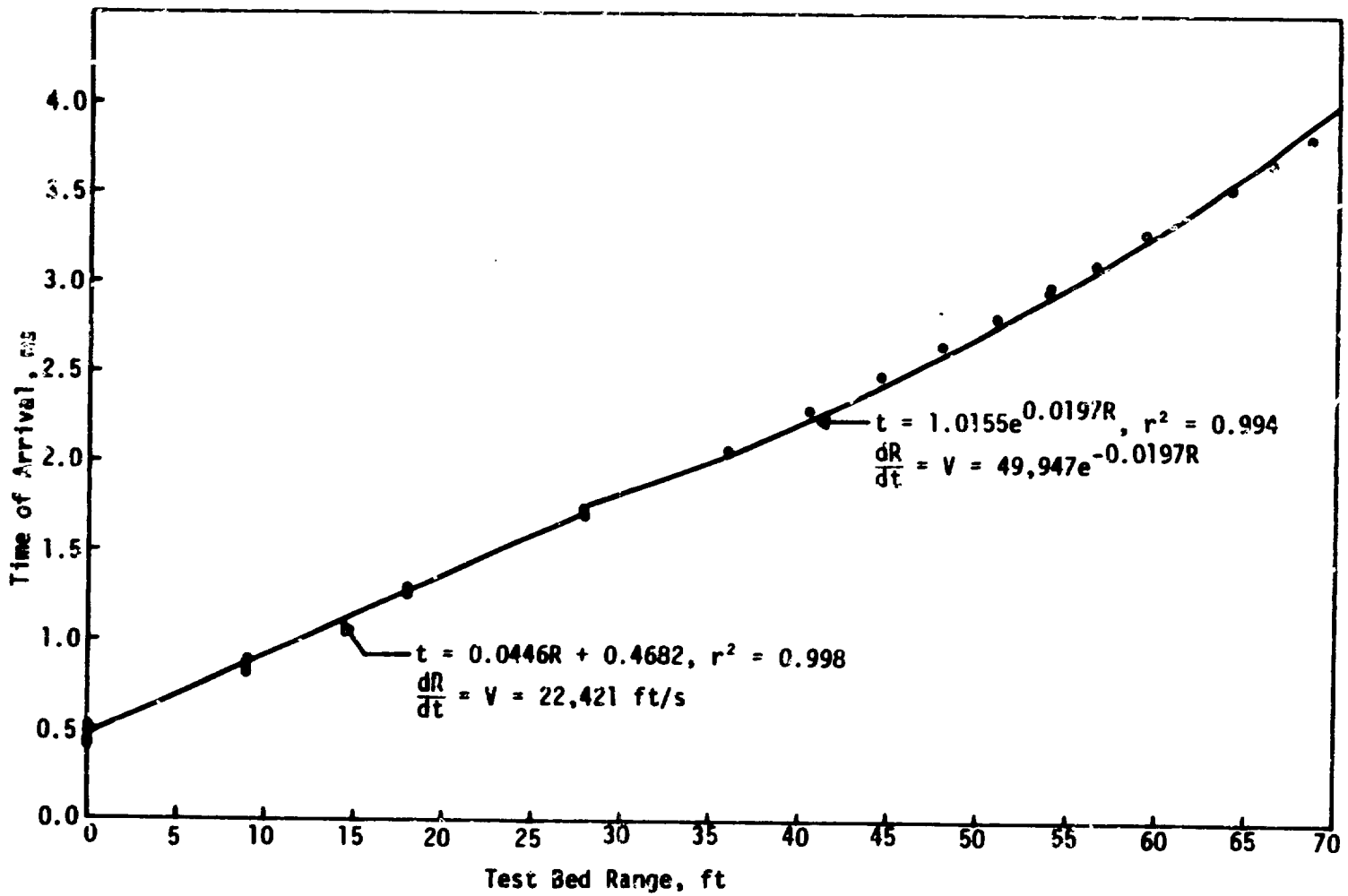

Figure 16. TA HEST 3 - Time of Arrival Versus Range

Table 1. WEAVE VELOCITY CALCULATIONS

Range, ft	Median Range, ft	Average TOA, ms	Δt, ms	ΔR, ft	$V\left(\frac{\Delta R}{\Delta t}\right)$, ft/s
27.9		1.710			
	31.90		0.360	8.0	22,222
35.9		2.070			
	38.15		0.221	4.5	20,361
40.4		2.291			
	42.40		0.197	4.0	20,304
44.4		2.488			
	46.15		0.184	3.5	19,021
47.9		2.672			
	49.40		0.149	3.0	20,134
50.9		2.821			
	52.35		0.158	2.9	18,354
53.8		2.979			
	55.15		0.145	2.7	18,620
56.5		3.124			
	57.85		0.159	2.7	16,981
59.2		3.283			
	60.45		0.133	2.5	18,796
61.7		3.416			
	62.85		0.136	2.3	16,911
64.0		3.552			
	65.15		0.131	2.3	17,557
66.3		3.686			
	67.40		0.140	2.2	15,714
68.5		3.823			

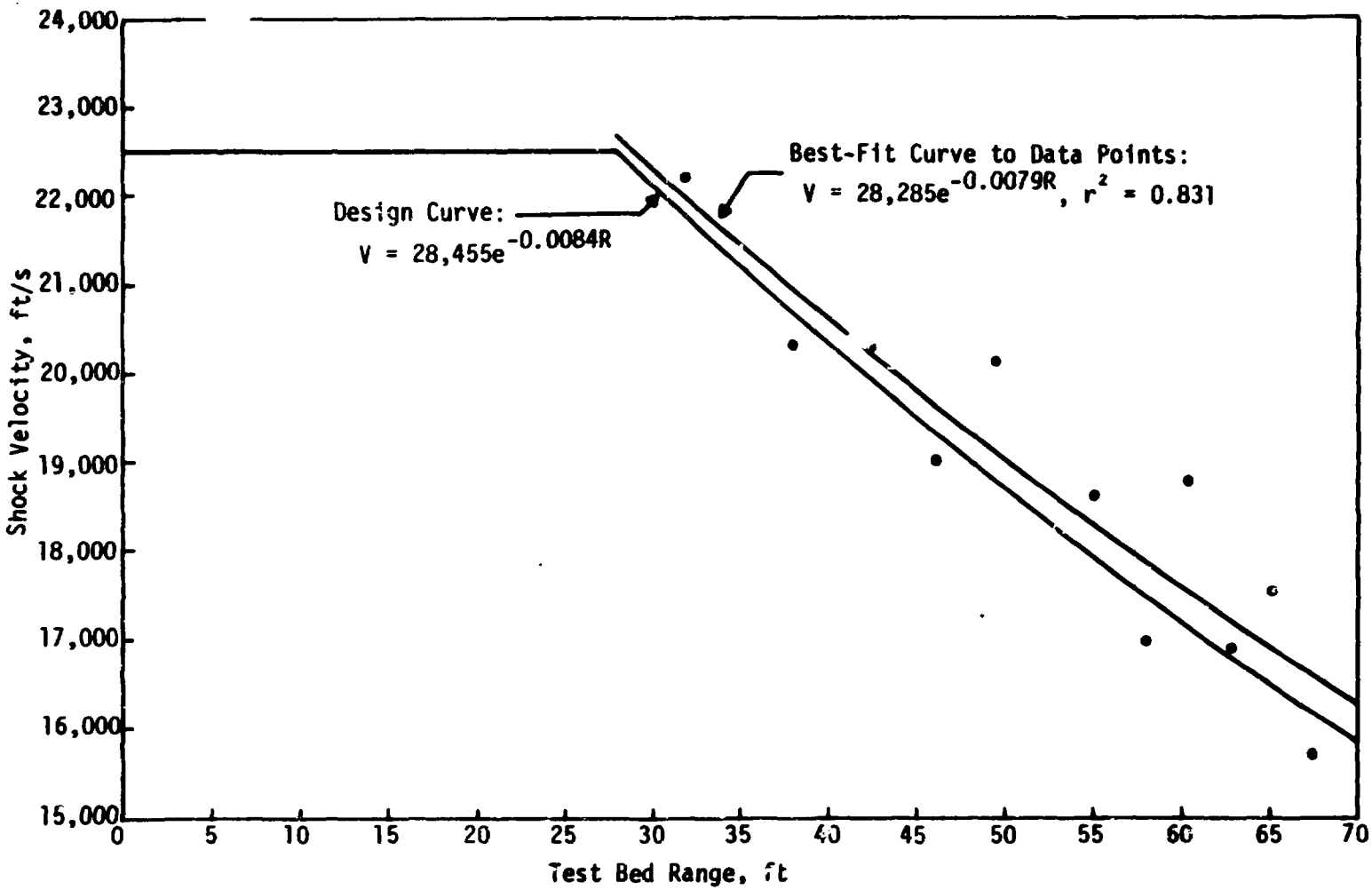

Figure 17. TA HEST 3 - Shock Velocity Versus Range Test Results for Weave and Design Curve

Becau e Hycam cameras run at regulated speeds in the low range, the photopole plots were done by using the camera's setting of 1,000 frames per second. While this number is not exact, it is probably correct to within 5 percent. The plots all indicate photopole impulses 2 psi-s to 5 psi-s below those of the pressure gages, an error probably explained by the film speed and the inertia of the photopoles.

The Troxler soil density measuring machine had been returned to the factory for repairs prior to TA HEST 3, so all of the density measures for this test came from can samples analyzed in the laboratory. The test bed gave an in situ density of 106 lb/ft^3 (from 3 surface samples), a dry density of 96 lb/ft^3, and a moisture content of 10.3 percent. Since these samples came from the surface, these densities are probably lower than for subsurface samples. The overburden had an in situ density of 88 lb/ft^3, a dry density of 84 lb/ft^3, and a moisture content of 4.8 percent (from 3 samples).

As a final note in this test series, measurements were made on the changes in elevation, before and after the tests, on all of the concrete gage canisters. While these displacements do not really correlate with any other related variable, it must be noted that the canisters dropped an average of 1.08 ft in TA HEST 3. This drop compares with displacements of 0.61 ft in TA HEST 2, and 0.945 ft in TA HEST 1.

SECTION V
CONCLUSIONS

The efforts of the Target Assessment HEST test series were successful in clearly defining the properties of Iremite in a foam HEST for nuclear simulation purposes, and in calibrating the det cord driver needed for a desired shock velocity. The results of this effort will be used by the Waterways Experiment Station (WES) in their test of a generic silo as part of a Defense Nuclear Agency (DNA) targeting research and test program. The relationship between the peak pressure obtained in a sweeping wave HEST and the Iremite charge density is described by the data in Figure 8. This graph of peak pressure versus charge density produced the usable function of

$$P = 1{,}717.8 \text{ psi } \left(\frac{C_D}{\text{lb/ft}^3}\right) \qquad P = 0.740 \text{ MPa } \left(\frac{C_D}{\text{kg/m}^3}\right) \tag{18}$$

for the future design of Iremite foam HESTS. By analyzing the data from this test series (and its antecedents) with the Wampler double-exponential peak pressure program, much of the data scatter due to human error has been eliminated in Figure 8. Equation 18 falls about 12 percent below the original design function of

$$P = 1{,}957.6 \text{ psi } \left(\frac{C_D}{\text{lb/ft}^3}\right) \qquad P = 0.843 \text{ MPa } \left(\frac{C_D}{\text{kg/m}^3}\right) \tag{19}$$

used for TA HEST 3; in a repetition of that test the HEST should be modified. However, this modification in design is straightforward.

Returning to the design procedure described above for TA HEST 3, one can merely substitute the new pressure-charge function of Equation 18 into the calculations. The charge-density-versus-range function can be recreated by using Equations 5 and 18 as

$$C_D = (5.65 \text{ lb/ft}^3)e^{-0.0142 \text{ (R/ft)}} \qquad C_D = (90.50 \text{ kg/m}^3)e^{-0.0466 \text{ (R/m)}} \tag{20}$$

Working through the math using Equation 9, the new space-width-versus-range equation for the TA HEST design parameters can be found as

$$S_C = (2.76 \text{ in})e^{0.142 \text{ (R/ft)}} \qquad S_C = (7.01 \text{ CM})e^{0.466 \text{ (R/m)}} \tag{21}$$

with two layers of Iremite. This function can be graphed and approximated appropriately to create a new stepped charge density HEST. According to the data from this test series, the redesign of TA HEST 3 with Equation 21 should yield the originally desired pressure range of 10,000 psi to 3,700 psi. A 7-inch cavity thickness and a 4-foot overburden height were used throughout this test series.

WES's calibration tests for their silo testing can be performed with the peak-pressure-versus-charge-density relationship above to check its validity with the clay soils of WES's test area in Kentucky for verification purposes. If the modified version of TA HEST 3 described here proves successful, then the desired 70-foot HEST needed for WES's test can be designed by merely repeating the explosive patterns of TA HEST 3 about sixfold. The 12-foot pieces of Iremite would be lengthened to 70 feet, and the det cord driver pattern would be repeated over the entire test bed width. A rough estimate of the explosives needed for a 70- by 70-foot test can be figured from the actual amount of explosives used in TA HEST 3. Since 1,545 pounds of Iremite was used in TA HEST 3, 12 percent more would be 1,730.4 pounds; for a 70-foot wide test bed, 10,094 pounds would be needed. Of course, WES's calibration tests will probably introduce further modifications into the HEST design produced for WES in this Target Assessment test series.

An AFWL Technical Report describing in detail the sizing considerations, design process, and data analysis done on this test series, the WES calibration tests, and the WES generic silo test is currently being written. It should be available from DDC by 30 September 1979.

APPENDIX A

PRESSURE VERSUS TIME PLOTS

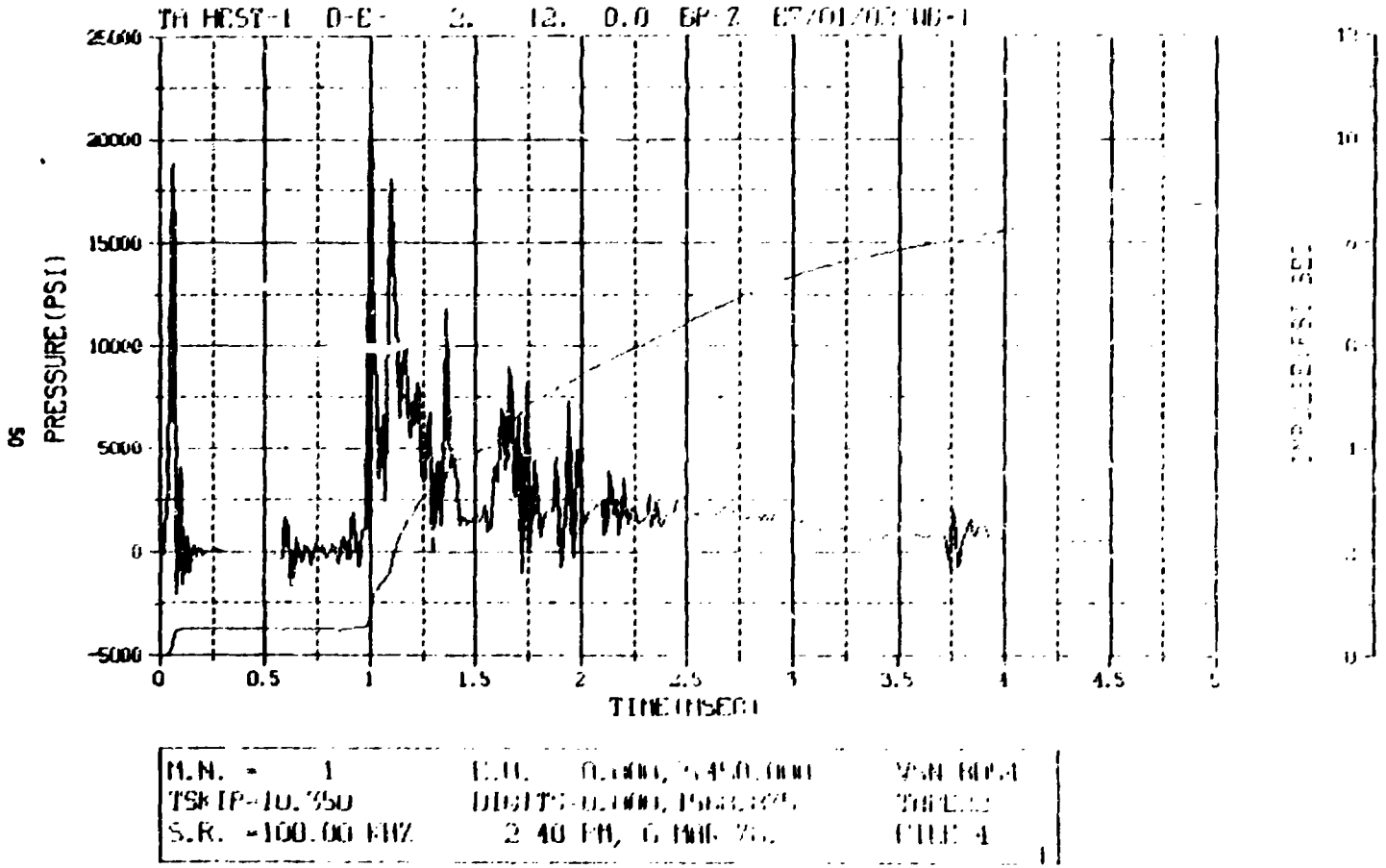
PRESSURE(PSI)
TIME(HSEC)
25000
20000
15000
10000
5000
0
-5000
0
0.5
1
1.5
2
2.5
3
3.5
4
4.5
5

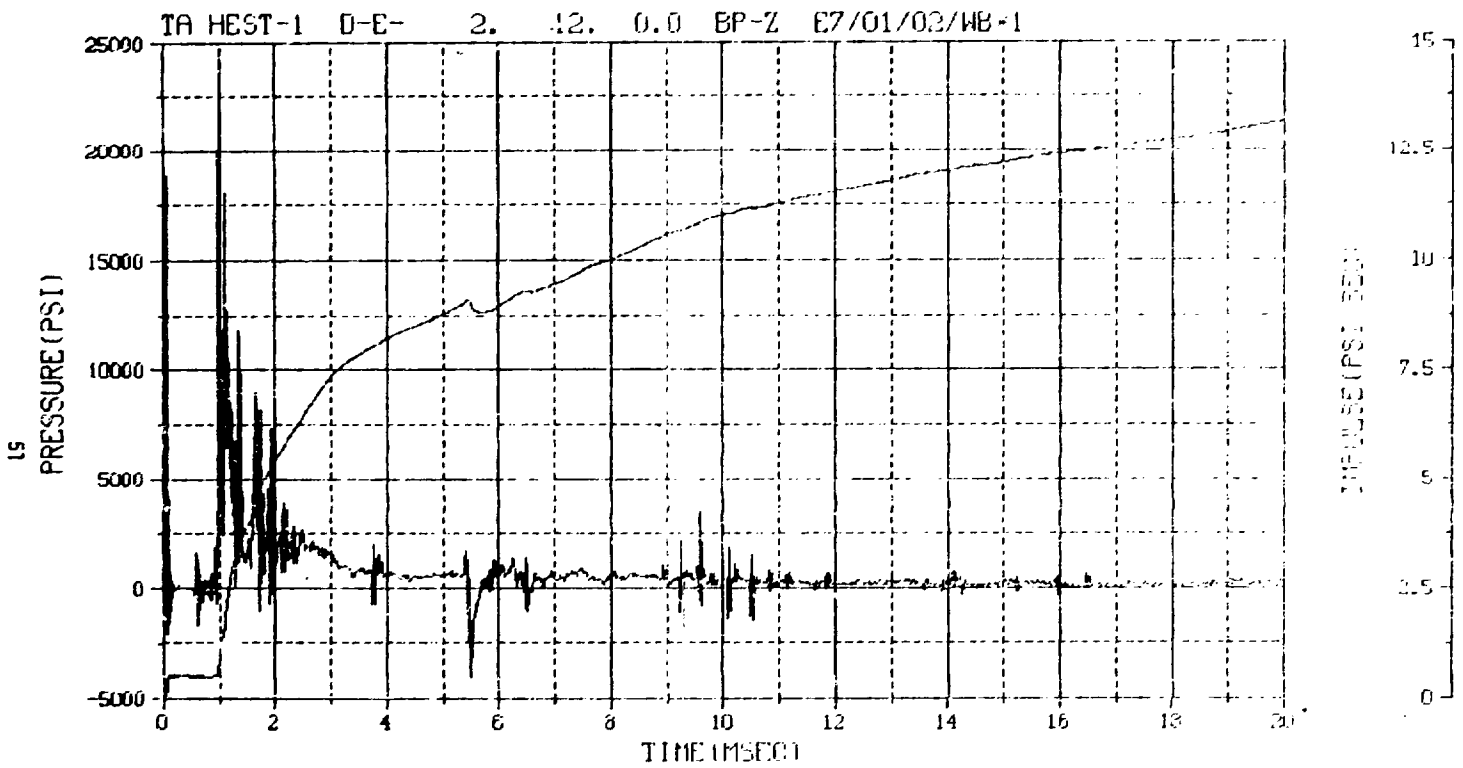
TA HEST-1 D-E- 2. 12. 0.0 BP-Z E7/01/02/WB-1
25000
20000
15000
10000
5000
0
-5000
PRESSURE(PSI)
0
2
4
6
8
10
12
14
16
18
20
TIME(MSEC)
15
12.5
10
7.5
5
2.5
0
M.N. = 1
TSKIP=10.350
S.R. =100.00 KHZ
E.U. =0.000,21450.000
DIGITS=0.000,1508.875
2 40 PM, 6 MAR 76.
VSN=BD54
TAPE22
FILE=4
1

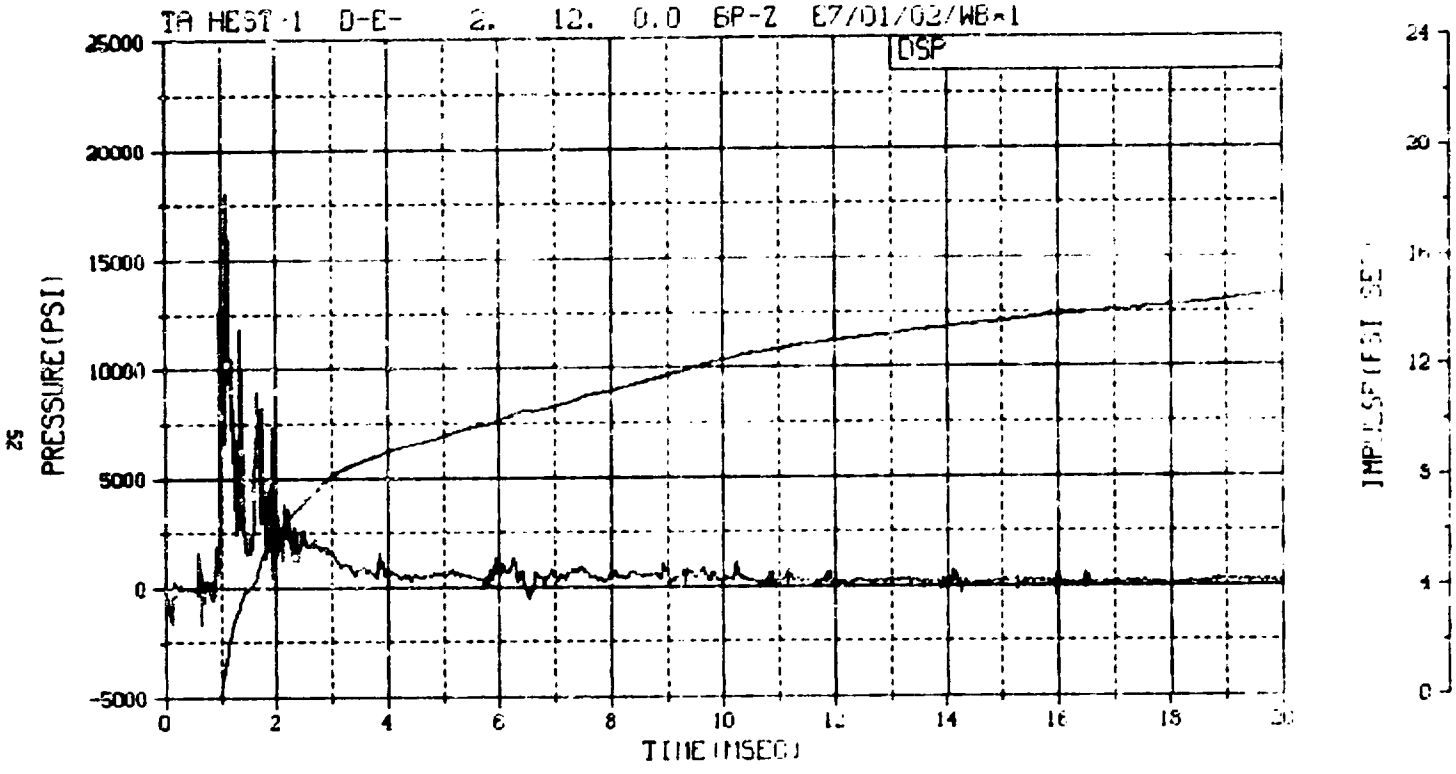

M.N. =80001	E.U. =0.000, 21450.000	VSN=
TSKIP=10.350	DIGITS=0.000, 1568.875	TAPE26
S.R. =50.00 KHZ	3 49 PM, 11 APR 78.	FILE=1

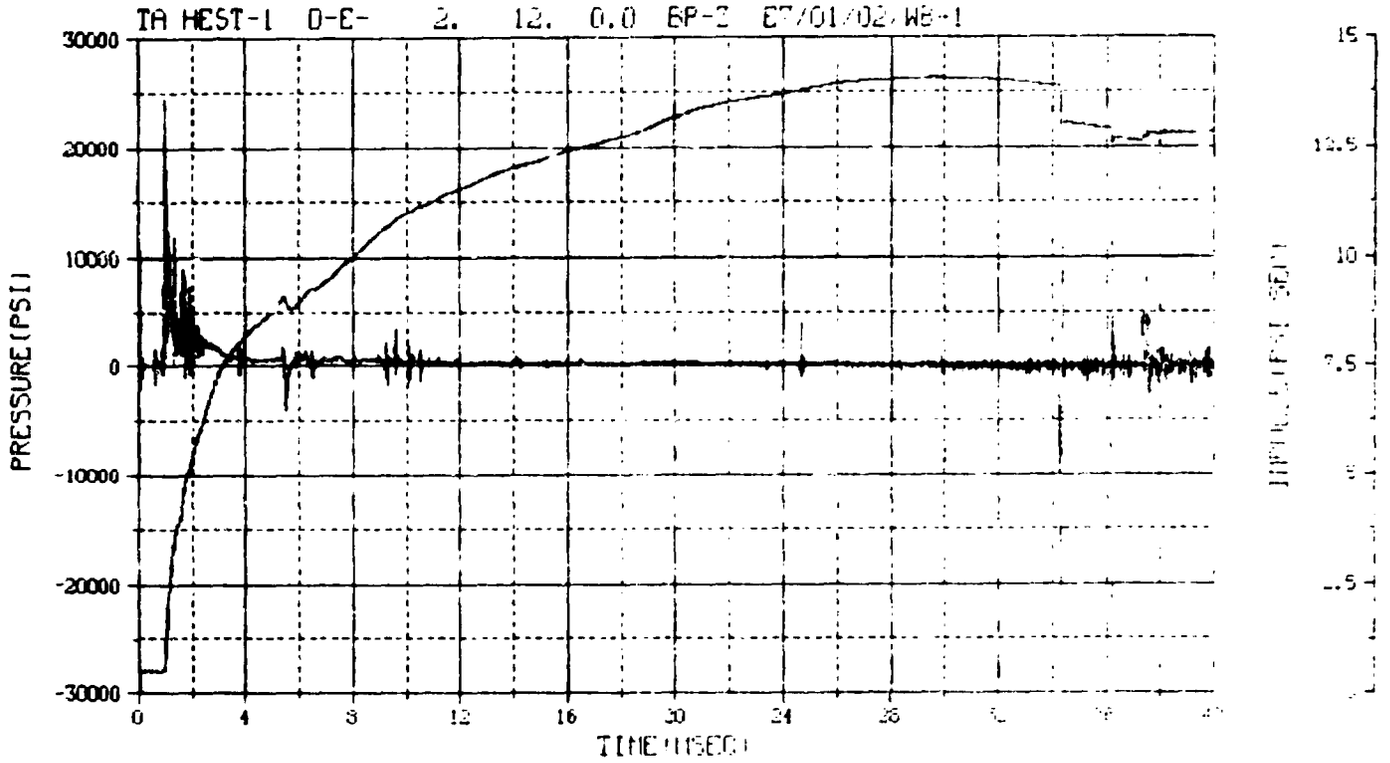

M.N. = 1	E.U. =0.000,21450.000	VSN=6054
TSKIP=10.350	DIGITS=0.000,15[illegible]	TAPE22
S.R. =100.00 KHZ	6 13 PM. [illegible] MAR [illegible]	FILE=4

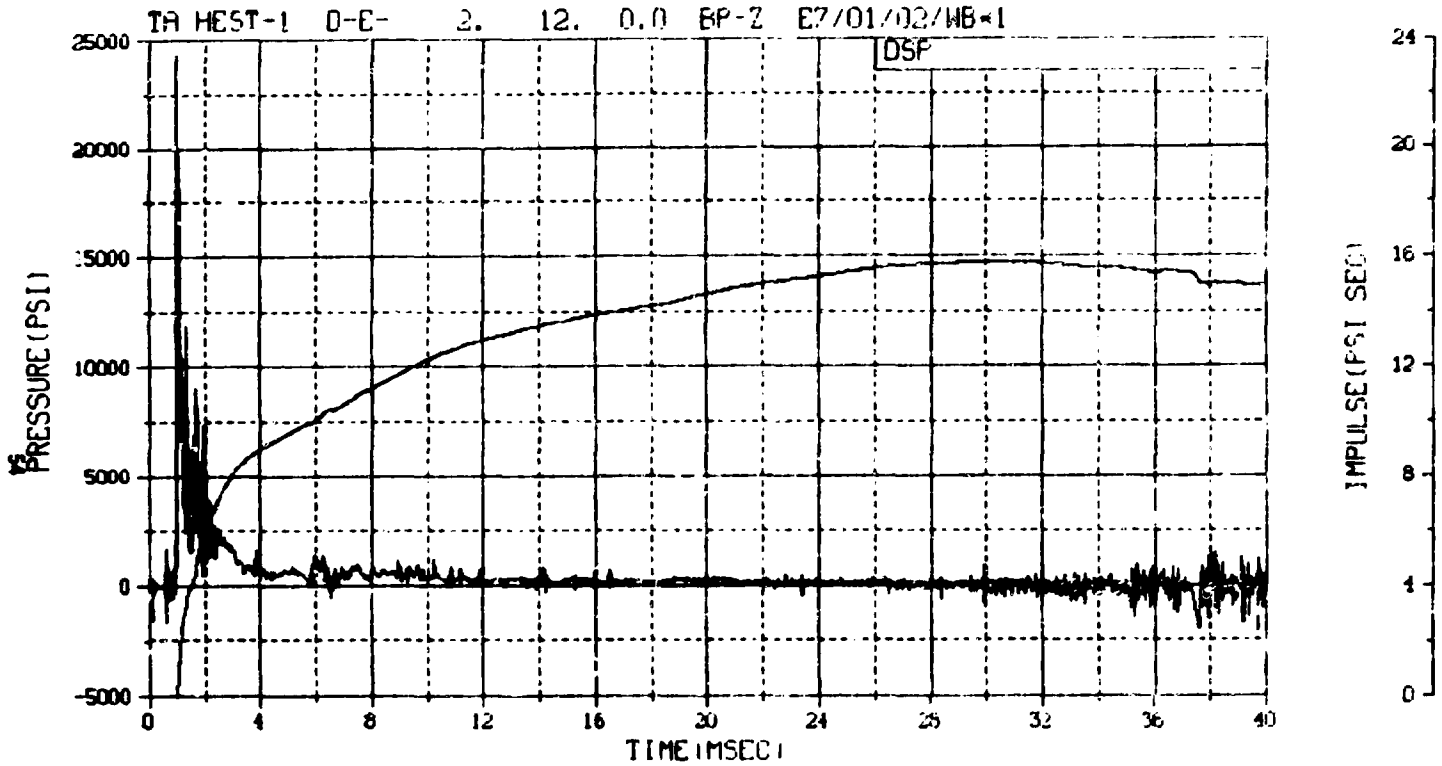

M.N. =80001	E.U. =0.000,21450.000	VSN=
TSKIP=10.350	DIGITS=0.000,1568.375	TAPE26
S.R. =50.00 KHZ	3 49 PM, 11 APR 78.	FILE=1

1

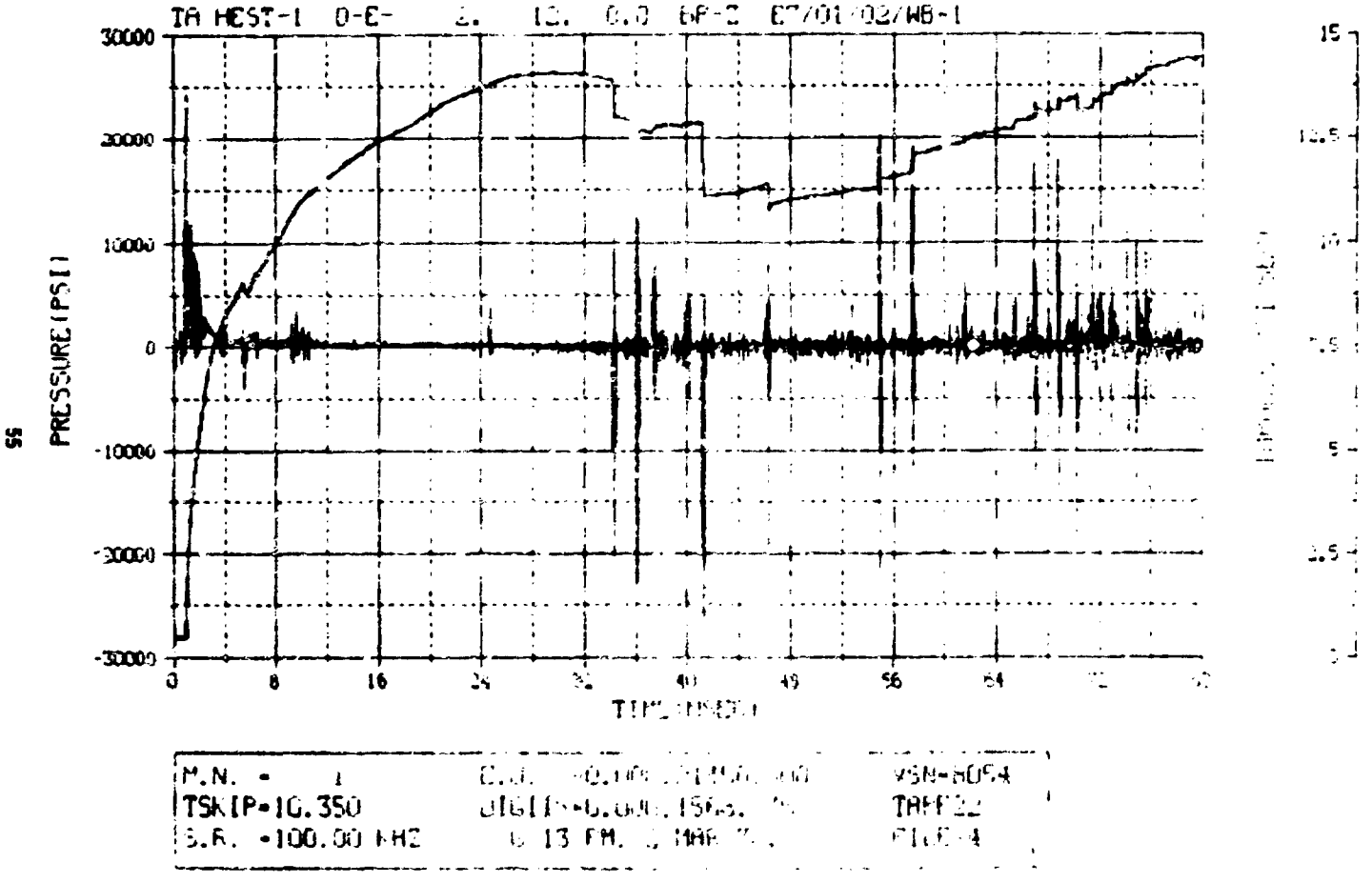
TA HEST-1 0-E-
30000
20000
10000
0
-10000
-30000
PRESSURE(PSI)
0
8
16
24
40
48
56
64
15
12.5
10
7.5
5
2.5
0
M.N. = 1
TSKIP=10.350
S.R. =100.00 KHZ
VSN=8054
TAPE22

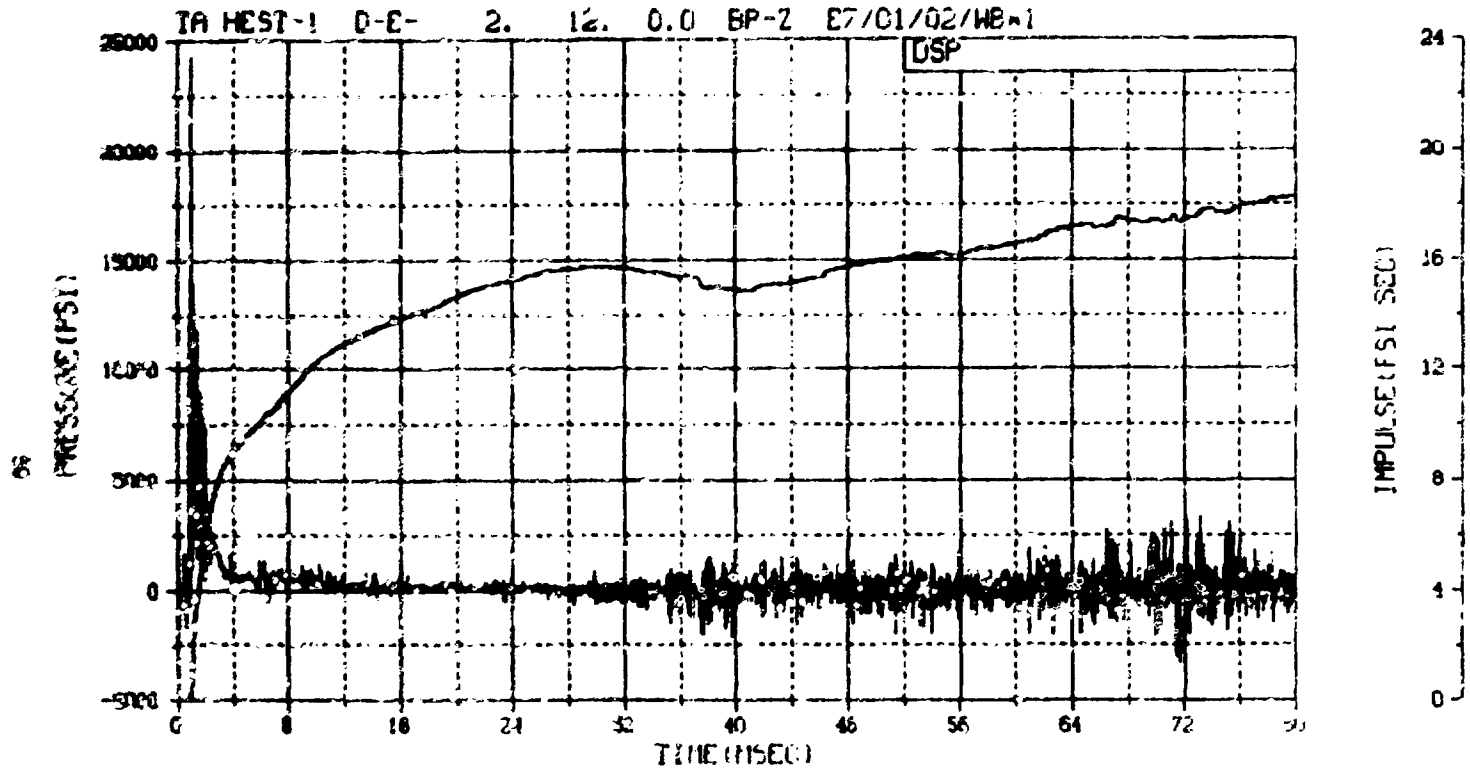

M.N. =80101	E.U. =0.000,21450.000	VSN=
TSNIP=10.350	DIGITS=0.000,1568.875	TAPE26
S.R. =50.00 KHZ	3 49 PM, 11 APR 78.	FILE=1

1

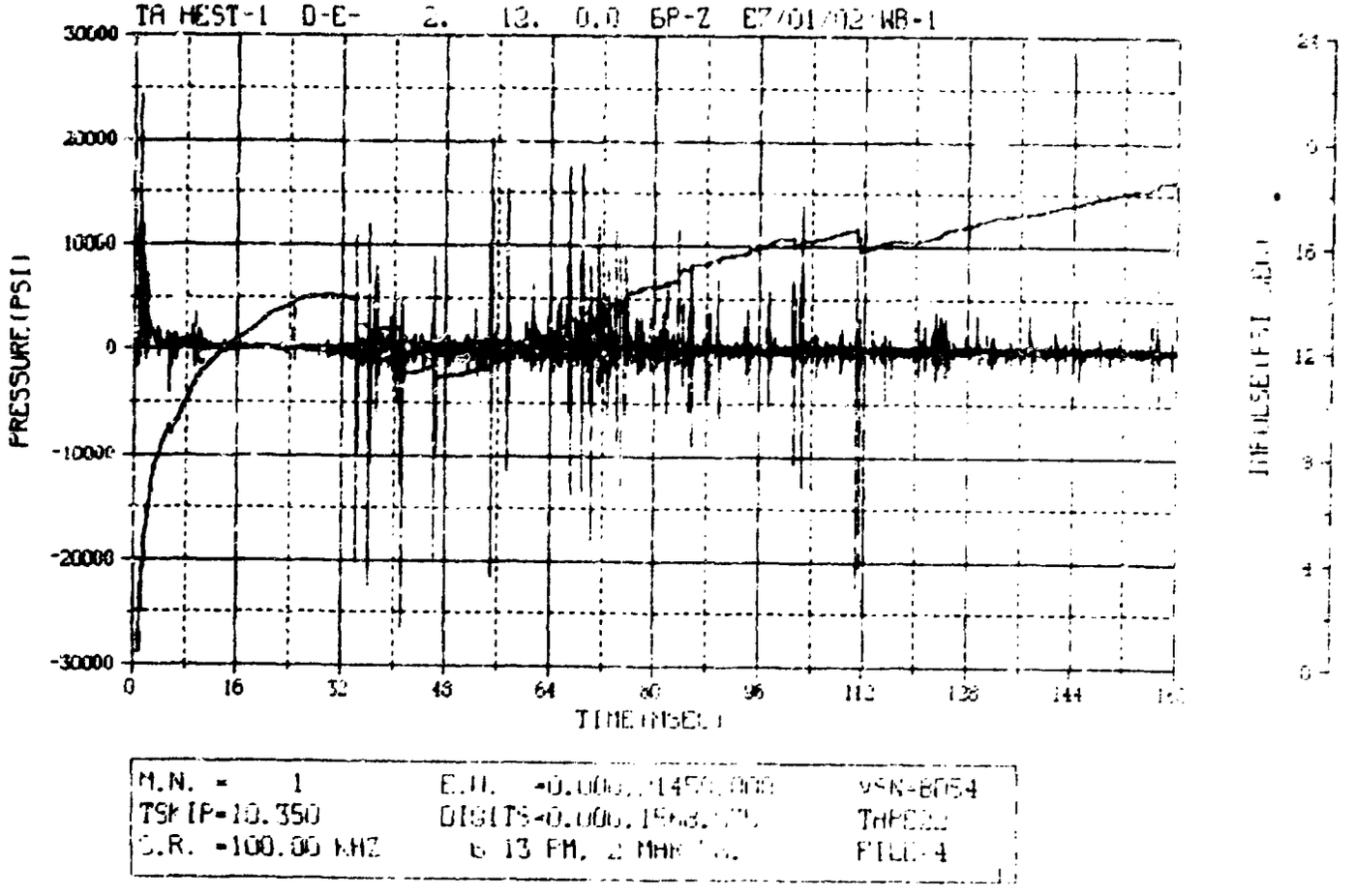
TA HEST-1 D-E- 2. 12. 0.0 BP-Z E7/01/02 WB-1
PRESSURE(PSI)
30000
20000
10000
0
-10000
-20000
-30000
0
16
32
48
64
80
96
112
128
144
TIME(MSEC)
M.N. = 1
TSKIP=10.350
S.R. =100.00 KHZ
E.U. =0.000,1450.000
DIGITS=0.000,1568.
6 13 PM, 2 MAR
VSN=8054
TAPE22
FILE-4

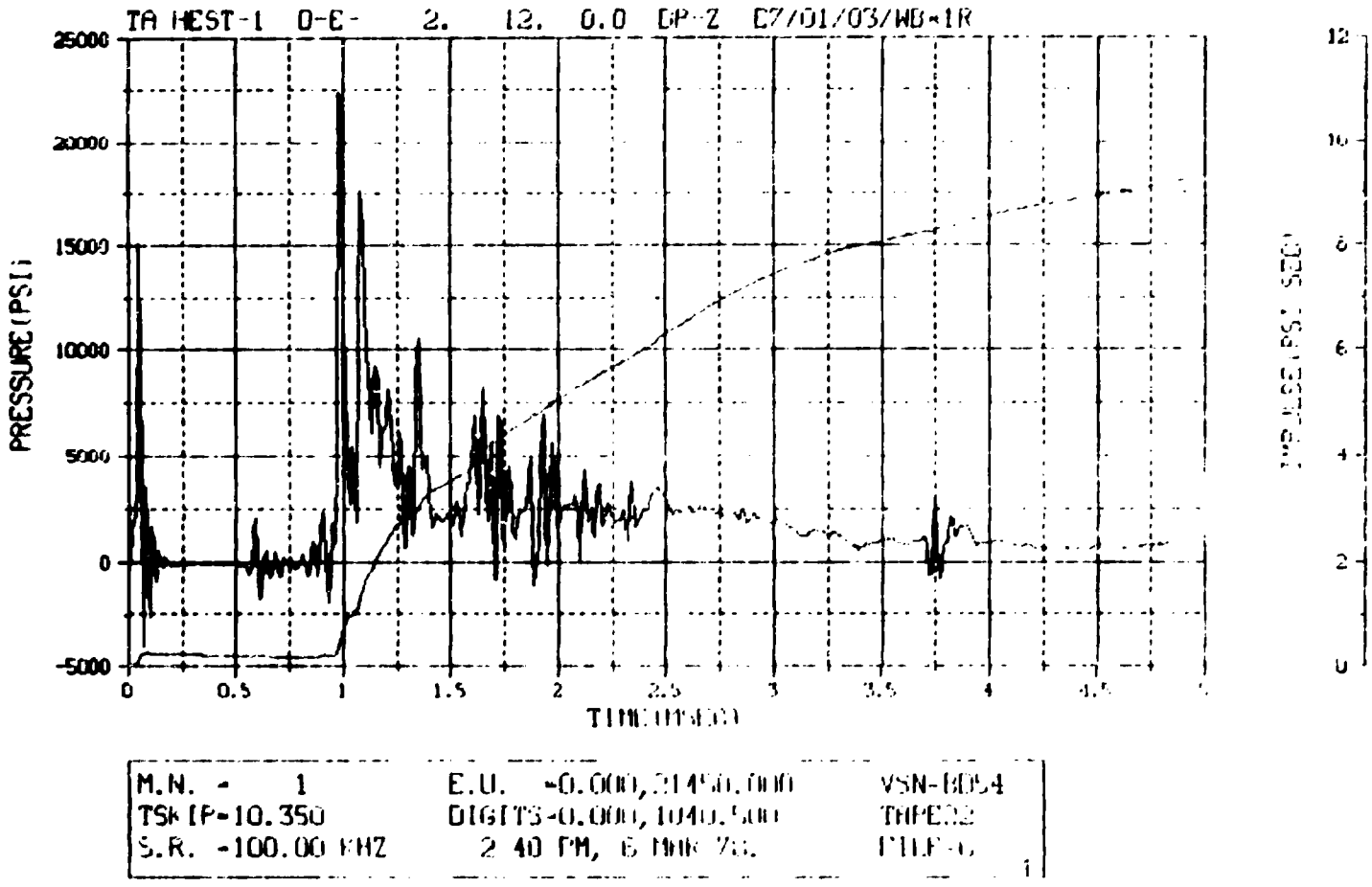
TA HEST-1 O-E- 2. 12. 0.0 DP-Z E7/01/03/WB*1R
PRESSURE(PSI)
25000
20000
15000
10000
5000
0
-5000
0
0.5
1
1.5
2
2.5
3
3.5
4
4.5
5
TIME(MSEC)
IMPULSE(PSI SEC)
12
10
8
6
4
2
0
M.N. - 1
TSKIP-10.350
S.R. -100.00 KHZ
E.U. -0.000,21450.000
DIGITS-0.000,1040.500
2 40 PM, 6 MAR 78.
VSN-BD54
TAPE22
FILE-6

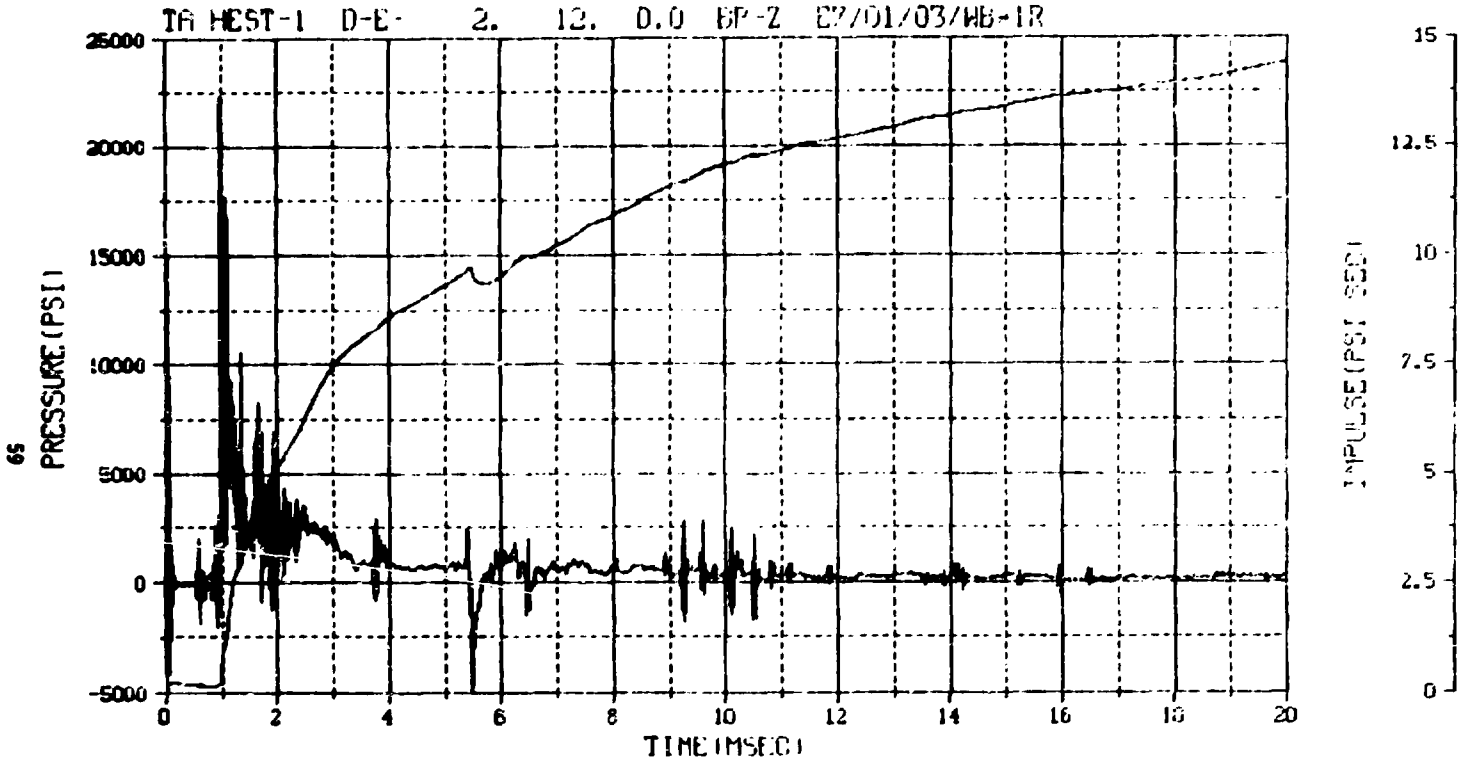
TA HEST-1 D-E- 2. 12. 0.0 BP-Z 87/01/03/WB-1R
PRESSURE(PSI)
65
25000
20000
15000
10000
5000
0
-5000
0
2
4
6
8
10
12
14
16
18
20
TIME(MSEC)
IMPULSE(PSI SEC)
15
12.5
10
7.5
5
2.5
0
M.N. - 1
E.U. -0.000,21450.000
VSN-BD54
TSKIP-10.350
DIGITS-0.000,1040.000
TAPE22
S.R. -100.00 KHZ
2 40 PM, 6 MAR 78.
FILE-6

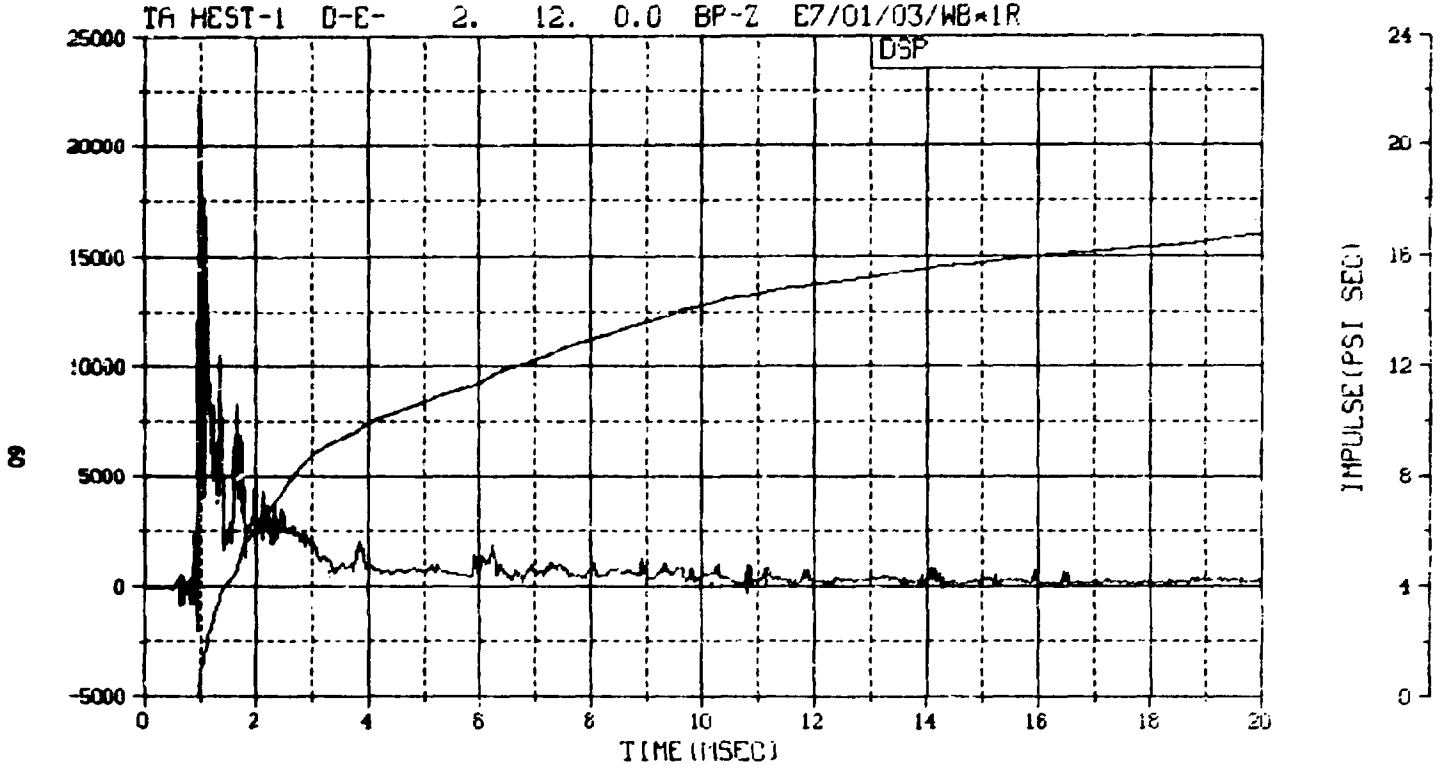
TA HEST-1 D-E- 2. 12. 0.0 BP-Z E7/01/03/WB×1R
DSP
25000
20000
15000
10000
5000
0
-5000
0
2
4
6
8
10
12
14
16
18
20
TIME(MSEC)
24
20
16
12
8
4
0
IMPULSE(PSI SEC)
M.N. =80001
TSKIP=10.350
S.R. =50.00 KHZ
E.U. =0.000,21450.000
DIGITS=0.000,1040.500
3 49 PM,11 APR 78.
VSN=
TAPE26
FILE=2
1

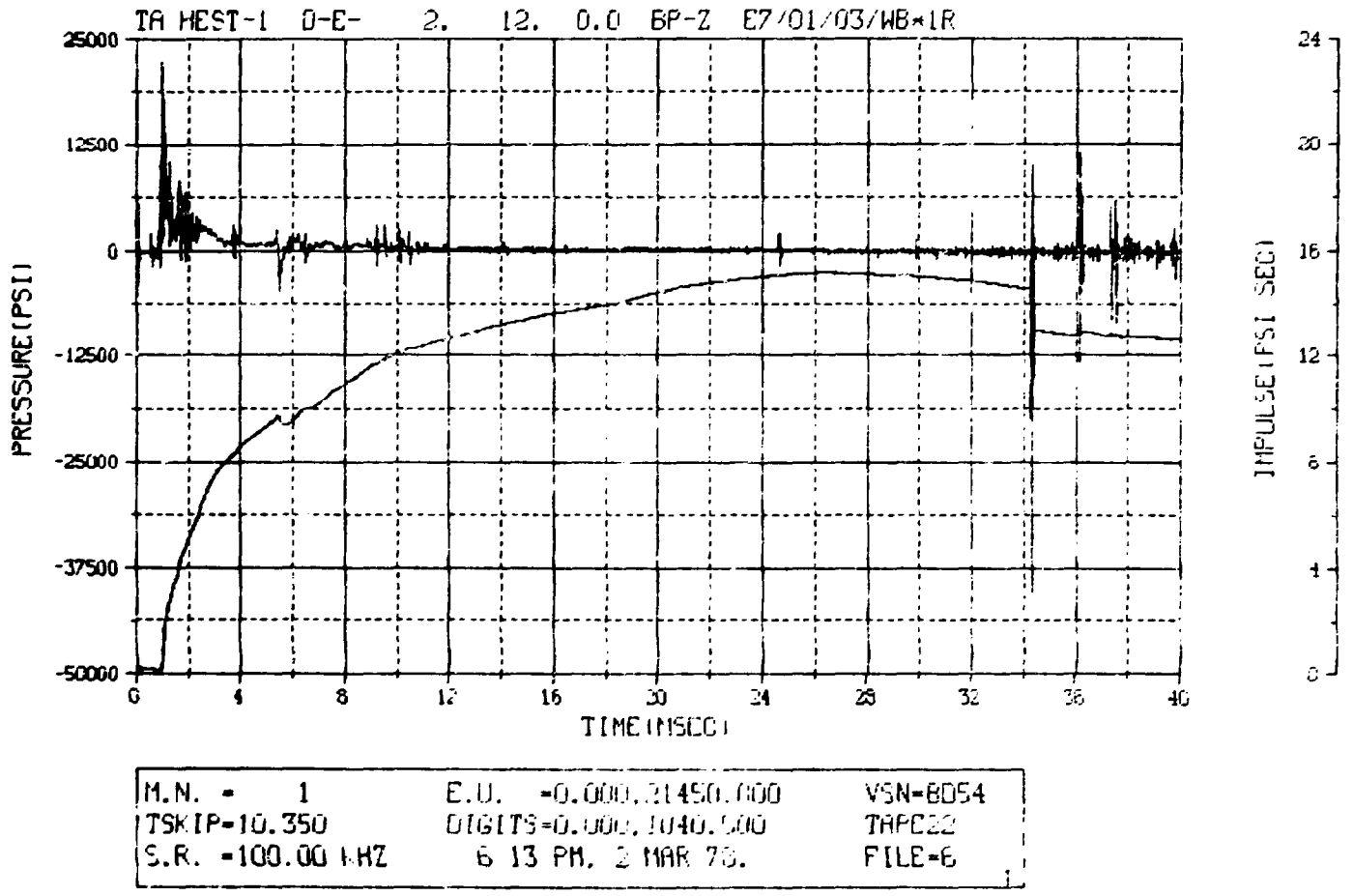
TA HEST-1 0-E- 2. 12. 0.0 BP-Z E7/01/03/WB×1R
25000
12500
0
-12500
-25000
-37500
-50000
PRESSURE(PSI)
0
4
8
12
16
20
24
28
32
36
40
TIME(MSEC)
24
20
16
12
8
4
0
IMPULSE(PSI SEC)
M.N. = 1
E.U. =0.000,21450.000
VSN=8054
TSKIP=10.350
DIGITS=0.000,1040.500
TAPE22
S.R. =100.00 KHZ
6 13 PM, 2 MAR 78.
FILE=6

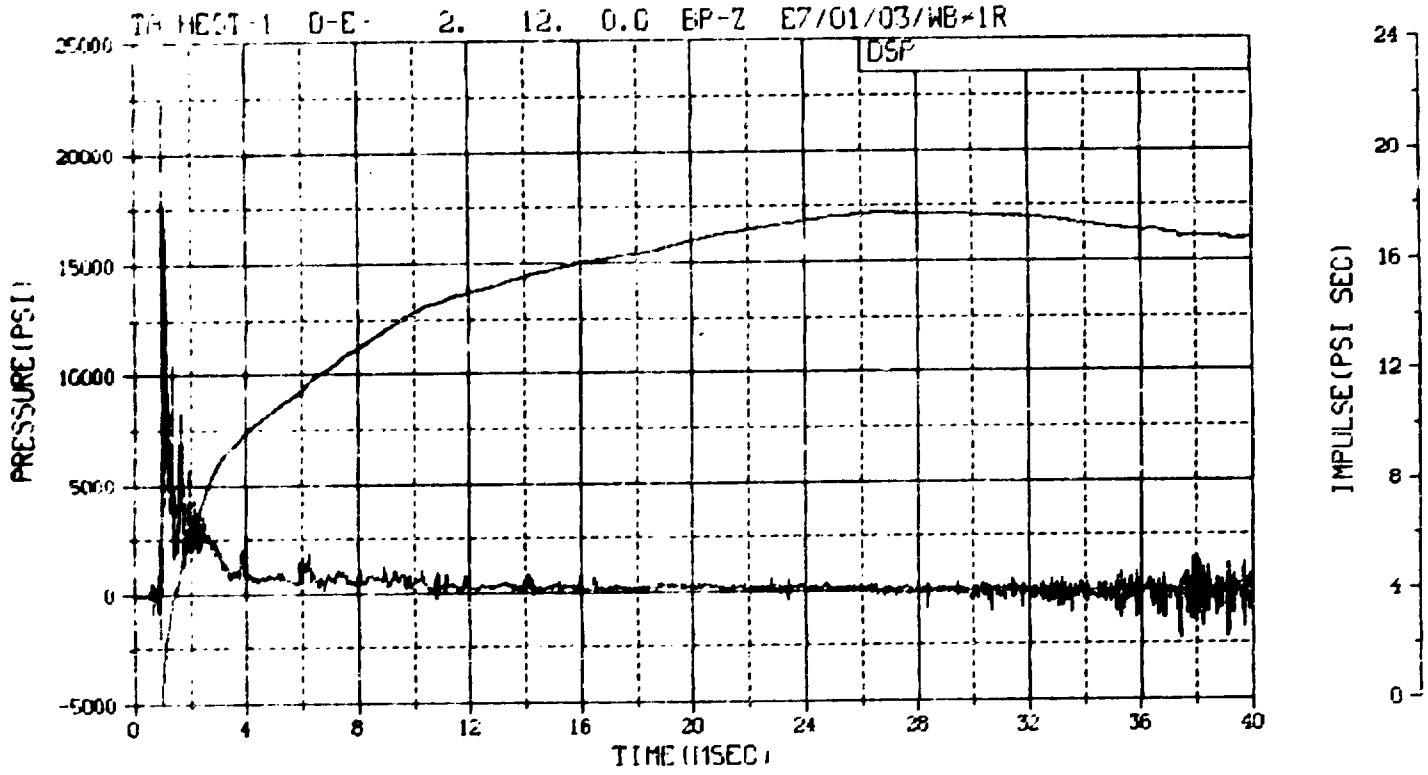

M.N. =80001	E.U. =0.000,21450.000	VSN=
TSMP=10.350	DIGITS=0.000,1040.500	TAPE26
S.R. =50.00 KHZ	3 49 PM,11 APR 78.	FILE=2

1

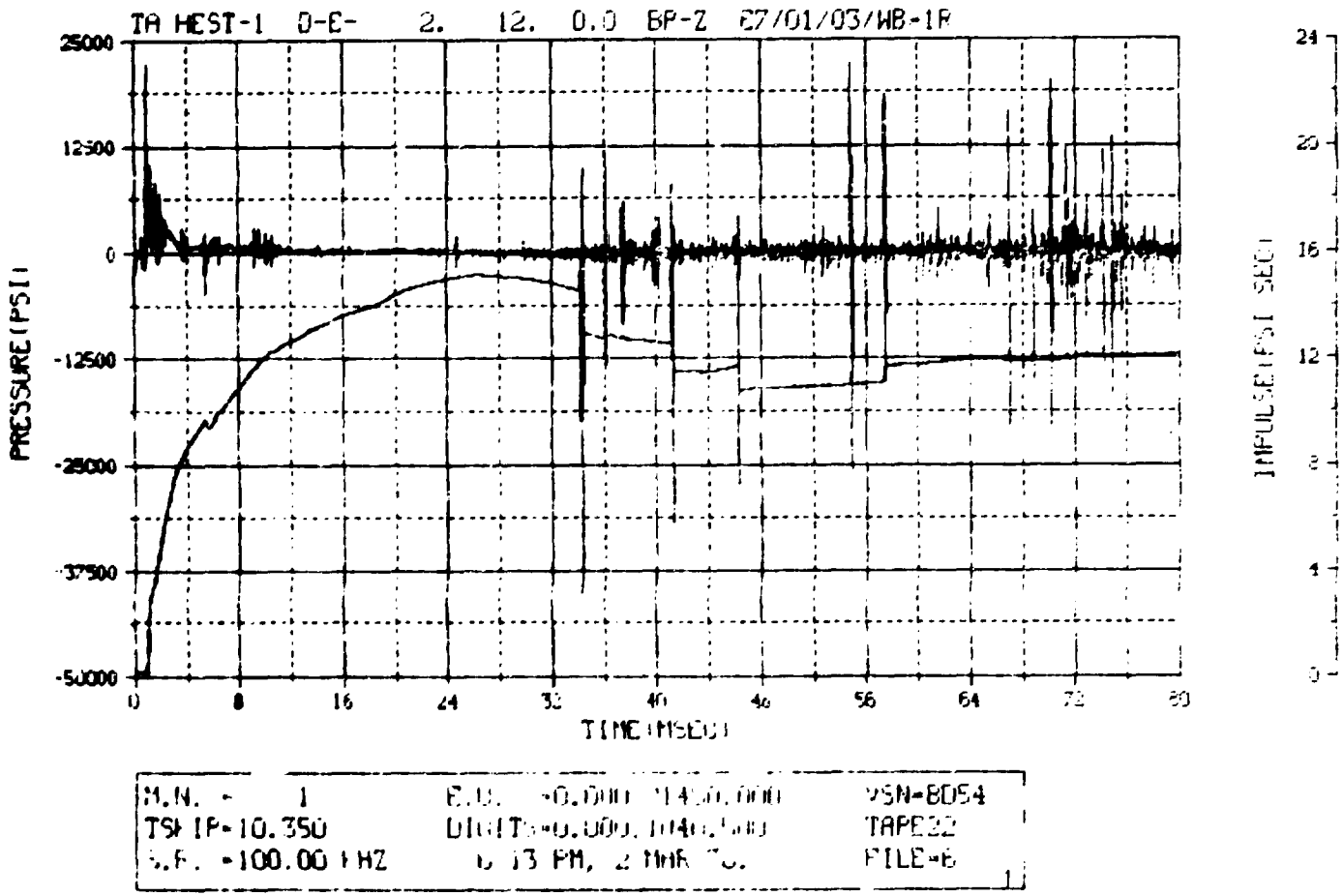
TA HEST-1 D-E- 2. 12. 0.0 BP-Z 67/01/03/WB-1R
PRESSURE(PSI)
25000
12500
0
-12500
-25000
-37500
-50000
0
8
16
24
32
40
48
56
64
72
80
TIME(MSEC)
24
20
16
12
8
4
0
M.N. = 1
TSKIP=10.350
S.R. =100.00 KHZ
VSN=BD54
TAPE22
FILE=6

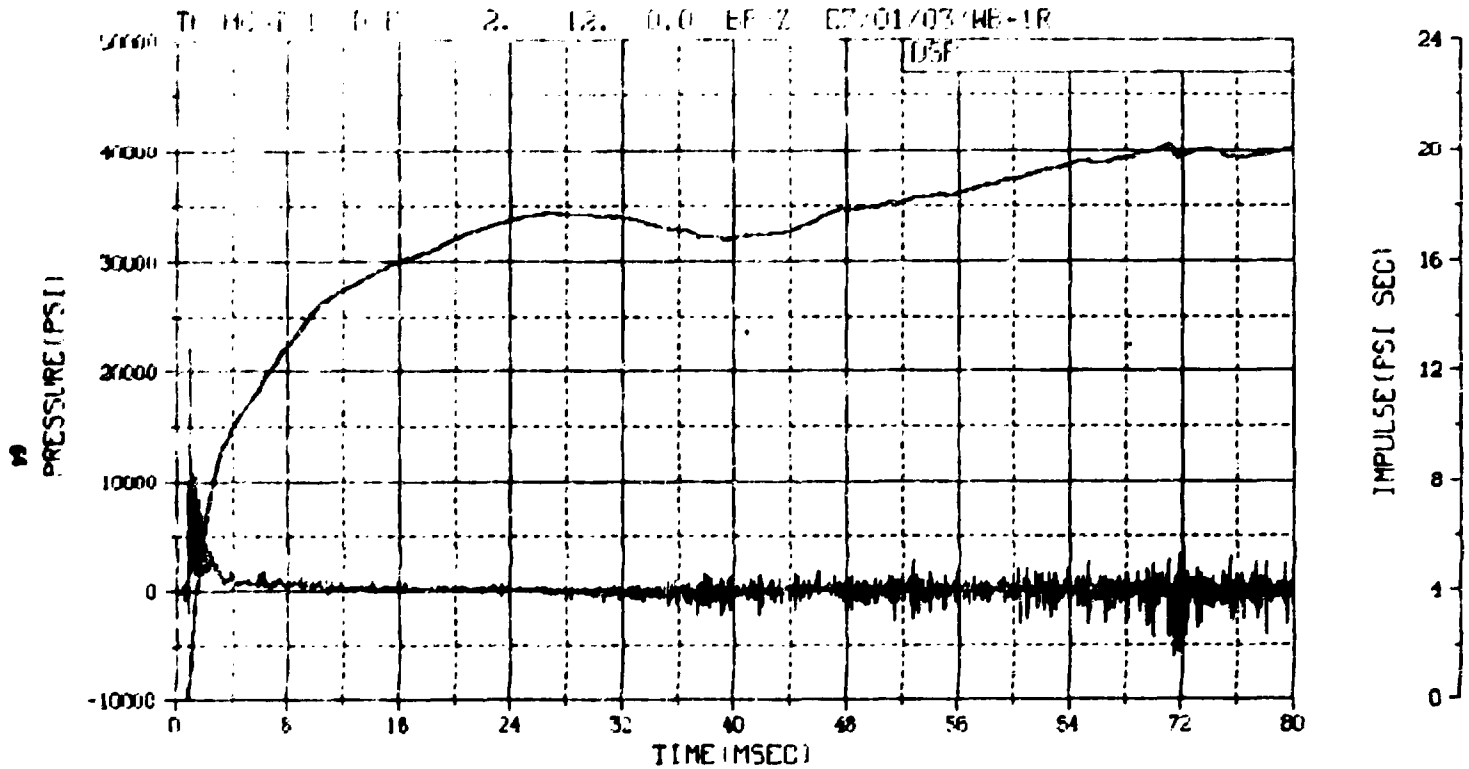

M.N. =80001	E.U. =0.000,21450.000	VSN=
TSMP=10.350	DIGITS=0.000,1040.500	TAPE26
S.F. =50.00 KHZ	3 49 PM,11 APR 78.	FILE=2

1

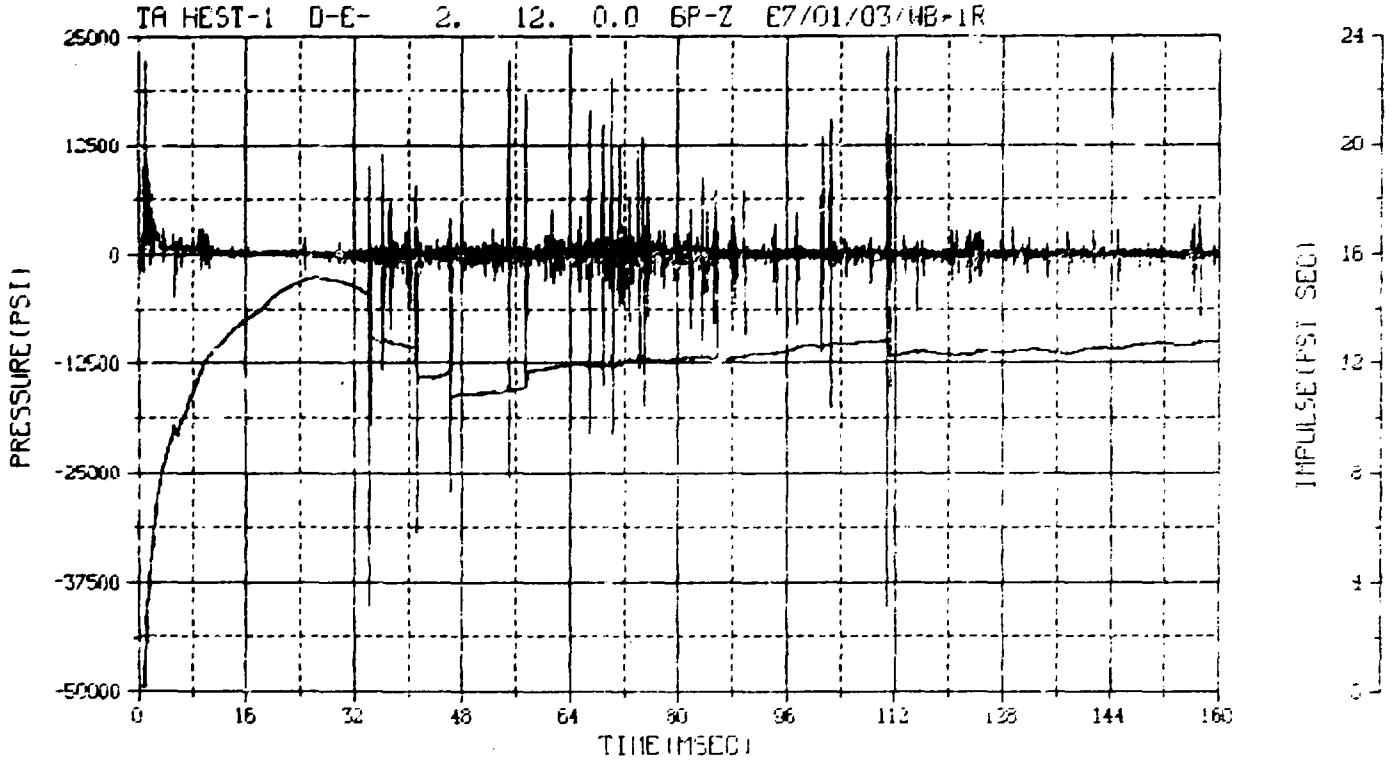

M.N. = 1	E.U. =0.000,21450.000	VSN=8054
TSKIP=10.350	DIGITS=0.000,1040.500	TAPE22
S.R. =100.00 KHZ	6 13 PM. 2 MAR 78.	FILE=6

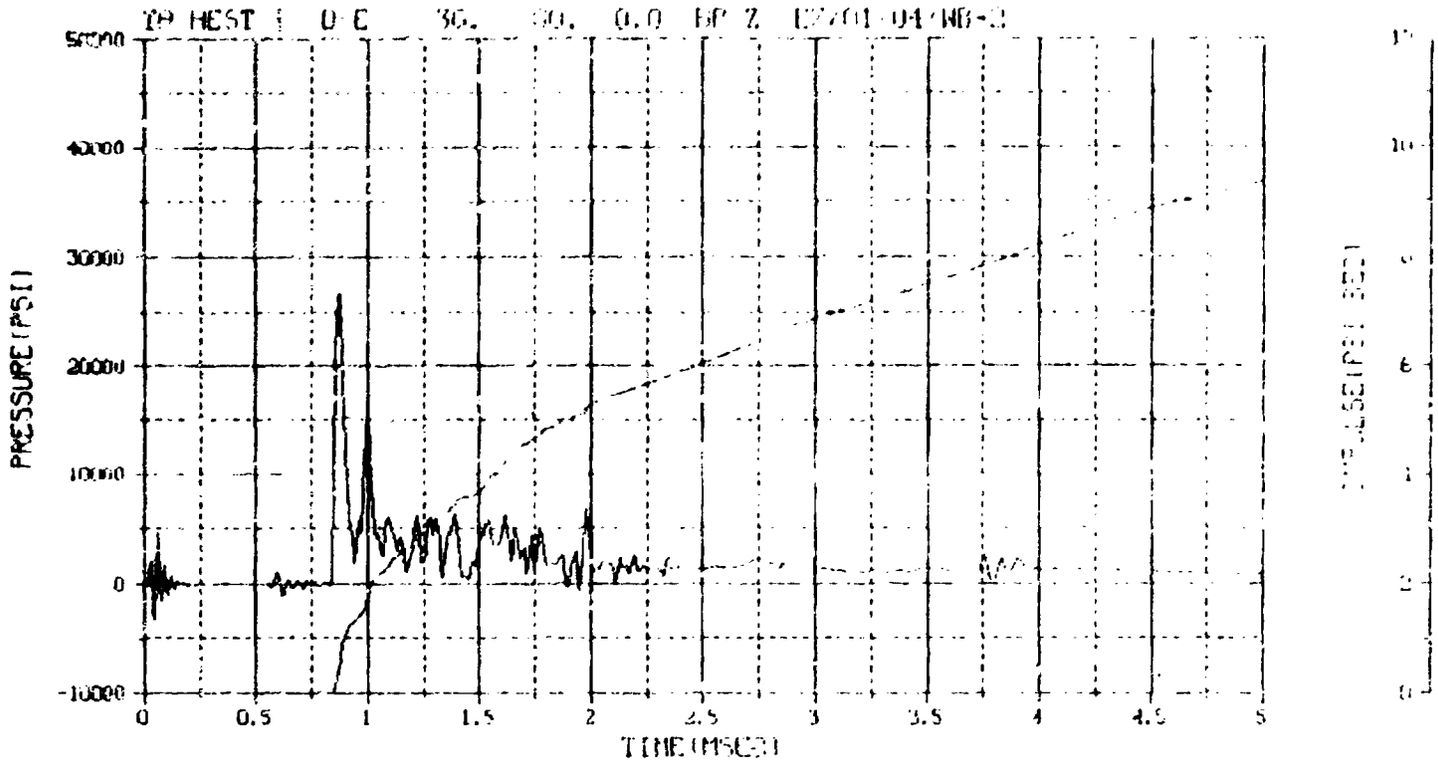
PRESSURE(PSI)
TIME(MSEC)
50000
40000
30000
20000
10000
0
-10000
0
0.5
1
1.5
2
2.5
3
3.5
4
4.5
5
M.N. = 2
TSKIP=10.350
S.R. =100.00 KHZ
2 40 PM, 6 MAR 78.
VSN-8054

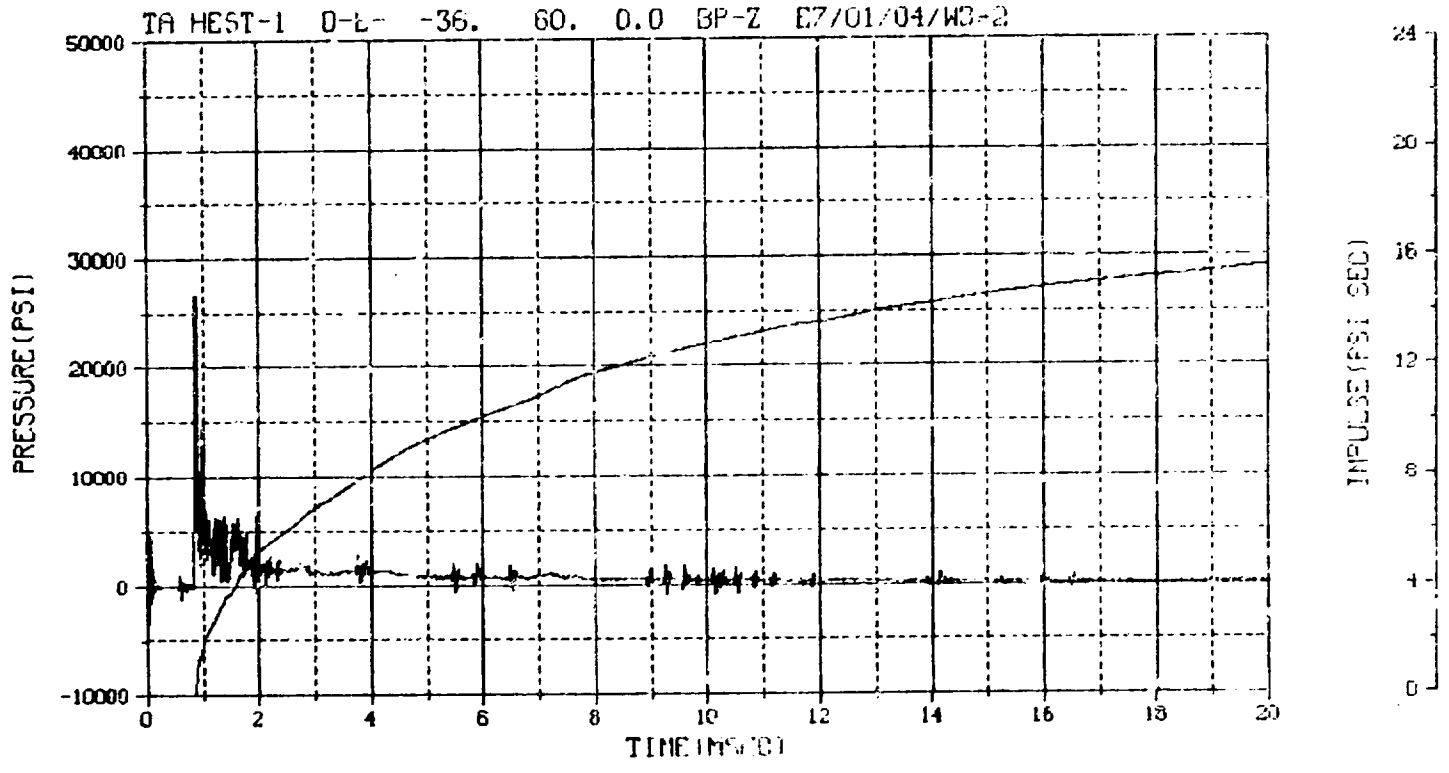

M.N. = 2	E.U. =0.000,25070.000	VSN=8054
TSKIP=10.350	DIGITS=0.000,1[illegible]5.000	TAPE22
S.R. =100.00 KHZ	2 40 PM, 6 MAR 78.	FILE=8

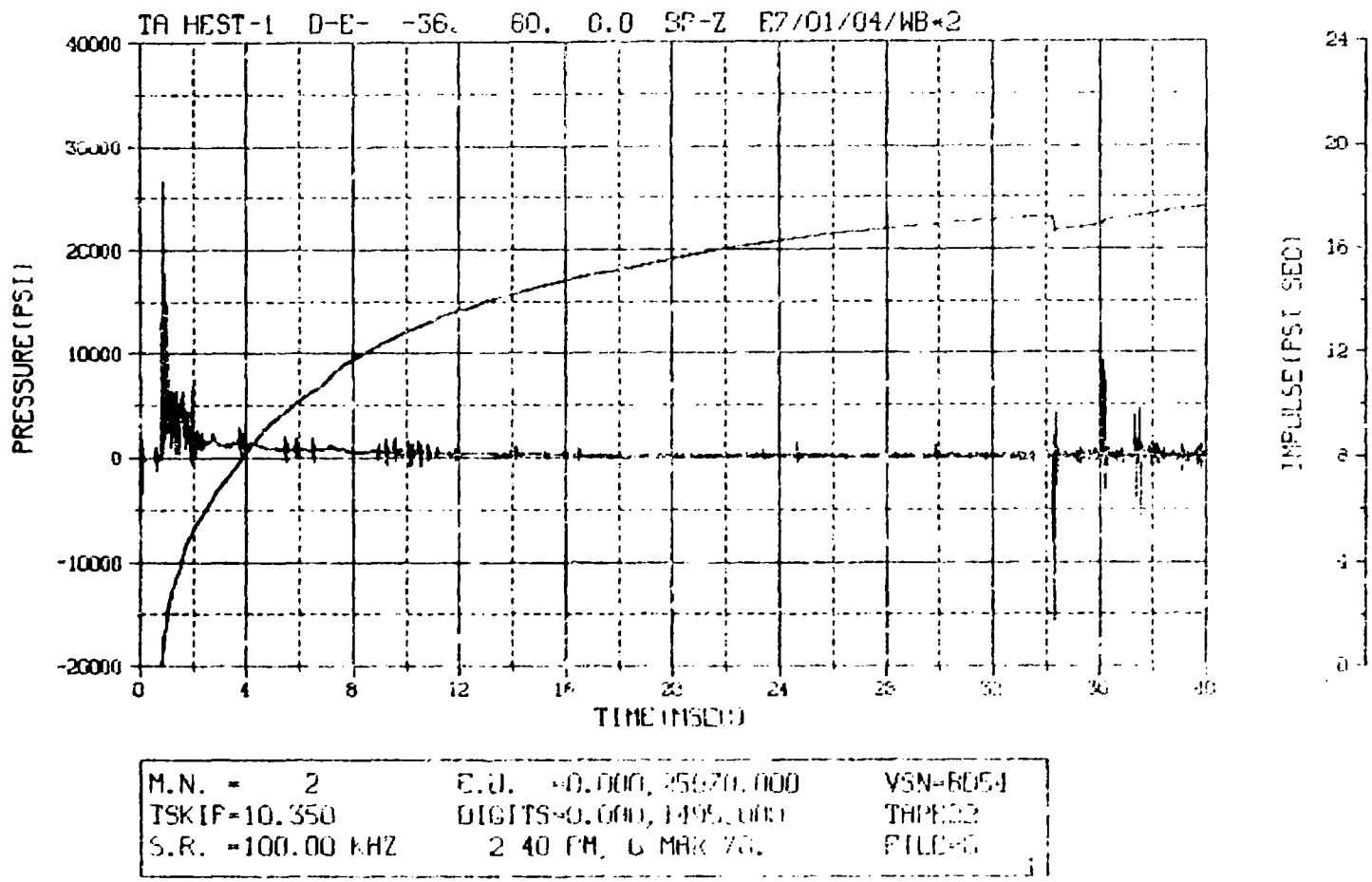
TA HEST-1 D-E- -36. 60. 0.0 SP-Z E7/01/04/WB*2
PRESSURE(PSI)
IMPULSE(PSI SEC)
TIME(MSEC)
M.N. = 2
TSKIP=10.350
S.R. =100.00 KHZ
E.U. =0.000, 25670.000
DIGITS=0.000, 1495.000
2 40 PM, 6 MAR 78.
VSN=BD54
TAPE22
FILE=6

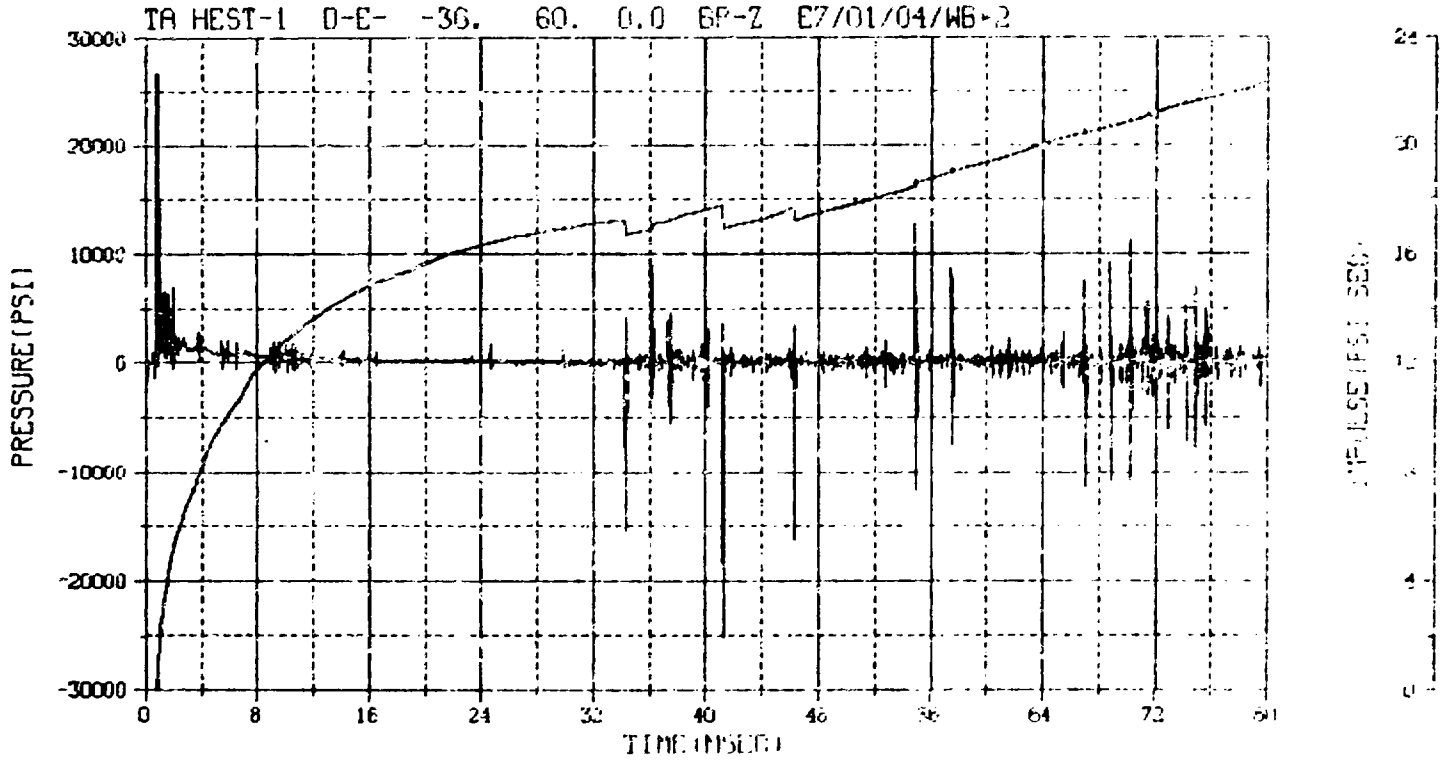

M.N. = 2	E.U. =0.000,25070.000	VSN=8054
TSKIP=10.350	DIGITS=0.000,1495.000	TAPE=2
S.R. =100.00 KHZ	2 40 PM, 6 MAR 78.	FILE=6

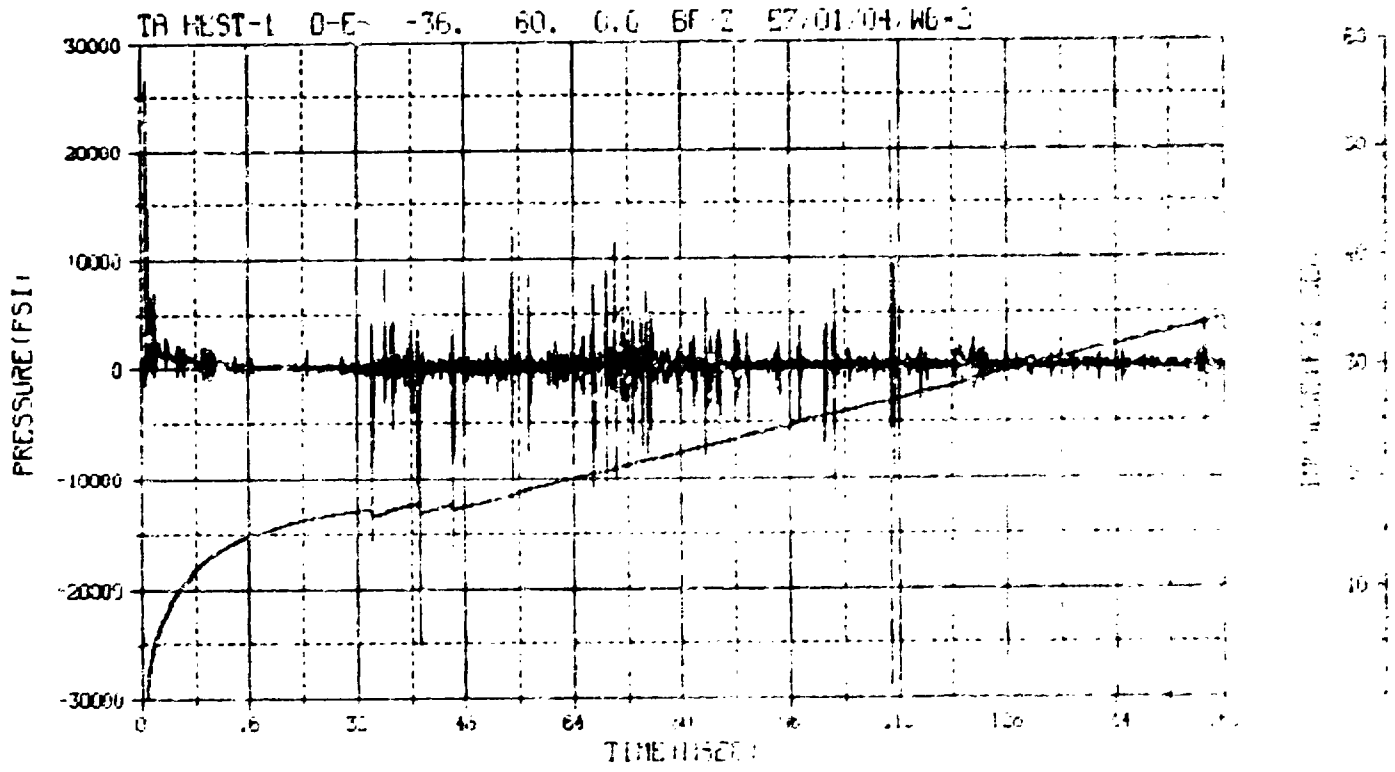
TA HEST-1 D-E- -36. 60. 0.0 BF 2 E7/01/04/WB-2
PRESSURE(PSI)
30000
20000
10000
0
-10000
-20000
-30000
0
.6
32
48
64
TIME(MSEC)
M.N. = 2
TSKIP=10.350
S.R. =100.00 KHZ
E.U. =0.000..5070.000
DIGITS=0.000.1495.000
6 13 FM, 3 MAR
VSN-E054
TAPE22
FILE-6

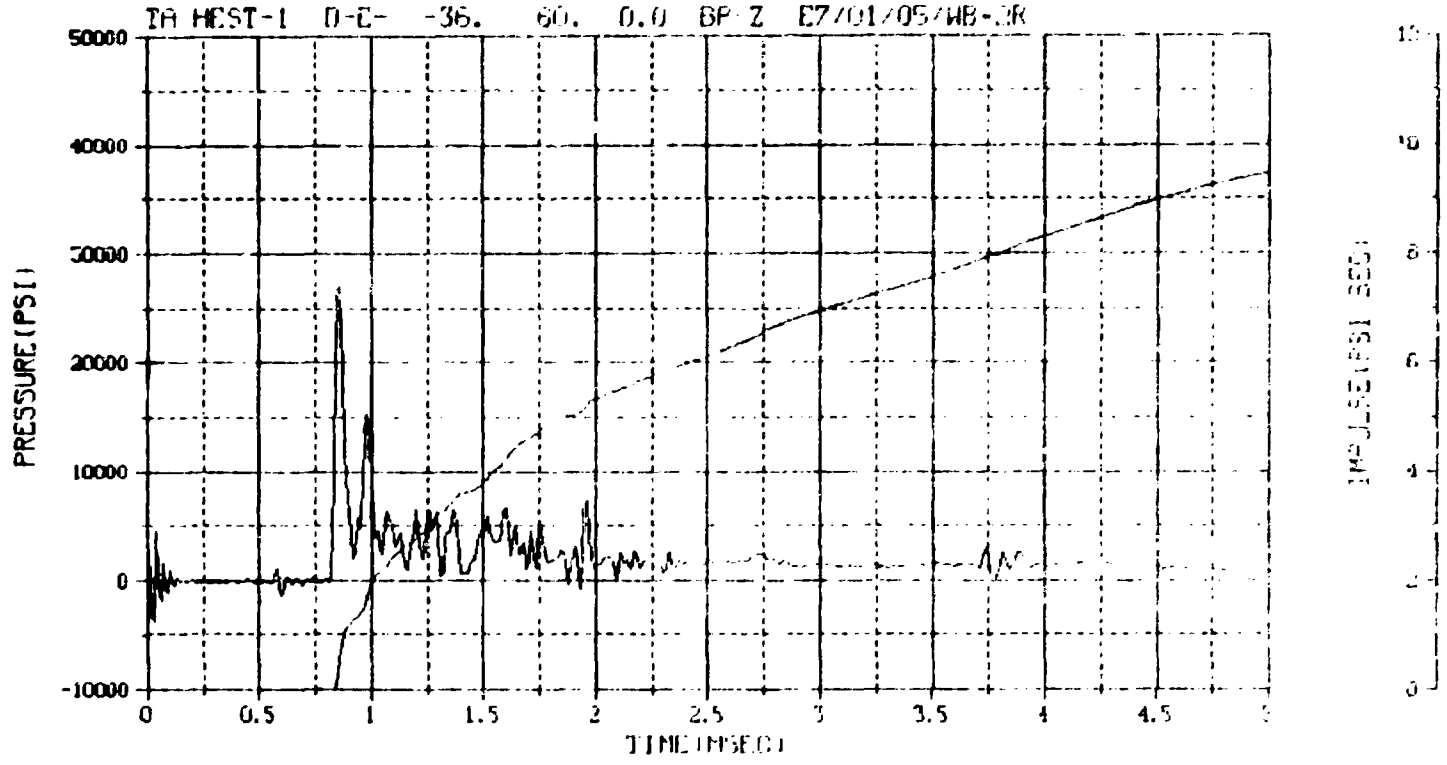
TR HEST-1 D-E- -36. 60. 0.0 BP Z E7/01/05/HB-.3R
50000
40000
30000
20000
10000
0
-10000
PRESSURE(PSI)
0
0.5
1
1.5
2
2.5
3
3.5
4
4.5
TIME(MSEC)
M.N. = 2
TSKIP=10.350
S.R. =100.00 KHZ
E.U. -0.000, 250/0.000
DIGITS=0.000, 1.201.500
2 40 PM, 6 MAR 78.
VSN-6054
TAPE22
FILE=10

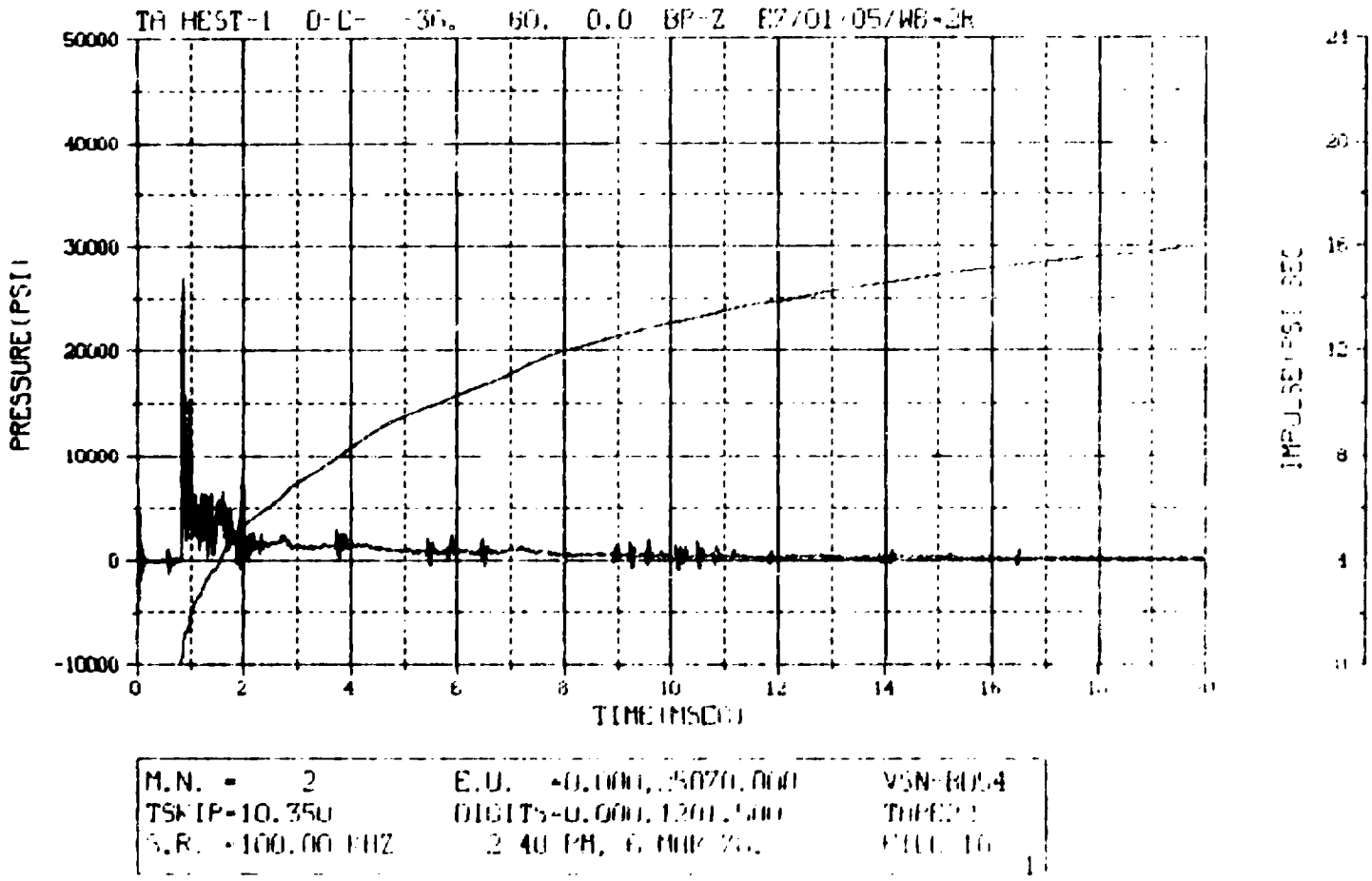
TA HEST-1 D-C- -36. 60. 0.0 BP-Z E7/01/05/WB-2R
PRESSURE(PSI)
50000
40000
30000
20000
10000
0
-10000
0
2
4
6
8
10
12
14
16
TIME(MSEC)
IMPULSE(PSI SEC)
M.N. = 2
TSKIP=10.350
S.R. =100.00 KHZ
E.U. =0.000,25070.000
DIGITS=0.000,1201.500
2 40 PM, 6 MAR 76.
VSN=BD54
TAPE
FILE 16

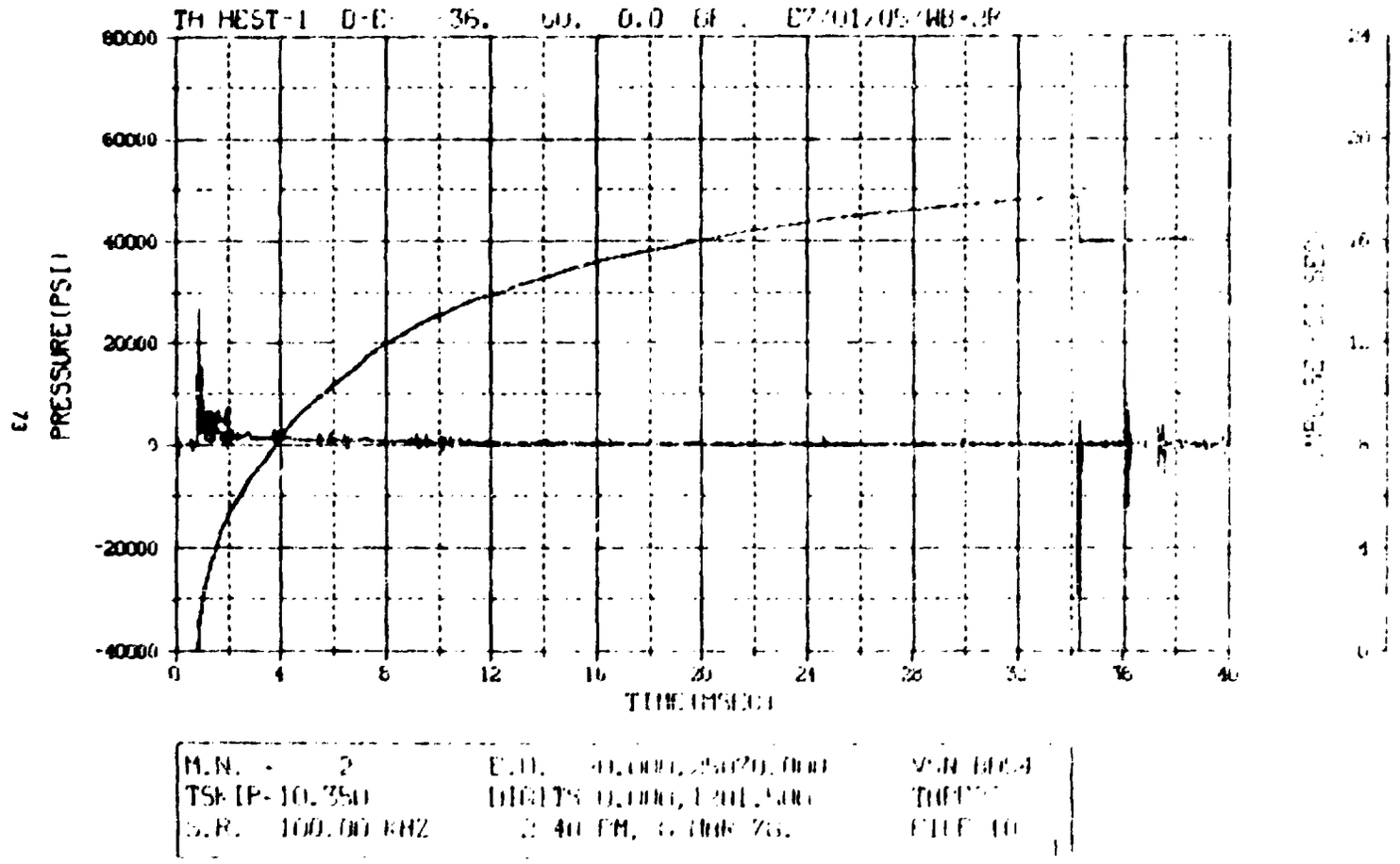
TH HEST-1 D-E 36. 60. 0.0 BF
PRESSURE(PSI)
80000
60000
40000
20000
0
-20000
-40000
0
4
8
12
16
20
24
28
32
36
40
TIME(MSEC)
M.N. - 2
TSKIP-10.350
S.R. 100.00 KHZ
DIGITS 0.000, 1201.500
2 40 PM, 6 MAR 78.

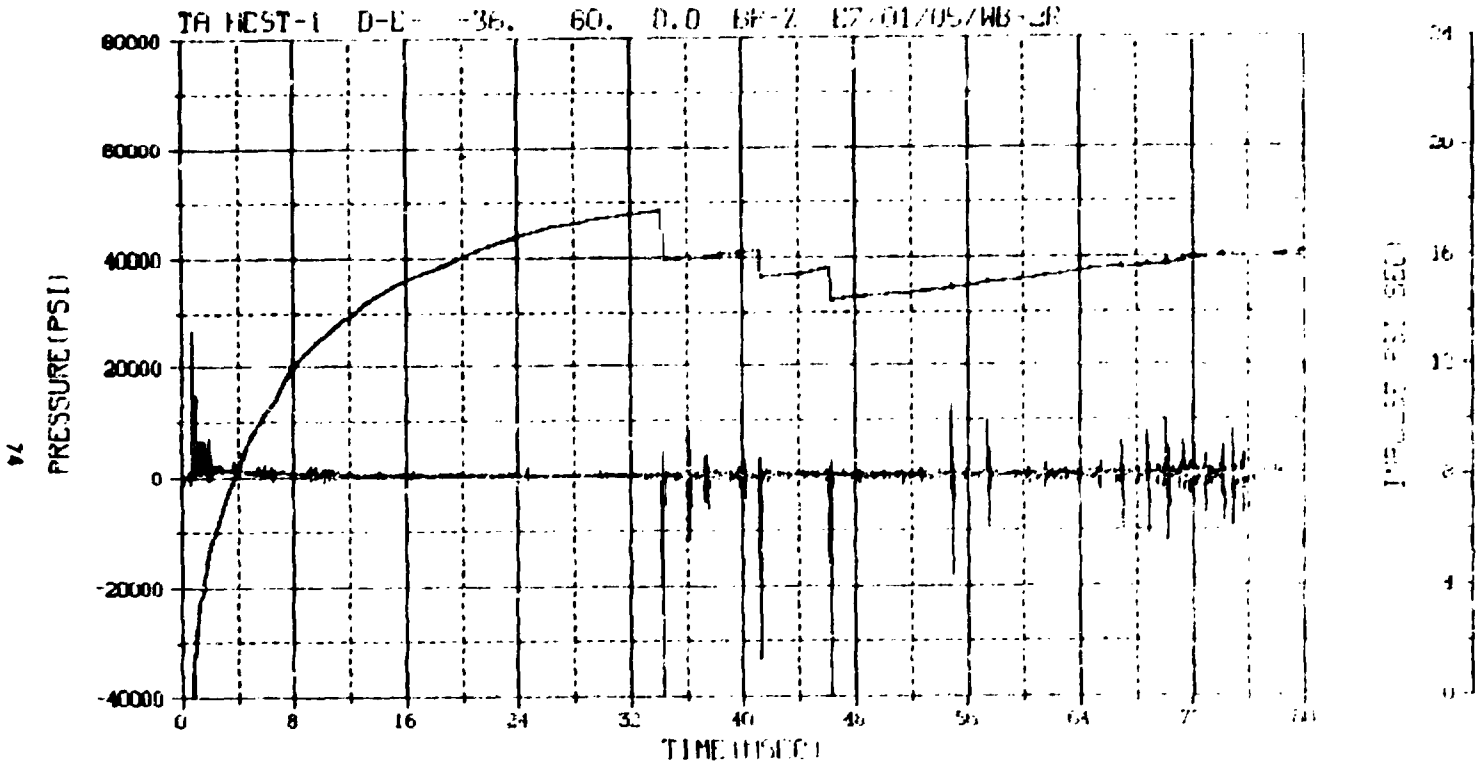

M.N. = 2	E.U. =0.000,[illegible]	VSN=[illegible]
TSKIP=10.350	DIGITS=0.000,[illegible]	[illegible]
S.R. =100.00 KHZ	2 40 PM, 6 MAR [illegible]	FILE=[illegible]

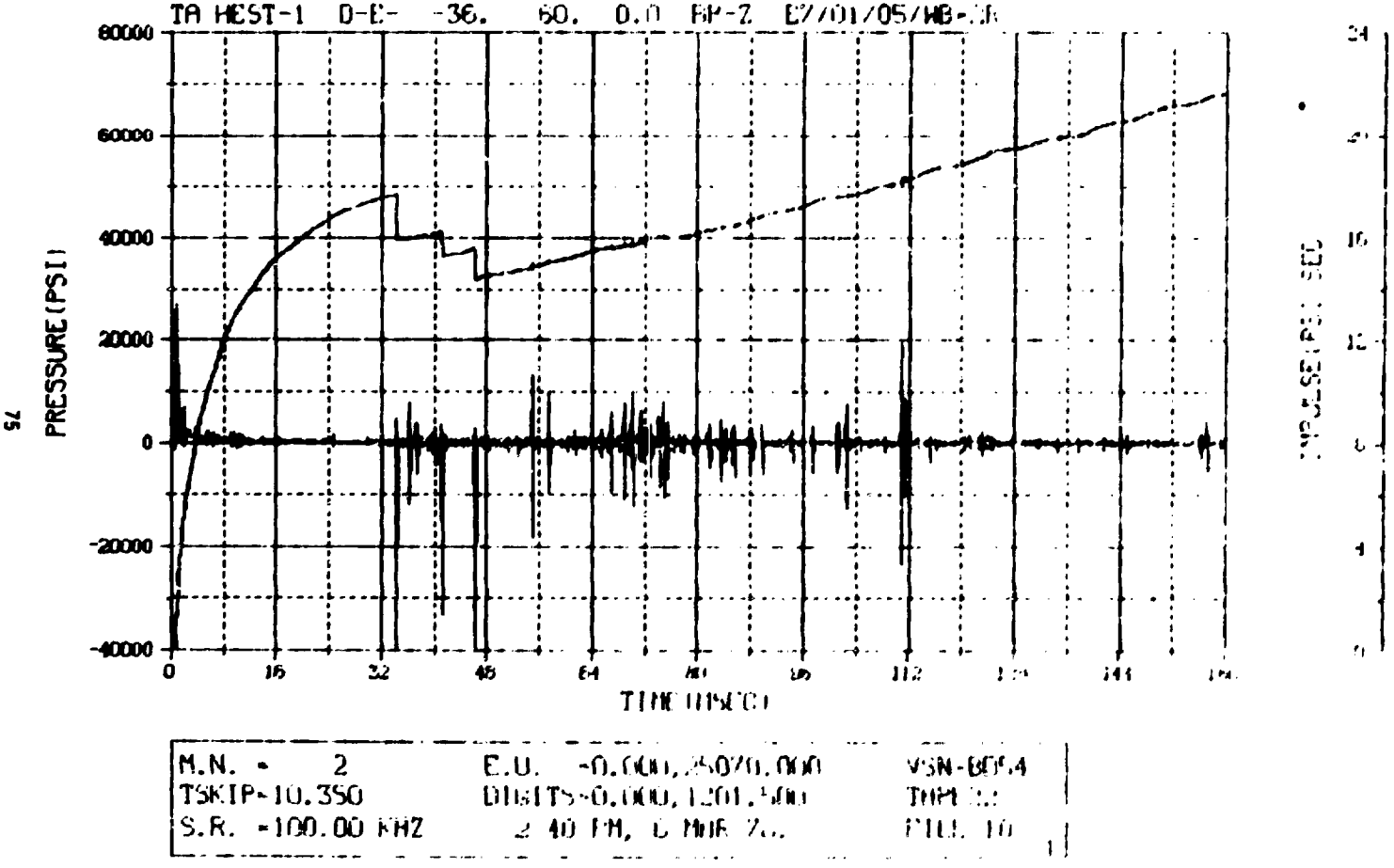
TA HEST-1 D-E- -36. 60. 0.0 BP-2
80000
60000
40000
20000
0
-20000
-40000
PRESSURE(PSI)
0
16
32
48
64
80
96
112
128
144
160
TIME(MSEC)
24
20
16
12
8
4
0
M.N. = 2
TSKIP=10.350
S.R. =100.00 KHZ

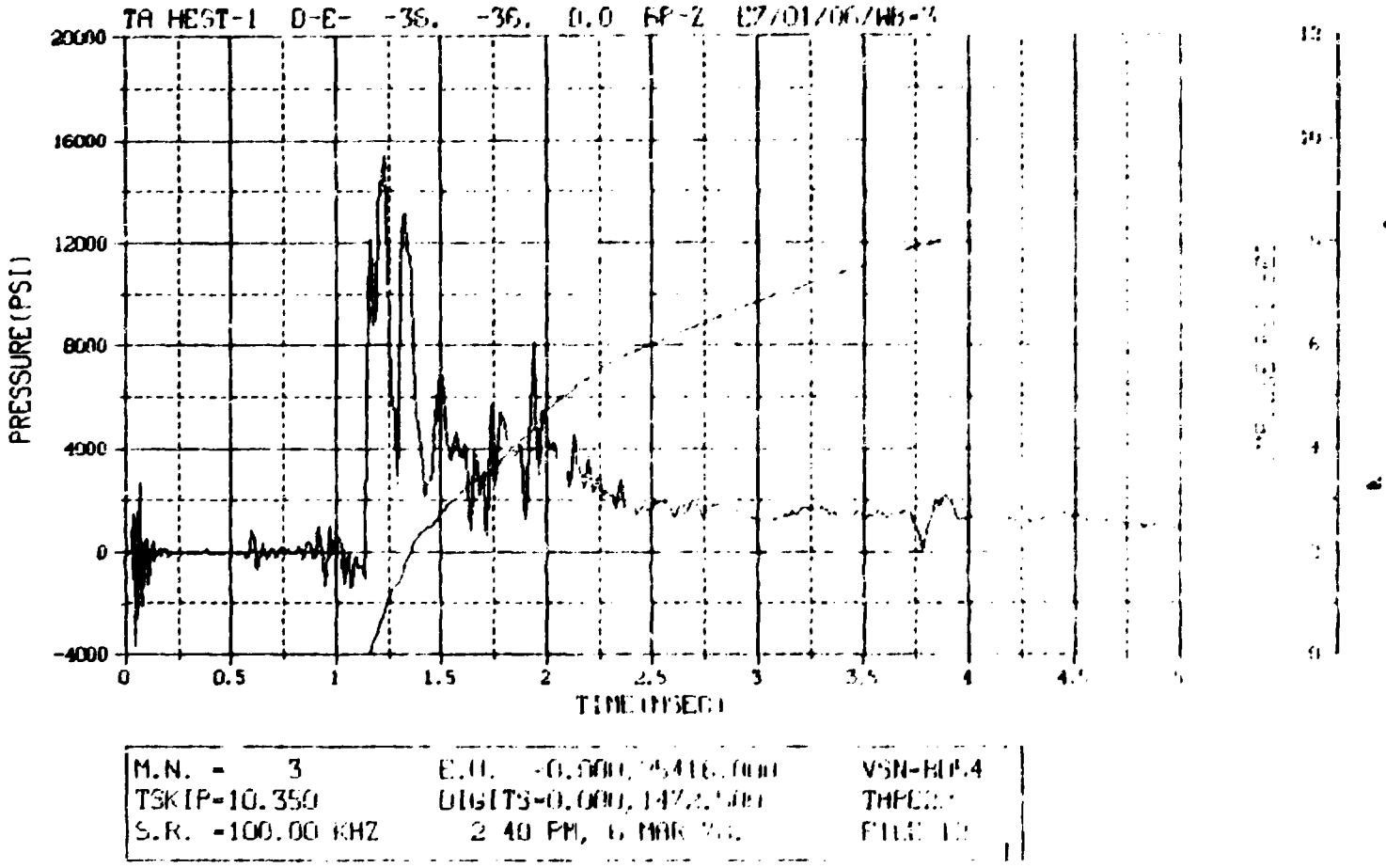
TA HEST-1 D-E- -36. -36. 0.0 RP-Z
20000
16000
12000
8000
4000
0
-4000
PRESSURE(PSI)
0
0.5
1
1.5
2
2.5
3
3.5
4
TIME(MSEC)
M.N. = 3
TSKIP=10.350
S.R. =100.00 KHZ

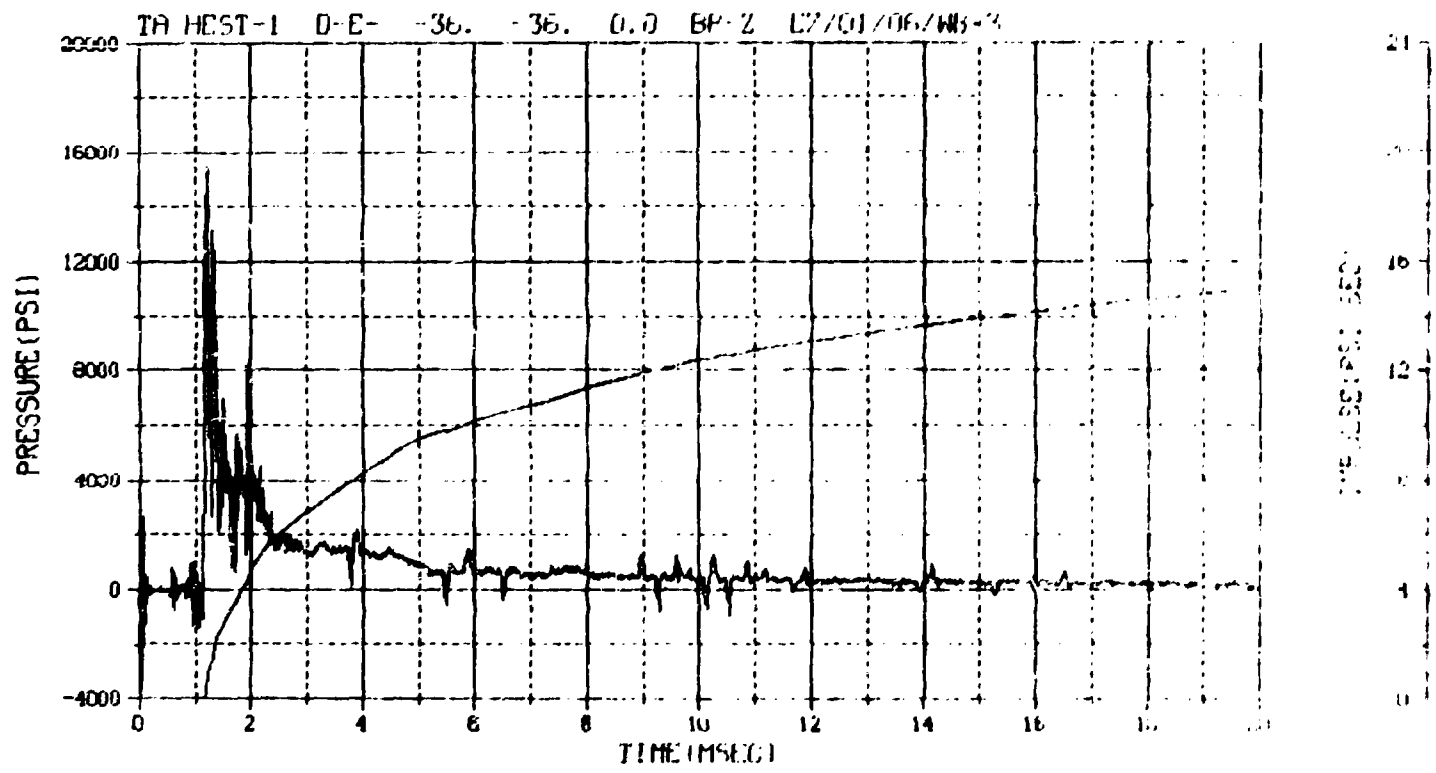

M.N. = 3	E.U. =0.000,25416.000	VSN-BD54
TSKIP=10.350	DIGITS=0.000,1472.500	TAPE22
S.R. =100.00 KHZ	2 40 PM, 6 MAR 78.	FILE 12

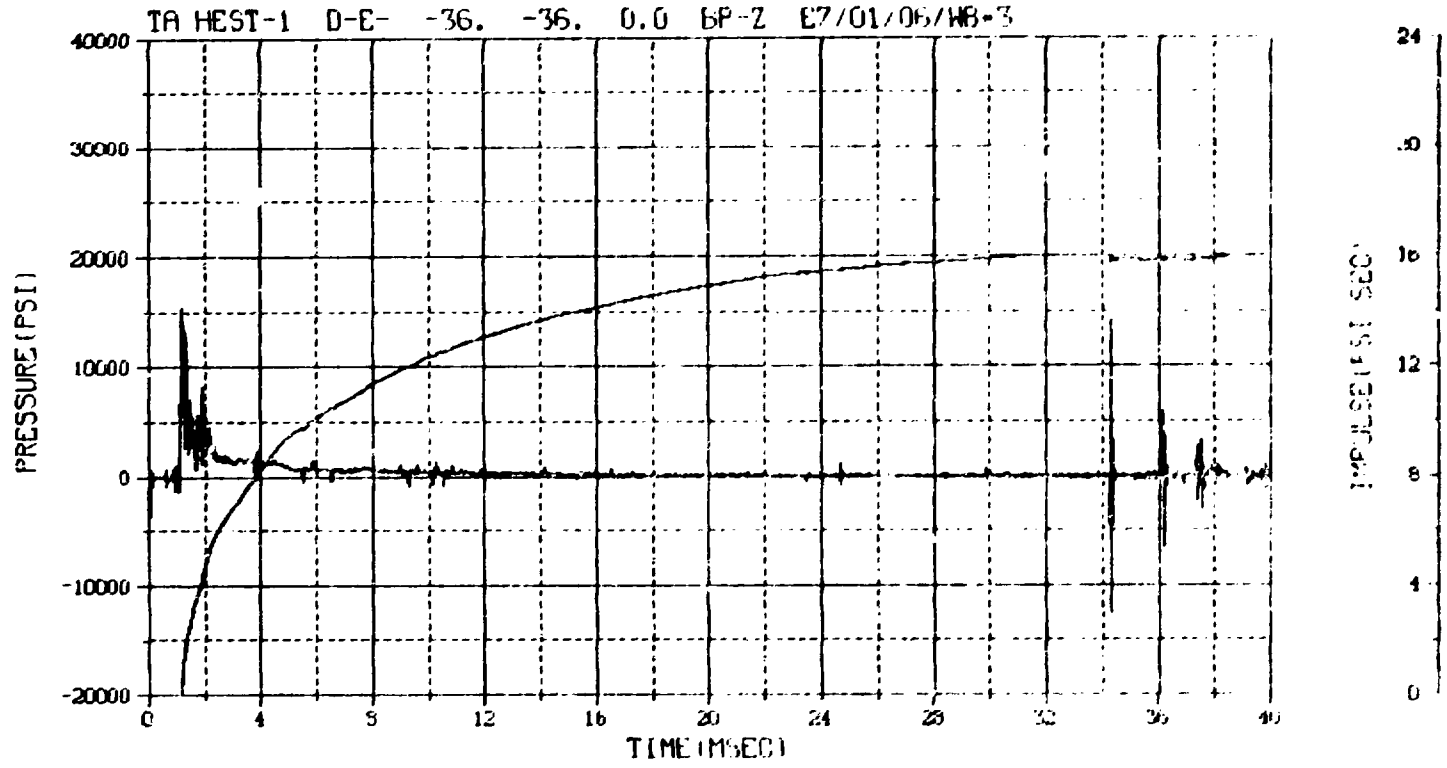

M.N. = 3	E.U. =0.000,25416.000	VSN=0004
TSKIP=10.350	DIGITS=0.000,1472.500	TAPE22
S.R. =100.00 KHZ	2 40 PM, 6 MAR 76.	FILE=12

1

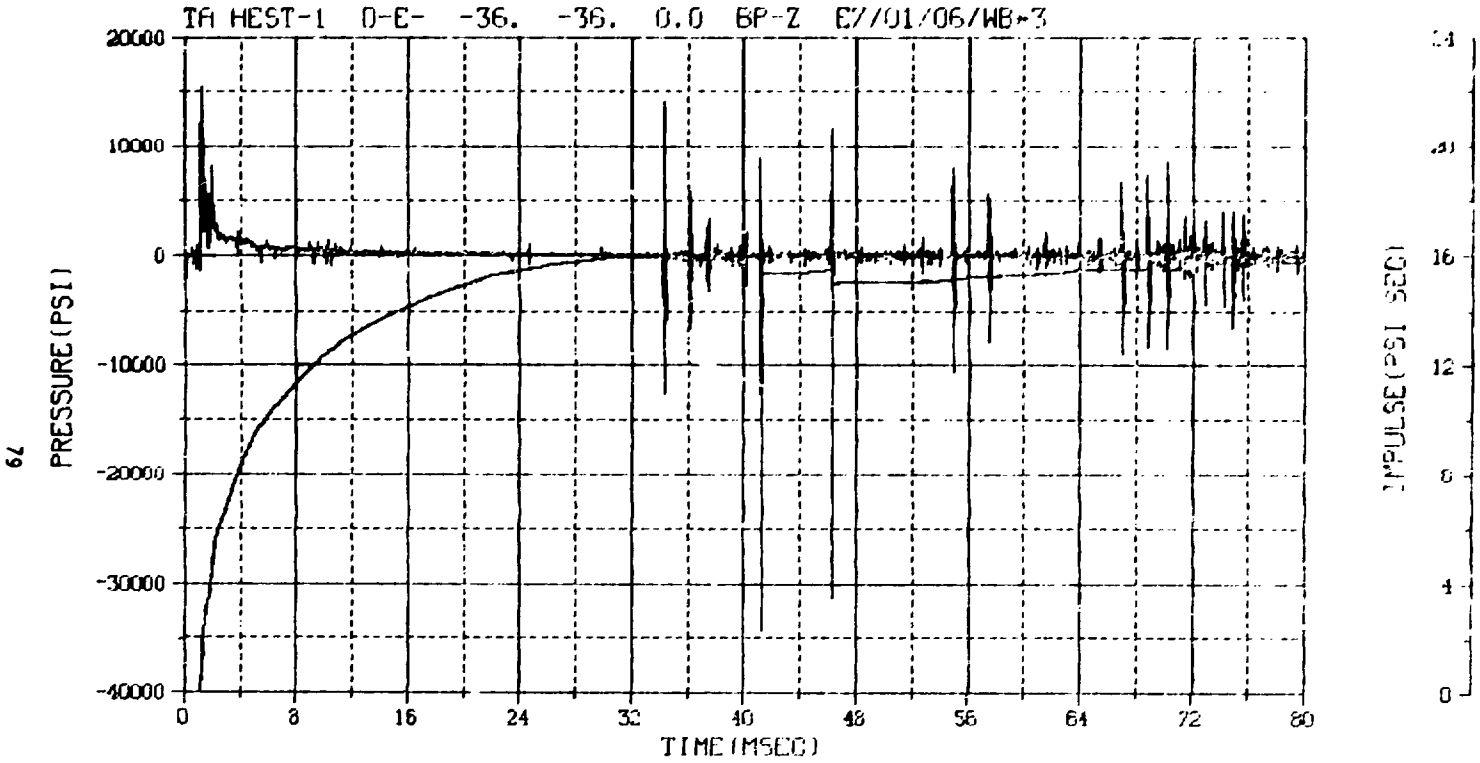

M.N. = 3	E.U. =0.000,25416.000	VSN=6054
TSKIP=10.350	DIGITS=0.000,1472.500	TAPE22
S.R. =100.00 KHZ	2 40 PM, 6 MAR 78.	FILE=12

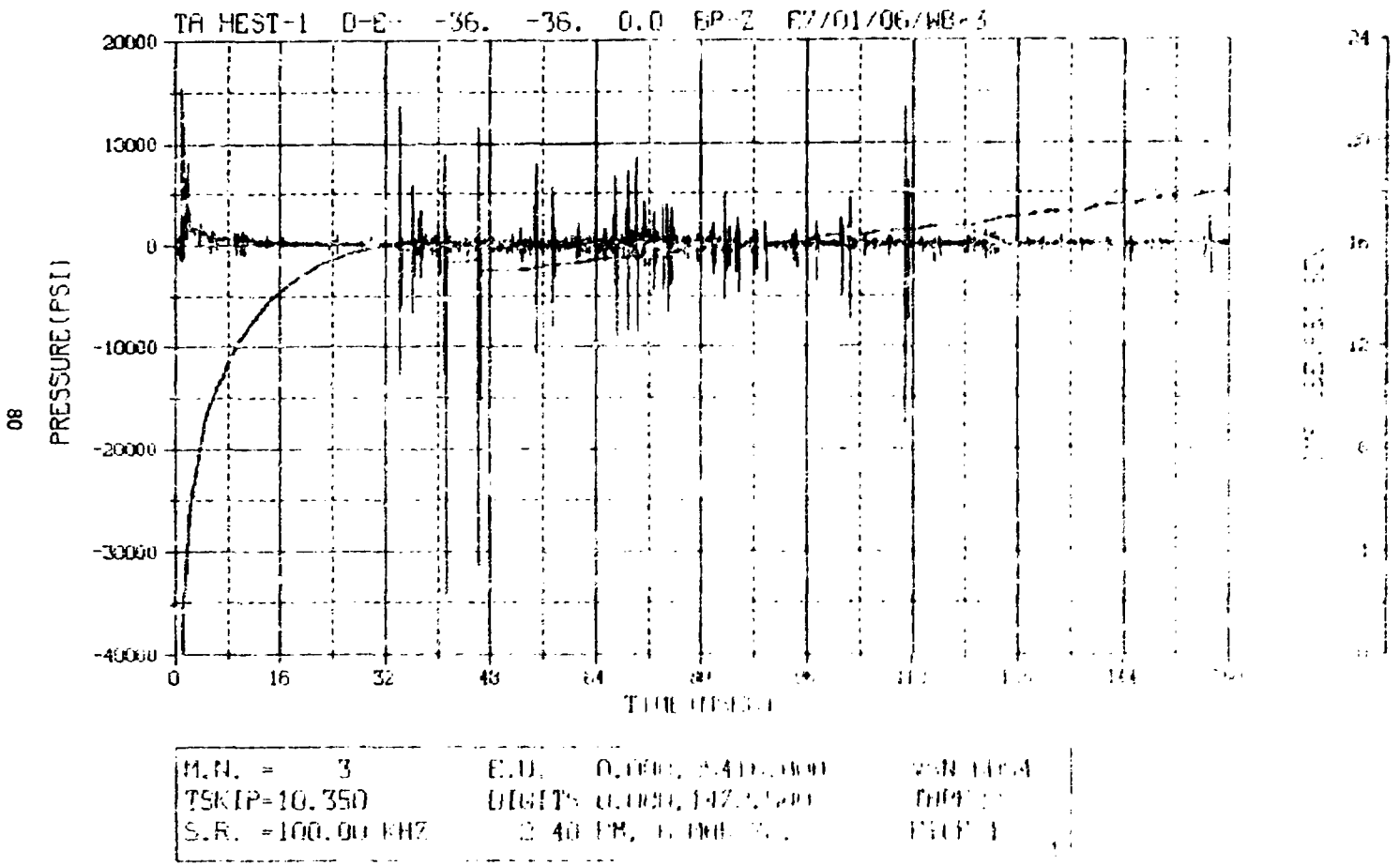
TA HEST-1 D-E -36. -36. 0.0 BP-Z FY/01/06/WB-3
20000
10000
0
-10000
-20000
-30000
-40000
PRESSURE(PSI)
0
16
32
48
64
M.N. = 3
TSKIP=10.350
S.R. =100.00 KHZ

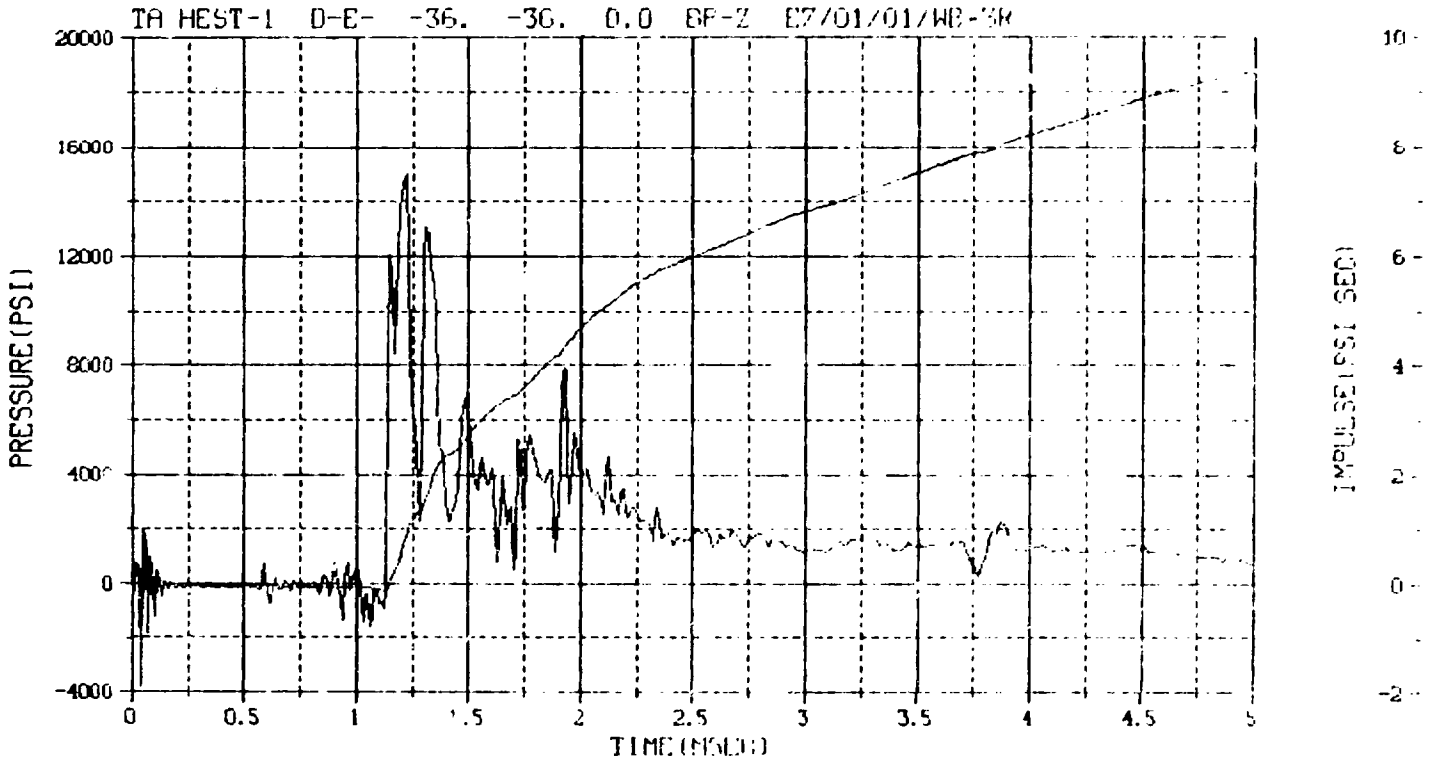
TA HEST-1 D-E- -36. -36. 0.0 BF-Z E7/01/01/WB-3R
PRESSURE(PSI)
IMPULSE(PSI SEC)
TIME(MSEC)
20000
16000
12000
8000
4000
0
-4000
10
8
6
4
2
0
-2
0
0.5
1
1.5
2
2.5
3
3.5
4
4.5
5
M.N. = 3
TSKIP=10.350
S.R. =100.00 KHZ
VSN-6054

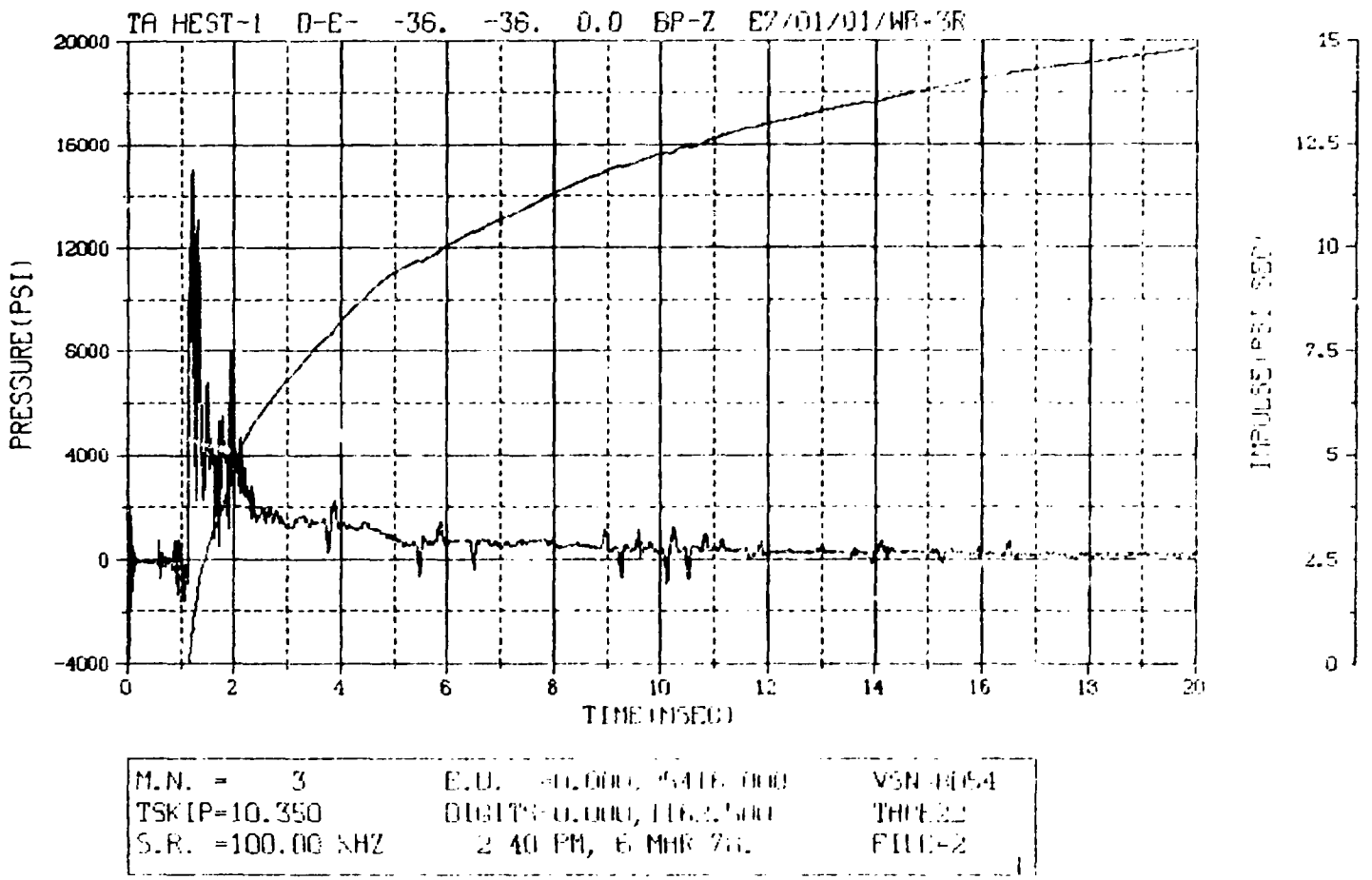
TA HEST-1 D-E- -36. -36. 0.0 BP-Z E7/01/01/WB-3R
PRESSURE(PSI)
20000
16000
12000
8000
4000
0
-4000
0
2
4
6
8
10
12
14
16
18
20
TIME(MSEC)
15
12.5
10
7.5
5
2.5
0
M.N. = 3
TSKIP=10.350
S.R. =100.00 KHZ
E.U.
DIGITS
2 40 PM, 6 MAR 78.
VSN
TAPE
FILE=2

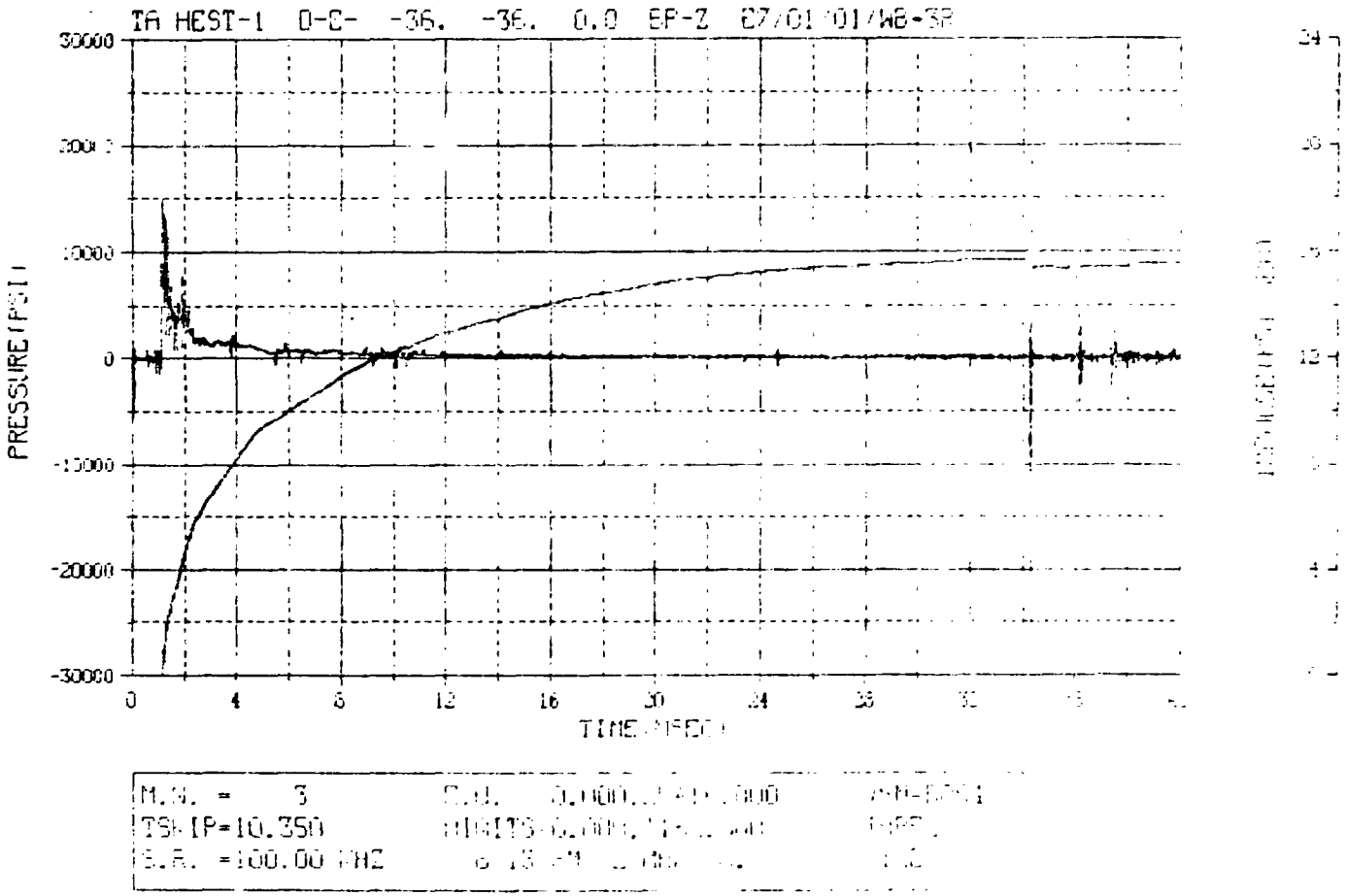
IA HEST-1 0-C- -36. -36. 0.0 EP-Z 87/01/01/WB-SP
30000
20000
10000
0
-10000
-20000
-30000
PRESSURE(PSI)
0
4
8
12
16
20
24
28
32
36
40
TIME(MSEC)
M.N. = 3
TSHIP=10.350
S.R. =100.00 KHZ

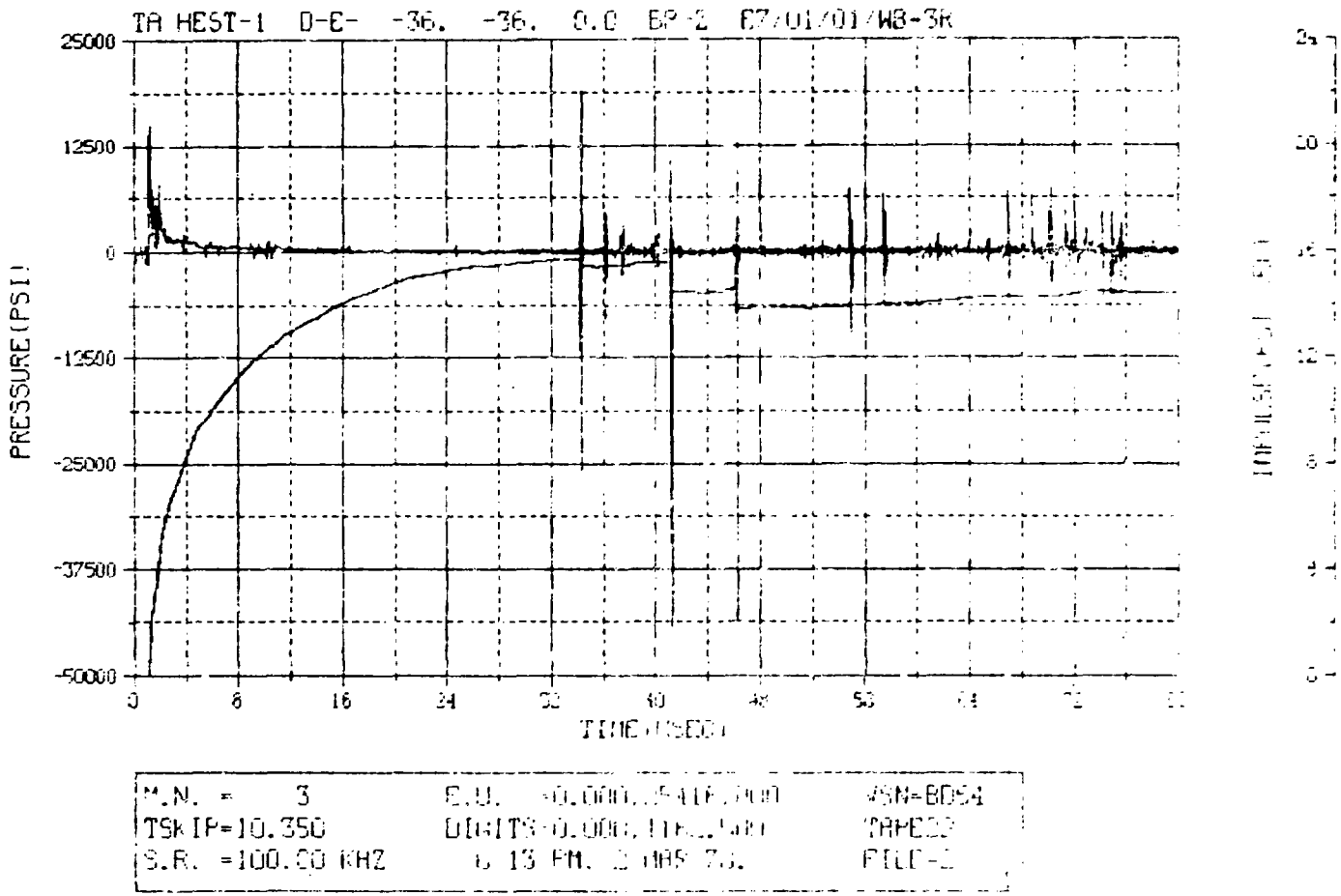
TA HEST-1 D-E- -36. -36. 0.0 BP-2 E7/01/01/WB-3R
PRESSURE(PSI)
25000
12500
0
-12500
-25000
-37500
-50000
0
8
16
24
32
40
48
56
64
72
80
TIME(MSEC)
M.N. = 3
TSKIP=10.350
S.R. =100.00 KHZ
E.U.
DIGITS
6 13 PM. 2 MAR 78.
VSN=BD54
TAPE
FILE

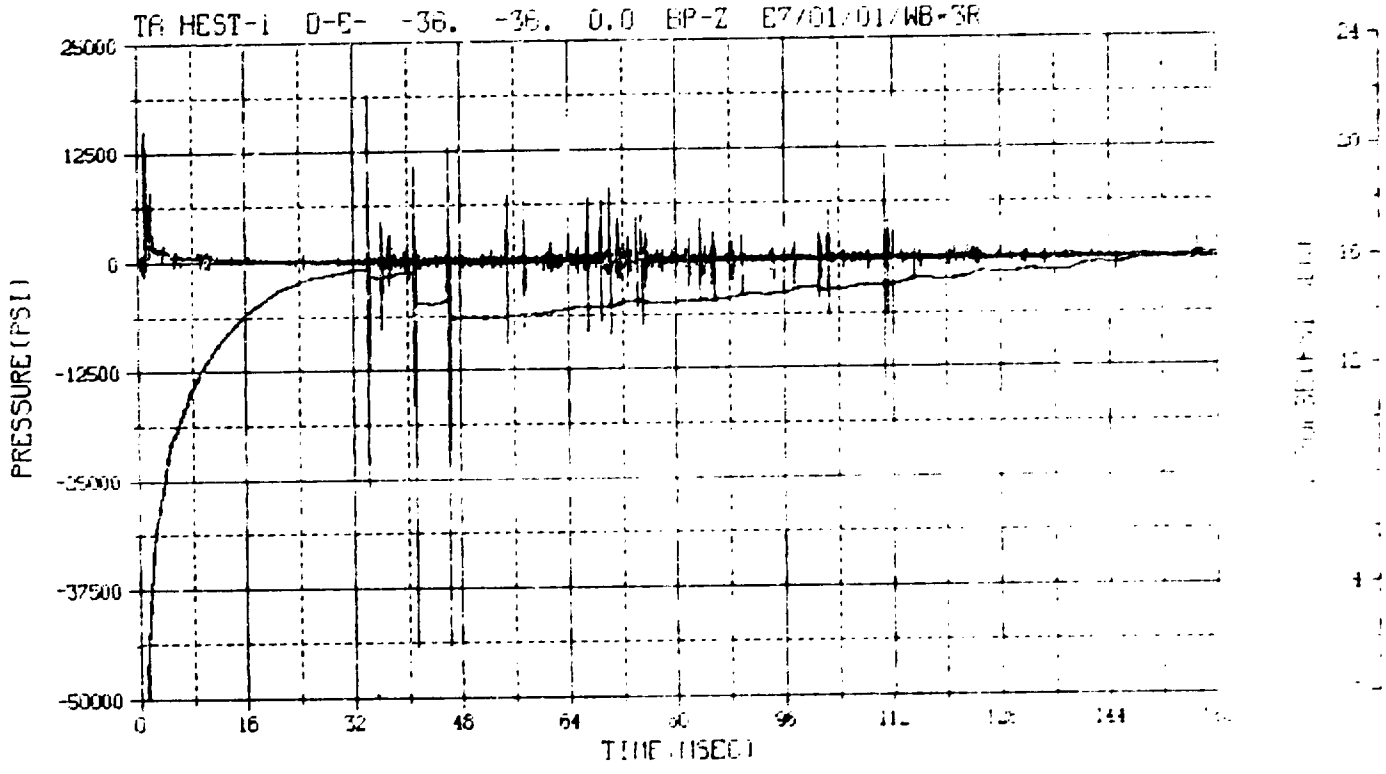
TR HEST-1 0-E- -36. -36. 0.0 BP-Z E7/01/01/WB-3R
25000
12500
0
-12500
-25000
-37500
-50000
PRESSURE (PSI)
0
16
32
48
64
80
96
112
128
144
TIME (MSEC)
24
20
16
12
8
4
M.N. = 3
TSKIP=10.350
S.R. =100.00 KHZ
6 13 PM,

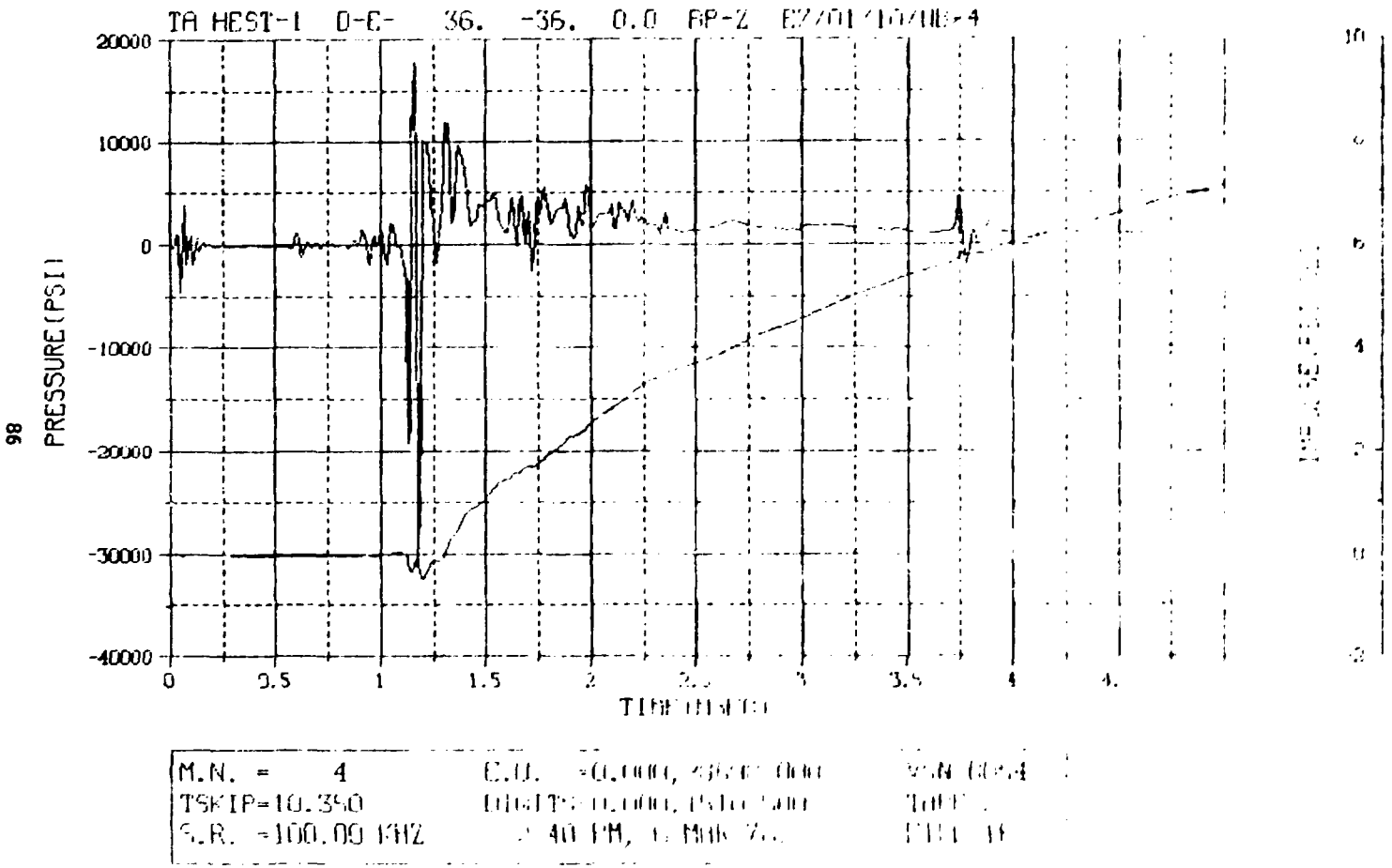
TA HEST-1 0-E- 36. -36. 0.0 BP-Z
20000
10000
0
-10000
-20000
-30000
-40000
PRESSURE(PSI)
0
0.5
1
1.5
2
3
3.5
4
4.
M.N. = 4
TSKIP=10.350
S.R. =100.00 KHZ

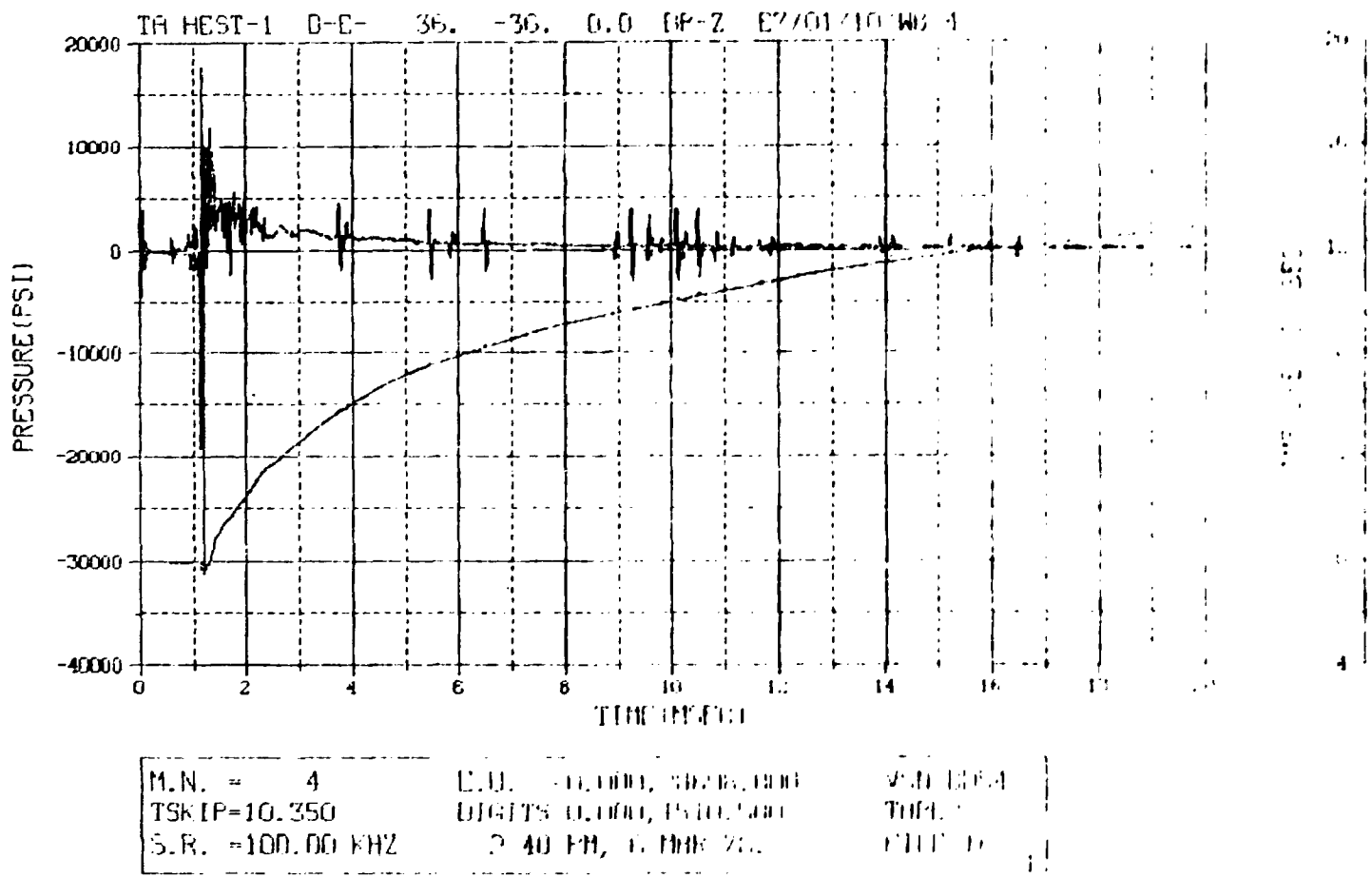
TA HEST-1 B-E- 36. -36. 0.0 BP-Z
20000
10000
0
-10000
-20000
-30000
-40000
PRESSURE(PSI)
0
2
4
6
8
10
12
14
16
M.N. = 4
TSKIP=10.350
S.R. =100.00 KHZ

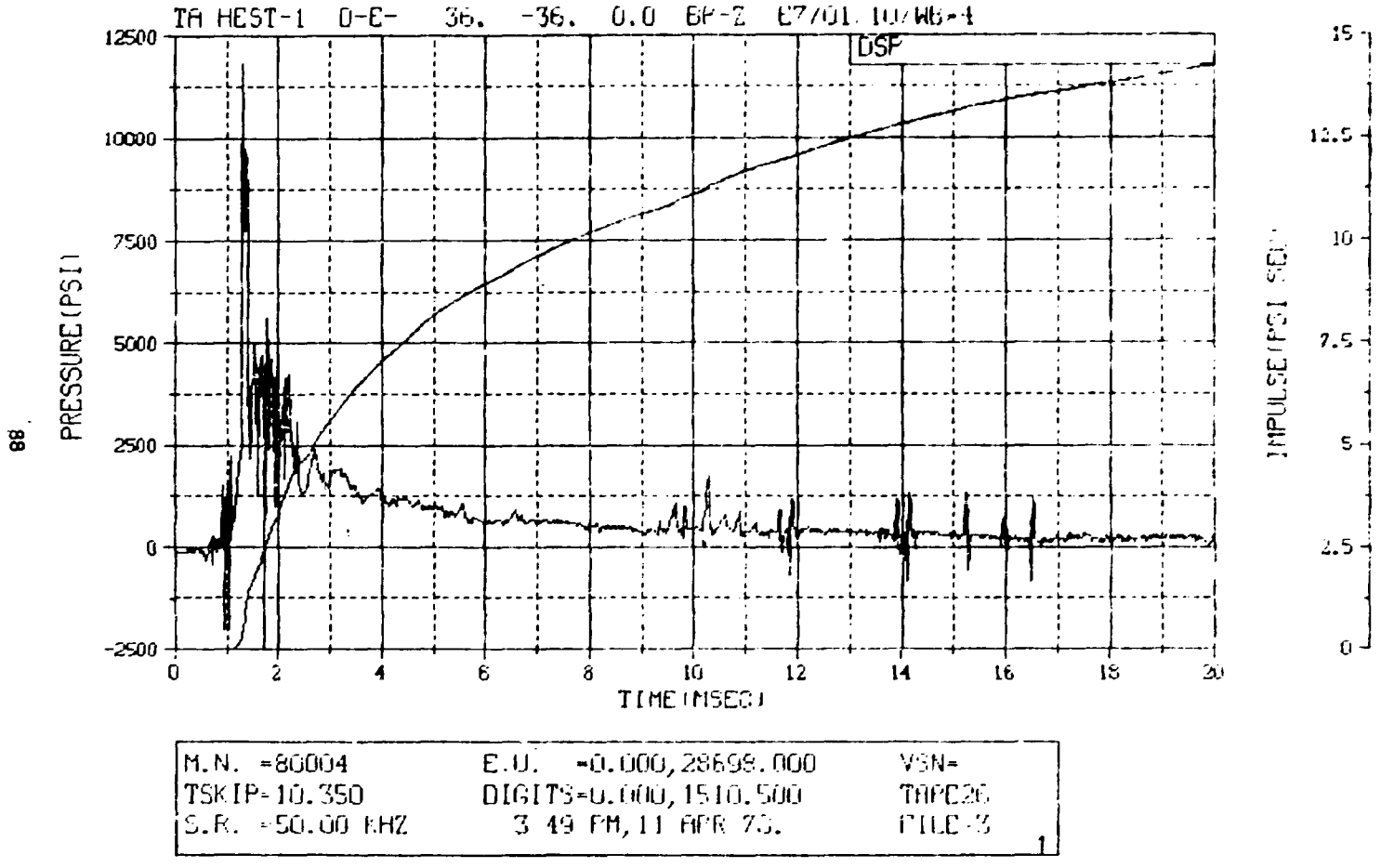
TA HEST-1 0-E- 36. -36. 0.0 BP-2 E7701 10/WB-4
DSF
PRESSURE(PSI)
IMPULSE(PSI SEC)
TIME(MSEC)
12500
10000
7500
5000
2500
0
-2500
0
2
4
6
8
10
12
14
16
18
20
15
12.5
10
7.5
5
2.5
0
M.N. =80004
E.U. =0.000,28698.000
VSN=
TSKIP=10.350
DIGITS=0.000,1510.500
TAPE26
S.R. =50.00 KHZ
3 49 PM, 11 APR 73.
FILE=3
1

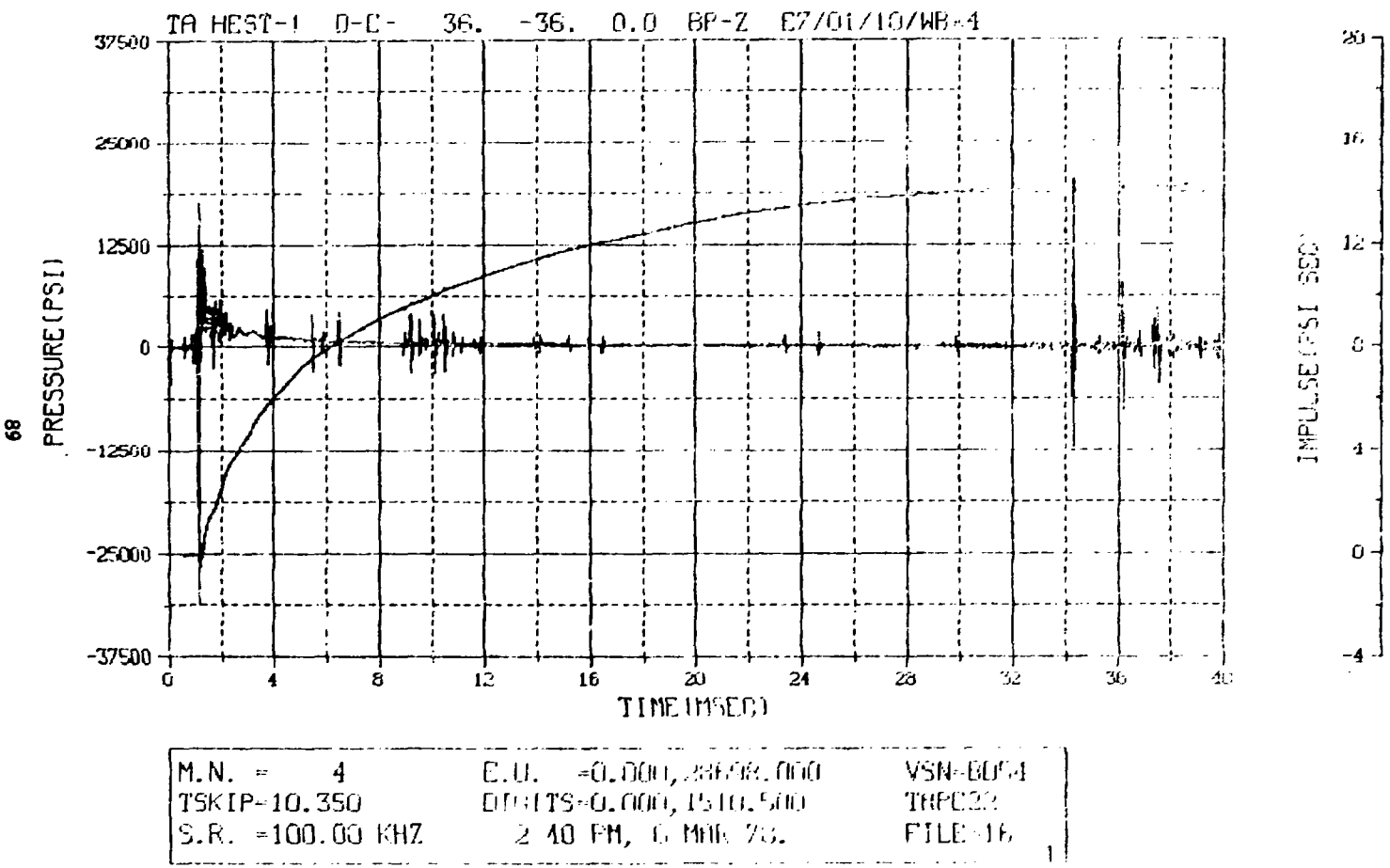
TA HEST-1 D-C- 36. -36. 0.0 BP-Z E7/01/10/WB=4
PRESSURE(PSI)
37500
25000
12500
0
-12500
-25000
-37500
0
4
8
12
16
20
24
28
32
36
40
TIME(MSEC)
IMPULSE(PSI SEC)
20
16
12
8
4
0
-4
M.N. = 4
TSKIP=10.350
S.R. =100.00 KHZ
E.U. =0.000,
DIGITS=0.000,
2 40 PM, 6 MAR 78.
VSN=BD54
TAPE22
FILE=16

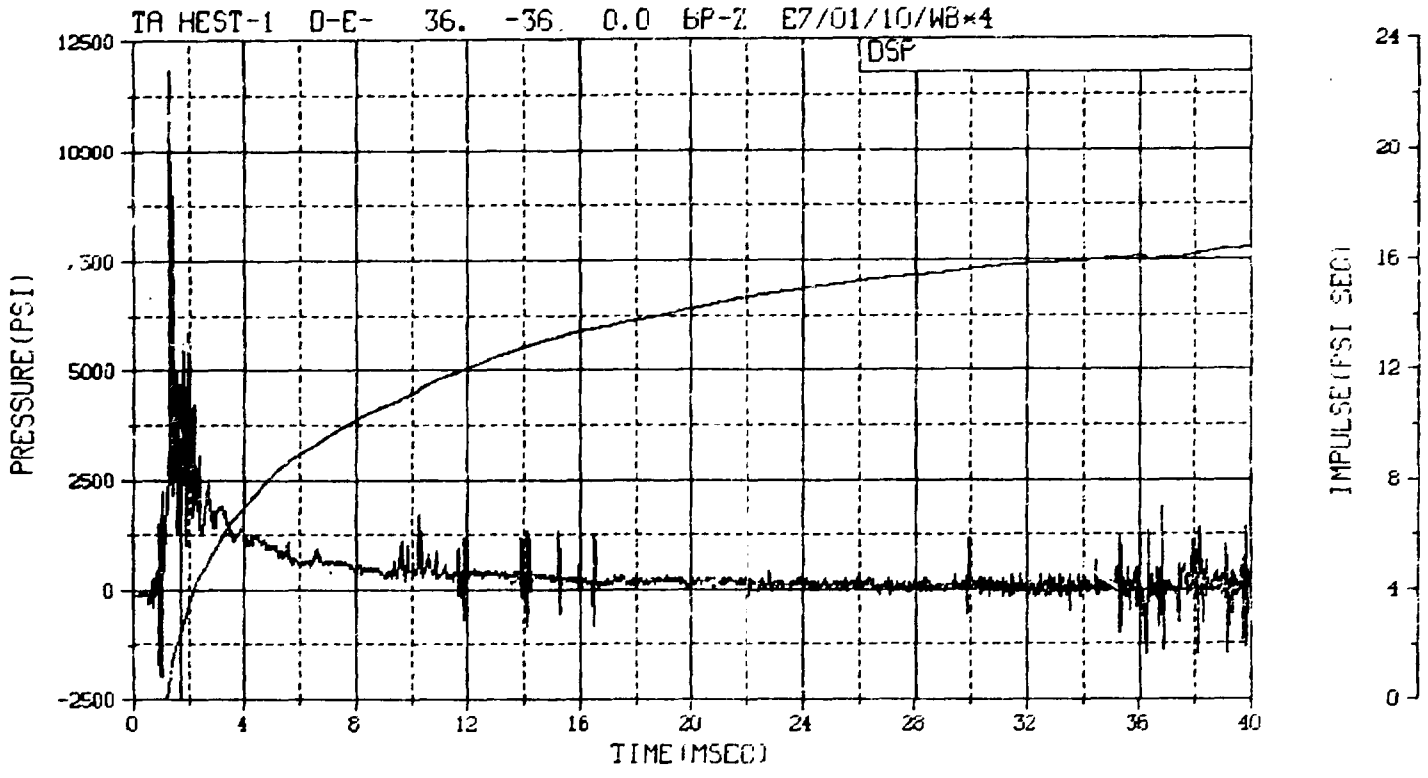

M.N. =80004	E.U. =0.000,28698.000	VSN=
TSKIP=10.350	DIGITS=0.000,1510.500	TAPE26
S.R. =50.00 KHZ	3 49 PM,11 APR 78.	FILE=3

1

06

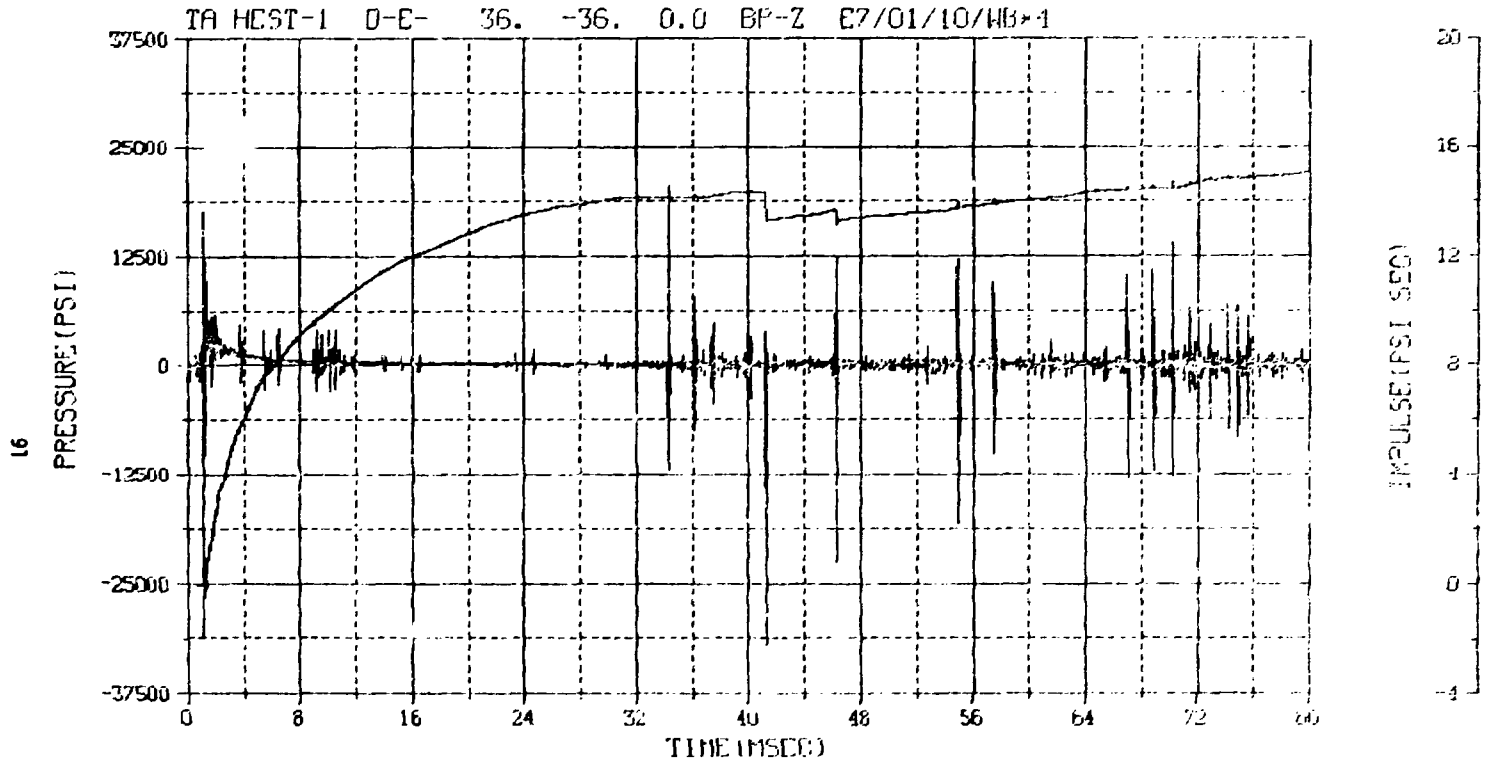

M.N. = 4	F.U. -0.000, 38608.000	VSN-6054
TSKIP=10.350	DIGITS-0.000, 15101.500	TAPE22
S.R. =100.00 KHZ	2:40 PM, 6 MAR 78.	FILE 16

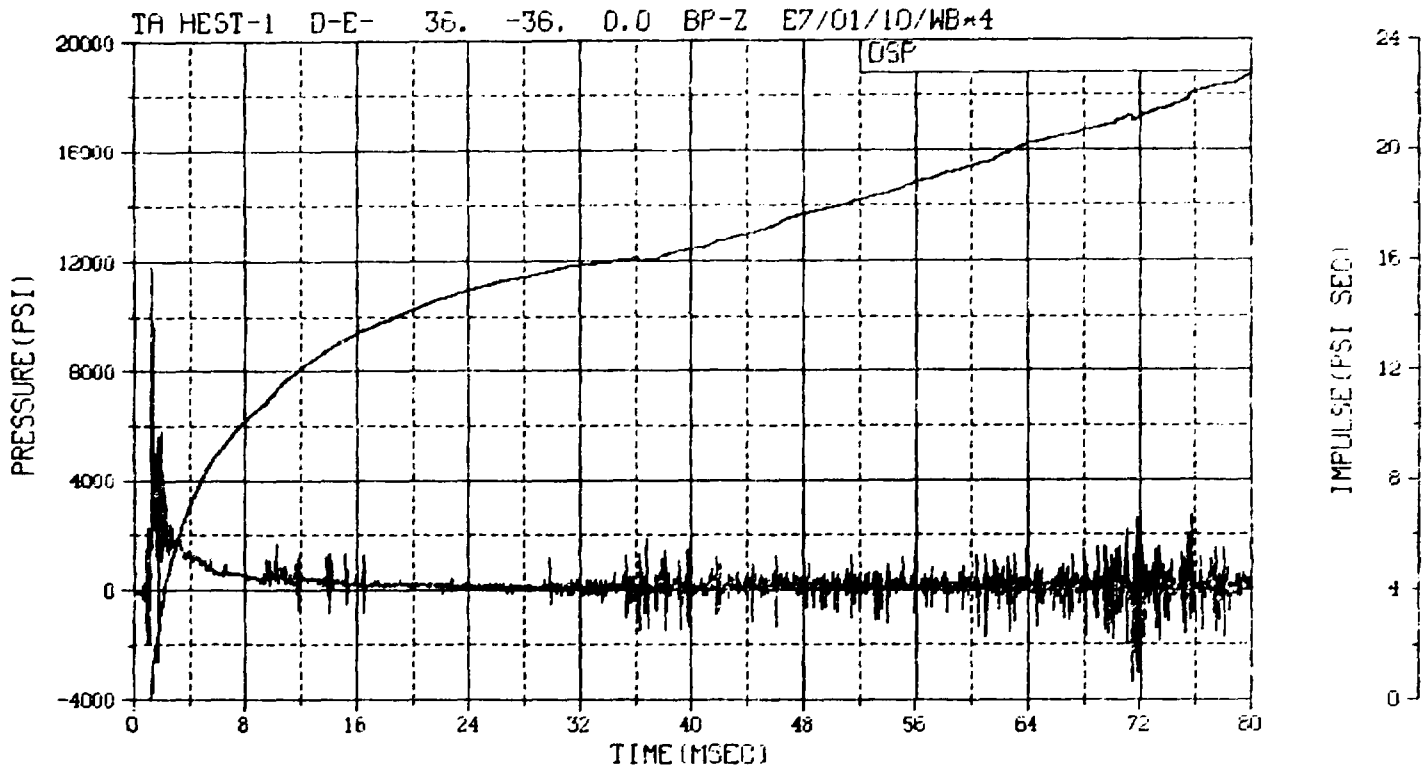

M.N. =80004	E.U. =0.000,28698.000	VSN=
TSKIP=10.350	DIGITS=0.000,1510.500	TAPE26
S.R. =50.00 KHZ	3 49 PM,11 APR 78.	FILE=3

1

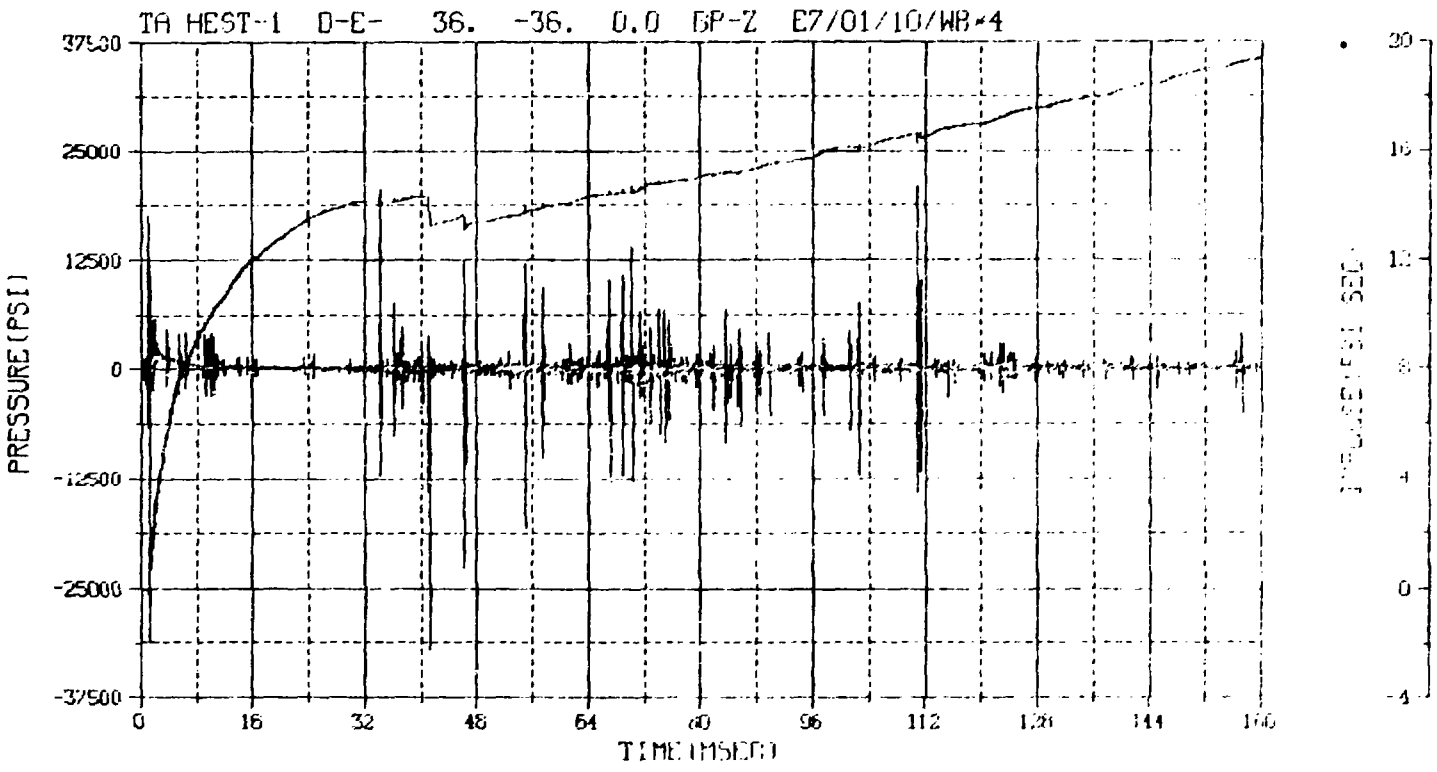

M.N. = 4	E.U. =0.000,28608.000	VSN=BD54
TSKIP=10.350	DIGITS=0.000,1510.500	TAPE22
S.R. =100.00 KHZ	2 40 PM, 6 MAR 7[illegible]	FILE=16

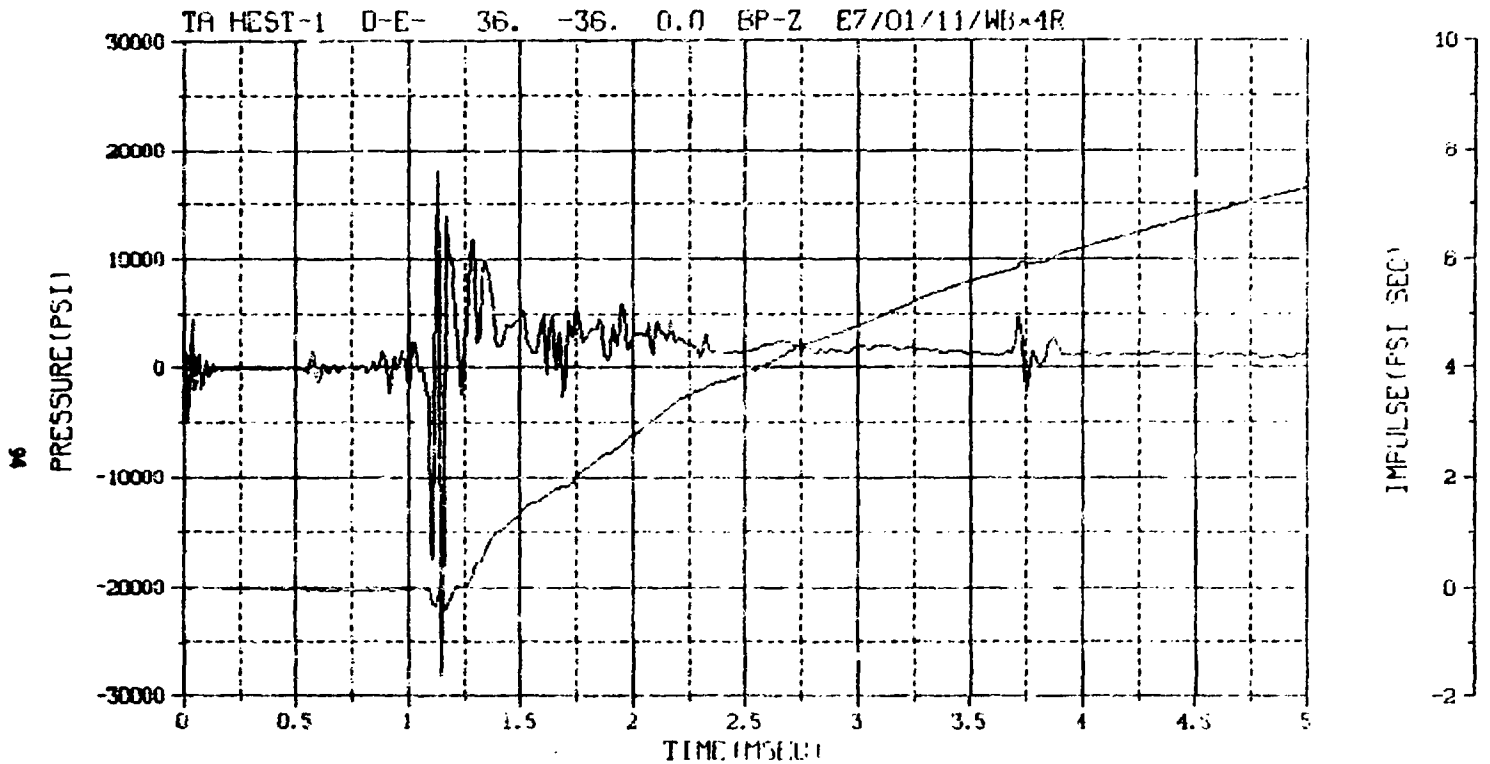

M.N. = 4	E.U. =0.000,[illegible]	VSN-8054
TSKIP=10.350	DIGITS=0.000,[illegible]	TAPE22
S.R. =100.00 KHZ	2 40 PM, 6 MAR 78.	FILE=18

1

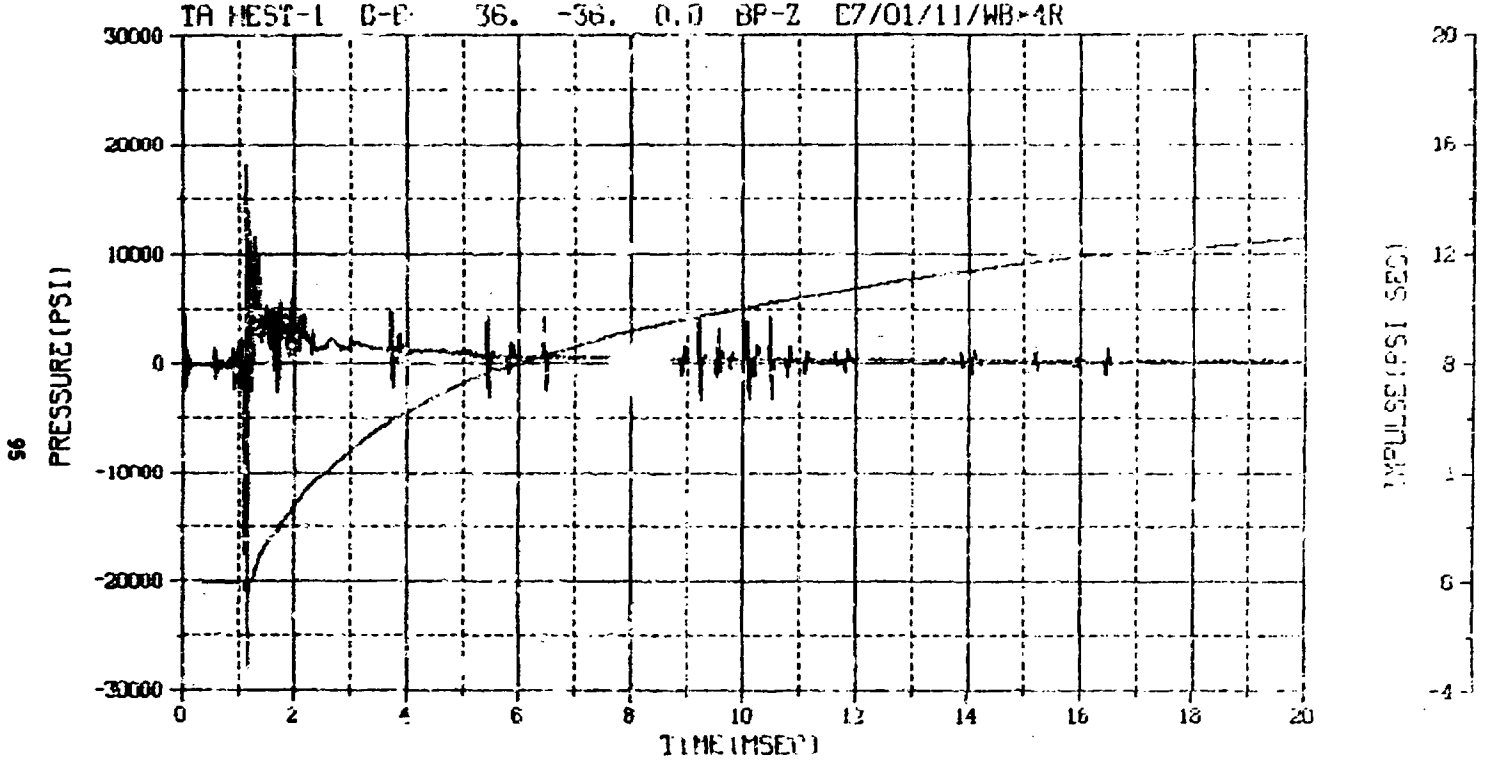
TA WEST-1 B-B' 36. -36. 0.0 BP-Z 87/01/11/WB=4R
30000
20000
10000
0
-10000
-20000
-30000
PRESSURE(PSI)
0
2
4
6
8
10
12
14
16
18
20
TIME(MSEC)
20
16
12
8
4
M.N. = 4
TSKIP=10.350
S.R. =100.00 KHZ
2 40 PM, 6 MAR 78.
VSN=8054
TAPE22
FILE=18

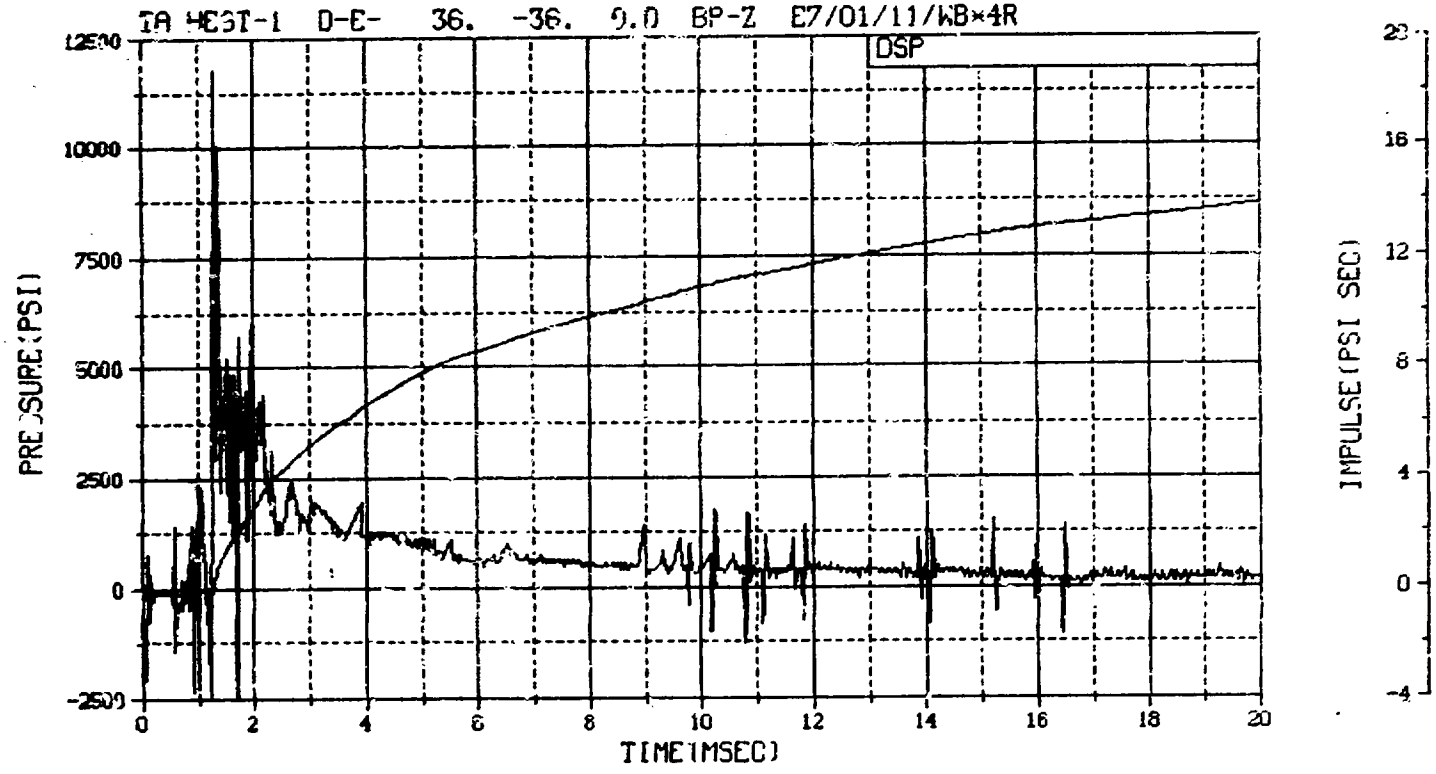

M.N. =80004	E.U. =0.000,28698.000	VSN=
TSKIP=10.350	DIGITS=0.000,1308.875	TAPE26
S.R. =50.00 KHZ	3 49 PM,11 APR 78.	FILE=4

1

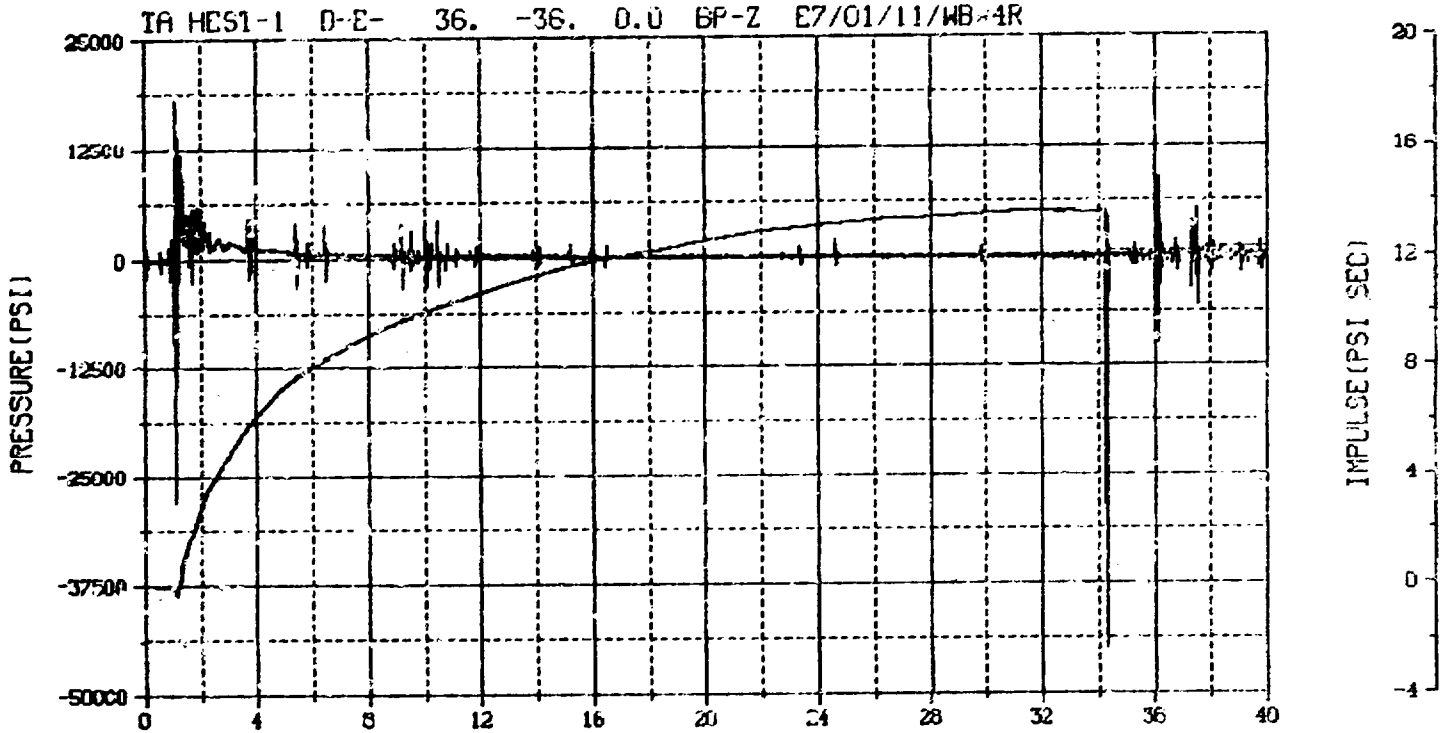

M.N. = 4	E.U. =0.000, 28698.000	VSN=BD54
T3KIP=10.350	DIGITS=0.000, 1308.375	TAPE22
S.R. =100.00 KHZ	2 40 PM, 6 MAR 78.	FILE=18

1

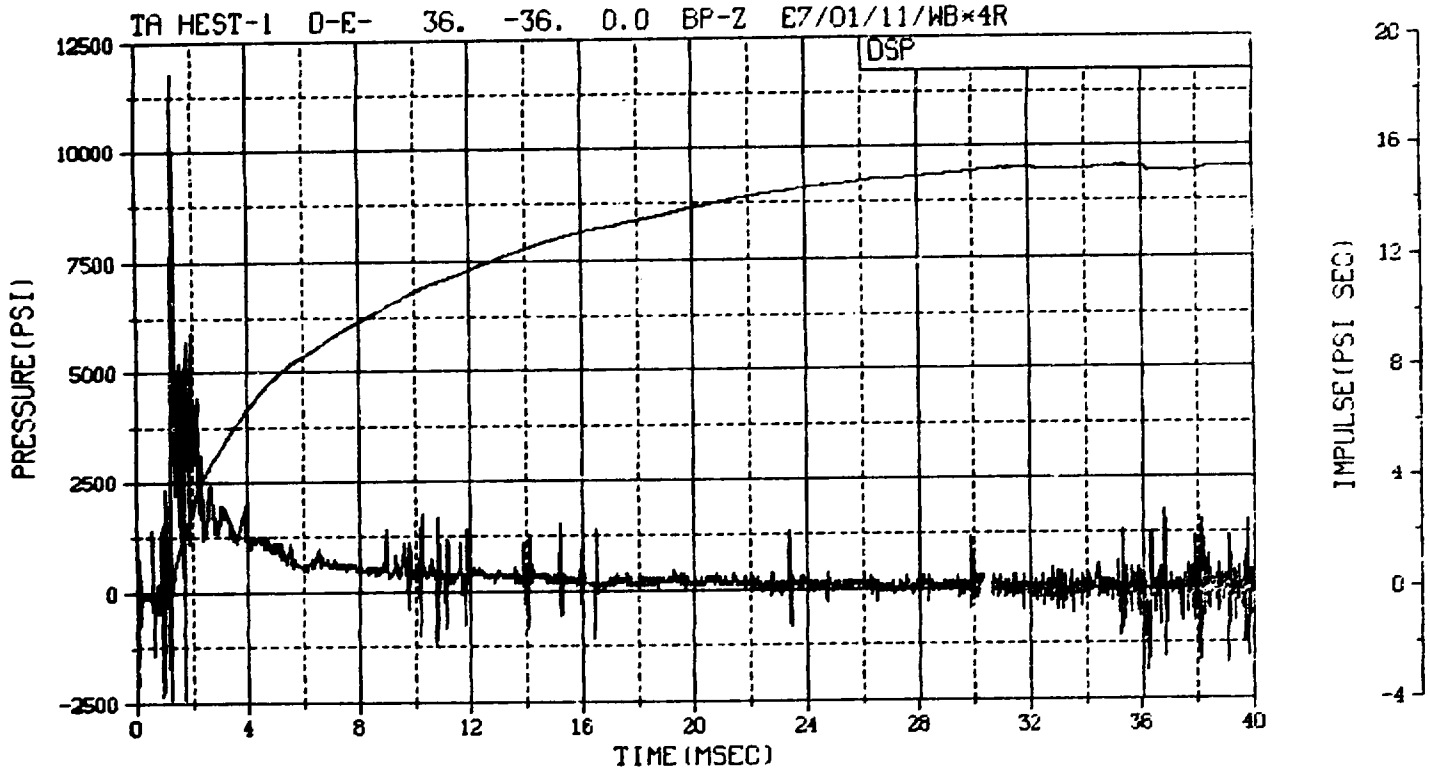

M.N. -80004	E.U. -0.000,28698.000	VSN=
TSKIP=10.350	DIGITS=0.000,1308.875	TAPE26
S.R. =50.00 KHZ	3 49 PM,11 APR 78.	FILE=4

1

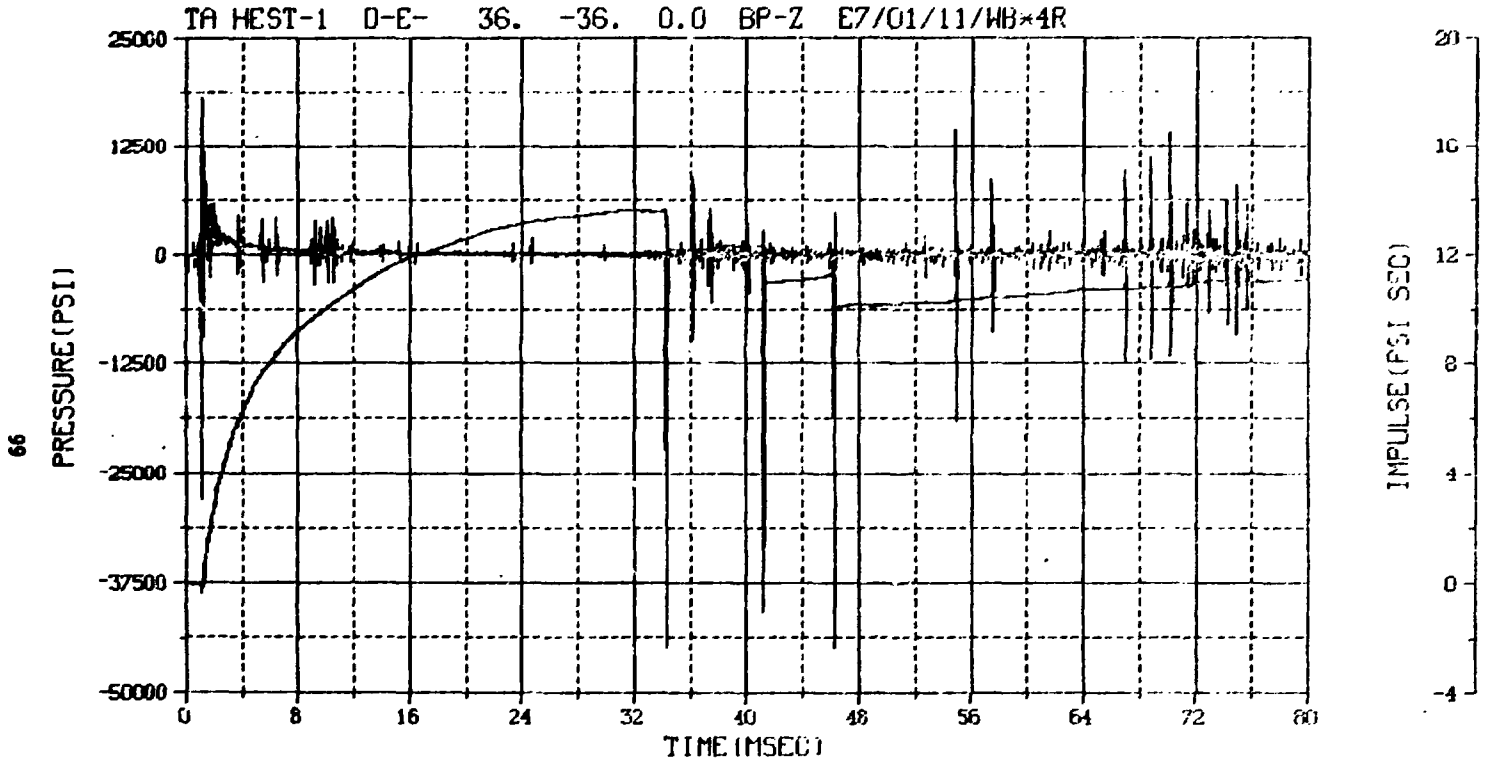

M.N. = 4	E.U. =0.000,28698.000	VSN=BD54
TSKIP=10.350	DIGITS=0.000,1308.875	TAPE22
S.R. =100.00 KHZ	2 40 PM, 6 MAR 78.	FILE=18

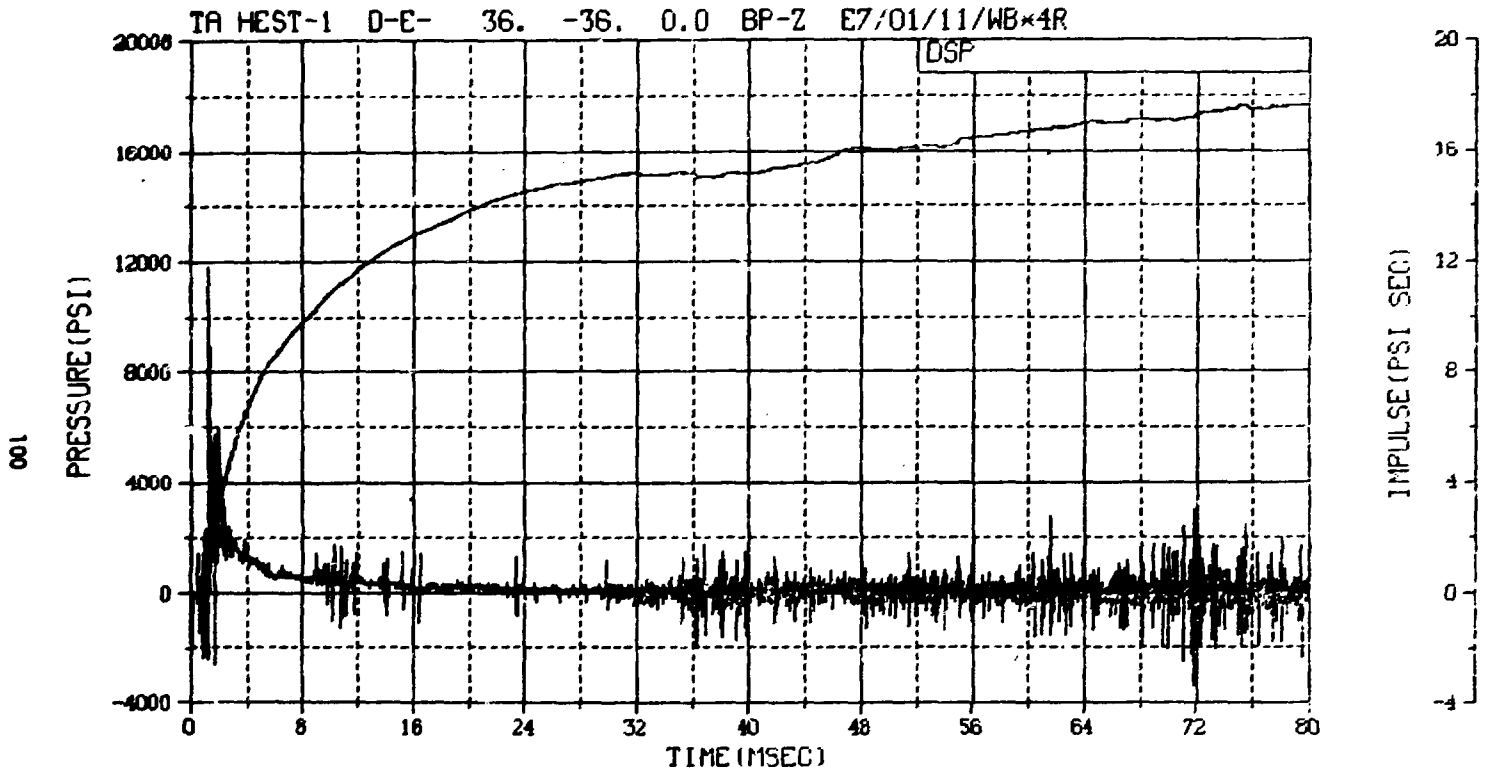

M.N. =80004	E.U. =0.000,28698.000	VSN=
TSKIP=10.350	DIGITS=0.000,1308.875	TAPE26
S.R. =50.00 KHZ	3 49 PM,11 APR 78.	FILE=4

1

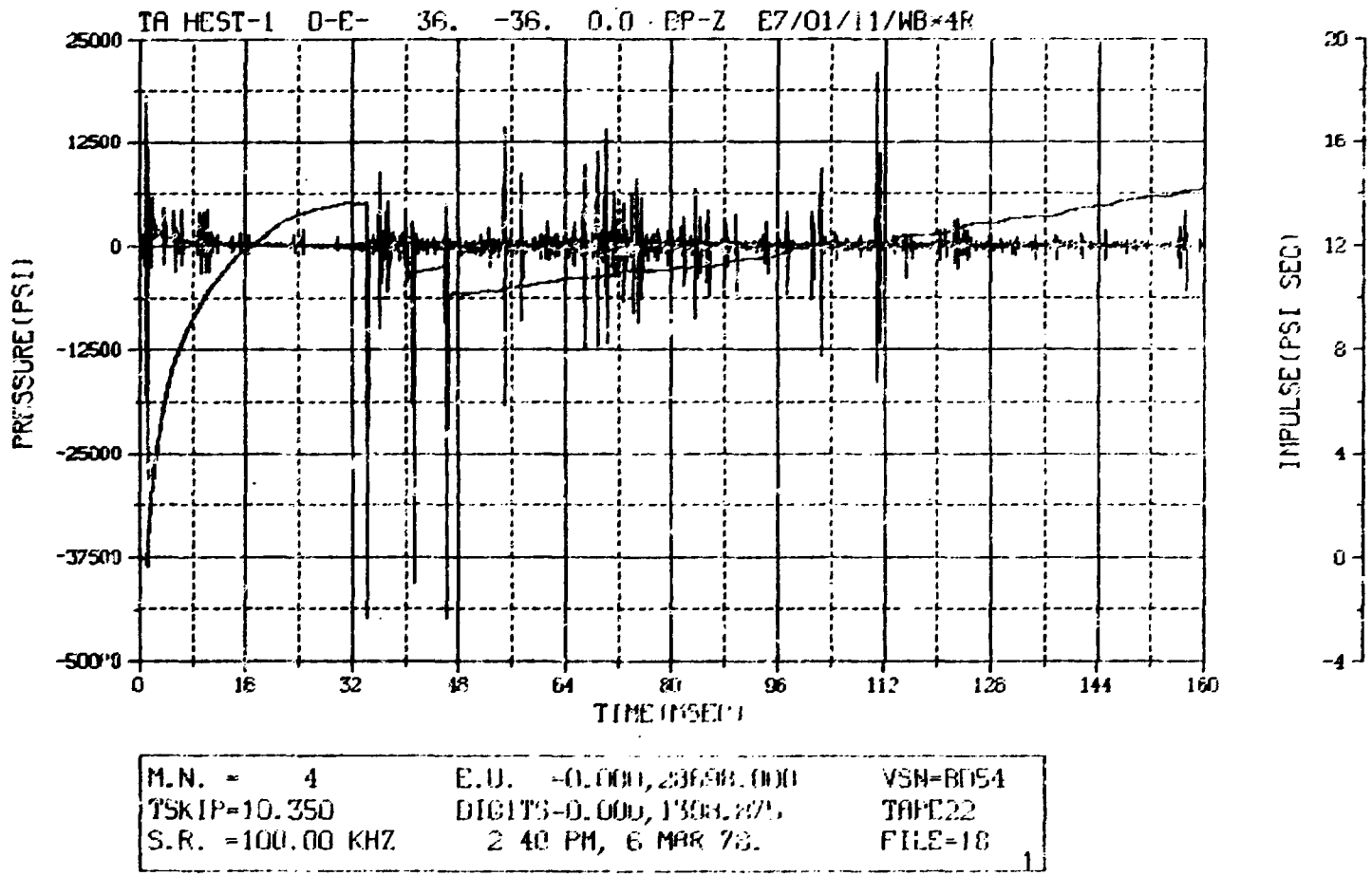
TA HEST-1 D-E- 36. -36. 0.0 BP-Z E7/01/11/WB*4R
PRESSURE(PSI)
25000
12500
0
-12500
-25000
-37500
-50000
0
16
32
48
64
80
96
112
128
144
160
TIME(MSEC)
IMPULSE(PSI SEC)
20
16
12
8
4
0
-4
M.N. = 4
TSKIP=10.350
S.R. =100.00 KHZ
E.U. =0.000,28698.000
DIGITS=0.000,1308.875
2 40 PM, 6 MAR 78.
VSN=BD54
TAPE22
FILE=18

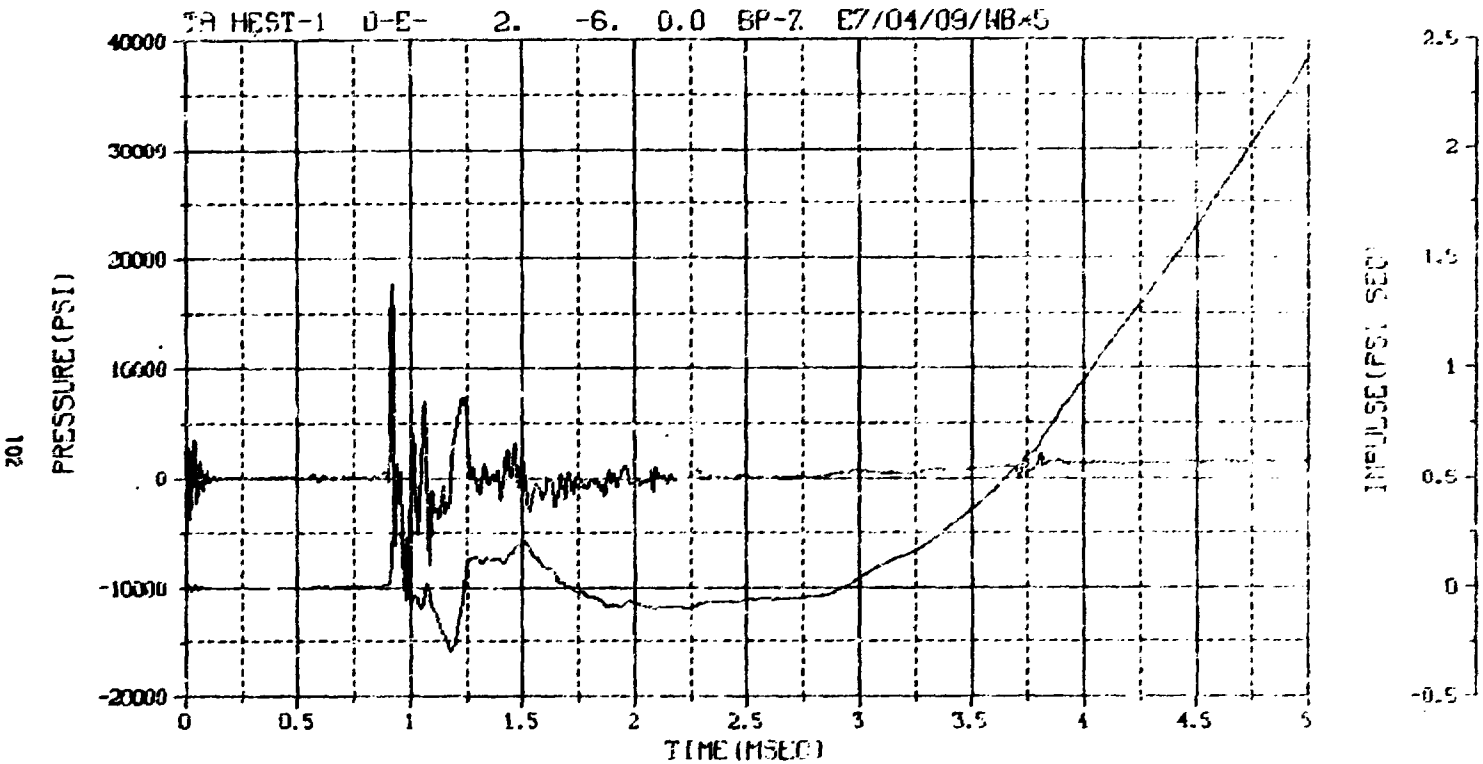

M.N. = 5	E.U. =0.000,5918.000	VSN=BD54
TSKIP=9.848	DIGITS=0.000,'61.000	TAPE22
S.R. =250.00 KHZ	2 40 PM, 6 MAR 78.	FILE=30

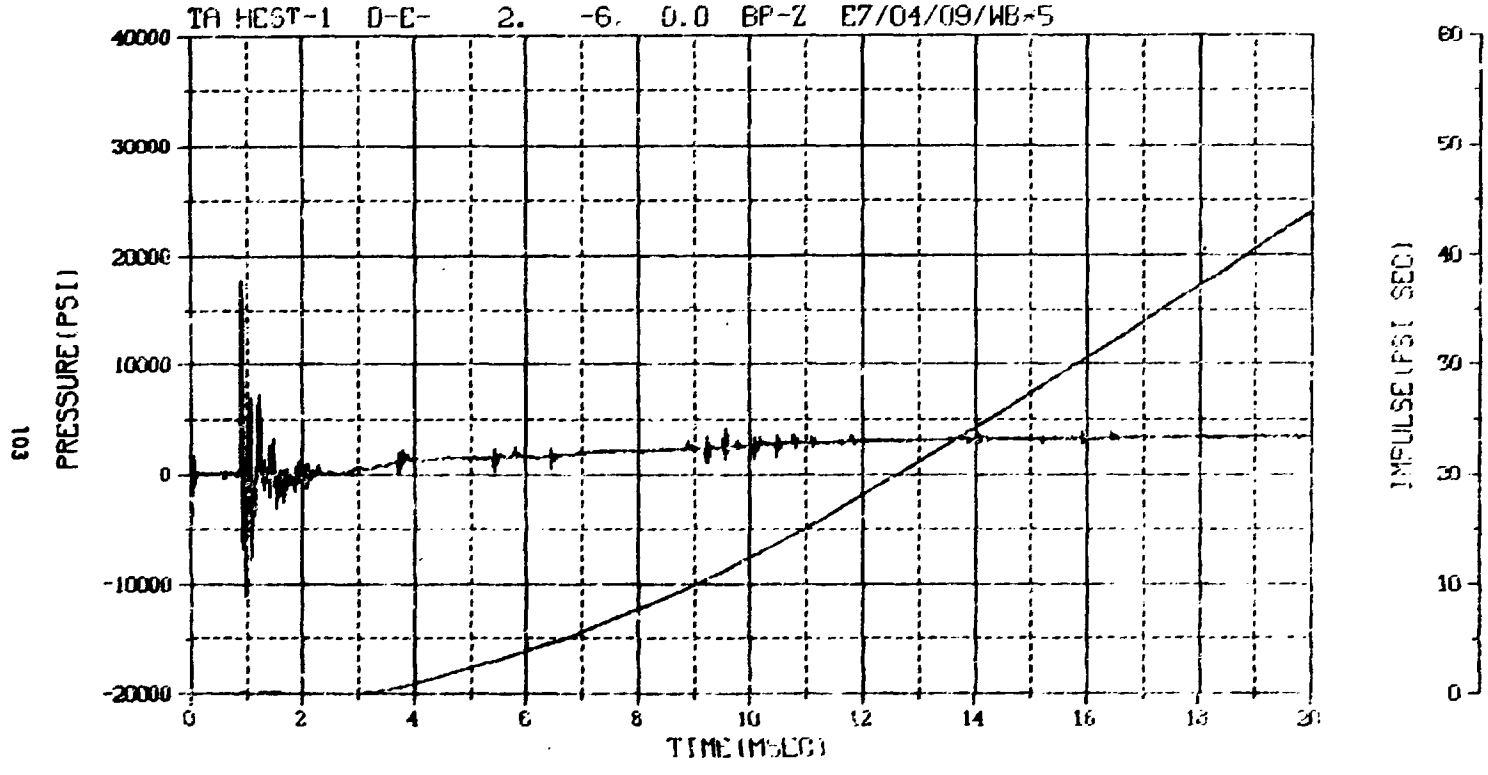
TA HEST-1 D-E- 2. -6. 0.0 BP-Z E7/04/09/WB=5
PRESSURE(PSI)
IMPULSE(PSI SEC)
TIME(MSEC)
40000
30000
20000
10000
0
-10000
-20000
60
50
40
30
20
10
0
0
2
4
6
8
10
12
14
16
18
M.N. = 5
E.U. =0.000,5918.000
VSN-BD54
TSKIP=9.848
DIGITS=0.000,5911.000
TAPE22
S.R. =250.00 KHZ
2 40 PM, 6 MAR 78.
FILE=30

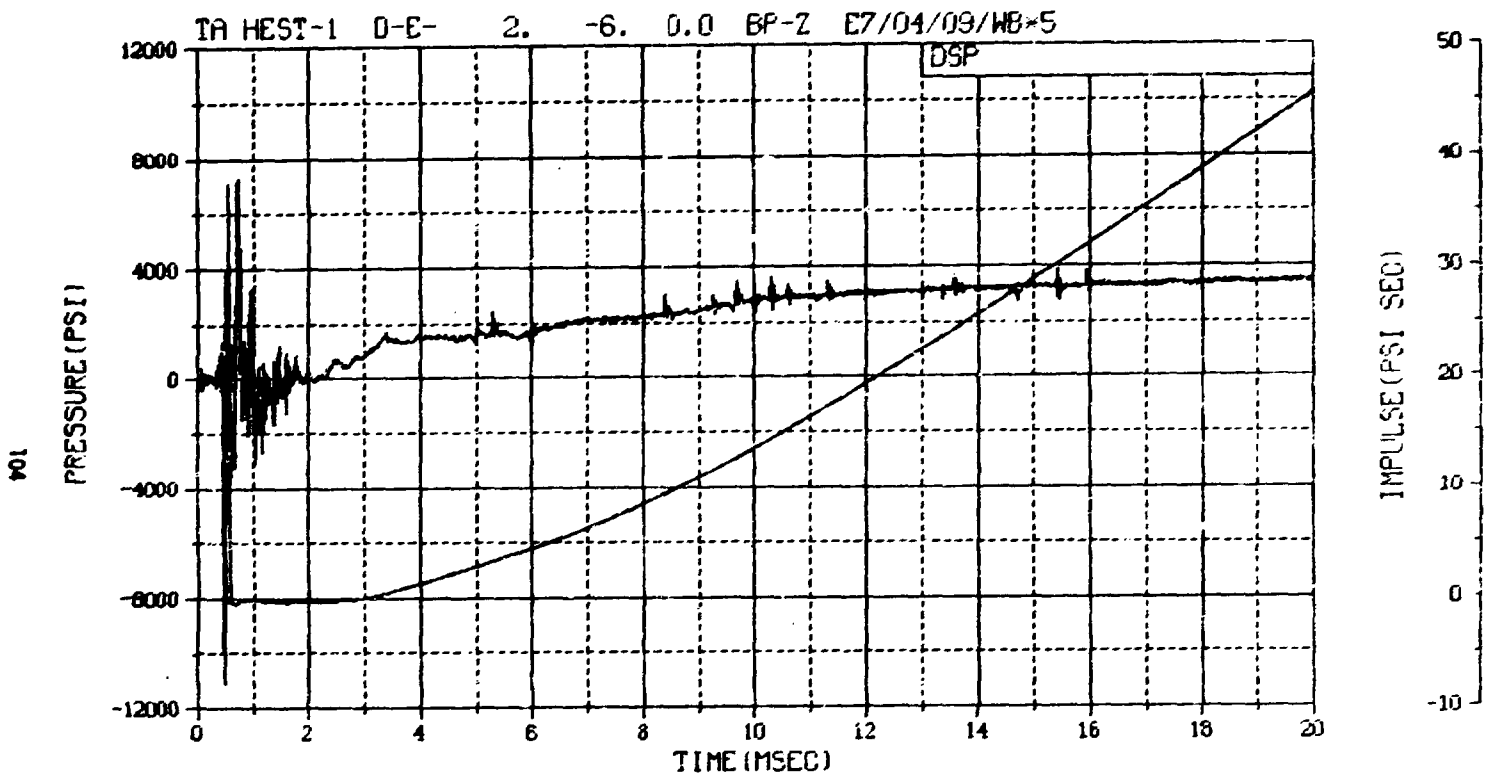

M.N. =80005	E.U. =0.000,5918.000	VSN=
TSKIP=10.350	DIGITS=0.000,561.000	TAPE26
S.R. =125.00 KHZ	3 49 PM,11 APR 78.	FILE=11

1

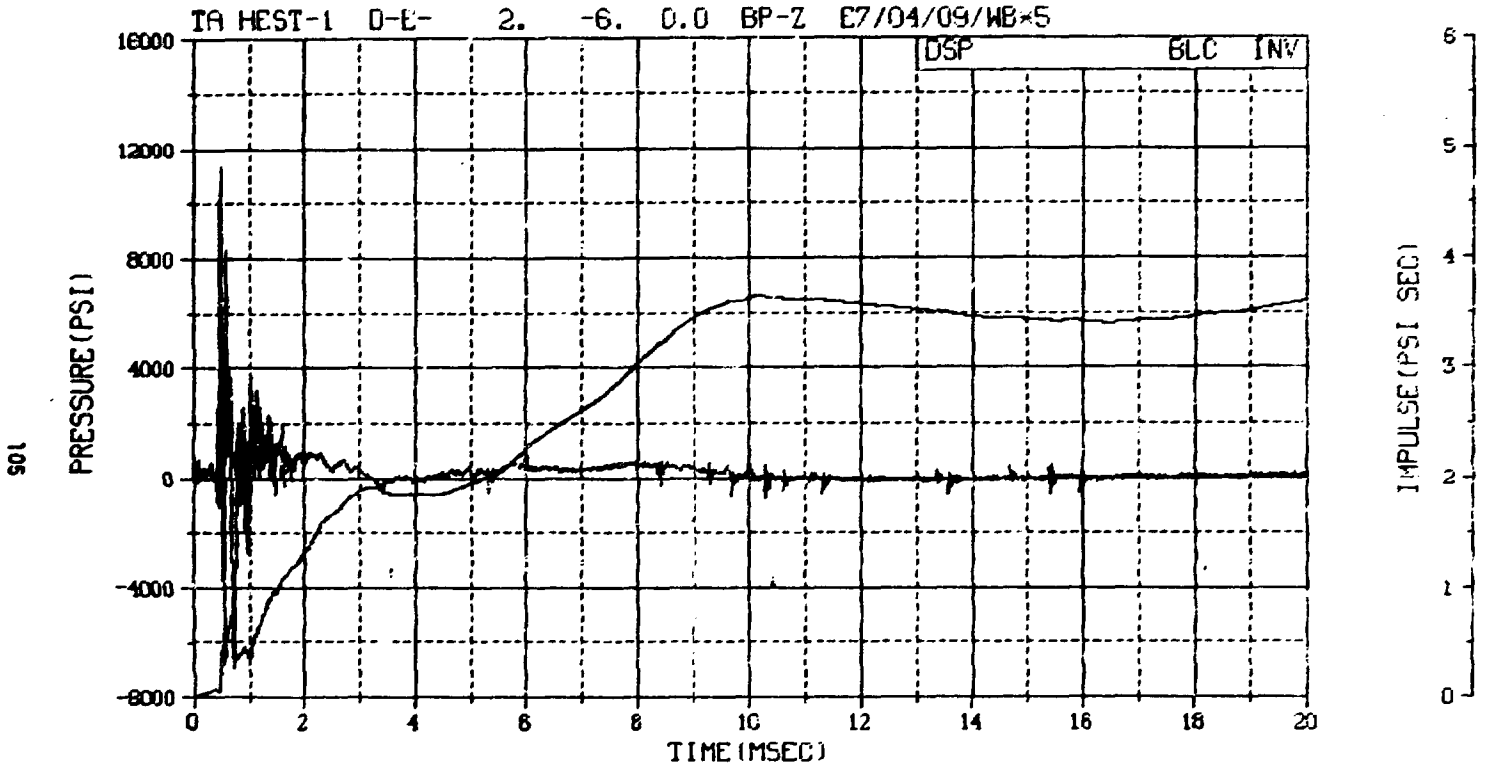
TA HEST-1 D-E- 2. -6. 0.0 BP-Z E7/04/09/WB×5
DSP
BLC INV
16000
12000
8000
4000
0
-4000
-8000
PRESSURE(PSI)
0
2
4
6
8
10
12
14
16
18
20
TIME(MSEC)
6
5
4
3
2
1
0
IMPULSE(PSI SEC)
M.N. =90005
E.U. =0.000,5918.000
VSN=
TSKIP=10.350
DIGITS=0.000,561.000
TAPE26
S.R. =125.00 KHZ
3 49 PM,11 APR 78.
FILE=12
1

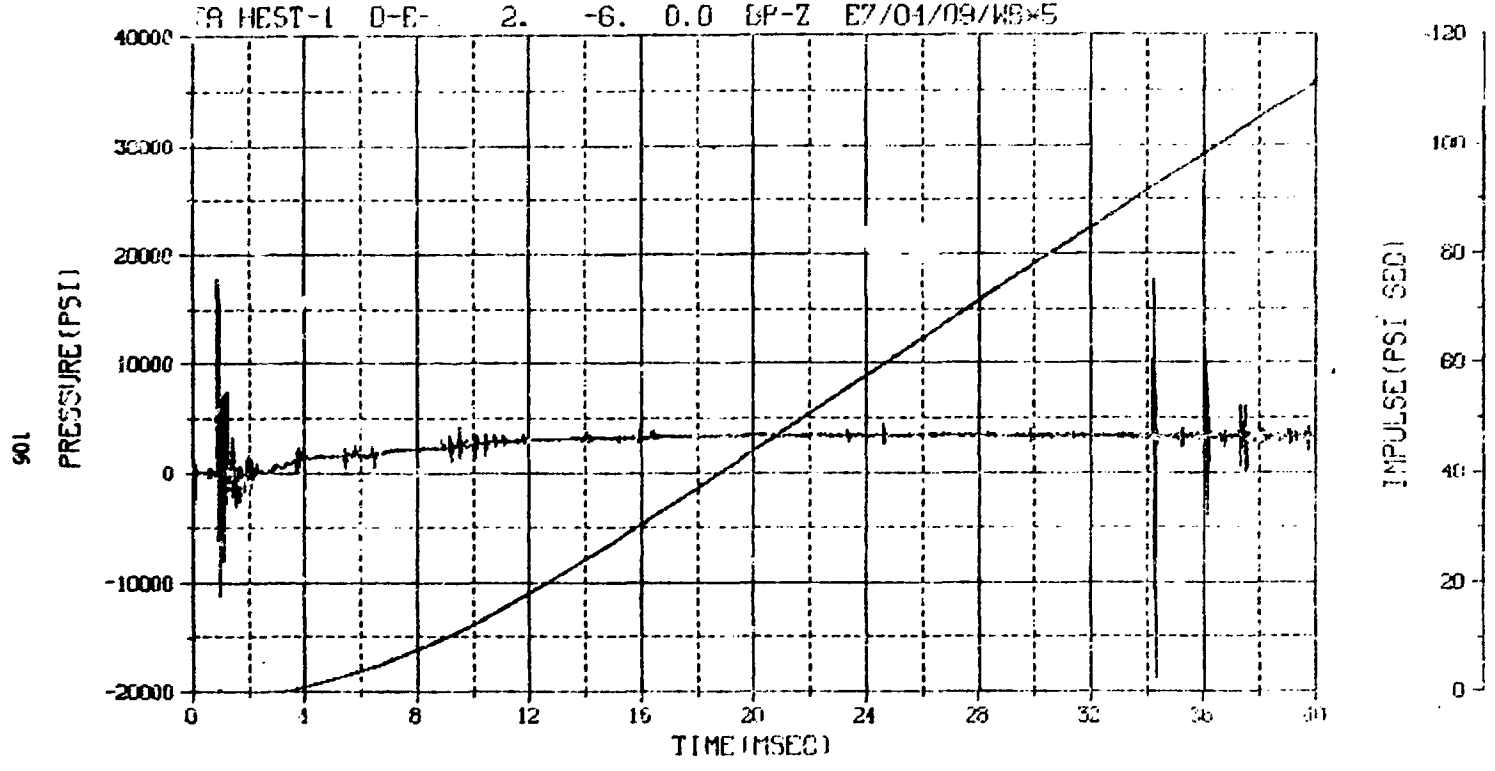

M.N. - 5	E.U. =0.000.5918.000	VSN=BD54
TSKIP=9.848	DIGITS=0.000,561.000	TAPE22
S.R. =250.00 KHZ	2 40 PM, 6 MAR 7[illegible]	FILE=30

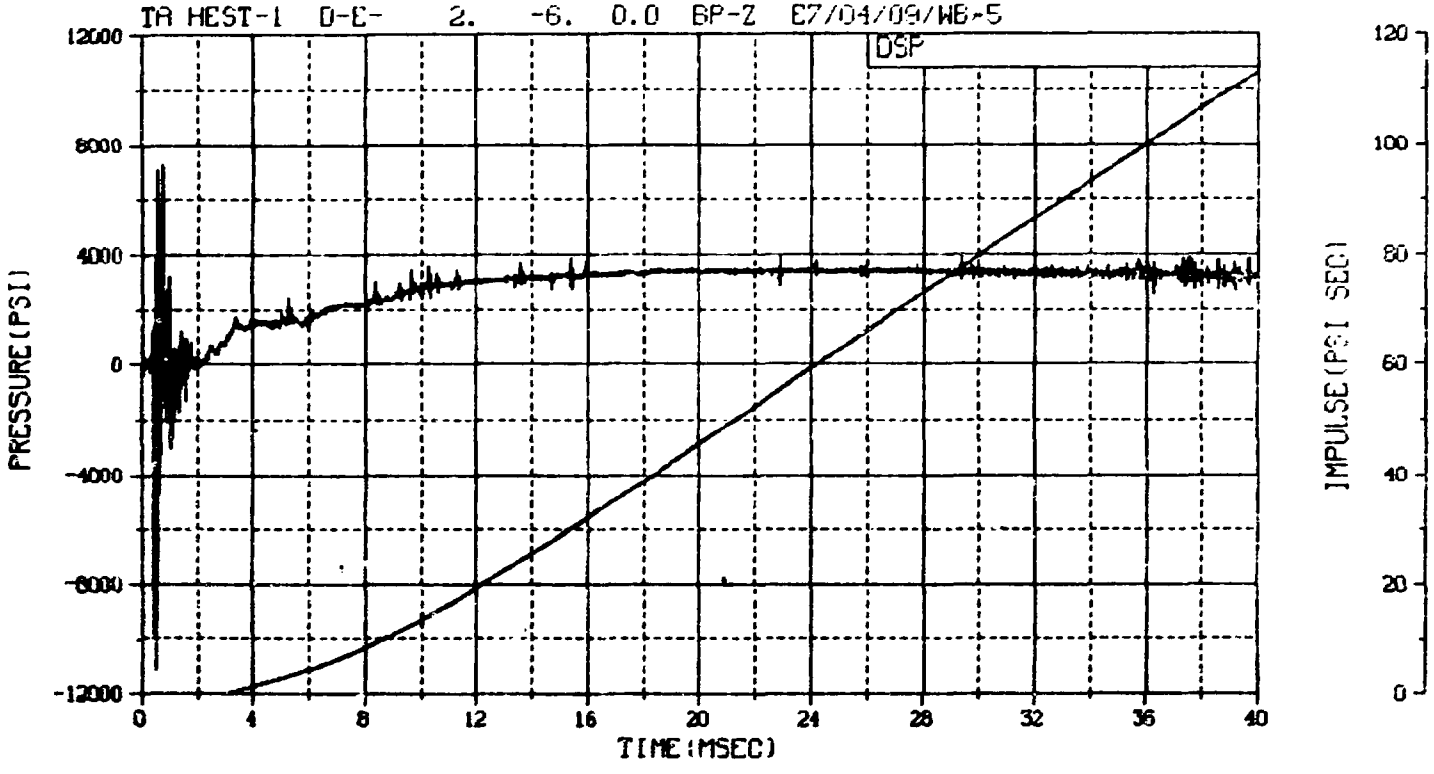

M.N. =80005	E.U. =0.000,5918.000	VSN=
TSKIP=10.350	DIGITS=0.000,561.000	TAPE26
S.R. =125.00 KHZ	3 49 PM,11 APR 78.	FILE=11

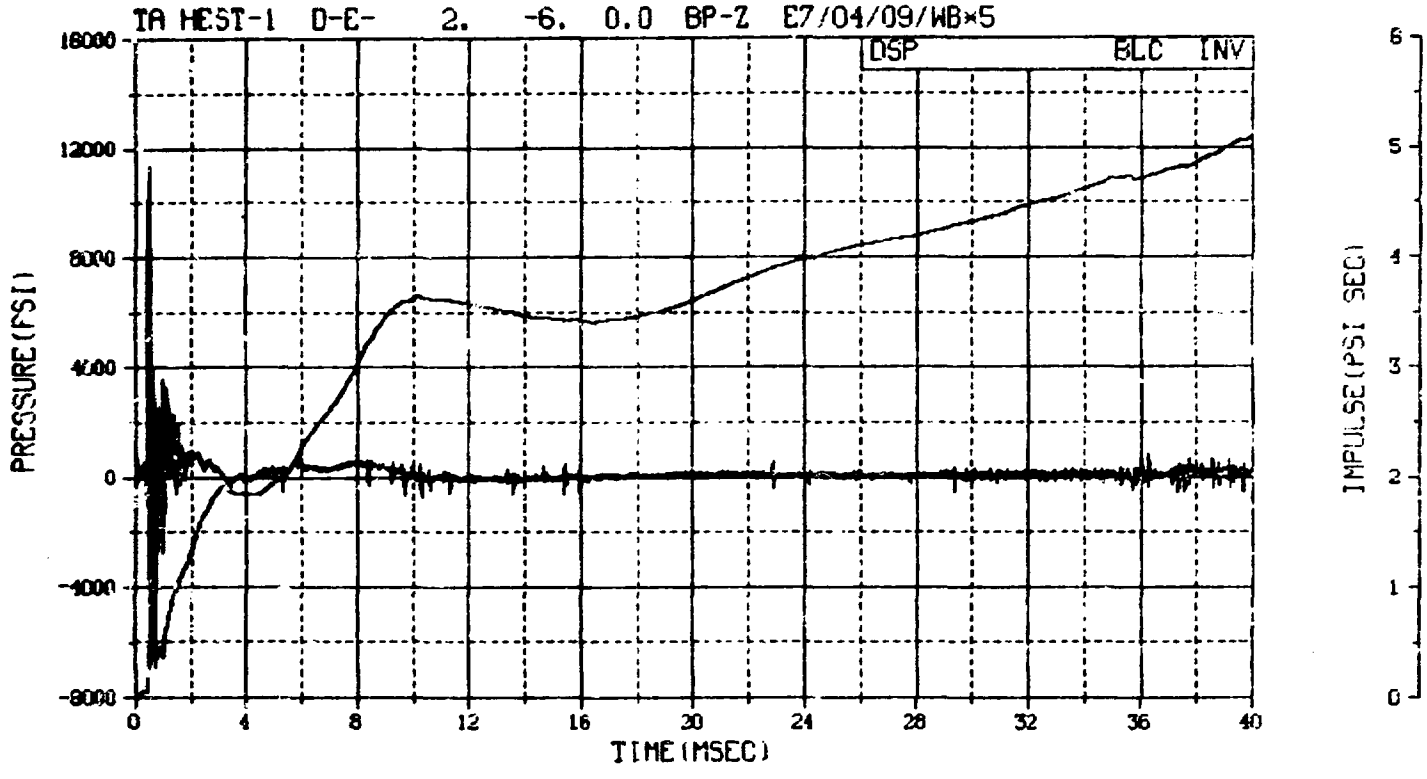

M.N. -90005	E.U. -0.000,5918.000	VSN-
TSKIP-10.350	DIGITS-0.000,561.000	TAPE26
S.R. -125.00 KHZ	3 49 PM, 11 APR 78.	FILE-12

1

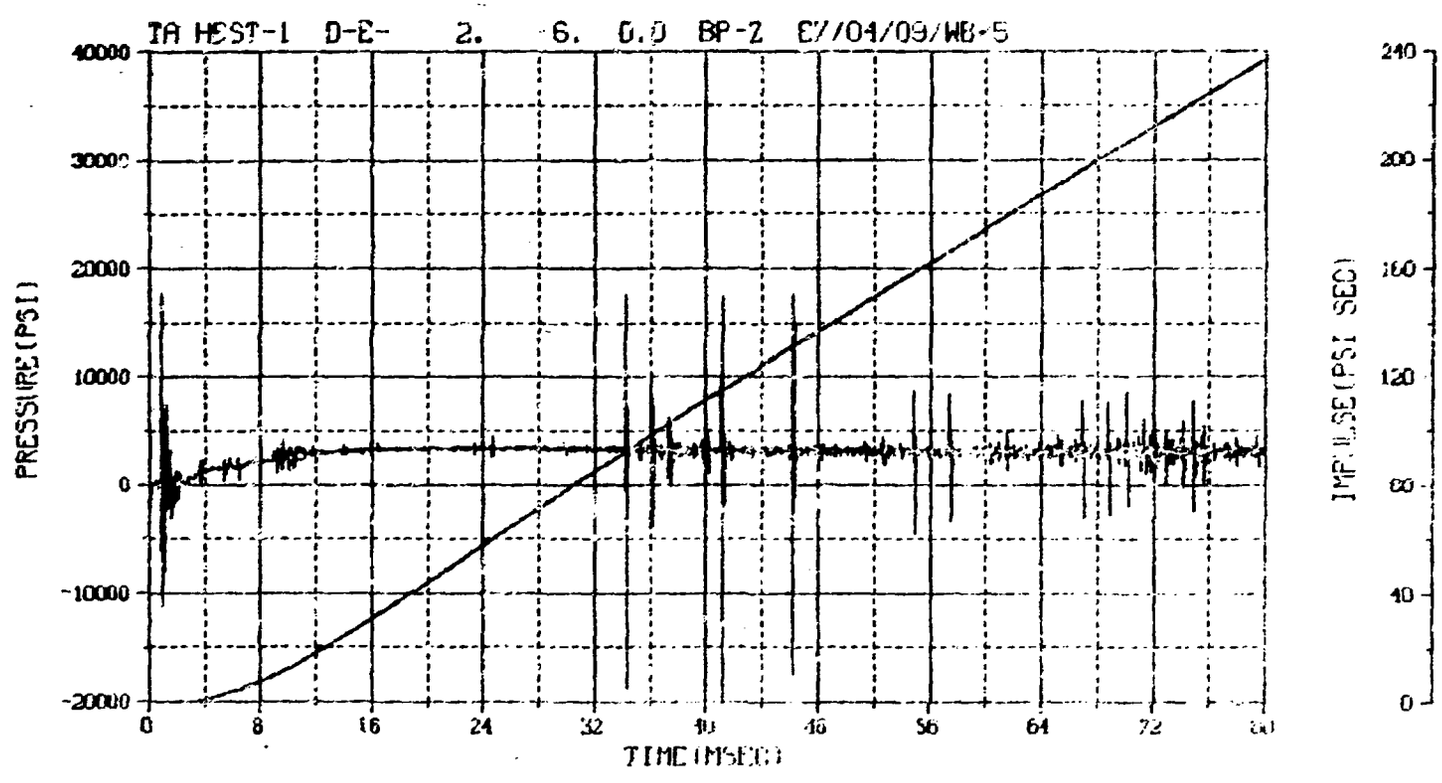

M.N. = 5	E.U. =0.000,5918.000	VSN=BD54
TSKIP=9.848	DIGITS 0.000,561.000	TAPE22
S.R. =250.00 KHZ	2 40 PM, 6 MAR 73.	FILE=30

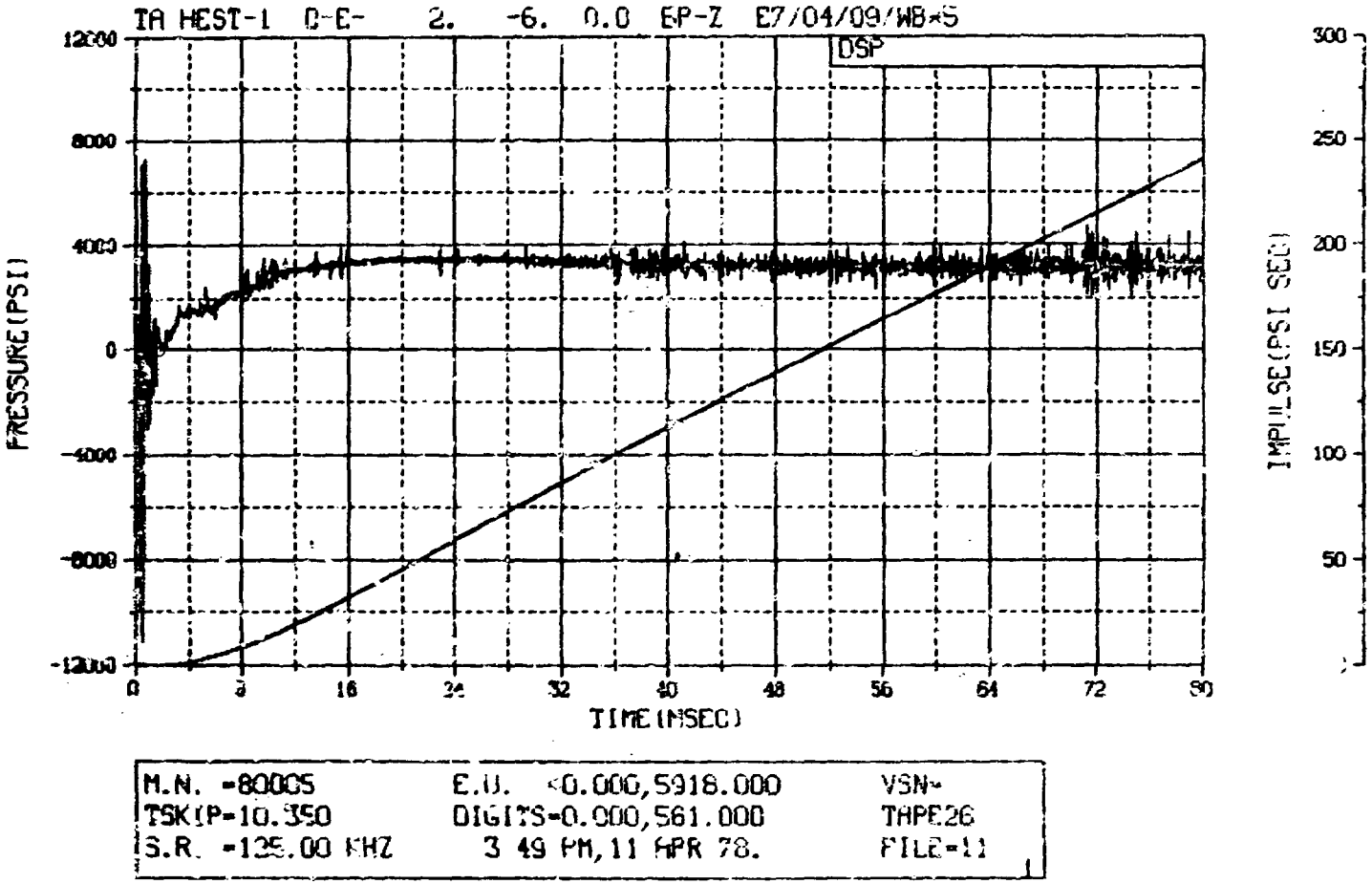
TA HEST-1 D-E- 2. -6. 0.0 EP-Z E7/04/09/WB×5
DSP
12000
8000
4000
0
-4000
-8000
-12000
0
8
16
24
32
40
48
56
64
72
80
PRESSURE(PSI)
IMPULSE(PSI SEC)
300
250
200
150
100
50
TIME(MSEC)
M.N. =80005
E.U. <0.000,5918.000
VSN=
TSK(P=10.350
DIGITS=0.000,561.000
TAPE26
S.R. =125.00 KHZ
3 49 PM,11 APR 78.
FILE=11

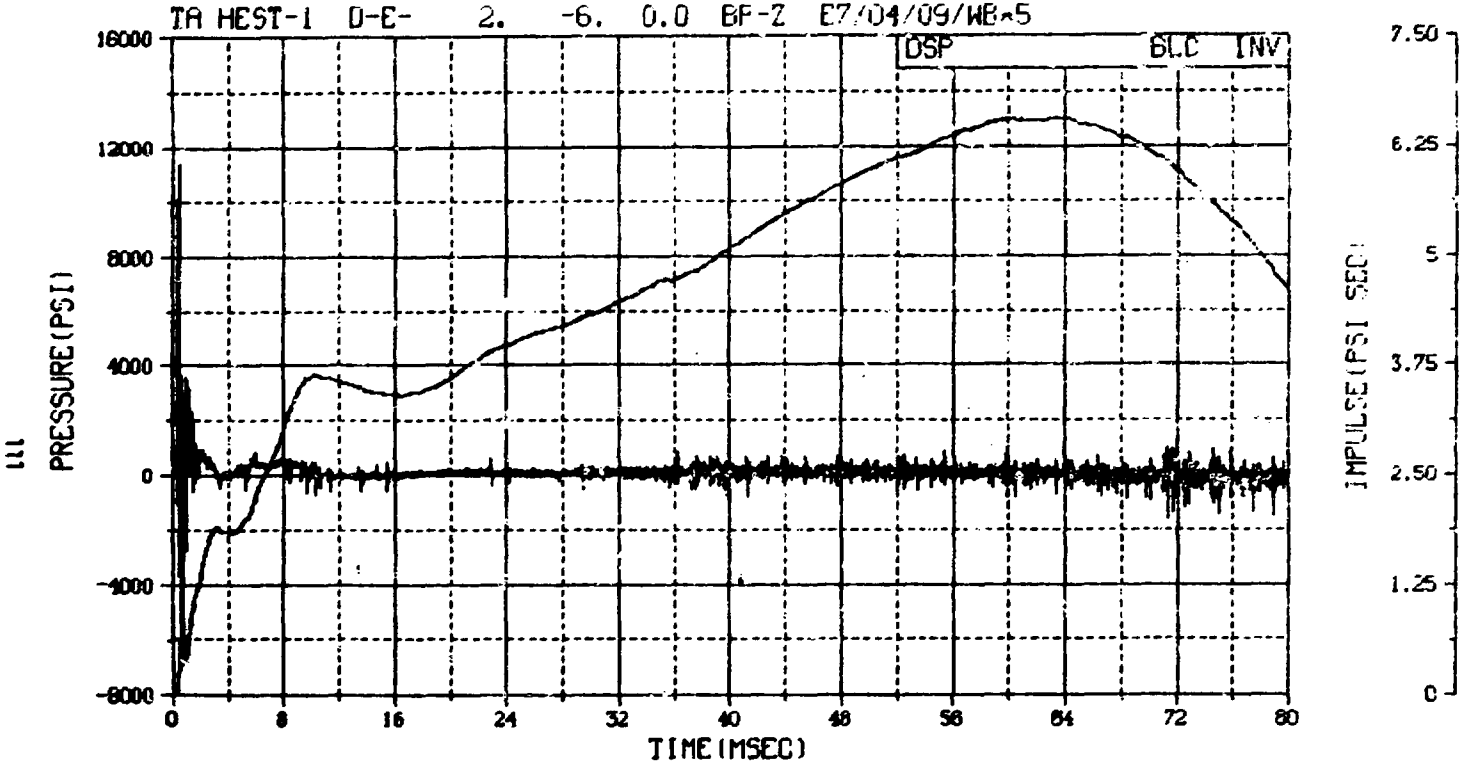

M.N. =90005	E.U. =0.000,5918.000	VSN=
TSKIP=10.350	DIGITS=0.000,561.000	TAPE26
S.R. =125.00 KHZ	3 49 PM, 11 APR 78.	FILE=12

1

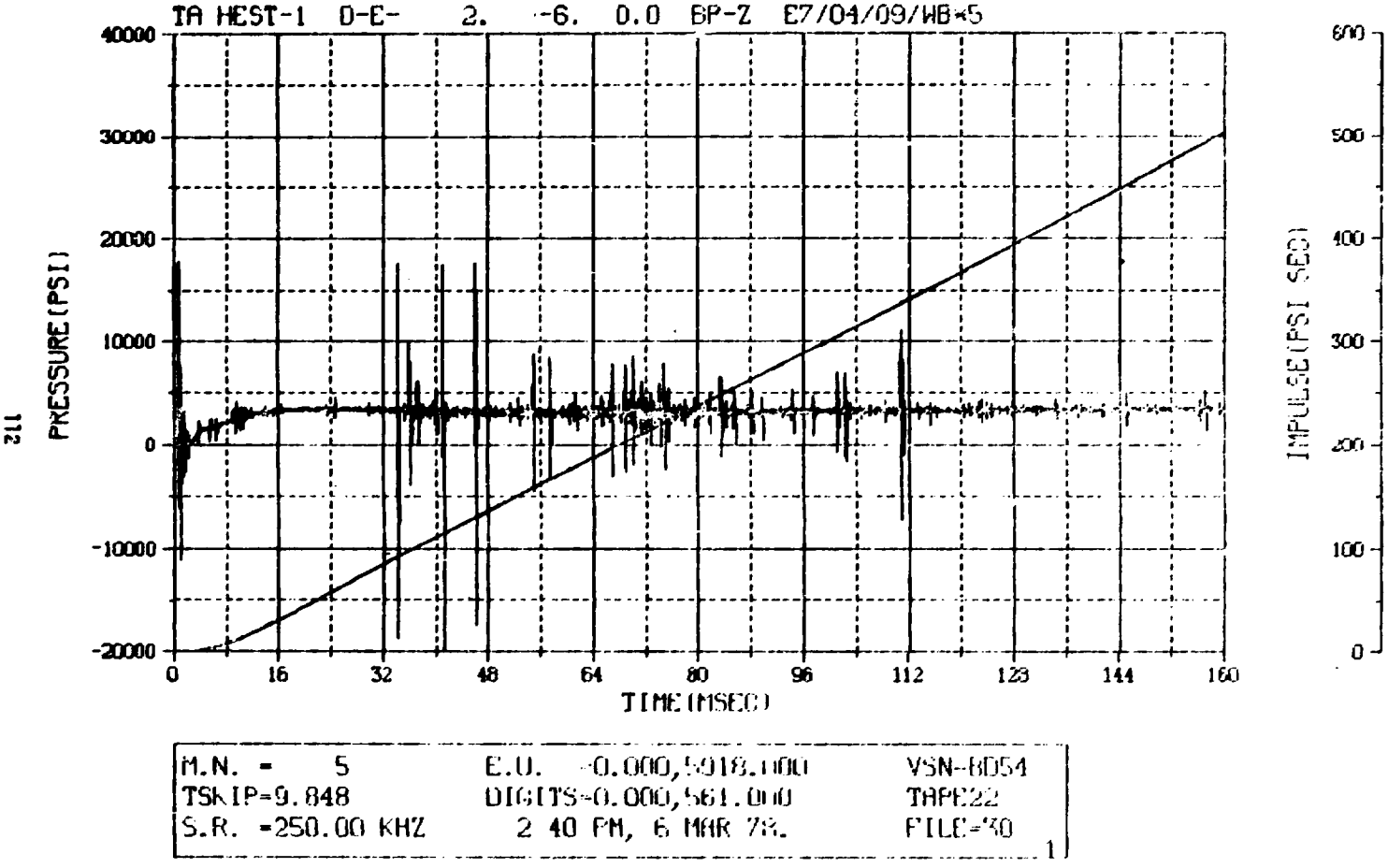
TA HEST-1 0-E- 2. -6. 0.0 BP-Z E7/04/09/WB*5
PRESSURE(PSI)
IMPULSE(PSI SEC)
TIME(MSEC)
40000
30000
20000
10000
0
-10000
-20000
600
500
400
300
200
100
0
0
16
32
48
64
80
96
112
128
144
160
M.N. = 5
E.U. -0.000,5018.1000
VSN-8054
TSKIP=9.848
DIGITS=0.000,561.000
TAPE22
S.R. =250.00 KHZ
2 40 PM, 6 MAR 78
FILE=30

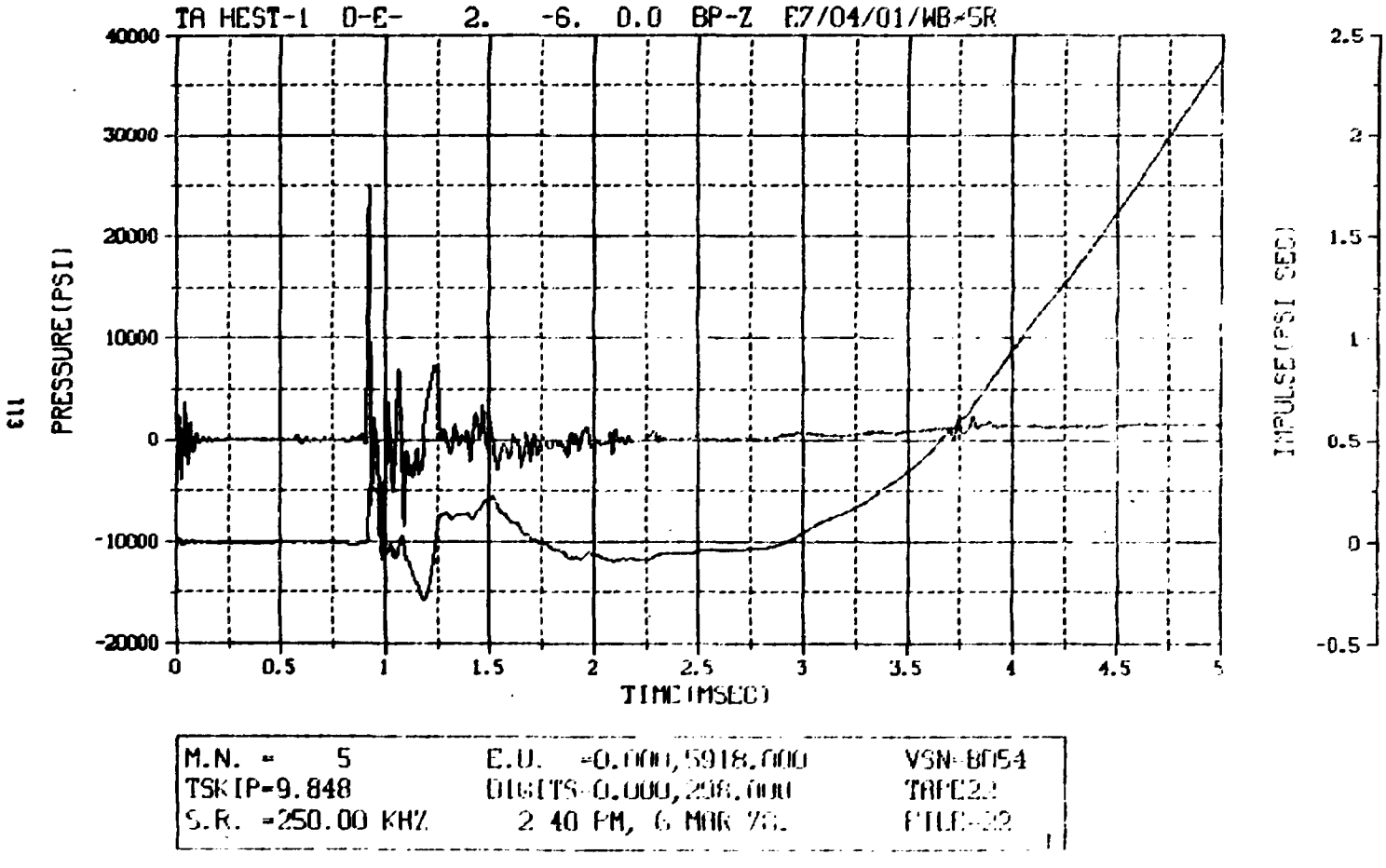
TA HEST-1 0-E- 2. -6. 0.0 BP-Z E7/04/01/WB*5R
PRESSURE(PSI)
IMPULSE(PSI SEC)
TIME(MSEC)
40000
30000
20000
10000
0
-10000
-20000
2.5
2
1.5
1
0.5
0
-0.5
0
0.5
1
1.5
2
2.5
3
3.5
4
4.5
5
M.N. = 5
E.U. =0.000,5918.000
VSN=8054
TSKIP=9.848
DIGITS=0.000,208.000
TAPE2?
S.R. =250.00 KHZ
2 40 PM, 6 MAR 76.
FILE=22

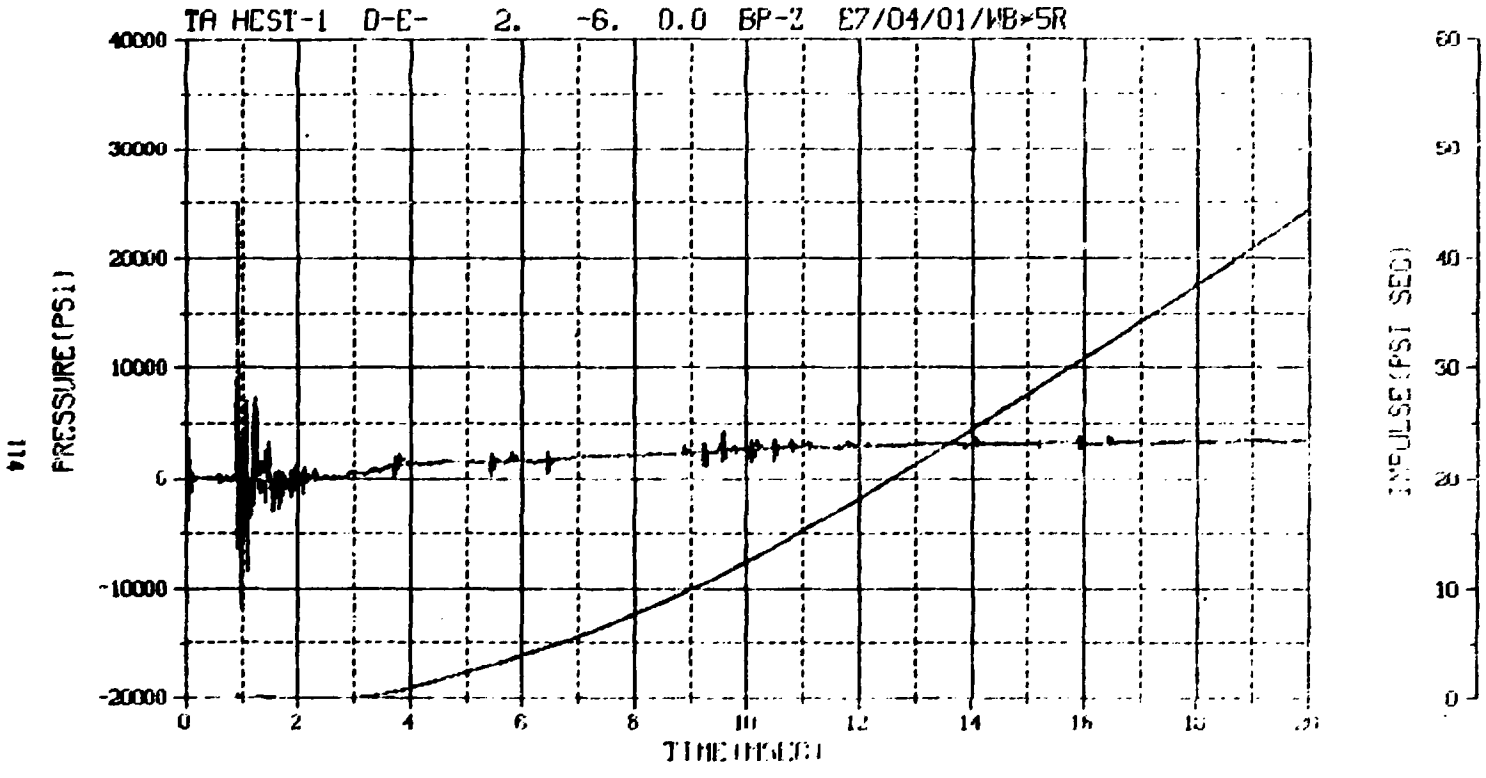
TA HEST-1 D-E- 2. -6. 0.0 BP-2 E7/04/01/WB*5R
40000
30000
20000
10000
0
-10000
-20000
0
2
4
6
8
10
12
14
16
18
20
PRESSURE(PSI)
60
50
40
30
20
10
0
M.N. = 5
E.U. =0.000,5918.000
VSN=BD54
TSKIP=9.848
DIGITS=0.000,208.000
TAPE22
S.R. =250.00 KHZ
2 40 PM, 6 MAR 7?
FILE=22

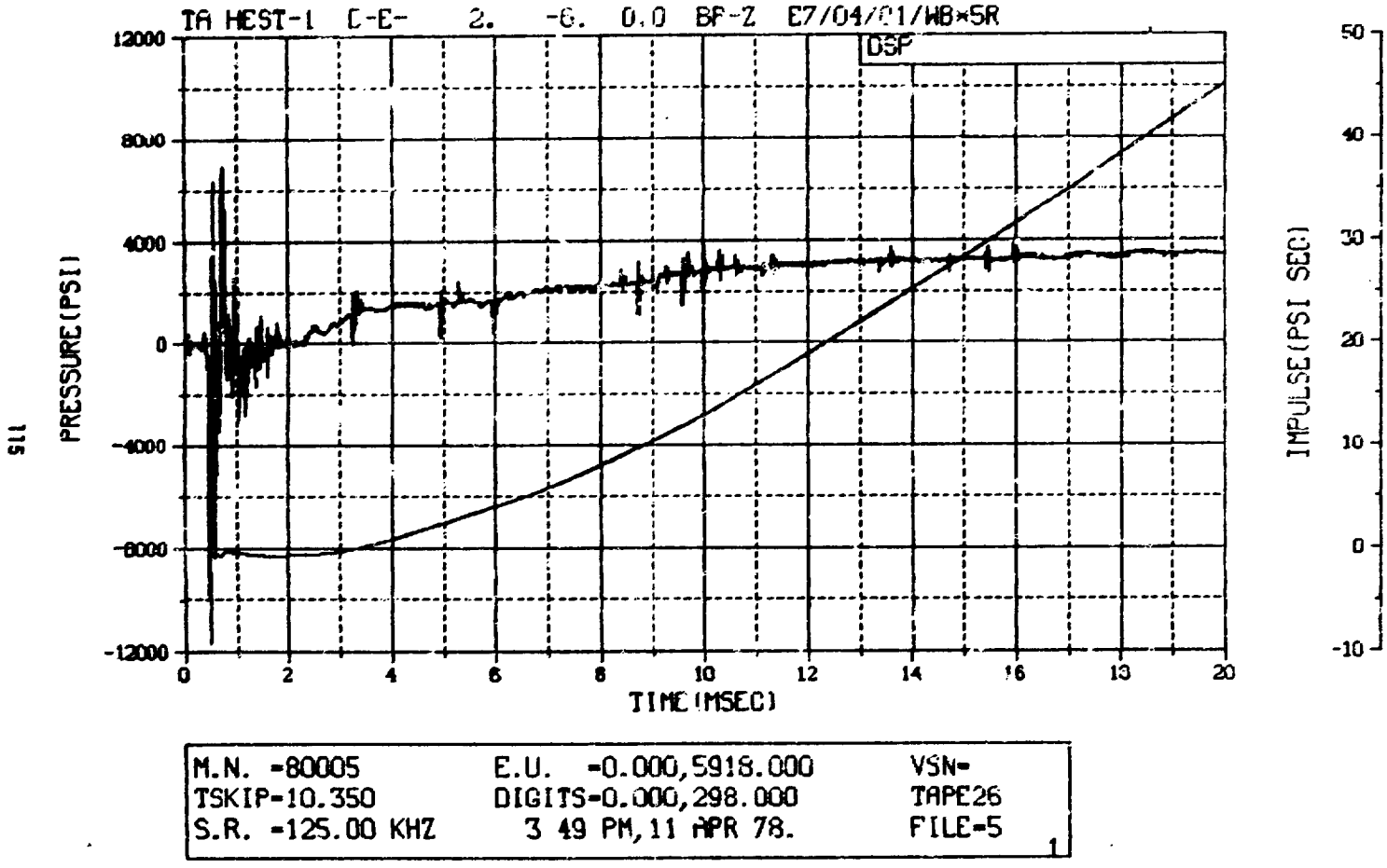
TA HEST-1 C-E- 2. -6. 0.0 BF-Z E7/04/01/WB×5R
DSP
PRESSURE(PSI)
IMPULSE(PSI SEC)
TIME(MSEC)
12000
8000
4000
0
-4000
-8000
-12000
50
40
30
20
10
0
-10
0
2
4
6
8
10
12
14
16
18
20
M.N. =80005
TSKIP=10.350
S.R. =125.00 KHZ
E.U. =0.000,5918.000
DIGITS=0.000,298.000
3 49 PM,11 APR 78.
VSN=
TAPE26
FILE=5

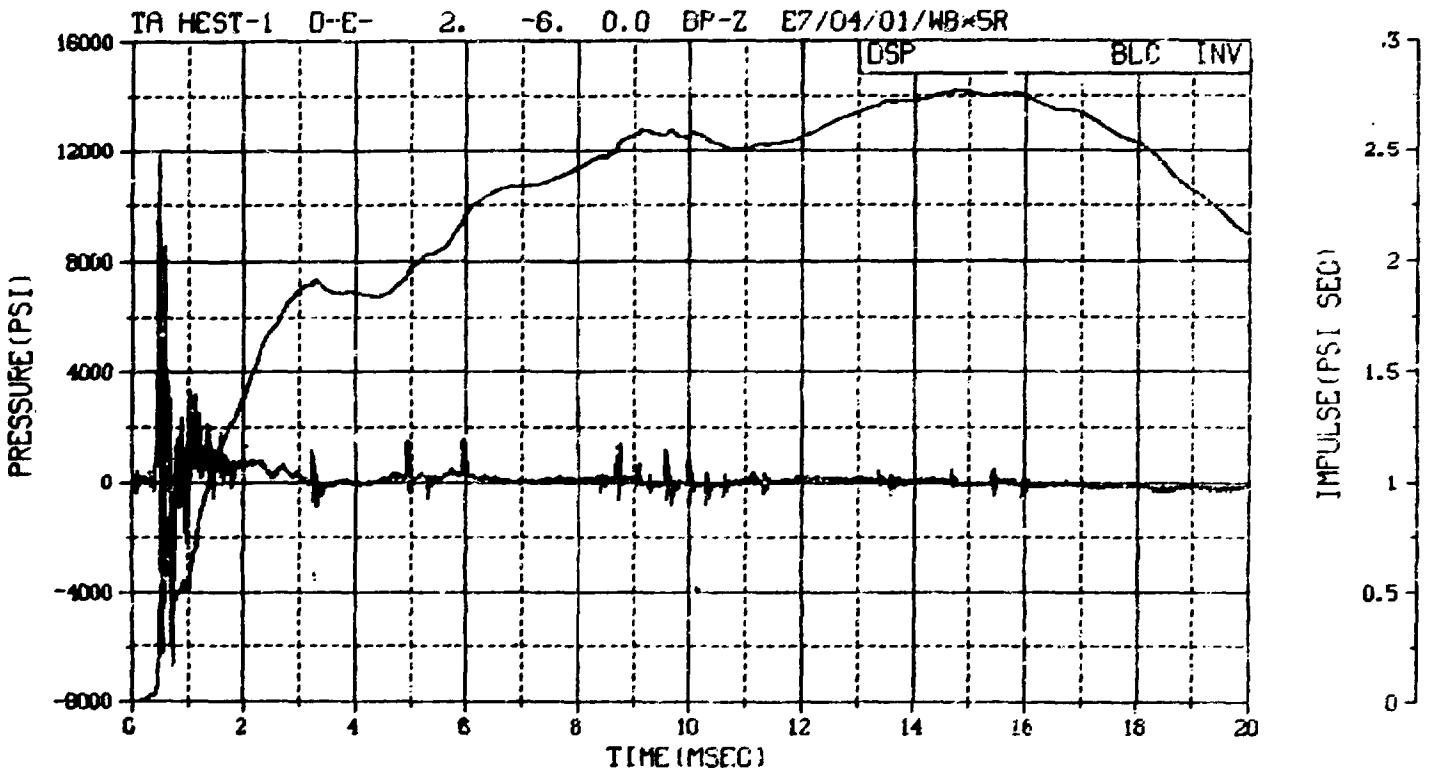

M.N. -90005	E.U. -0.000,5918.000	VSN-
TSKIP-10.350	DIGITS-0.000,298.000	TAPE26
S.R. -125.00 KHZ	3 49 PM,11 APR 78.	FILE-6

1

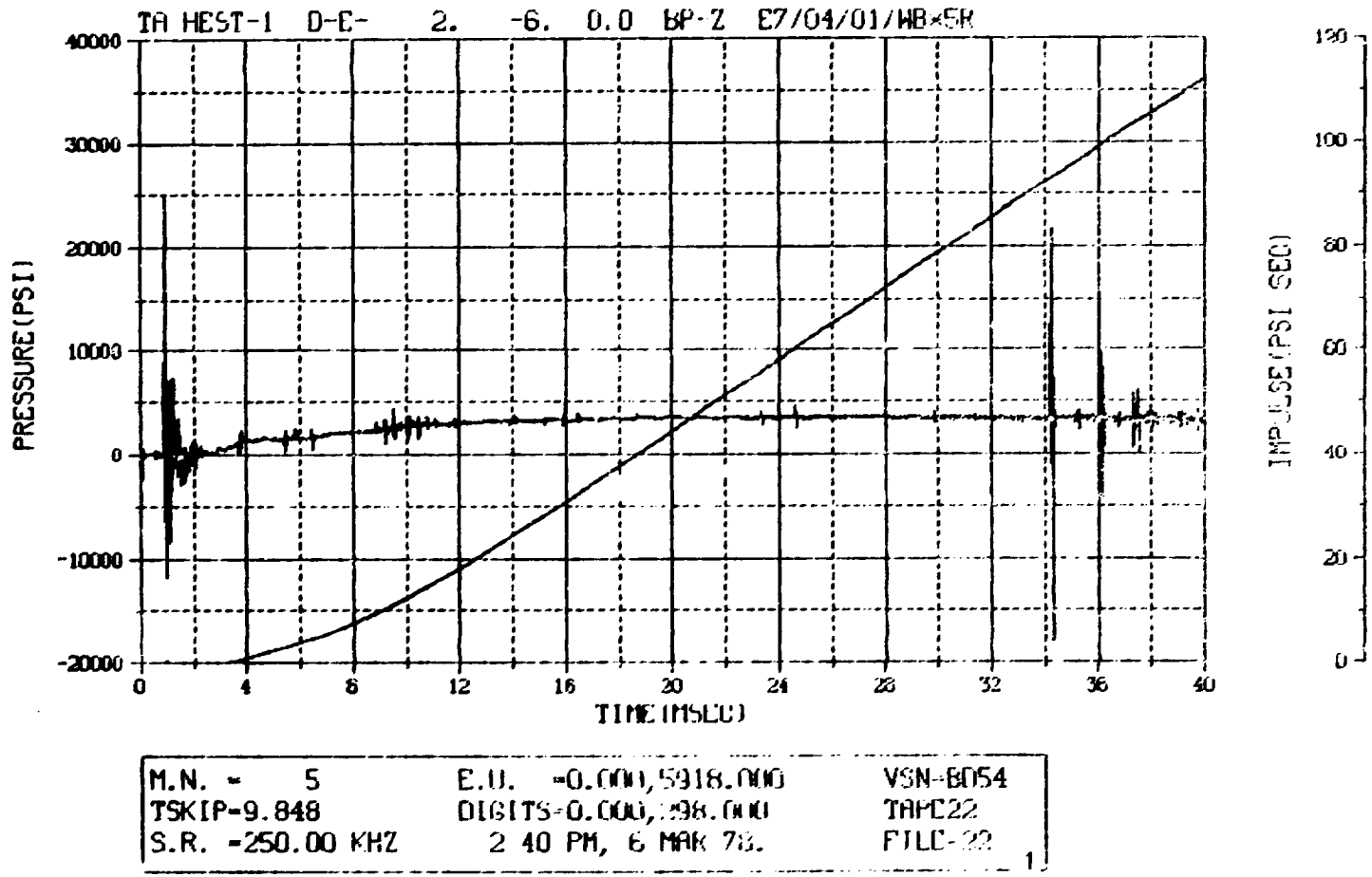
TA HEST-1 D-E- 2. -6. 0.0 BP-Z E7/04/01/WB×5R
PRESSURE(PSI)
IMPULSE(PSI SEC)
TIME(MSEC)
40000
30000
20000
10000
0
-10000
-20000
120
100
80
60
40
20
0
0
4
8
12
16
20
24
28
32
36
40
M.N. = 5
E.U. =0.000,5918.000
VSN=BD54
TSKIP=9.848
DIGITS=0.000,4096.000
TAPE22
S.R. =250.00 KHZ
2 40 PM, 6 MAR 78.
FILE=22
1

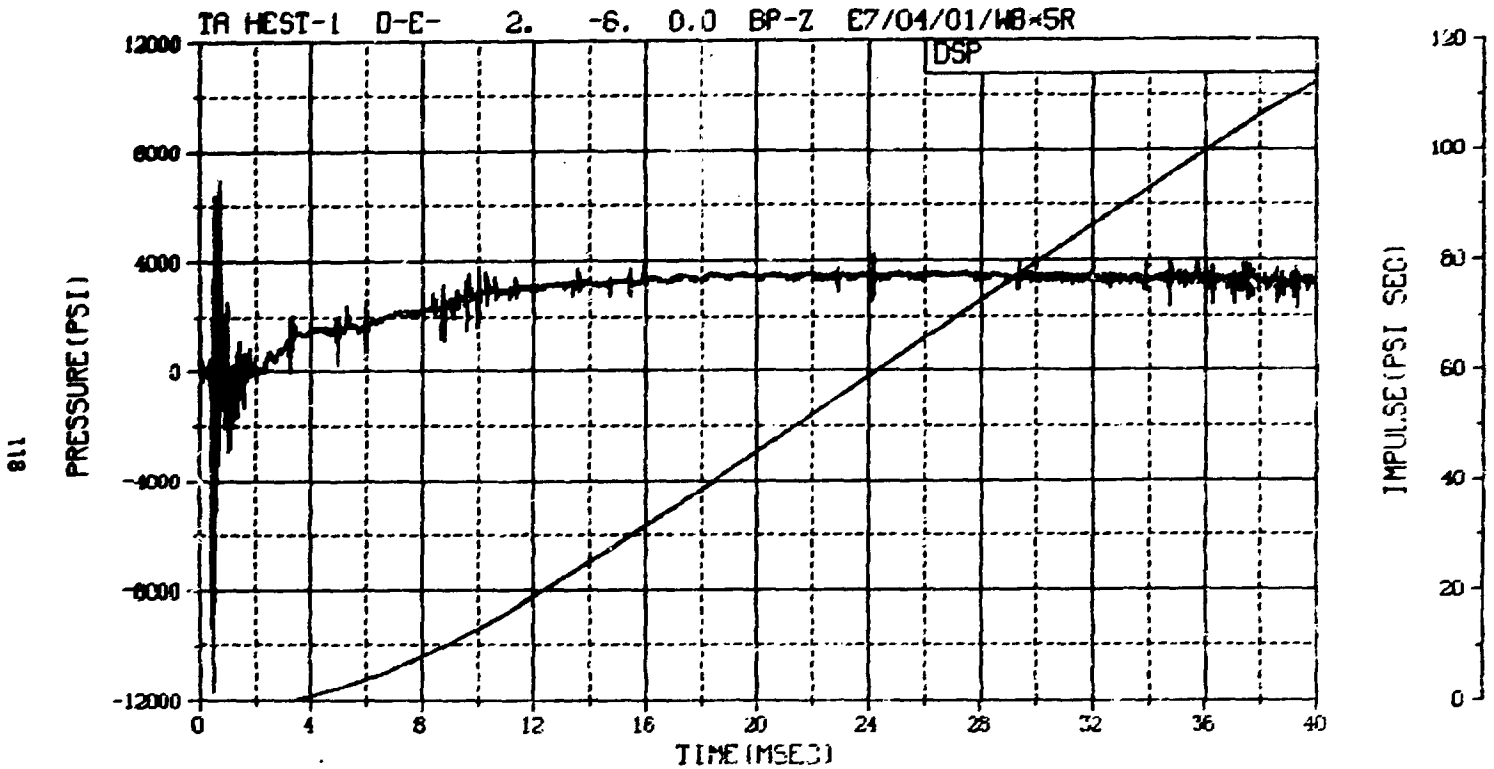

M.N. =80005	E.U. =0.000,5918.000	VSN=
TSKIP=10.350	DIGITS=0.000,298.000	TAPE25
S.R. =125.00 KHZ	3 49 PM,11 APR 78.	FILE=5

1

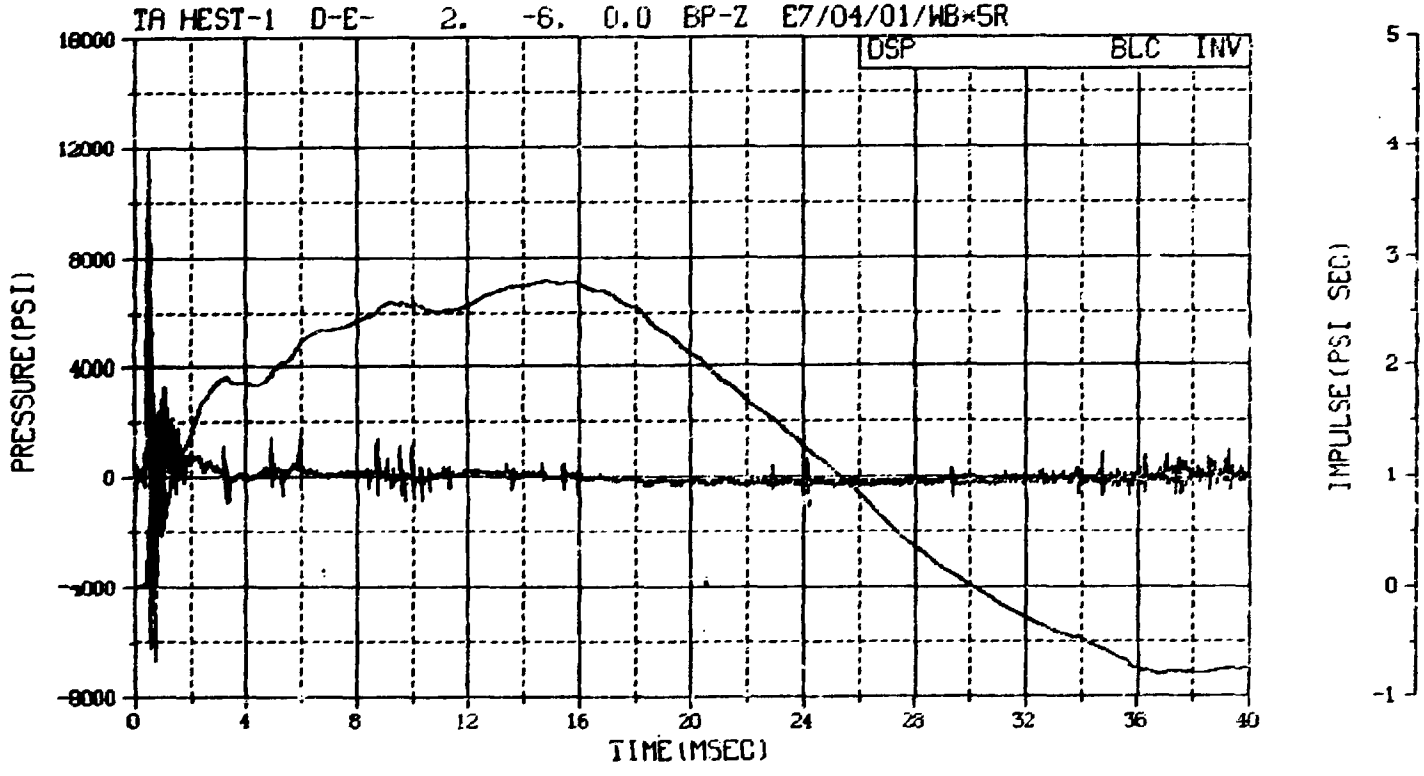

M.N. =90005	E.U. =0.000,5918.000	VSN=
TSKIP=10.350	DIGITS=0.000,298.000	TAPE26
S.R. =125.00 KHZ	3 49 PM,11 APR 78.	FILE=6

1

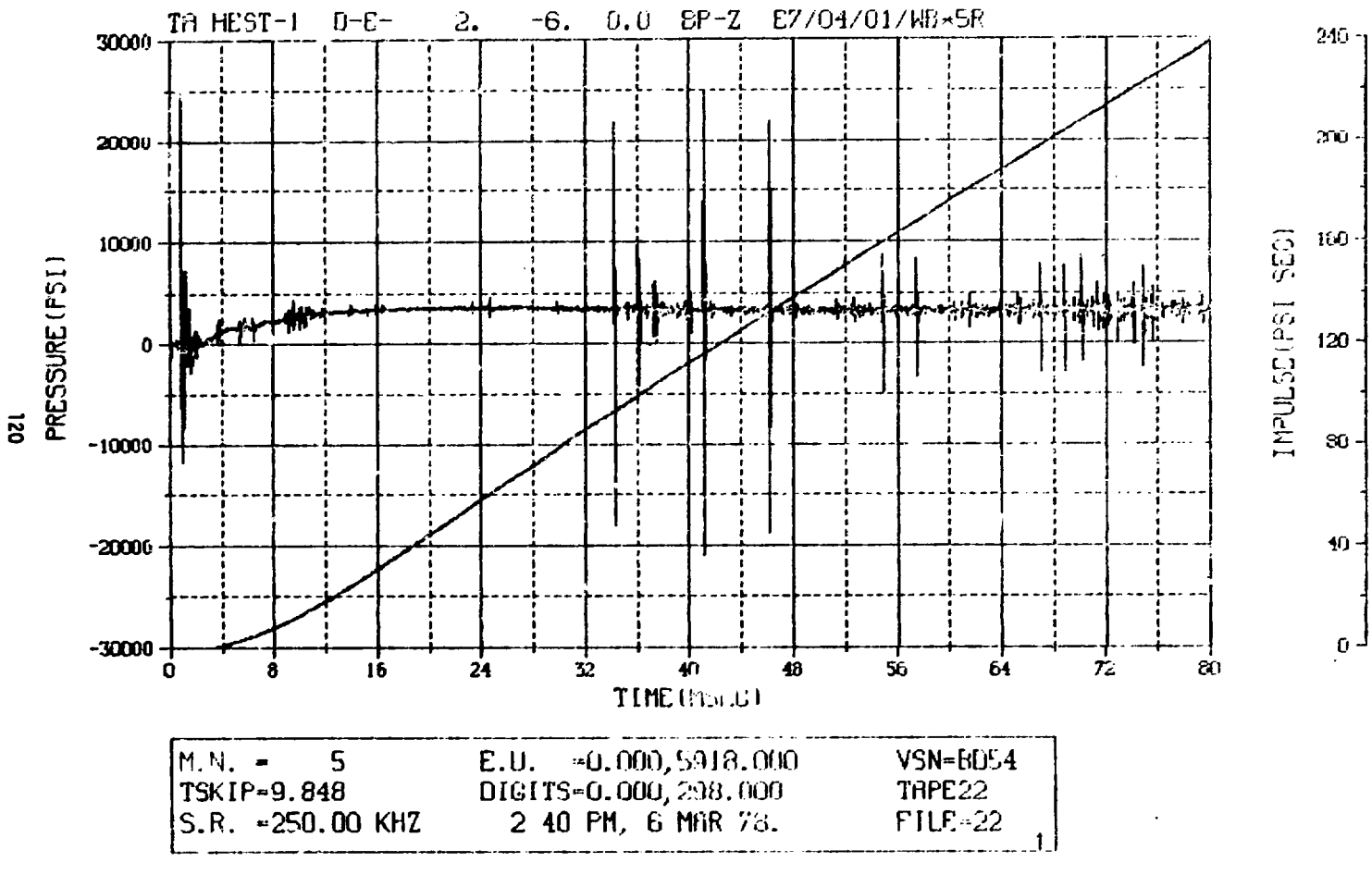
TA HEST-1 D-E- 2. -6. 0.0 BP-Z E7/04/01/WB×5R
PRESSURE(PSI)
30000
20000
10000
0
-10000
-20000
-30000
0
8
16
24
32
40
48
56
64
72
80
TIME(MSEC)
IMPULSE(PSI SEC)
240
200
160
120
80
40
0
M.N. = 5
E.U. =0.000,5918.000
VSN=BD54
TSKIP=9.848
DIGITS=0.000,208.000
TAPE22
S.R. =250.00 KHZ
2 40 PM, 6 MAR 78.
FILE=22

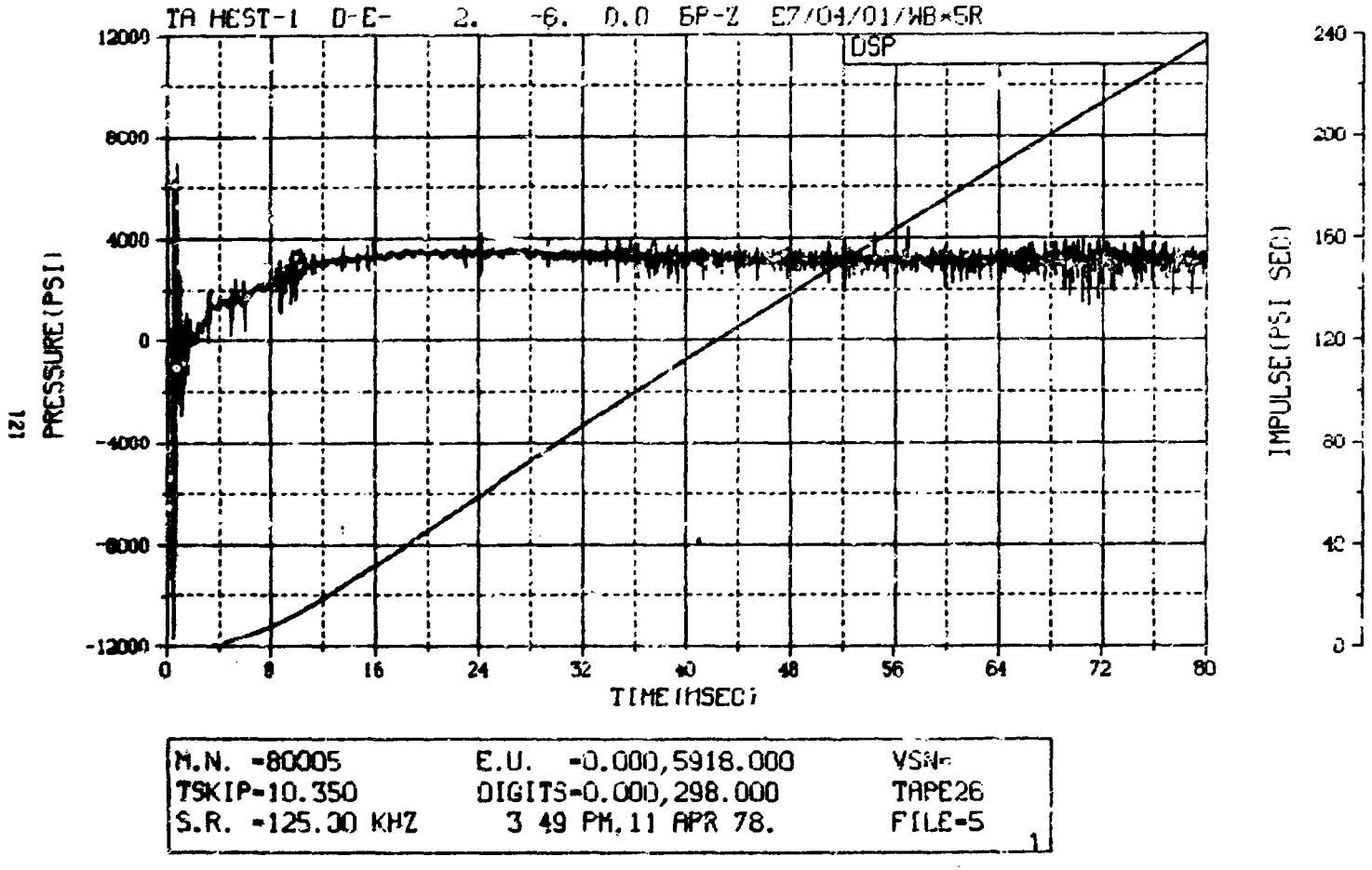
TA HEST-1 D-E- 2. -6. 0.0 BP-Z 87/04/01/WB*SR
DSP
12000
8000
4000
0
-4000
-8000
-12000
PRESSURE(PSI)
121
0
8
16
24
32
40
48
56
64
72
80
TIME(MSEC)
240
200
160
120
80
40
0
IMPULSE(PSI SEC)
M.N. =80005
E.U. =0.000,5918.000
VSN=
TSKIP=10.350
DIGITS=0.000,298.000
TAPE26
S.R. =125.00 KHZ
3 49 PM,11 APR 78.
FILE=5
1

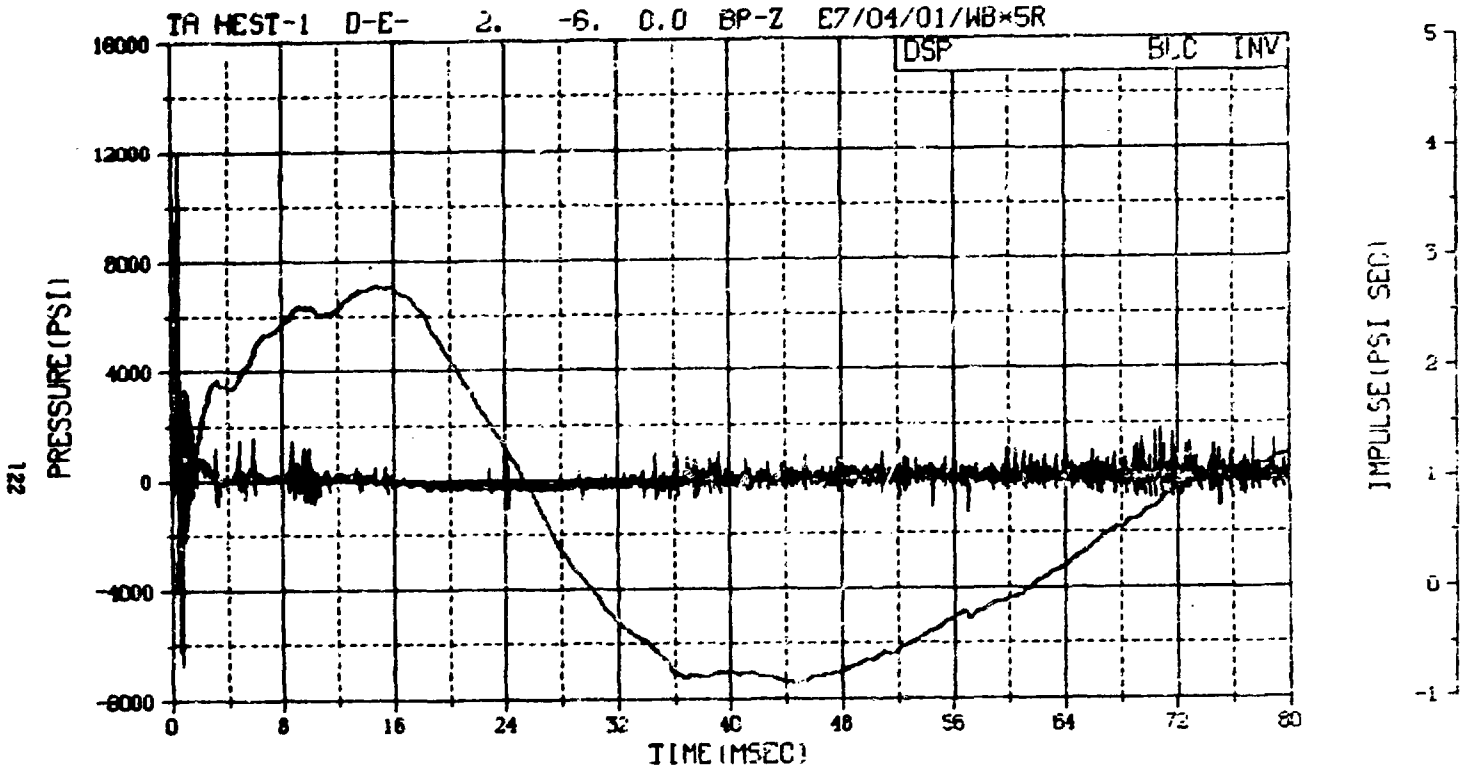

M.N. =90005	E.U. =0.000,5918.000	VSN=
TSKIP=10.350	DIGITS=0.000,298.000	TAPE26
S.R. =125.00 KHZ	3 49 PM,11 APR 78.	FILE=6

1

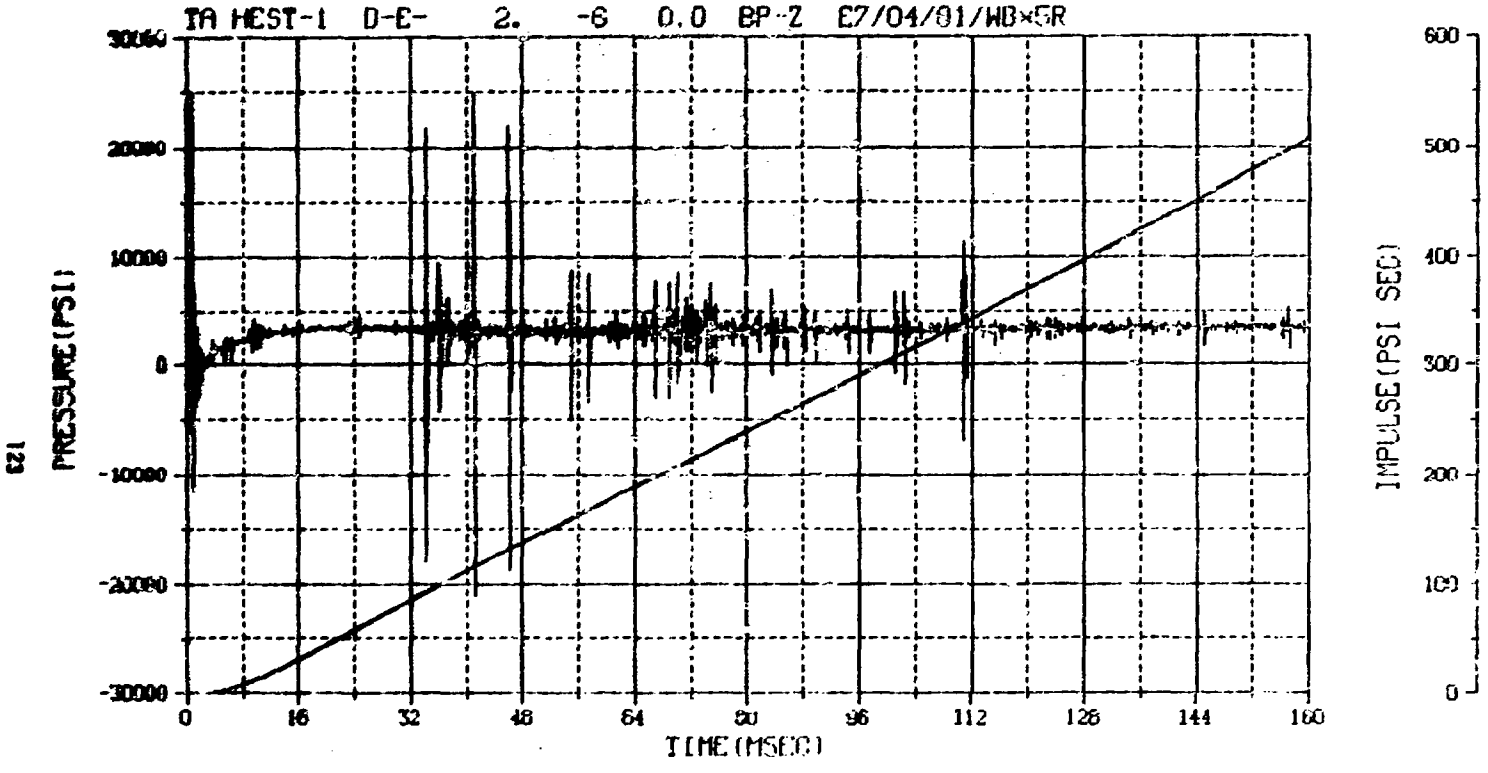

M.N. = 5	C.U. -40.000, 5418.000	VSN=BD54
TSKIP=9.848	DIGITS=0.000, 238.000	TAPE22
S.R. =250.00 KHZ	2.40 PM, 6 MAR 76.	FILE=22

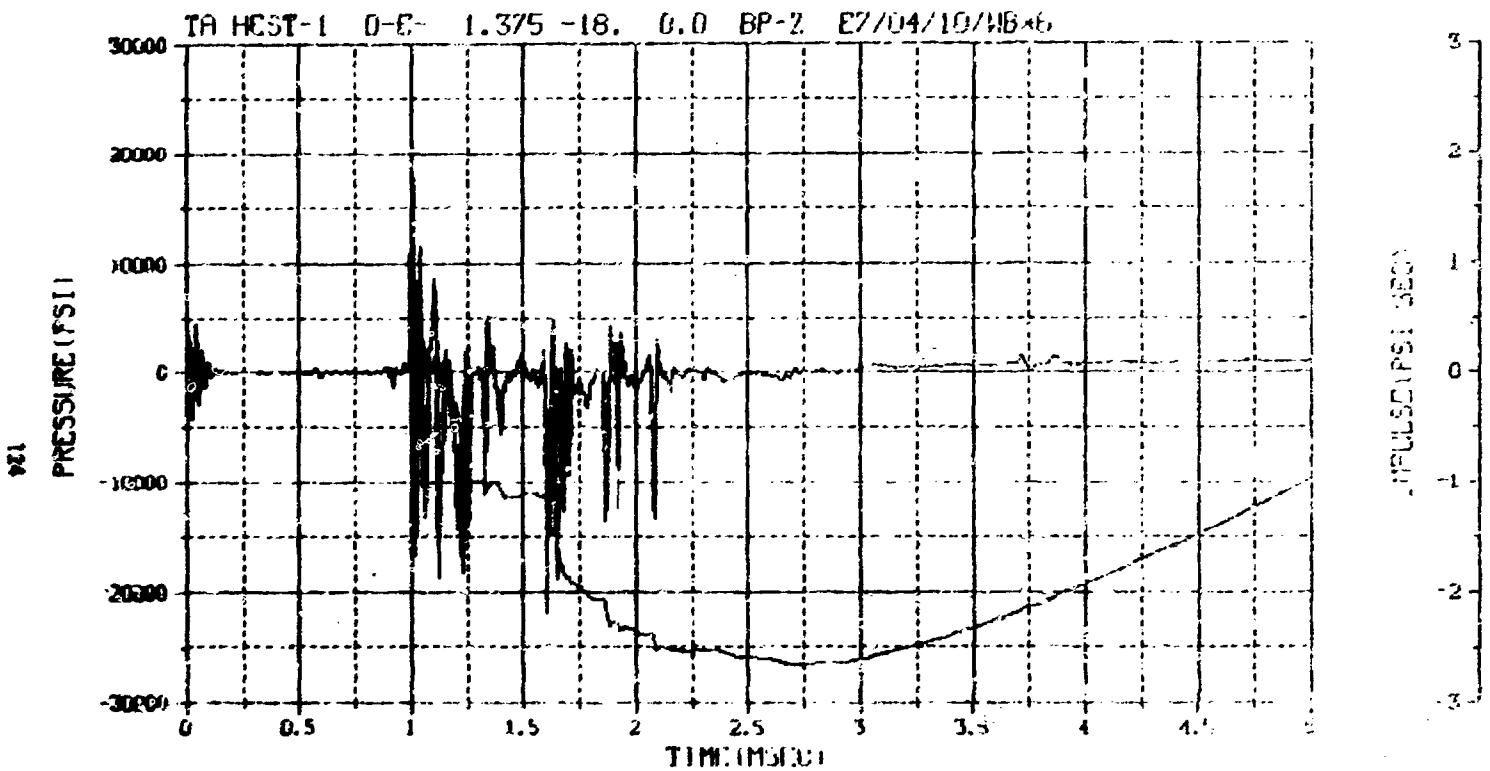

M.N. = 6	E.U. =0.000,4924.000	VSN=BD54
TSKIP=9.848	DIGITS=0.000,565.940	TYPE22
S.R. =250.00 KHZ	2 40 PR, 6 MHR 76.	FILE =32

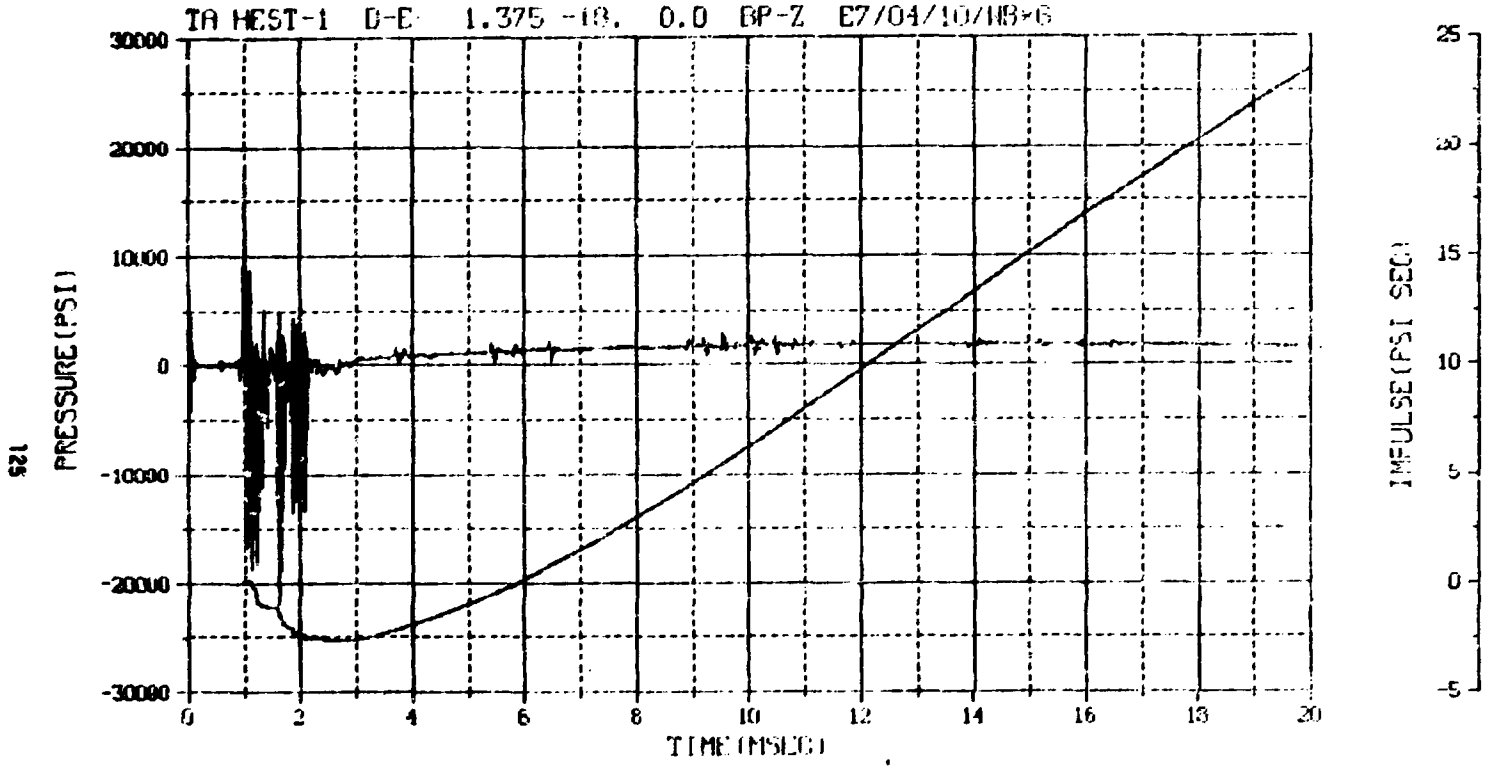
TA HEST-1 D-E 1.375 -18. 0.0 BP-Z E7/04/10/NB=6
PRESSURE(PSI)
125
30000
20000
10000
0
-10000
-20000
-30000
0
2
4
6
8
10
12
14
16
18
20
TIME(MSEC)
IMPULSE(PSI SEC)
25
20
15
10
5
0
-5
M.N. = 6
C.U. =0.000,5924.000
VSN=BD54
TSKIP=9.848
DIGITS=0.000,'55.'48
TAPE22
S.R. =250.00 KHZ
2 40 PM, 6 MAR 78.
PTLE=32
1

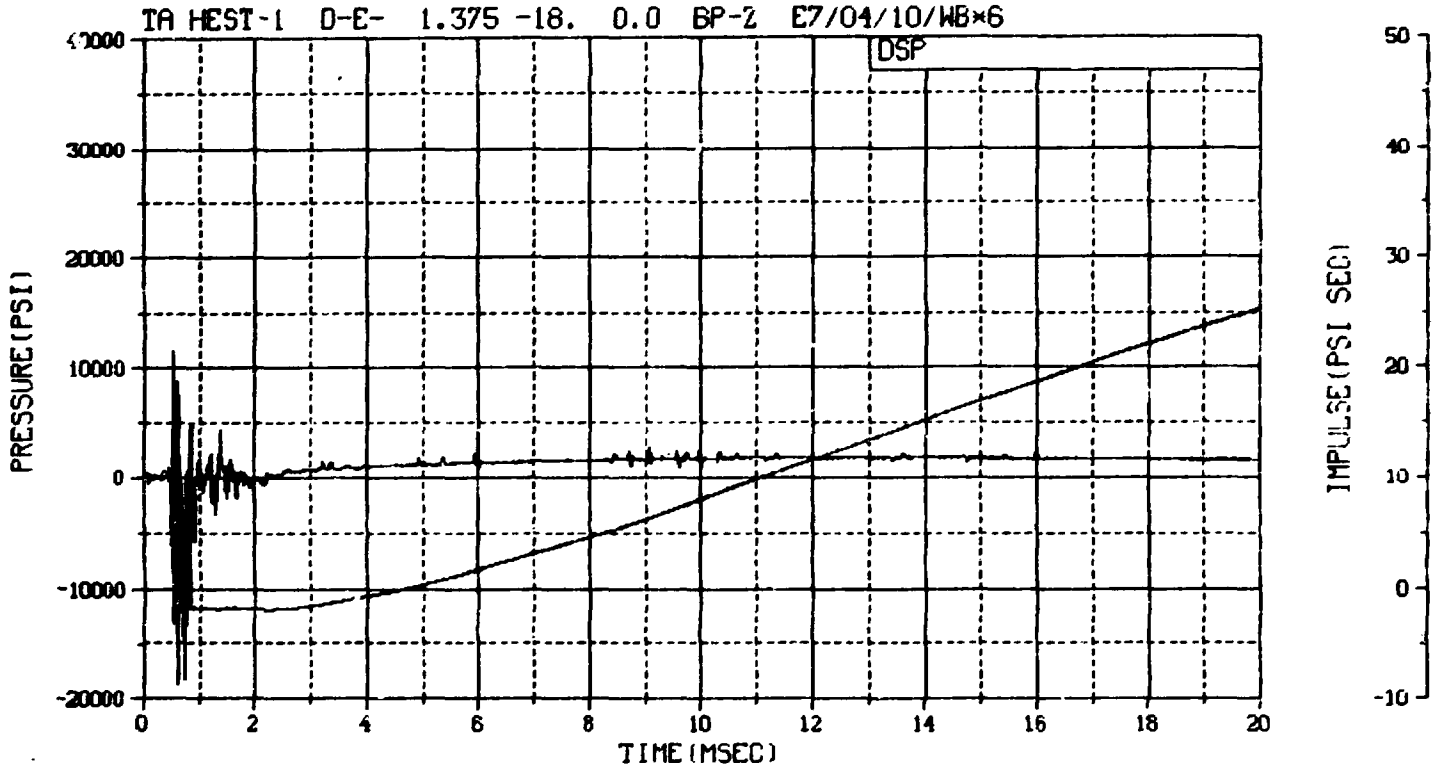

M.N. -80006	E.U. -0.000,5924.000	VSN-
TSKIP-10.350	DIGITS-0.000,555.500	TAPE26
S.R. -125.00 KHZ	3 49 PM,11 APR 78.	FILE-13

1

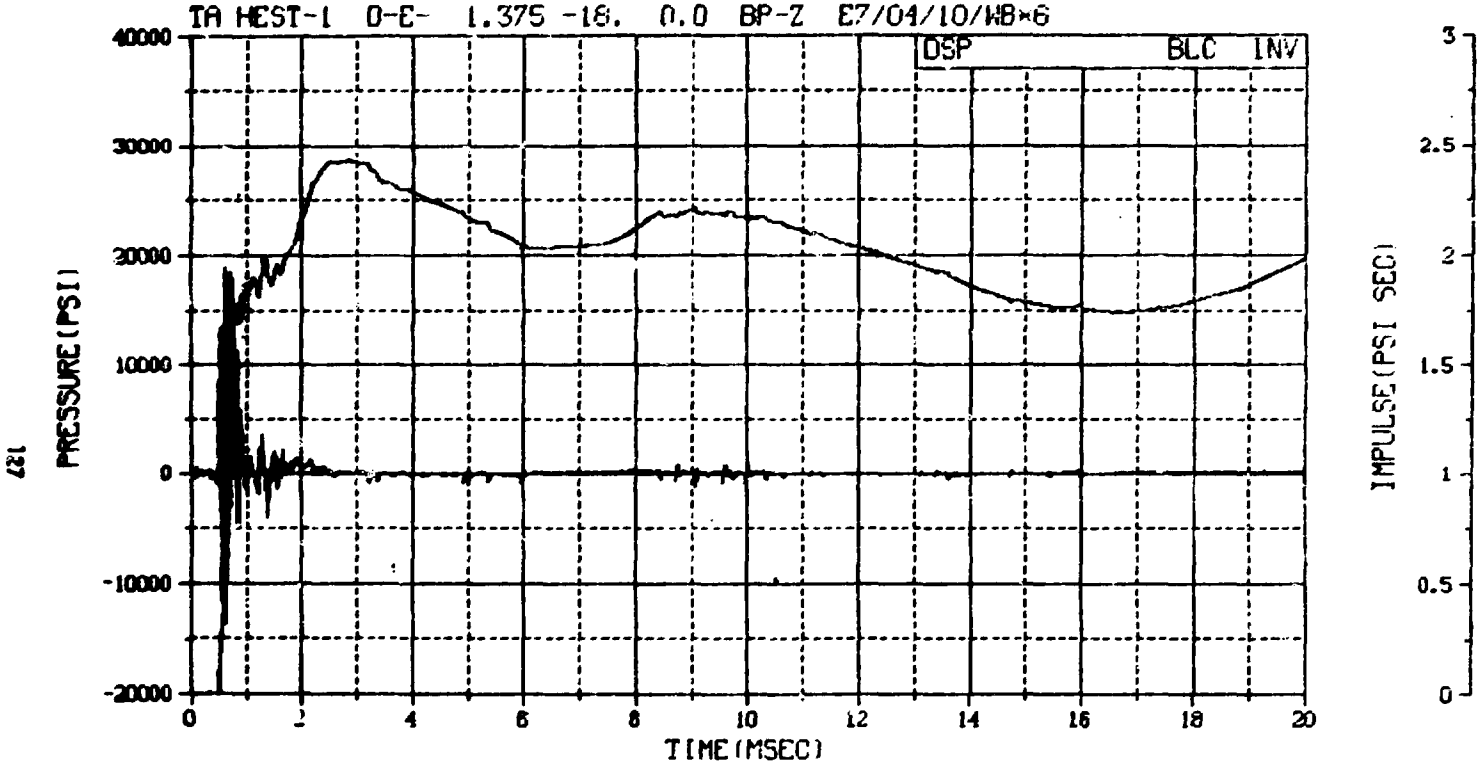

M.N. =90006	E.U. =0.000,5924.000	VSN=
TSKIP=10.350	DIGITS=0.000,555.500	TAPE26
S.R. =125.00 KHZ	3 49 PM,11 APR 78.	FILE=14

1

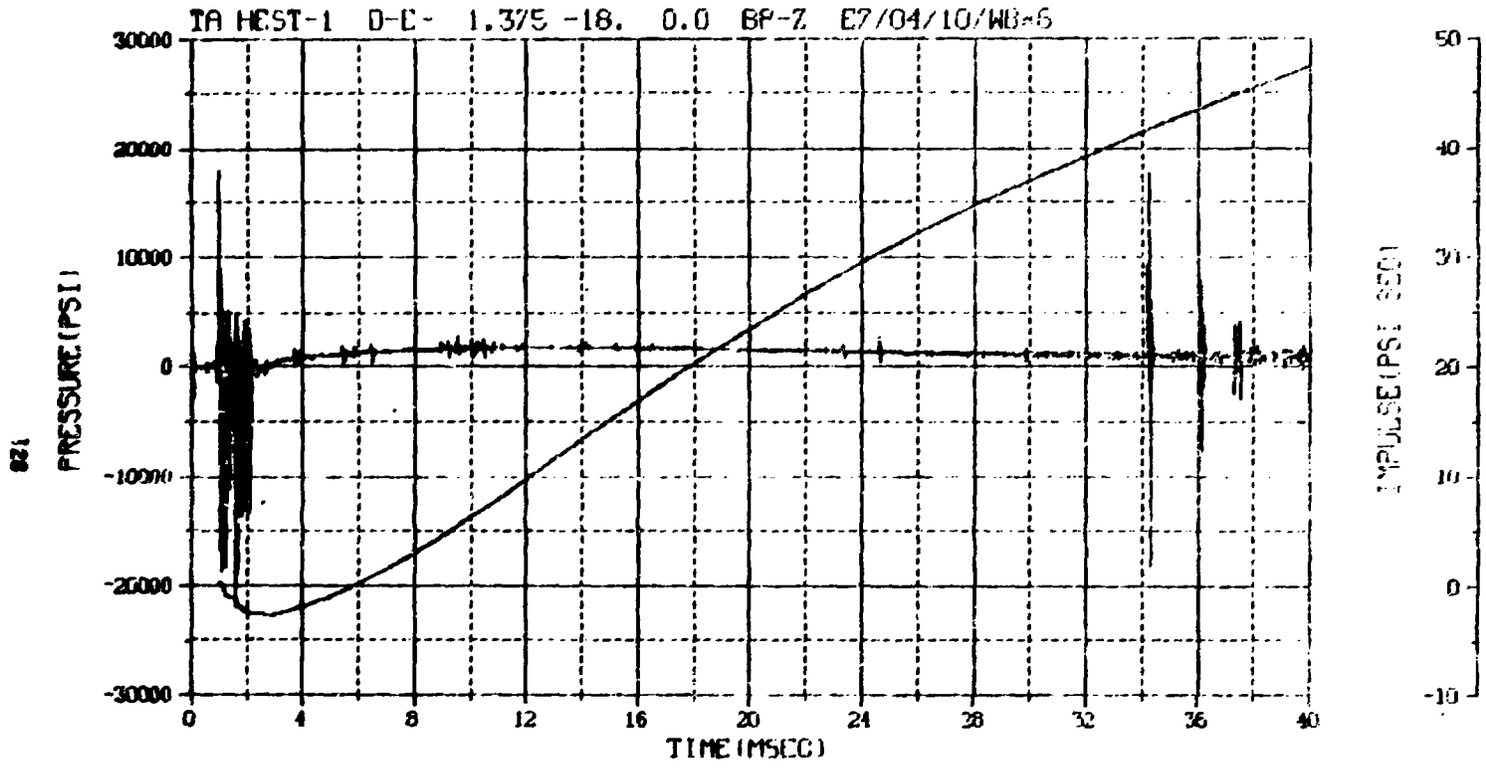

M.N. = 6	E.U. =0.000,5024.000	VSN=0054
TSKIP=9.848	DIGITS=0.000,555.500	TAPE22
S.R. =250.00 KHZ	2 40 PM, 6 MAR 78.	FILE=32

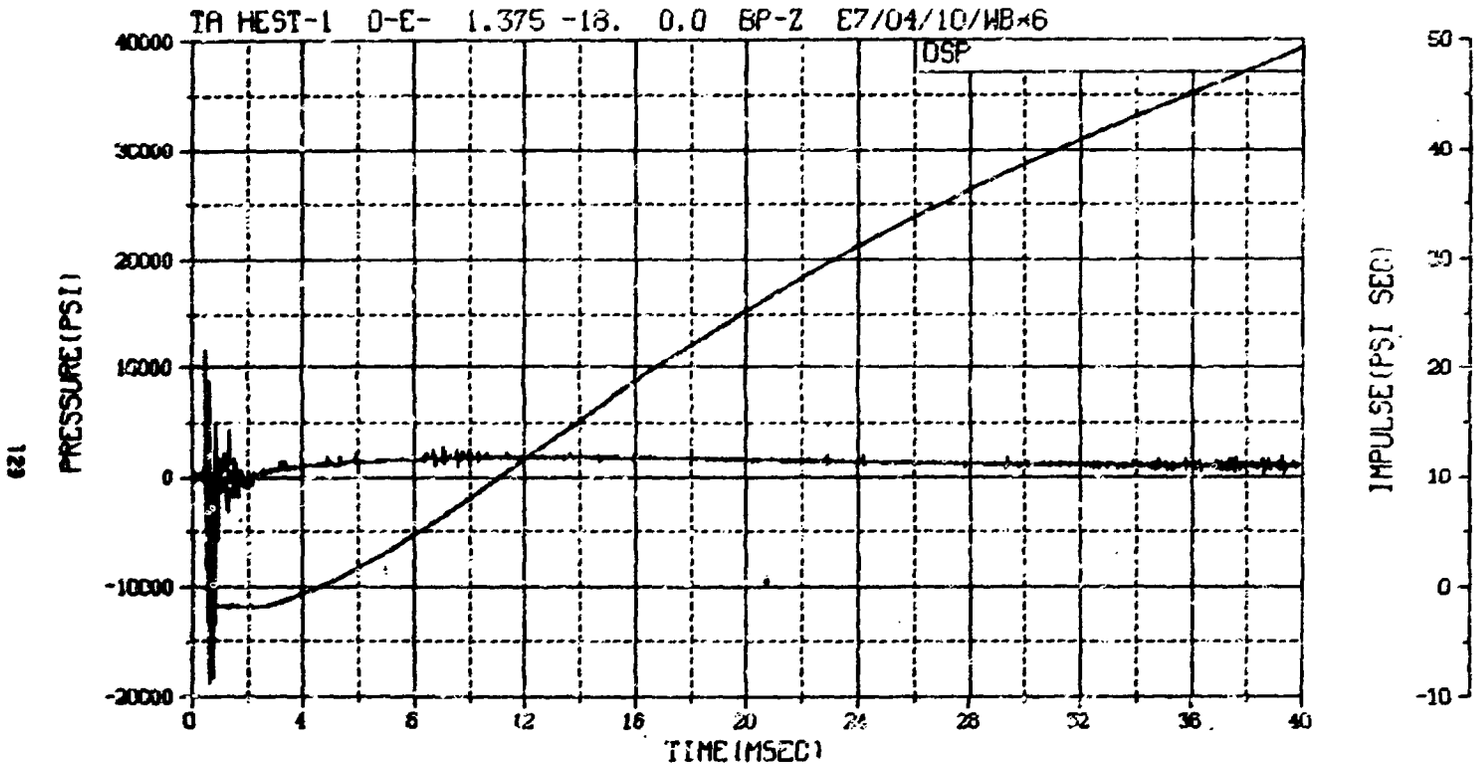

M.N. -80006	E.U. -0.000,5924.000	VSN=
TSKIP=10.350	DIGITS=0.000,555.500	TAPE26
S.R. =125.00 KHZ	3 49 PM, 11 APR 78.	FILE=13

1

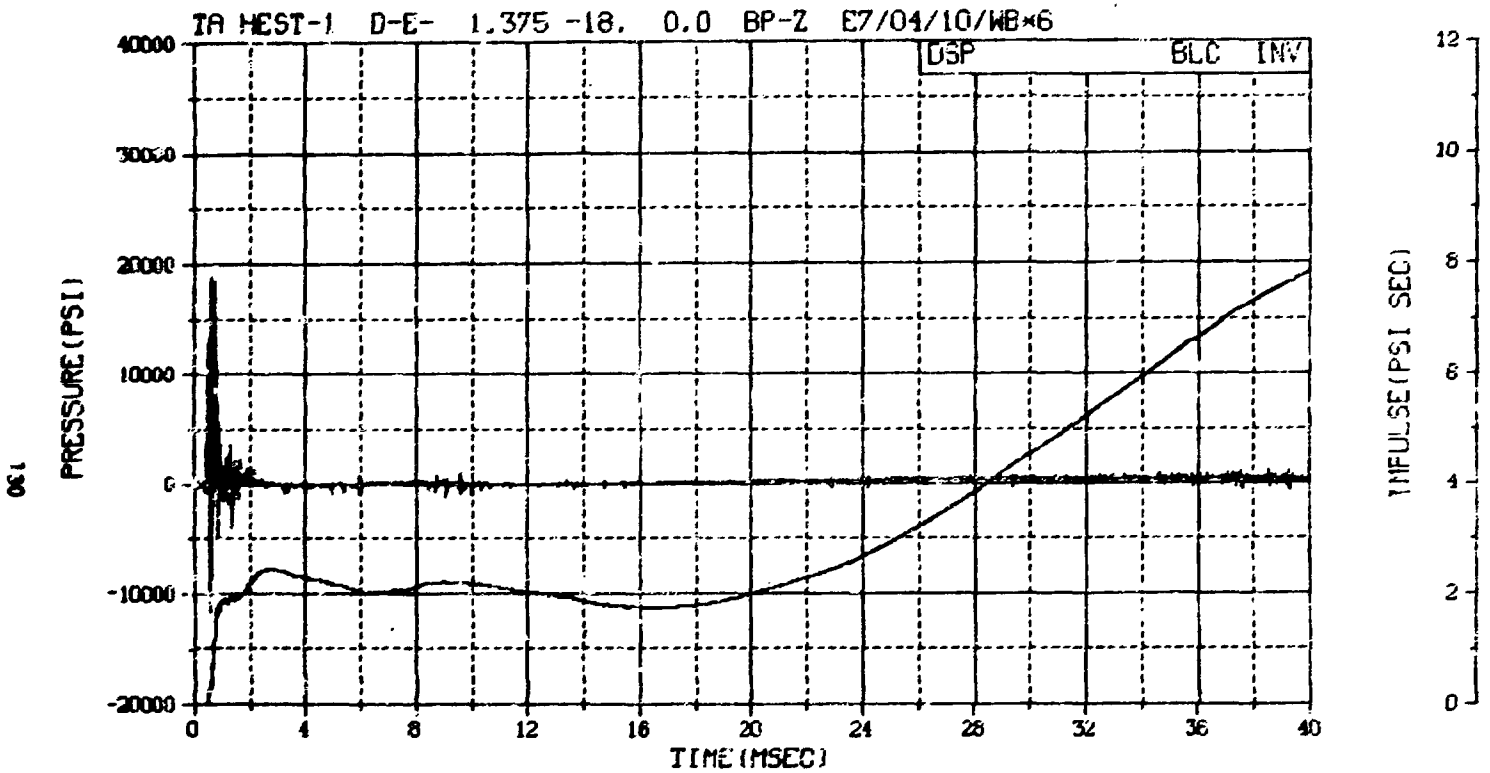

M.N. -90006	E.U. -0.000,5924.000	VSN=
TSKIP=10.350	DIGITS=0.000,555.500	TAPE26
S.R. =125.00 KHZ	3 49 PM, 11 APR 78.	FILE=14

1

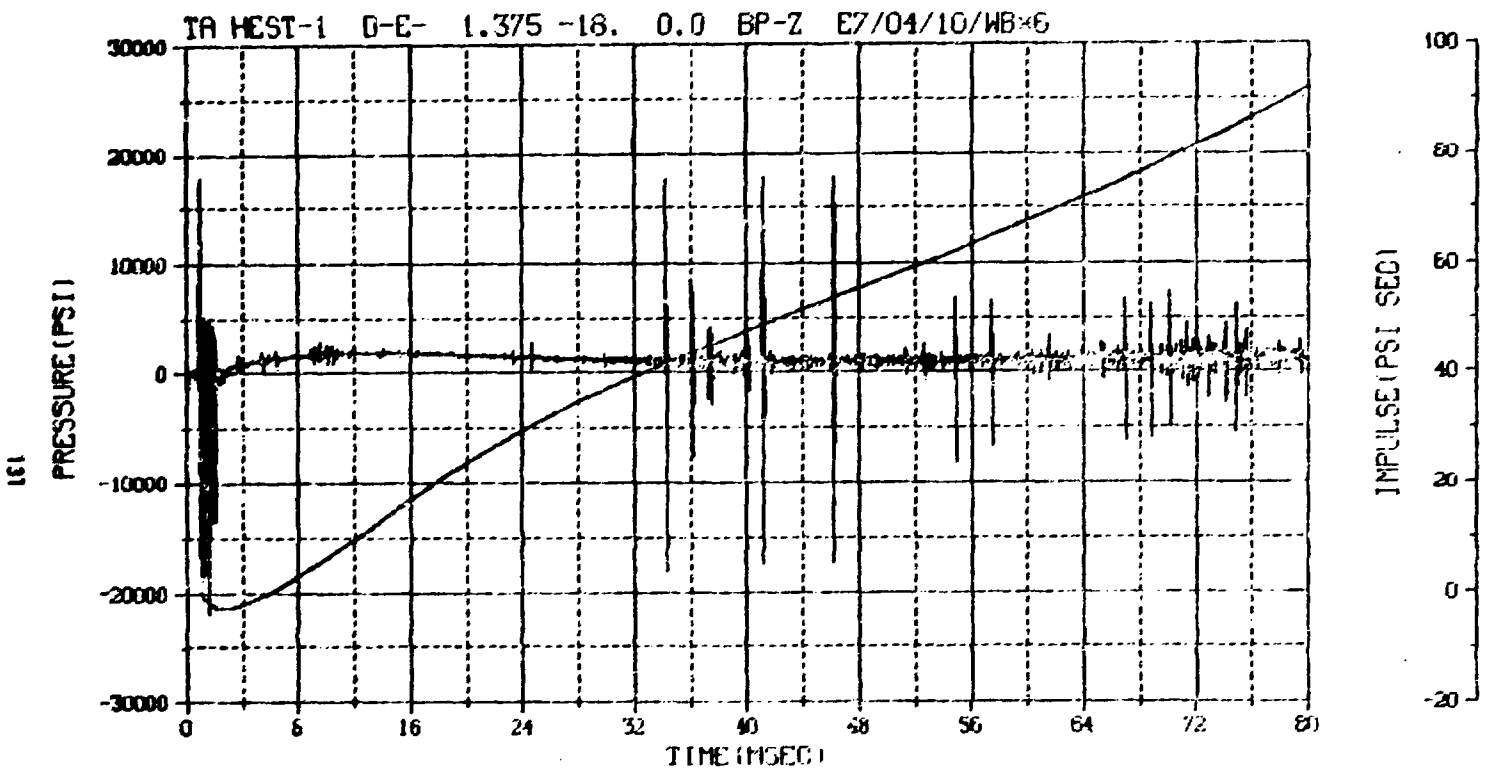

M.N. = 6	E.U. =0.000,5424.000	VSN=8054
TSKIP=9.848	DIGITS=0.000,565.500	TAPE22
S.R. =250.00 KHZ	2 40 PM, 6 MAR 78	FILE=32

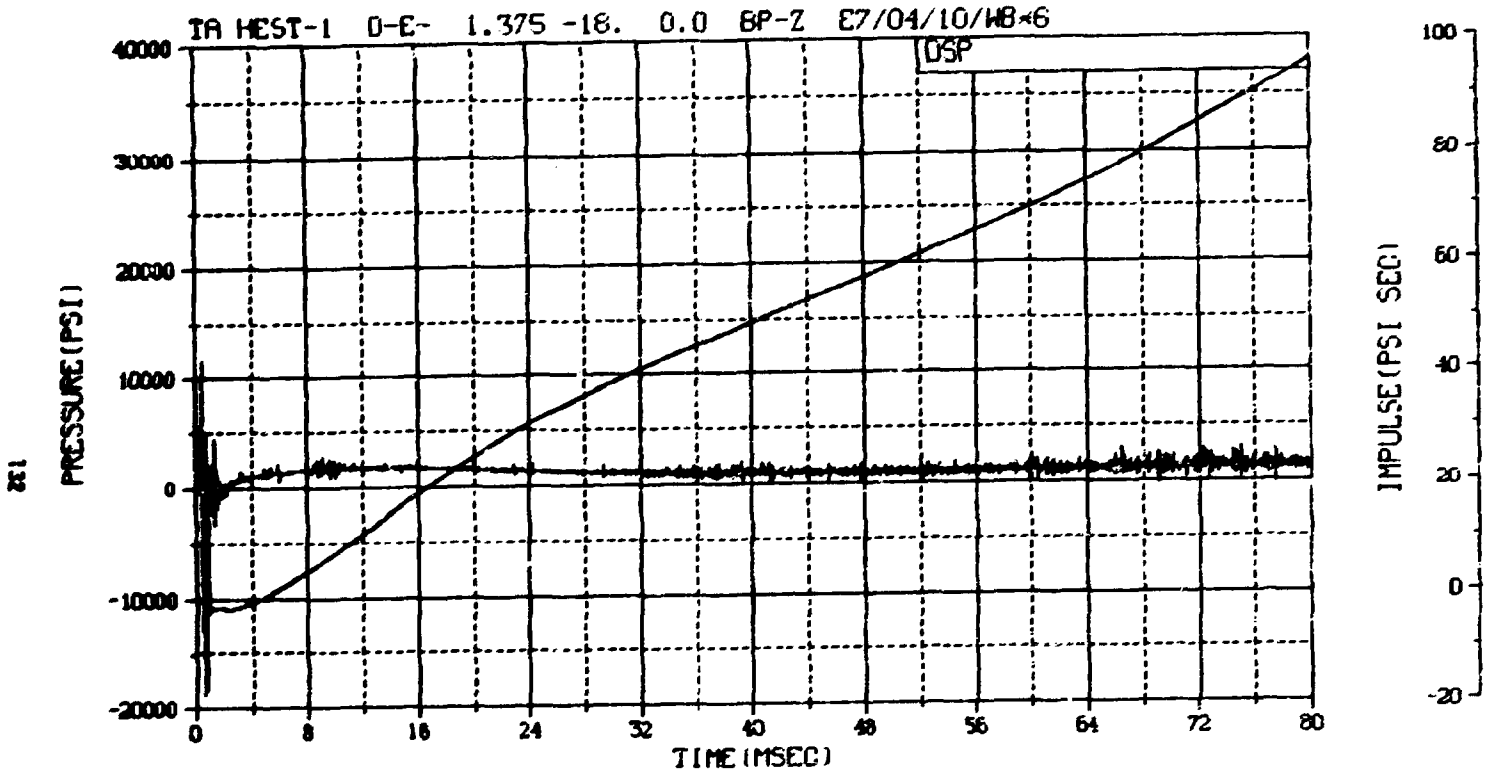

M.N. -80006	E.U. -0.000,5924.000	VSN=
TSKIP=10.350	DIGITS=0.000,555.500	TAPE26
S.R. =125.00 KHZ	3 49 PM,11 APR 78.	FILE=13

1

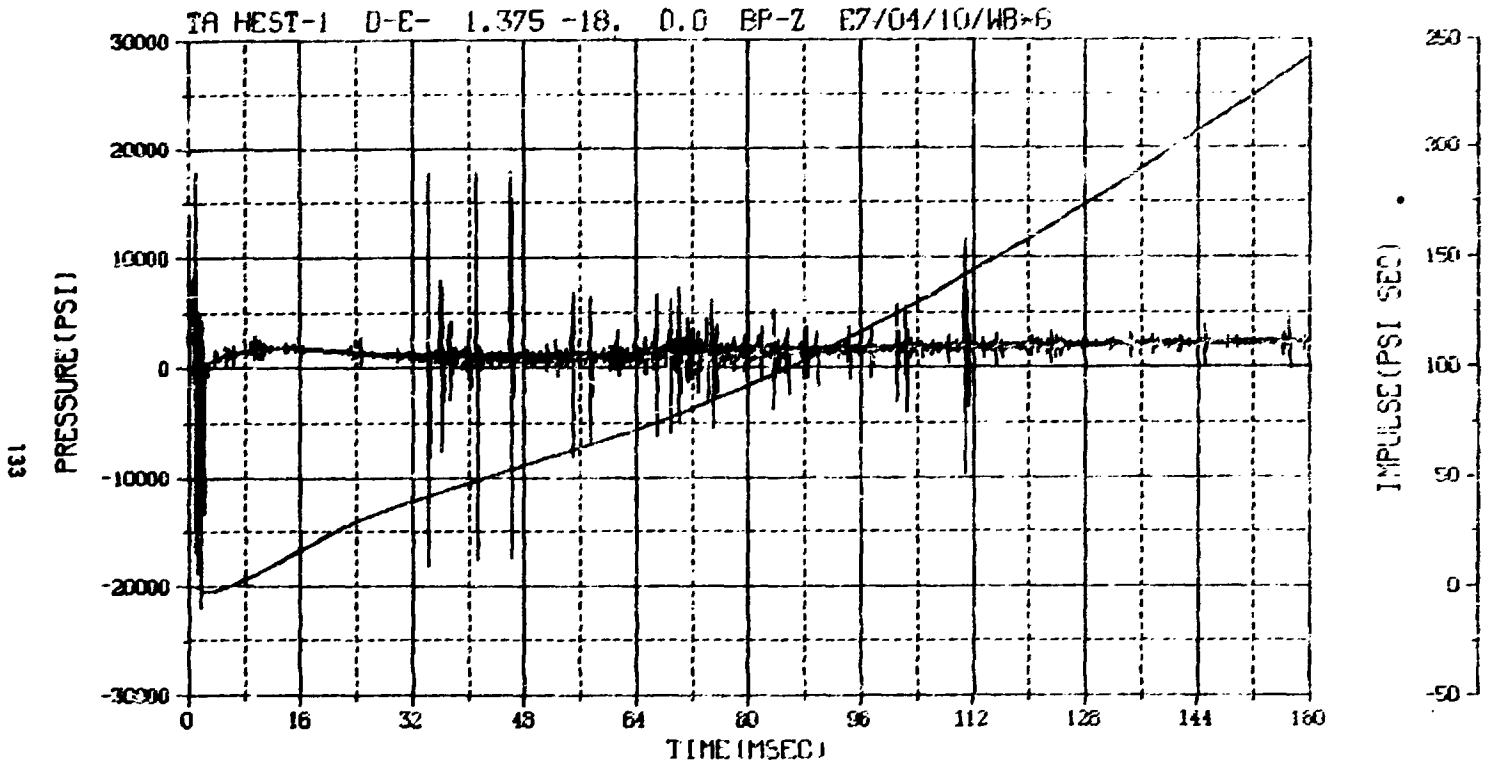

M.N. = 6	E.U. =0.000,5924.000	VSN=8054
TSKIP=9.848	DIGITS=0.000,555.500	TAPE22
S.R. =250.00 KHZ	2 40 PM, 6 MAR 78.	FILE=32

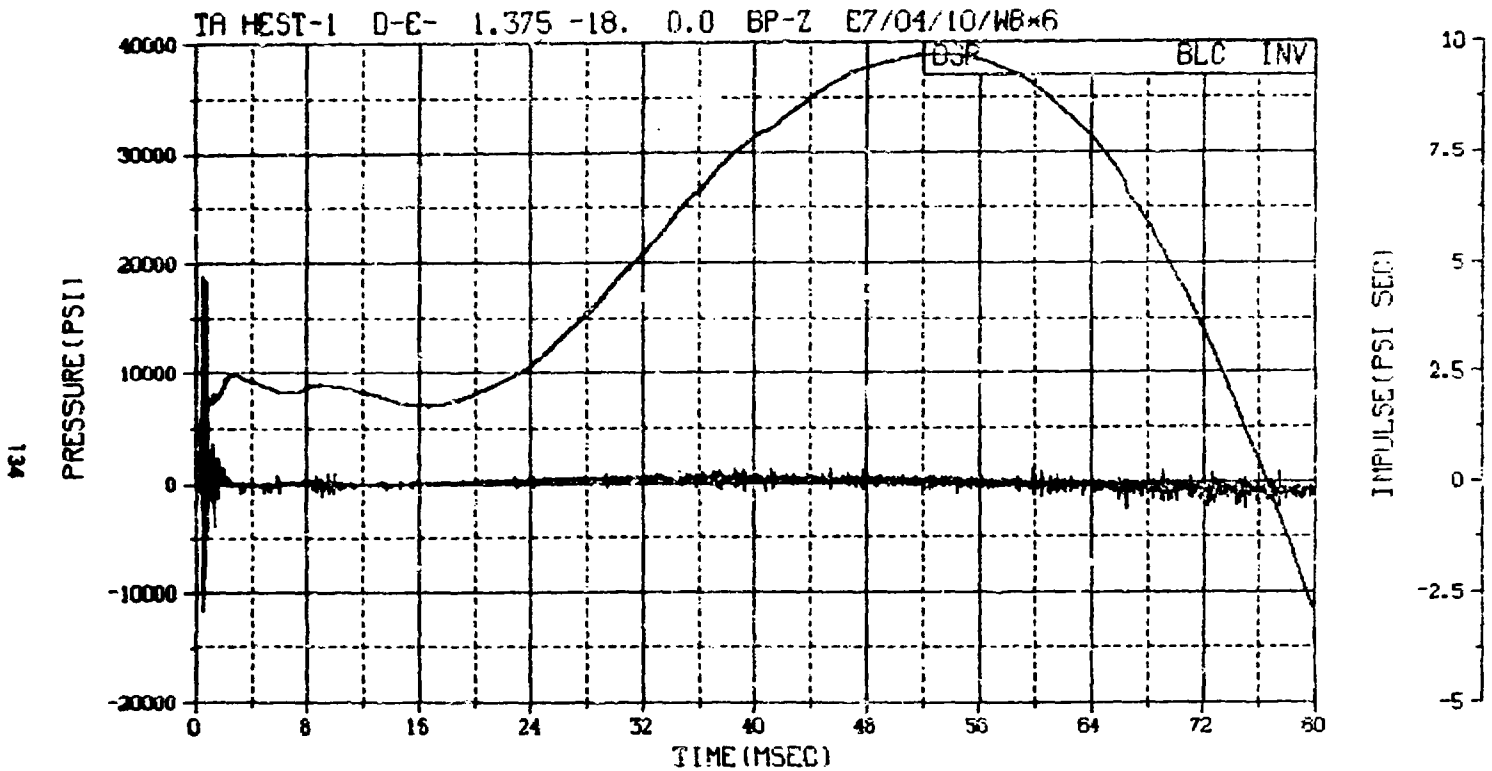
TA HEST-1 D-E- 1.375 -18. 0.0 BP-Z E7/04/10/W8×6
DSP
BLC INV
PRESSURE(PSI)
IMPULSE(PSI SEC)
TIME(MSEC)
40000
30000
20000
10000
0
-10000
-20000
10
7.5
5
2.5
0
-2.5
-5
0
8
16
24
32
40
48
56
64
72
80
M.N. =90006
E.U. =0.000,5924.000
VSN=
TSKIP=10.350
DIGITS=0.000,535.500
TAPE26
S.R. =125.00 KHZ
3 49 PM,11 APR 78.
FILE=14

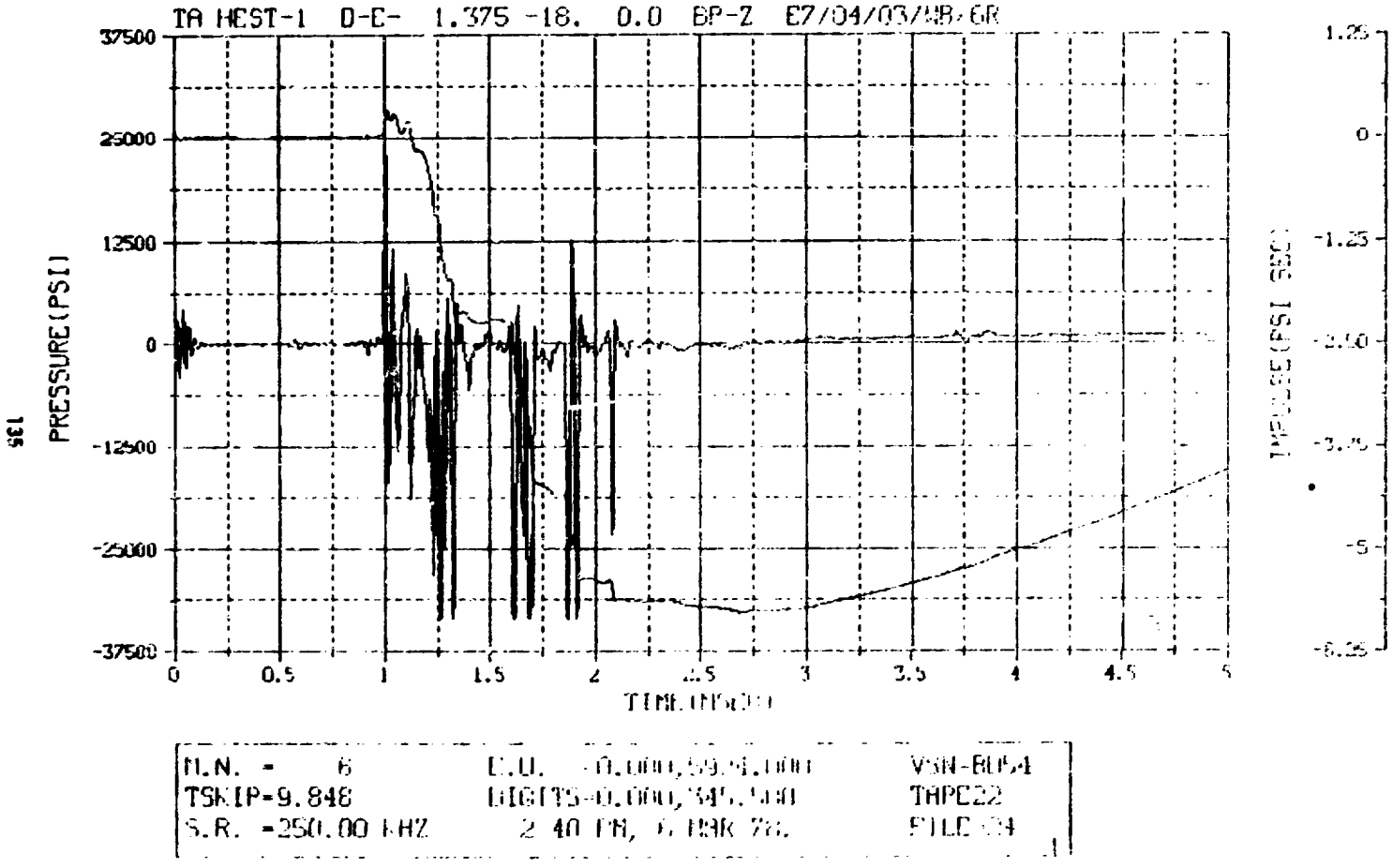
TA WEST-1 D-E- 1.375 -18. 0.0 BP-Z E7/04/03/WB-6R
37500
25000
12500
0
-12500
-25000
-37500
PRESSURE(PSI)
0
0.5
1
1.5
2
2.5
3
3.5
4
4.5
5
1.25
0
-1.25
-2.5
-3.75
-5
-6.25
N.N. = 6
TSKIP=9.848
S.R. =250.00 HZ
VSN-BUF4
TAPE22

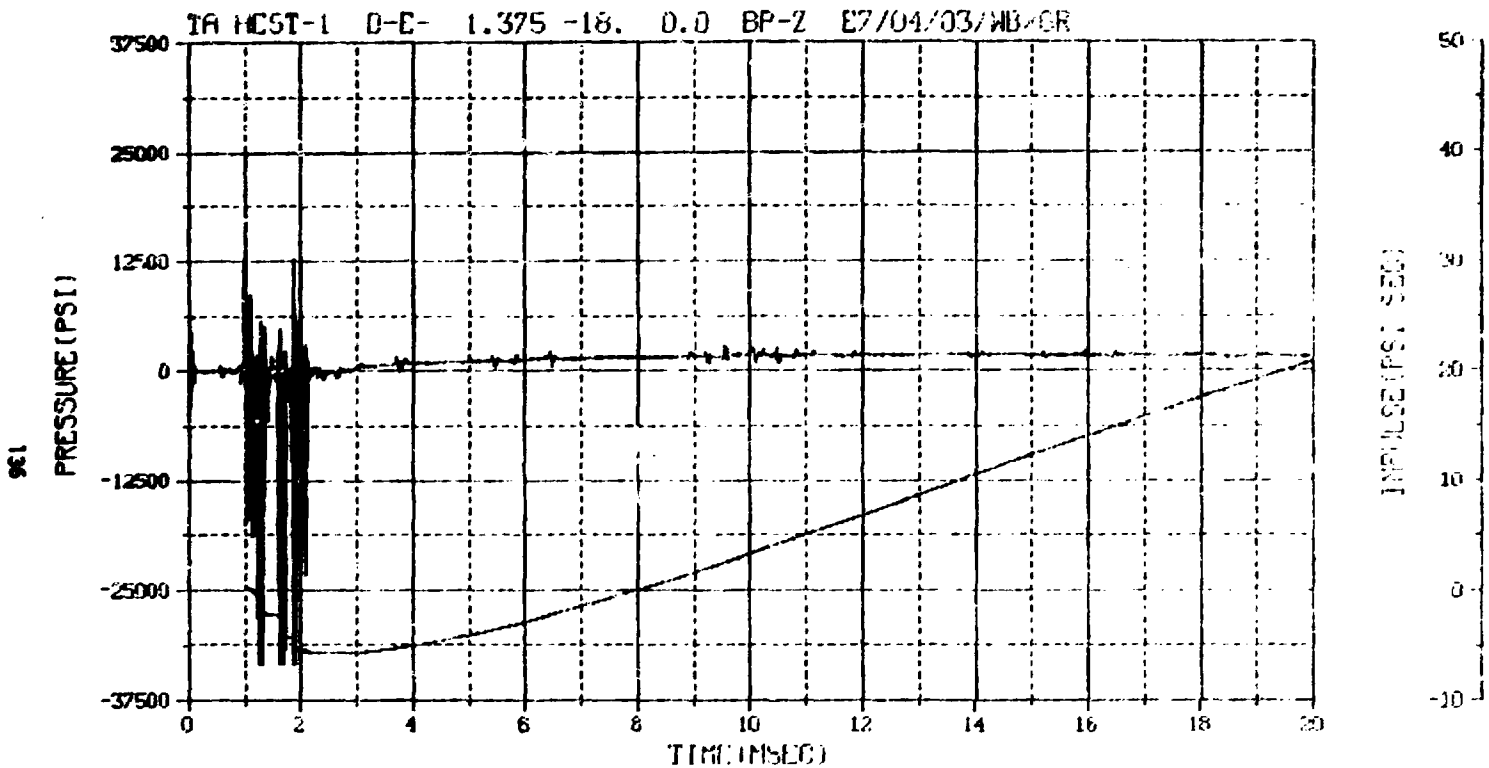

M.N. = 6	E.U. =0.000,5924.000	VSN=0054
TSKIP=9.848	DIGITS=0.000,345.000	TAPE22
S.R. =250.00 KHZ	2 40 PM, 6 MAR 78.	FILE=24

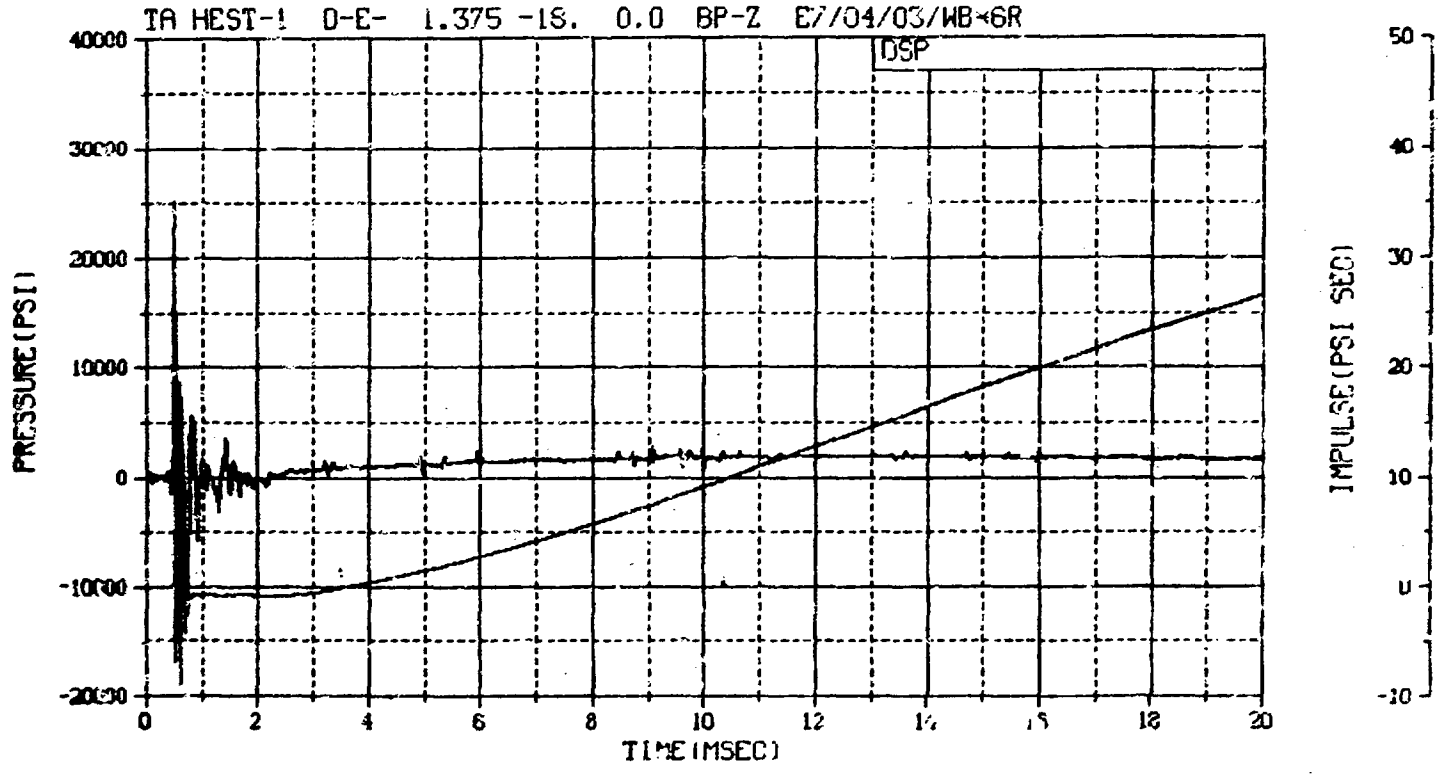

M.N. =80006	E.U. =0.000,5924.000	VSN=
TSKIP=10.350	DIGITS=0.000,345.500	TAPE26
S.R. =125.00 KHZ	3 49 PM,11 APR 78.	FILE=7

1

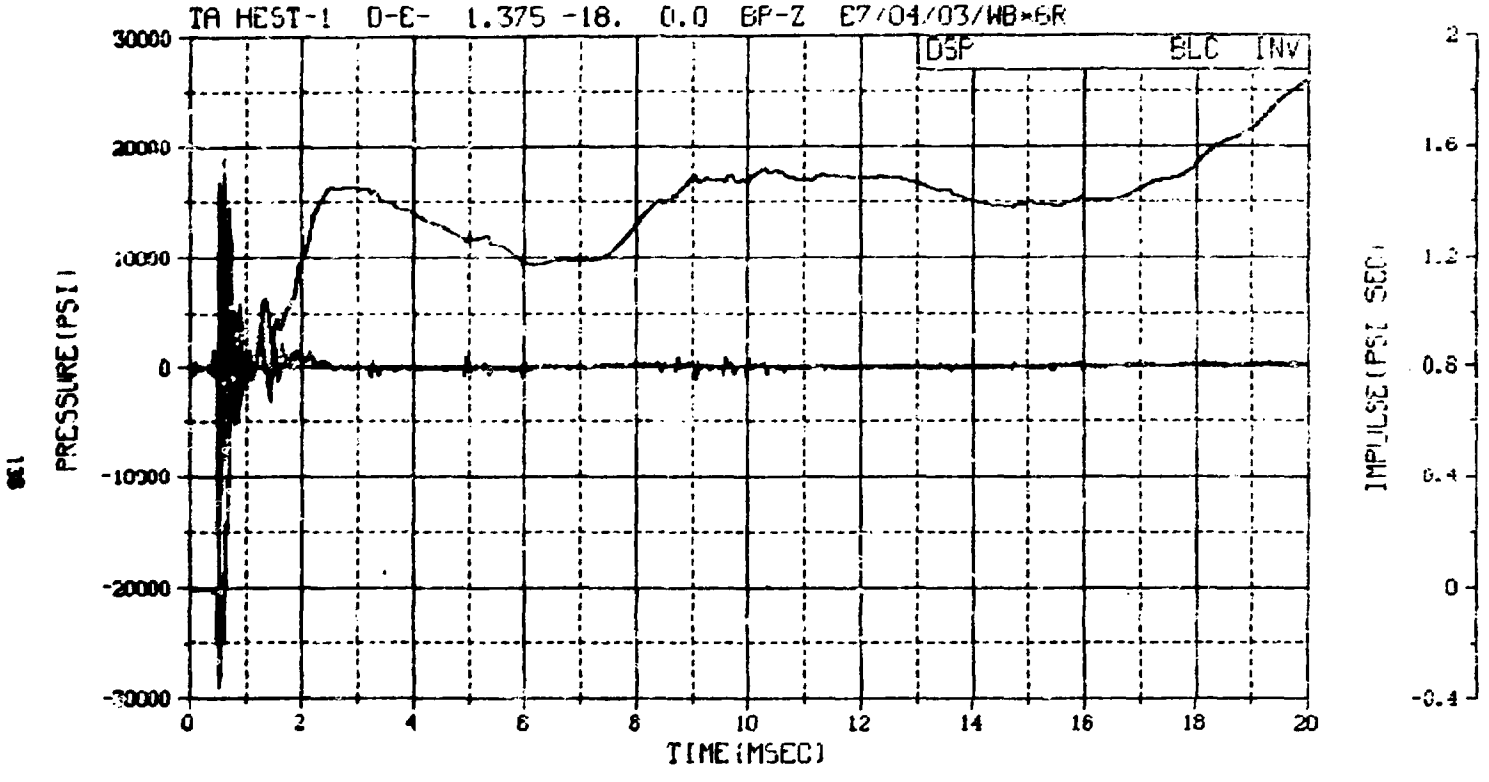

M.N. =90006	E.U. -0.000,5924.000	VSN=
TSMP=10.350	DIGITS=0.000,345.500	TAPE26
S.R. =125.00 KHZ	3 49 PM, 11 APR 78.	FILE=8

1

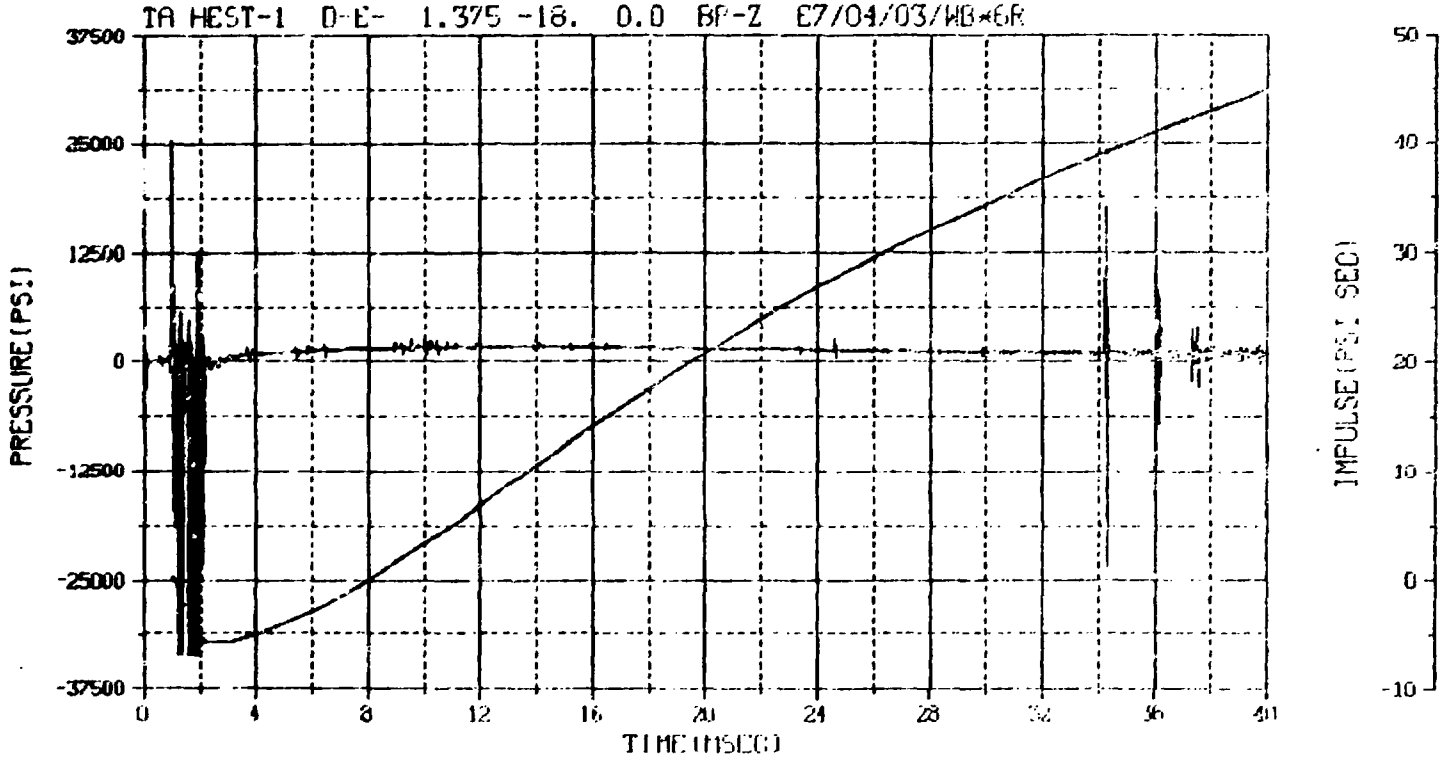
TA HEST-1 D-E- 1.375 -18. 0.0 BP-Z E7/04/03/WB*6R
37500
25000
12500
0
-12500
-25000
-37500
PRESSURE(PSI)
0
4
8
12
16
20
24
28
32
36
40
TIME(MSEC)
50
40
30
20
10
0
-10
IMPULSE(PSI SEC)
M.N. = 6
E.U. -0.000,7024.000
VSN=6054
TSKIP=9.848
DIGITS=0.000,3445.500
TAPE22
S.R. =250.00 KHZ
2 40 PM, 6 MAR 76.
FILE=24

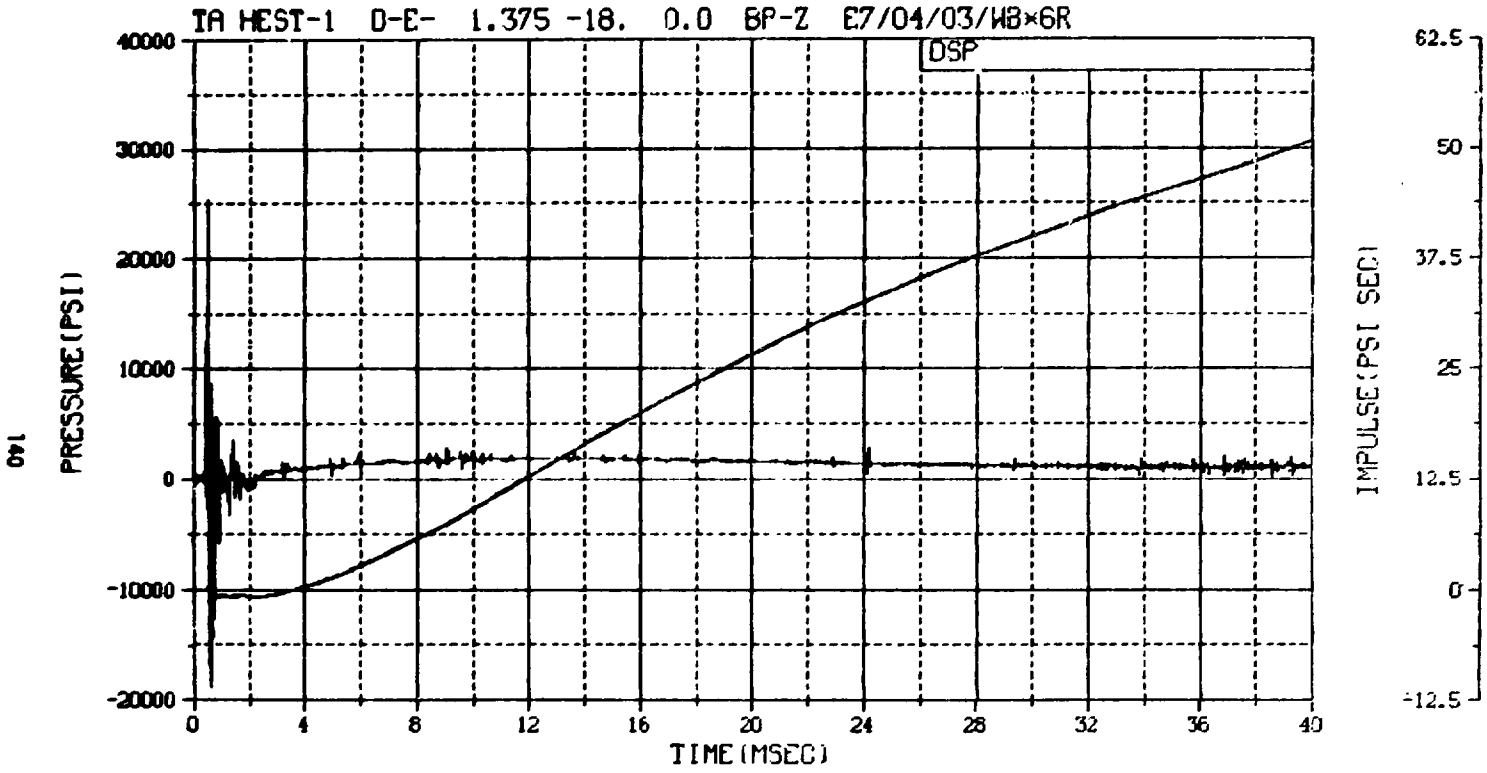

M.N. =80006	E.U. =0.000,5924.000	VSN=
TSKIP=10.350	DIGITS=0.000,345.500	TAPE26
S.R. =125.00 KHZ	3 49 PM,11 APR 78.	FILE=7

1

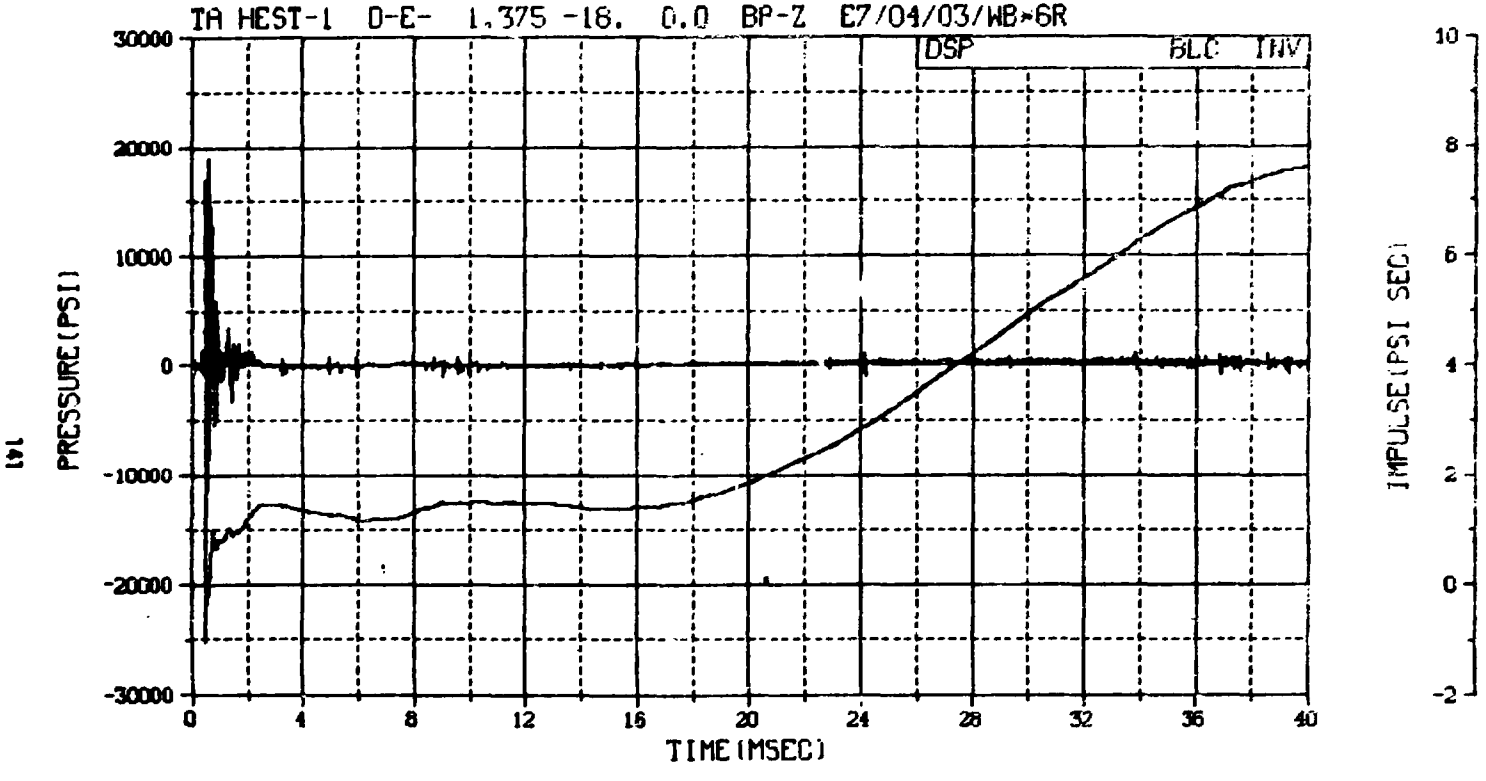

M.N. =90006	E.U. =0.000,5924.000	VSN=
TSKIP=10.350	DIGITS=0.000,345.500	TAPE26
S.R. =125.00 KHZ	3 49 PM,11 APR 78.	FILE=8

1

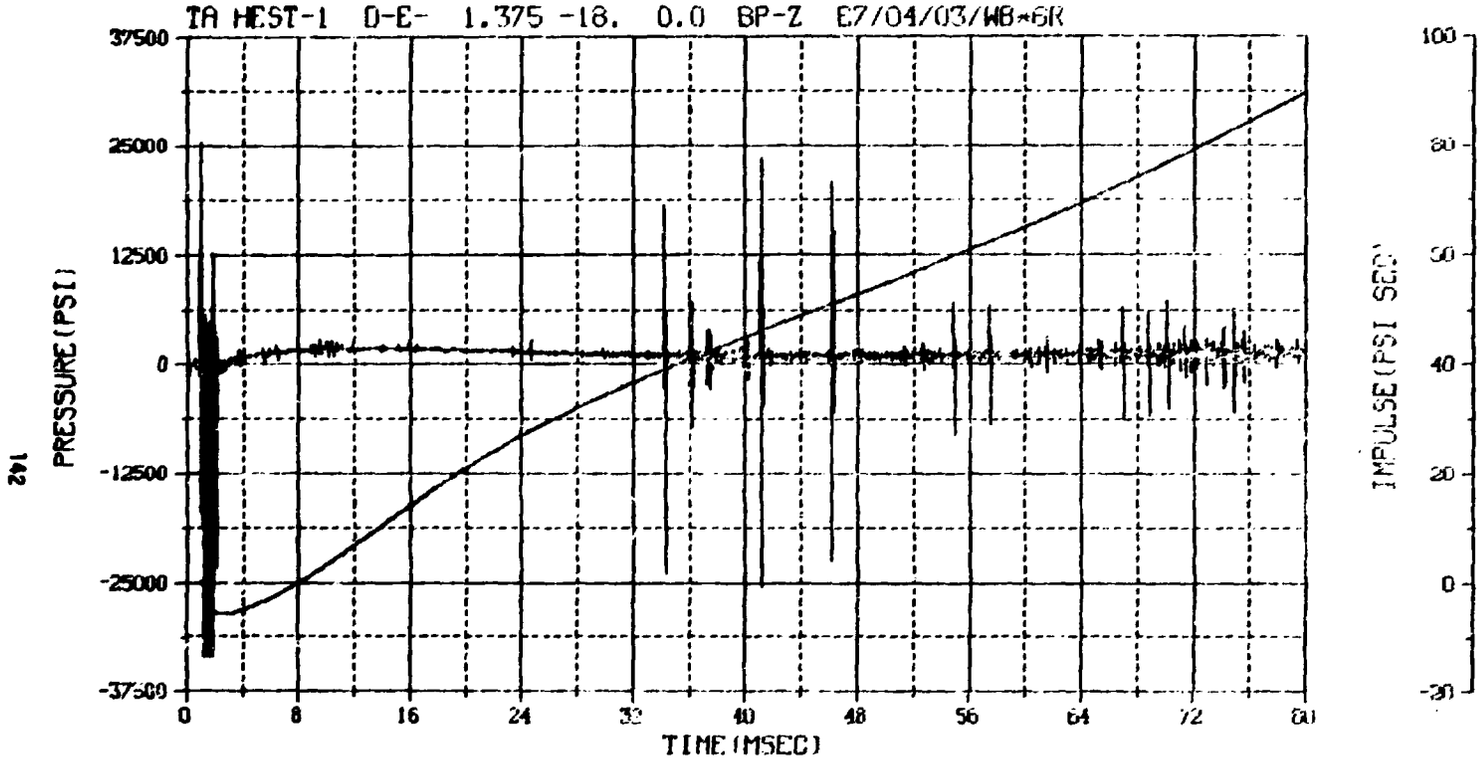

M.N. = 6	E.U. =0.000,5924.000	VSN=BD54
TSKIP=9.848	DIGITS=0.000,345.500	TAPE22
S.R. =250.00 KHZ	2 40 PM, 6 MAR 78.	FILE=24

1

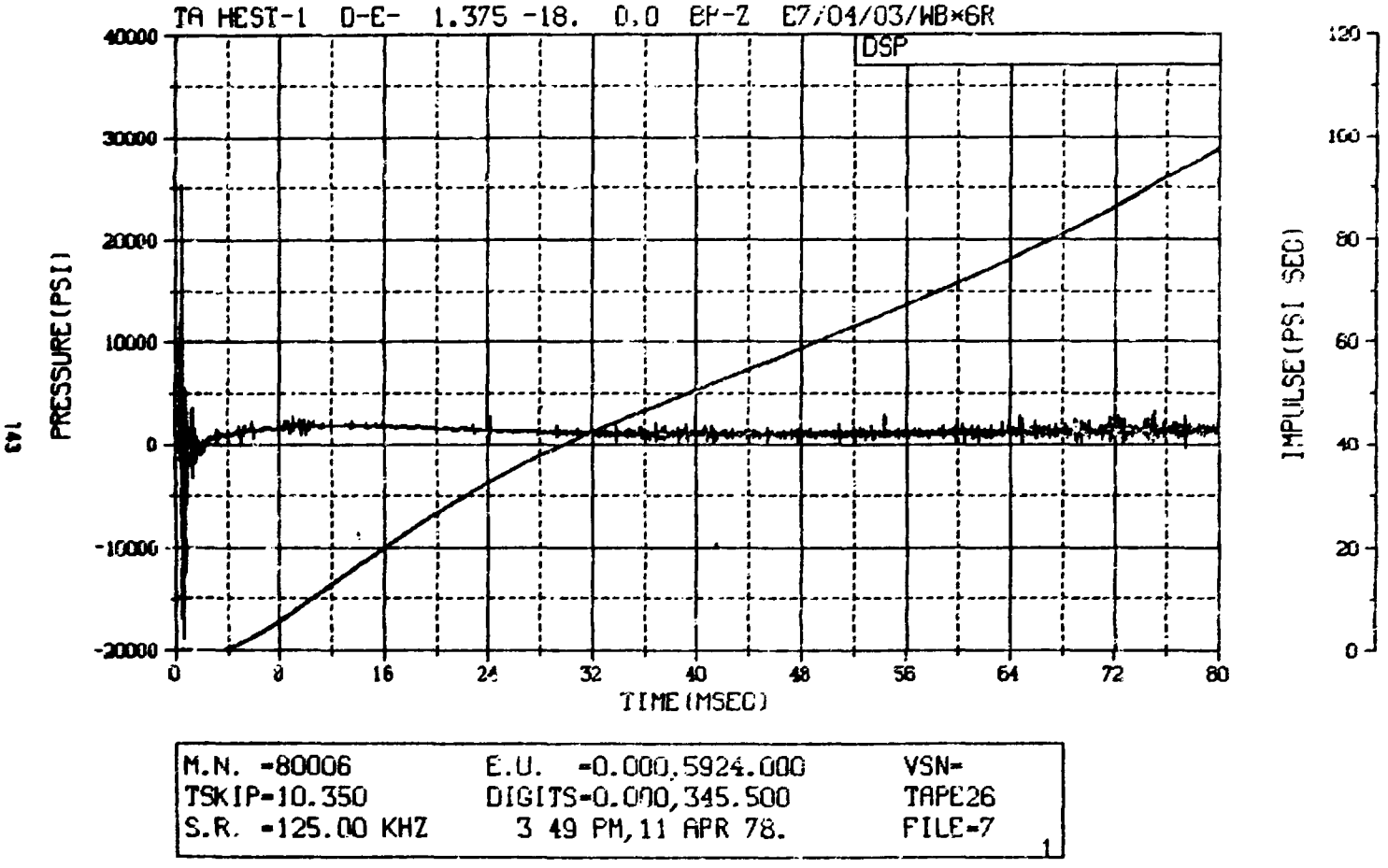
TA HEST-1 D-E- 1.375 -18. 0.0 EP-Z E7/04/03/WB×6R
DSP
PRESSURE(PSI)
IMPULSE(PSI SEC)
TIME(MSEC)
40000
30000
20000
10000
0
-10000
-20000
120
100
80
60
40
20
0
0
8
16
24
32
40
48
56
64
72
80
M.N. =80006
E.U. =0.000,5924.000
VSN=
TSKIP=10.350
DIGITS=0.000,345.500
TAPE26
S.R. =125.00 KHZ
3 49 PM,11 APR 78.
FILE=7

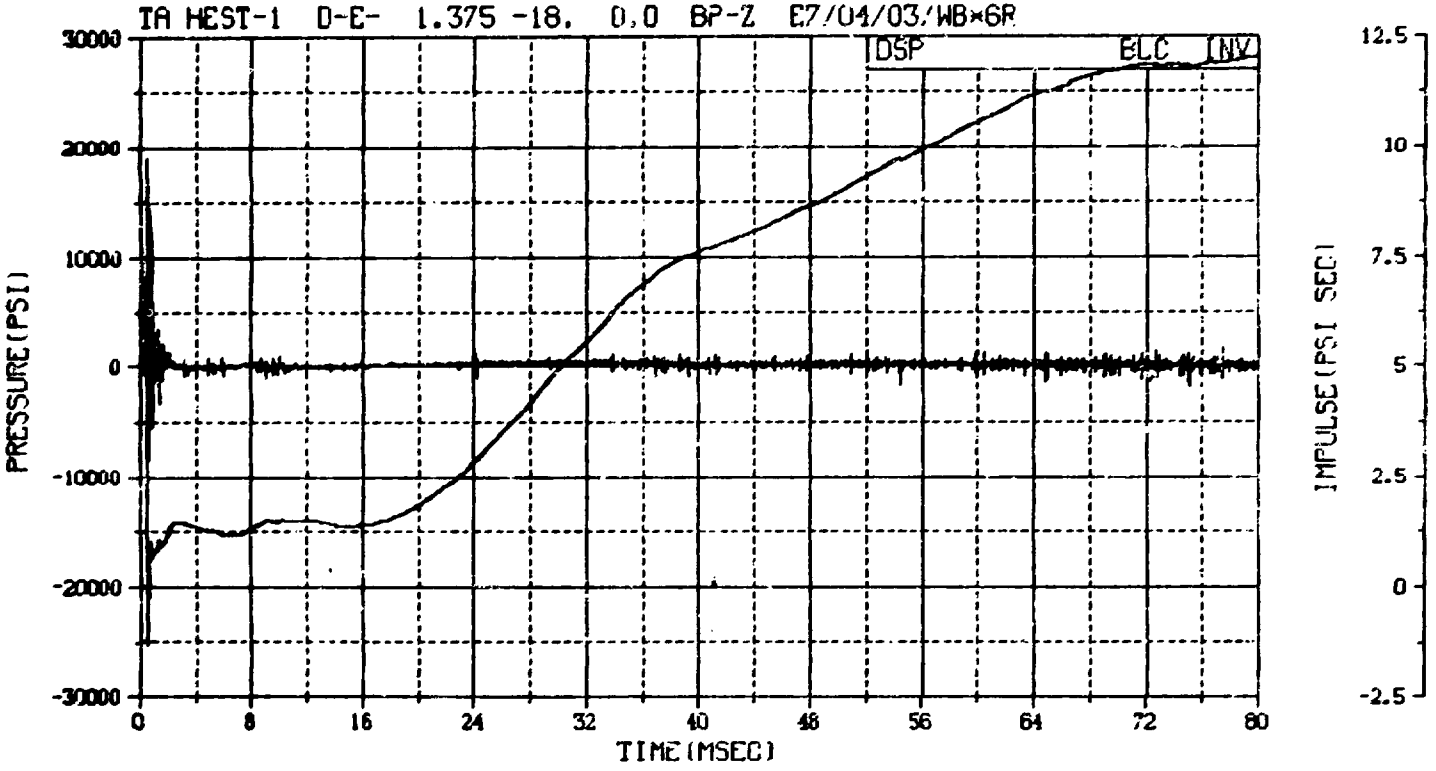

M.N. =90006	E.U. =0.000,5924.000	VSN=
TSKIP=10.350	DIGITS=0.000,345.500	TAPE26
S.R. =125.00 KHZ	3 49 PM,11 APR 78.	FILE=8

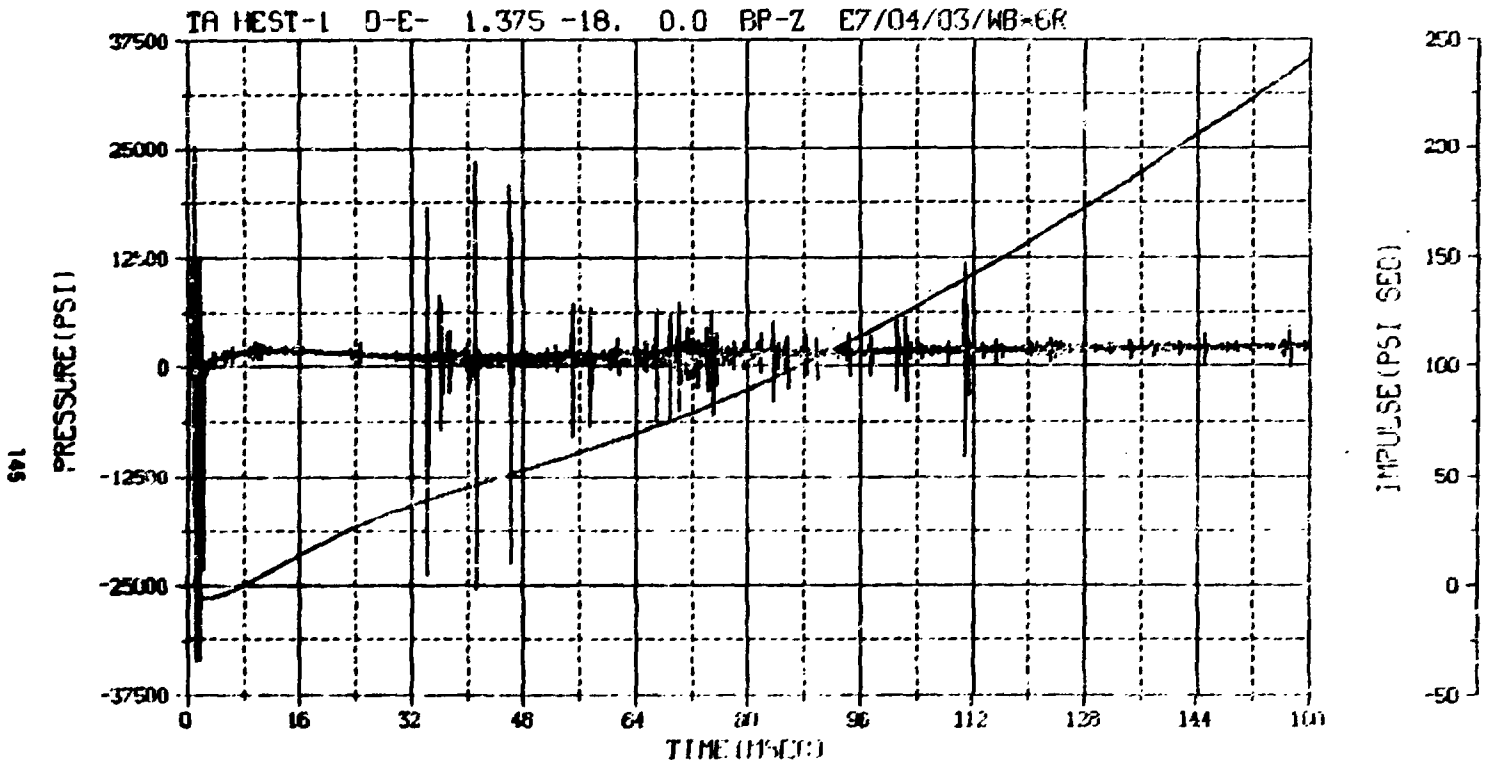
TA HEST-1 D-E- 1.375 -18. 0.0 BP-Z E7/04/03/WB=6R
PRESSURE(PSI)
IMPULSE(PSI SEC)
TIME(MSEC)
37500
25000
12500
0
-12500
-25000
-37500
250
200
150
100
50
0
-50
0
16
32
48
64
80
96
112
128
144
160
M.N. = 6
TSKIP=9.848
S.R. =250.00 KHZ
VSN=BD54
TAPE22
FILE=24

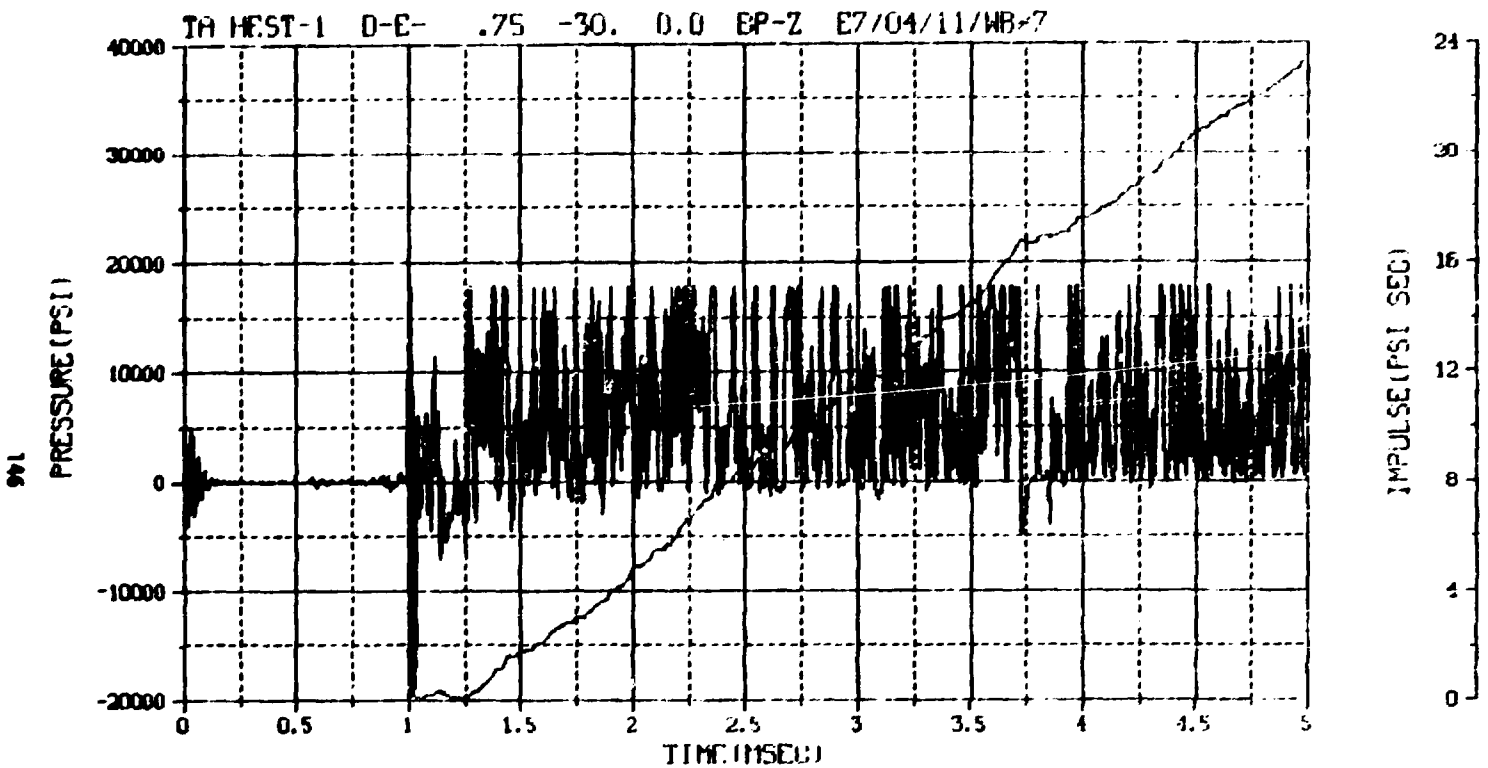

M.N. = 7	E.U. -0.000,5953.000	VSN=BG54
TSKIP=9.848	DIGITS-0.000,580.000	TAPE22
S.R. =250.00 KHZ	2 40 PH, 6 MAR 7..	FILE=34

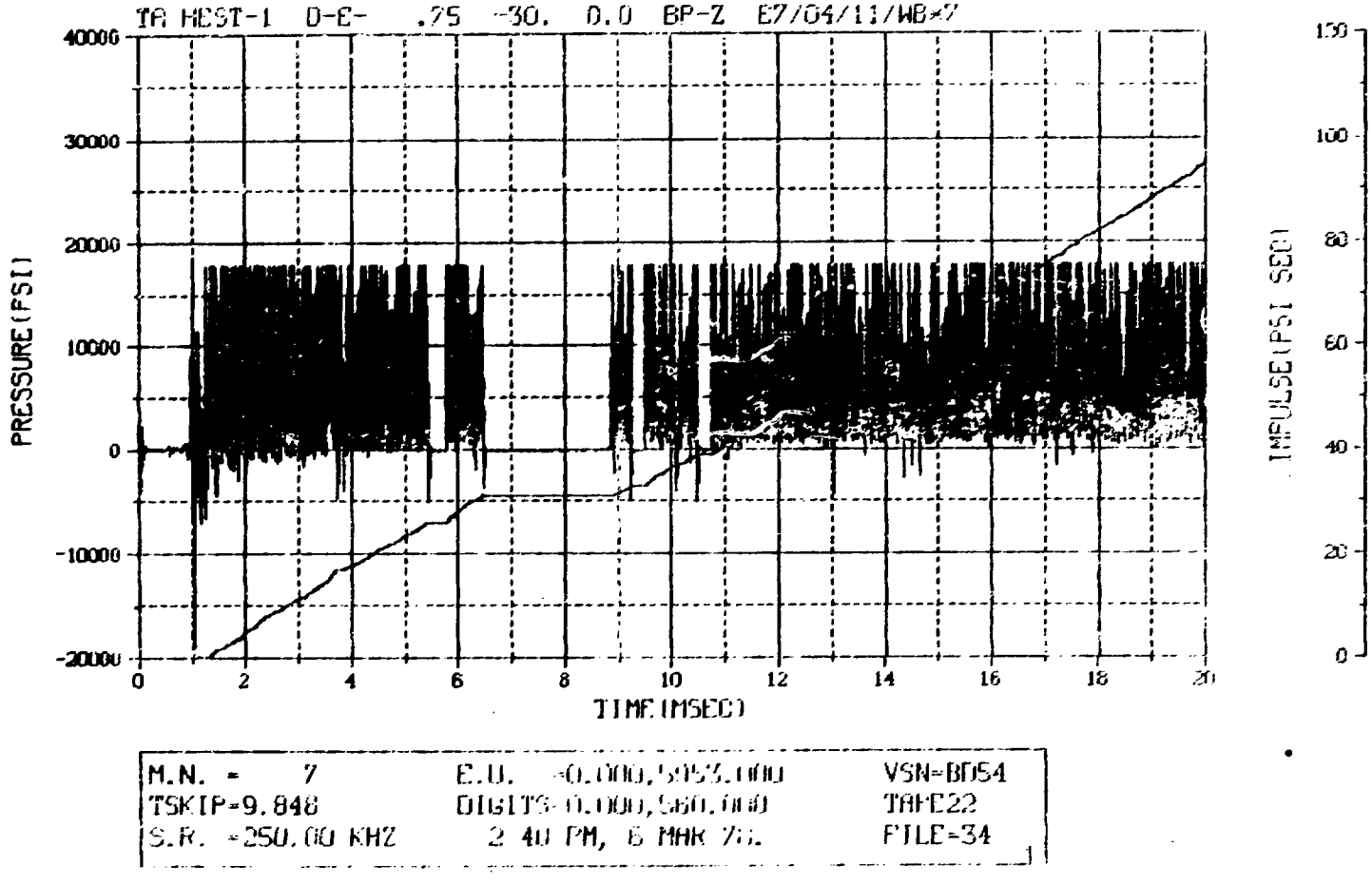
TA HOST-1 D-E- .25 -30. 0.0 BP-Z E7/04/11/WB#7
PRESSURE(PSI)
IMPULSE(PSI SEC)
TIME(MSEC)
40000
30000
20000
10000
0
-10000
-20000
100
80
60
40
20
0
2
4
6
8
10
12
14
16
18
20
M.N. = 7
TSKIP=9.848
S.R. =250.00 KHZ
E.U. =0.000,5853.000
DIGITS=0.000,4860.000
2 40 PM, 6 MAR 7?
VSN=BD54
TAPE22
FILE=34

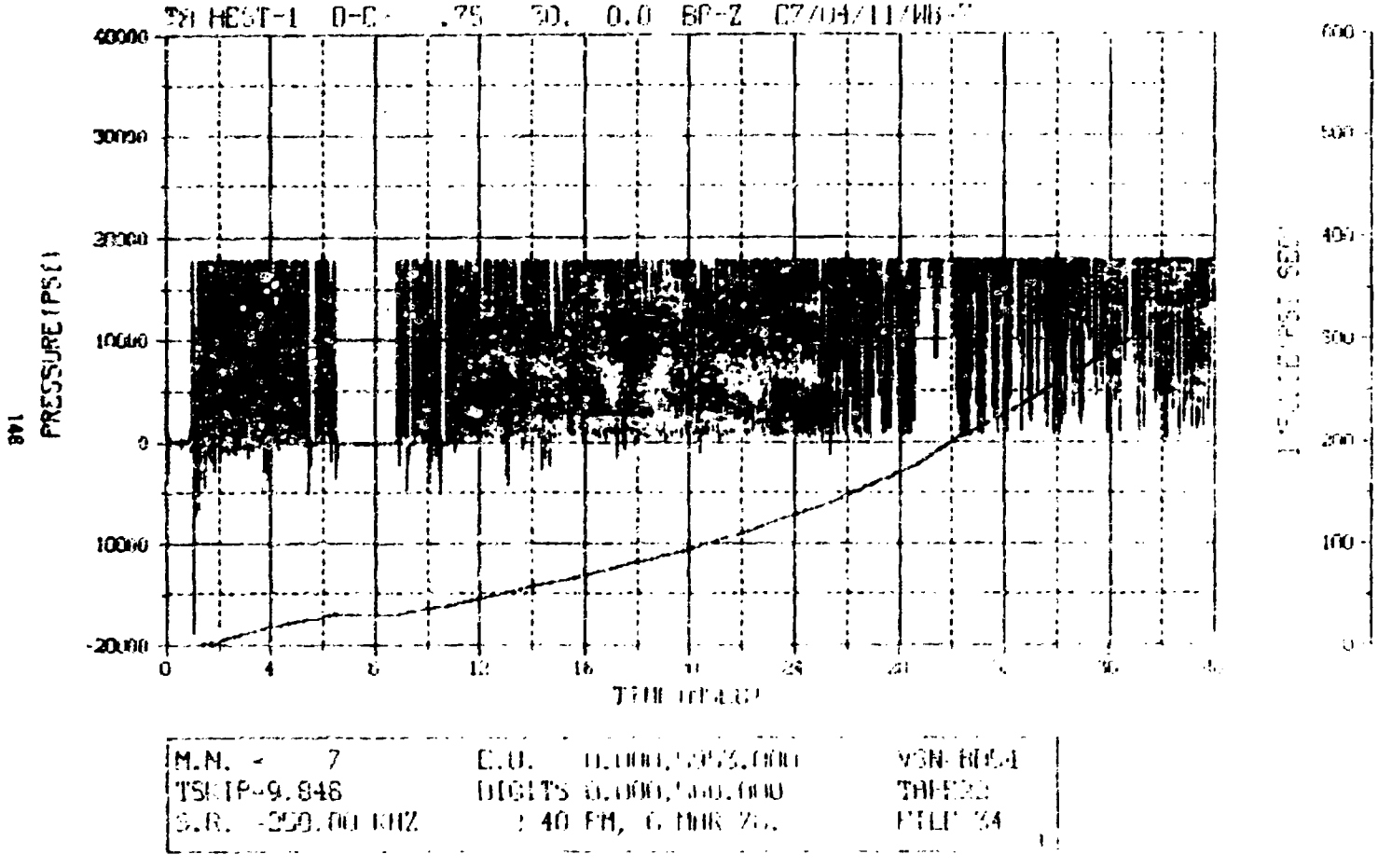
PRESSURE (PSI)
40000
30000
20000
10000
0
-10000
-20000
0
4
8
12
16
20
24
28
32
36
40
600
500
400
300
200
100
0

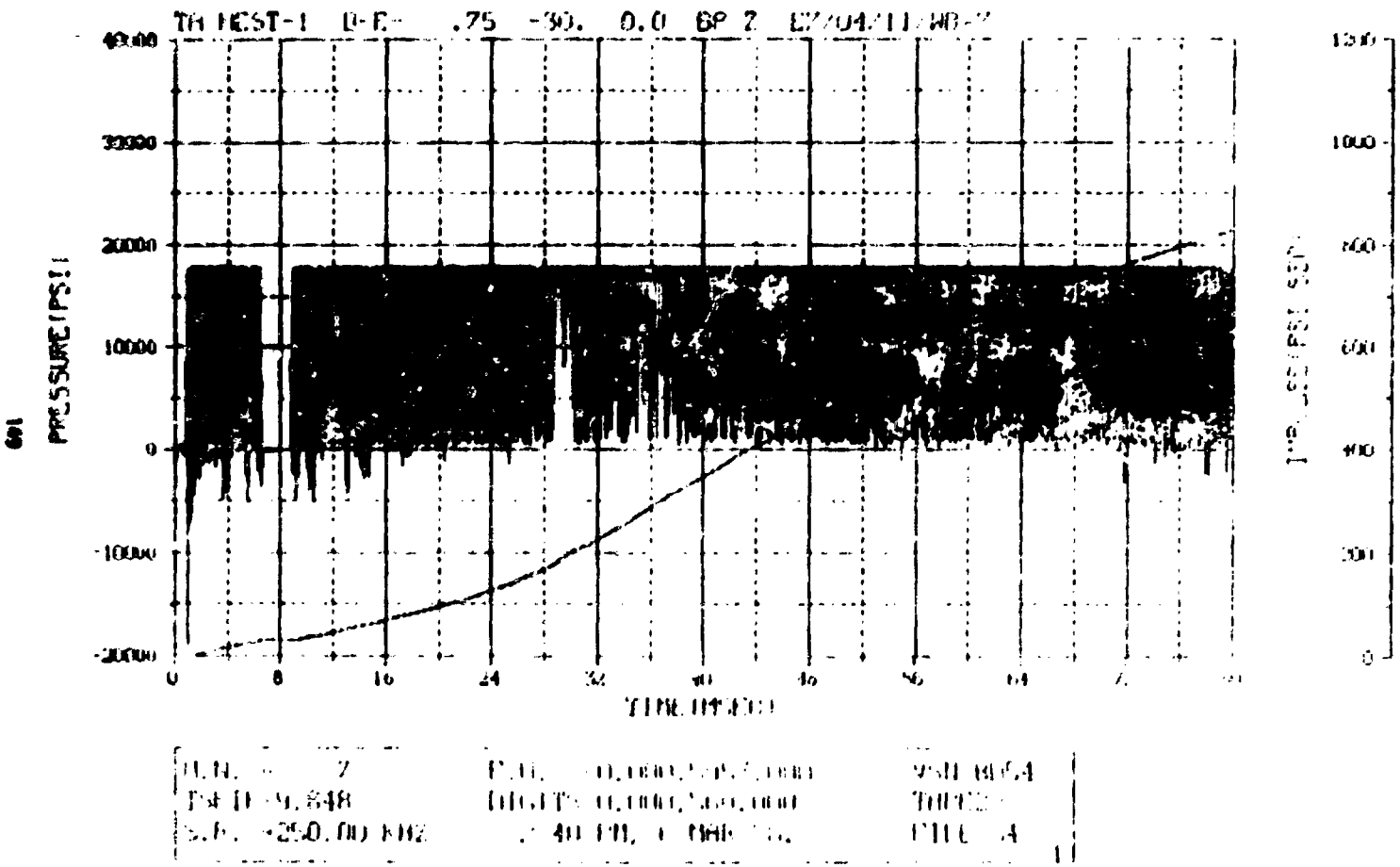
TA MEST-1 D-E- .75 -30. 0.0 BP 2
PRESSURE(PSI)
40000
30000
20000
10000
0
-10000
-20000
0
8
16
24
32
40
48
56
64
1000
600
400
0
TIME(MSEC)
S.R. +250.00 KHZ

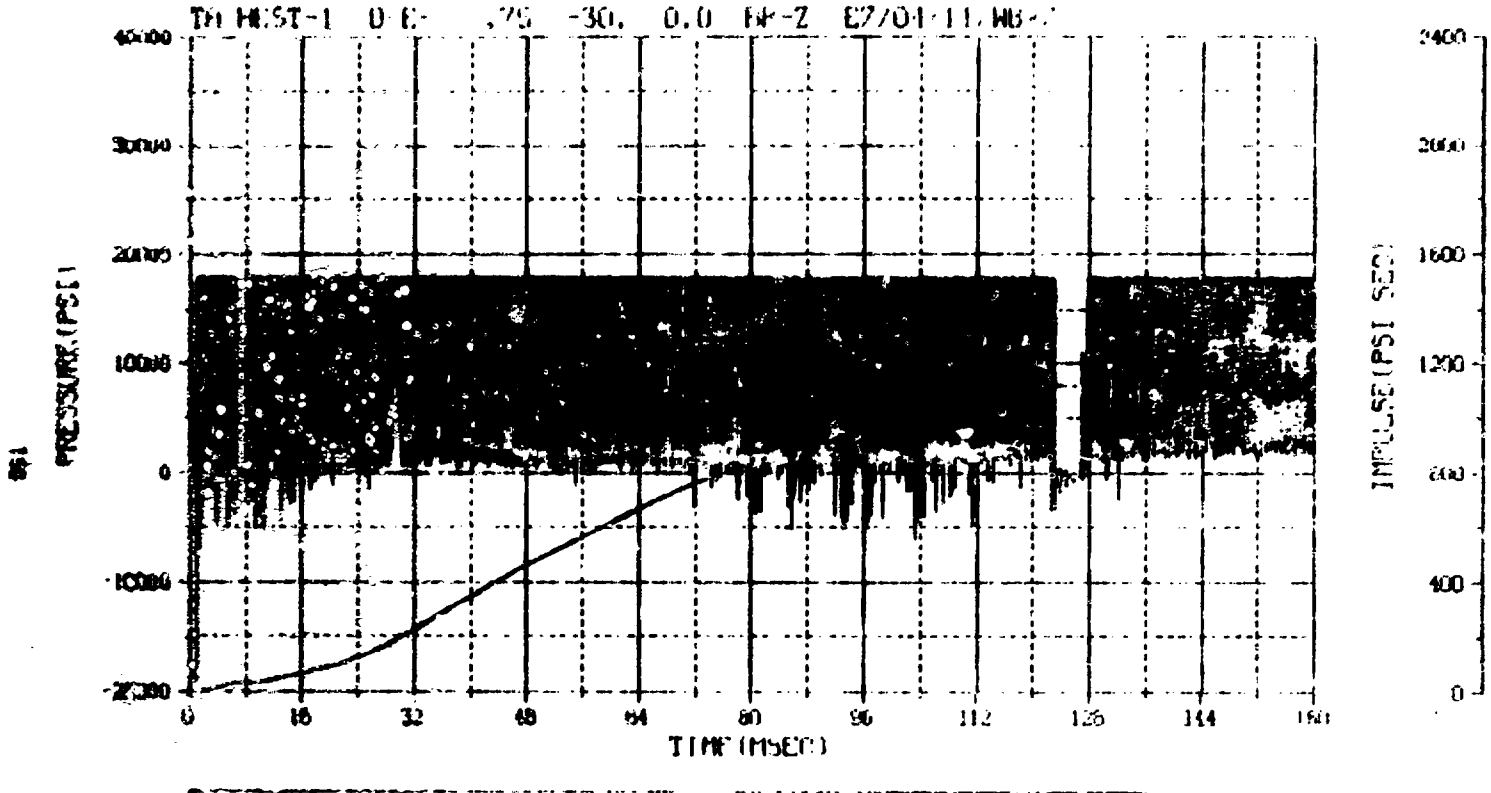

P.N. = 7	E.U. -0.000,5953.000	VSN-BD54
TSCIP-9.848	DIGITS-0.000,560.000	TAPE22
C.R. -250.0 KHZ	2:40 PM, 6 MAR 7..	FILE 34

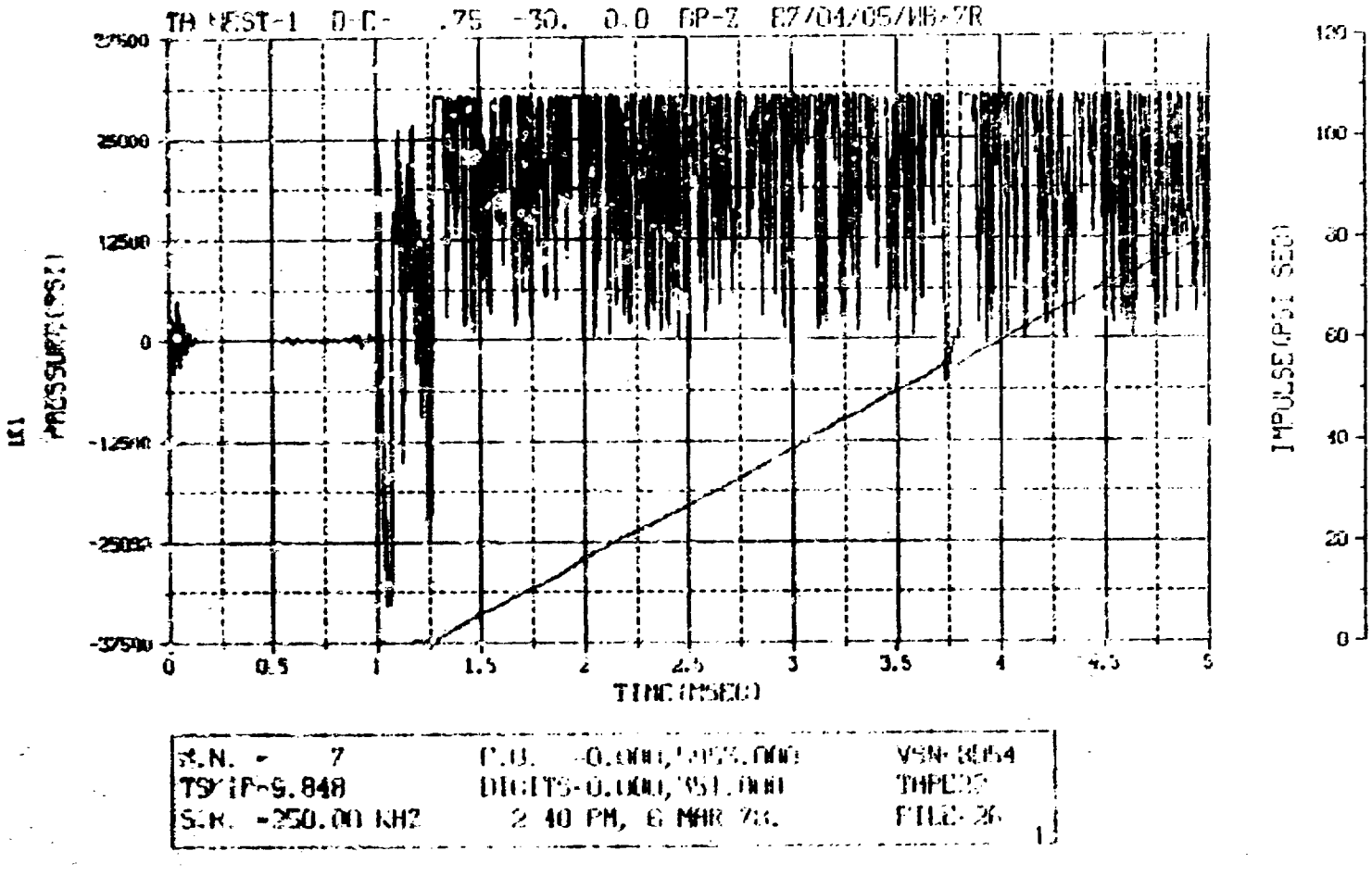
TA NEST-1 D-C- .75 -30. 0.0 BP-Z E7/04/05/WB-7R
PRESSURE(PSI)
IMPULSE(PSI SEC)
TIME(MSEC)
37500
25000
12500
0
-12500
-25000
-37500
0
0.5
1
1.5
2
2.5
3
3.5
4
4.5
5
120
100
80
60
40
20
0
S.N. - 7
TSKIP-9.848
S.R. -250.00 KHZ
DIGITS-0.000,351.000
2 40 PM, 6 MAR 78.
VSN-8054
FILE-26

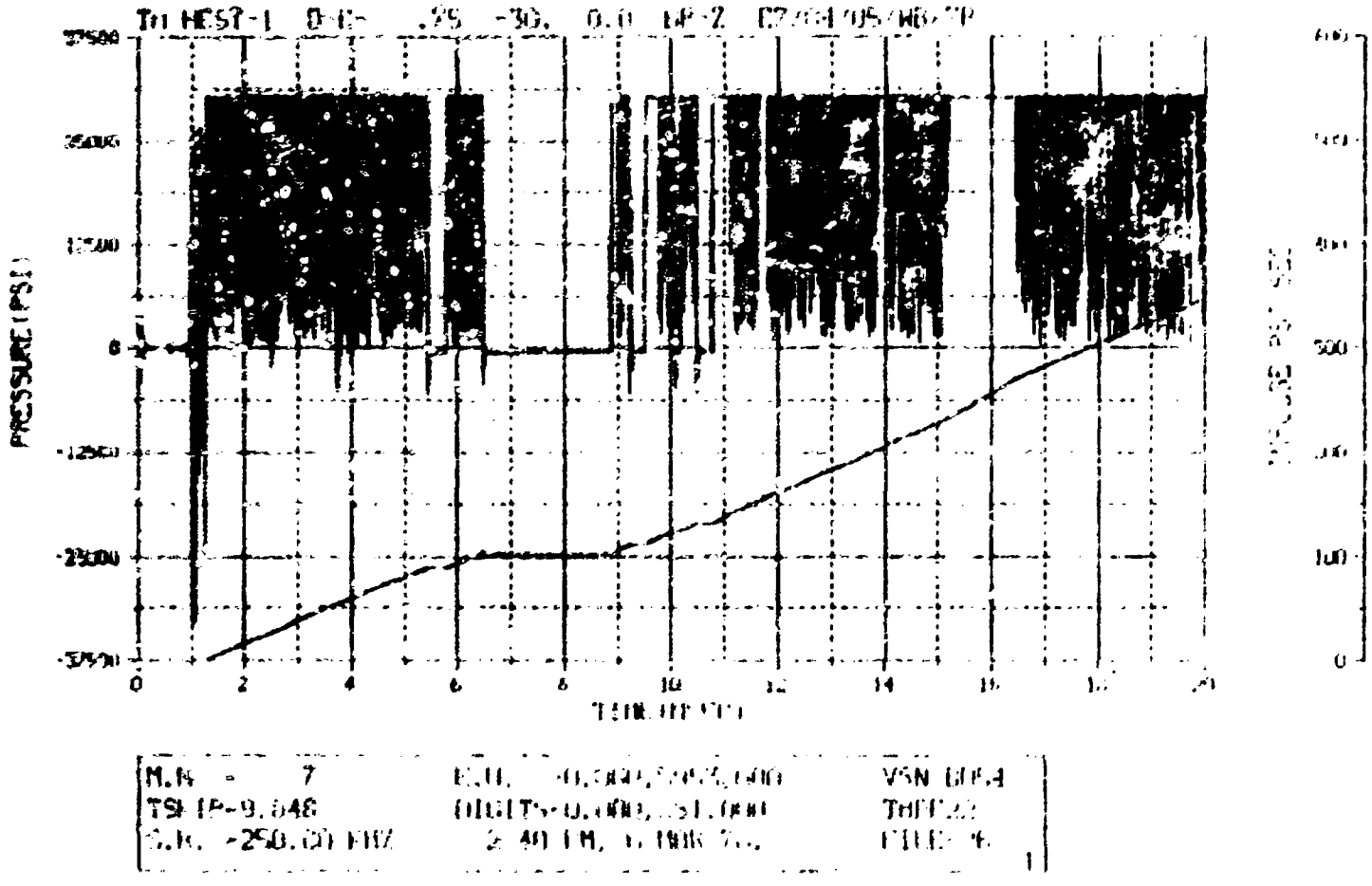
PRESSURE (PSI)
TIME (MSEC)
M.N = 7
TSKIP=9.048
S.R. =250.00 KHZ
VSN
THEE
FILE

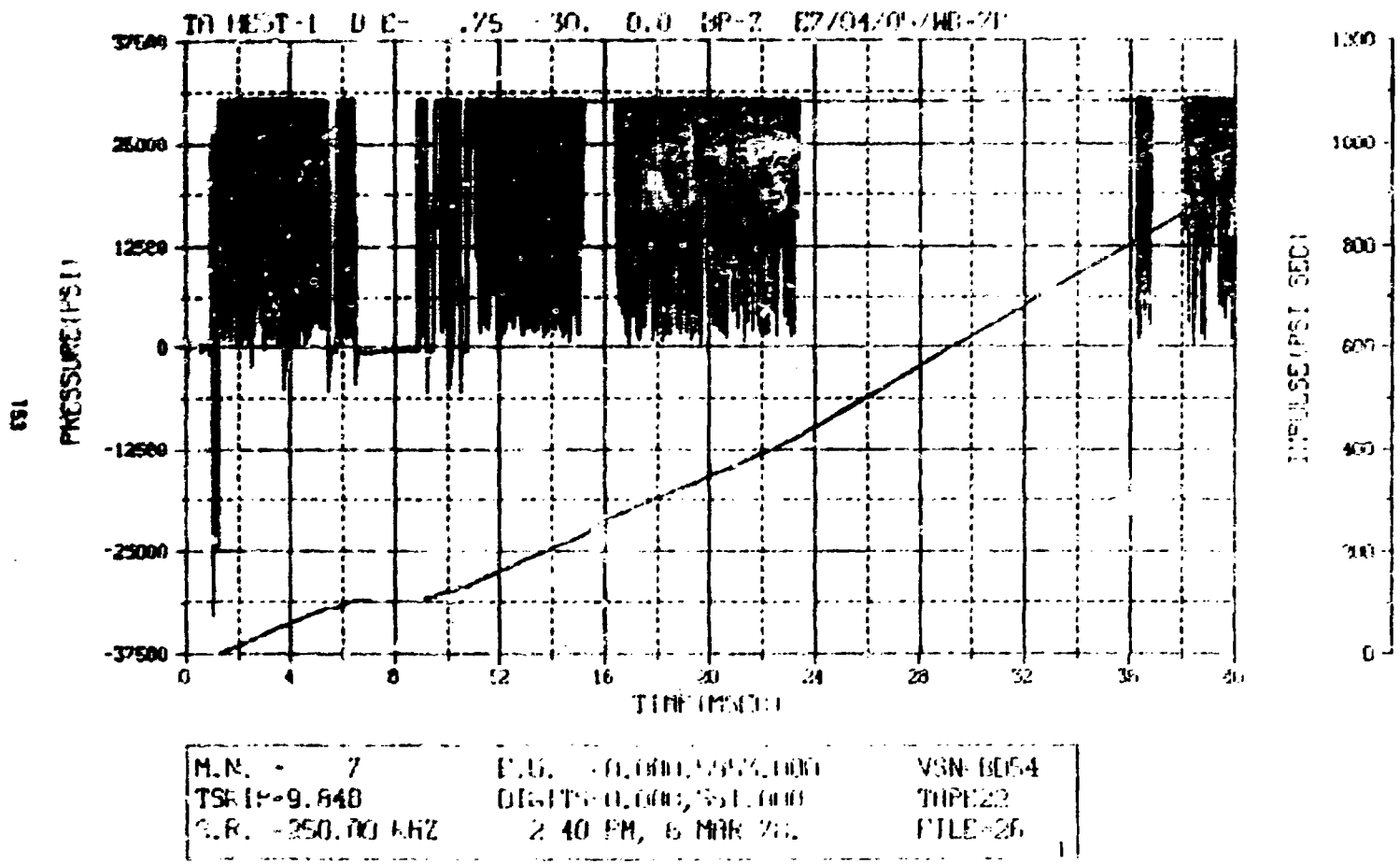
37500
25000
12500
0
-12500
-25000
-37500
0
4
8
12
16
20
24
28
32
36
40
1200
1000
800
600
400
200
0

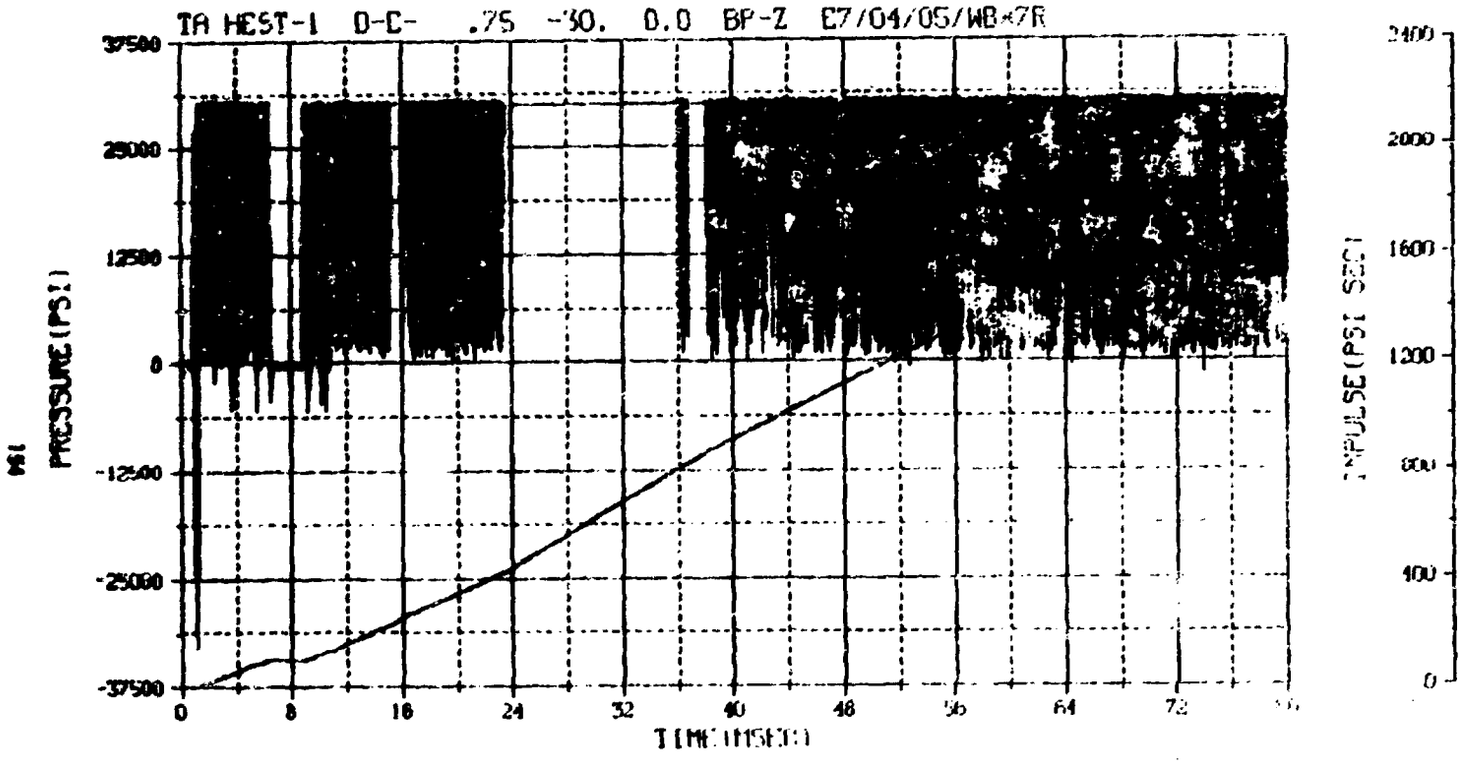

M.N. = 7	E.U. -0.000,5953.000	VSN=BD54
TSKIP=9.848	DIGITS=0.000,351.000	TAPE22
S.R. =250.00 KHZ	2 40 PM, 6 MAR 7[illegible]	FILE[illegible]

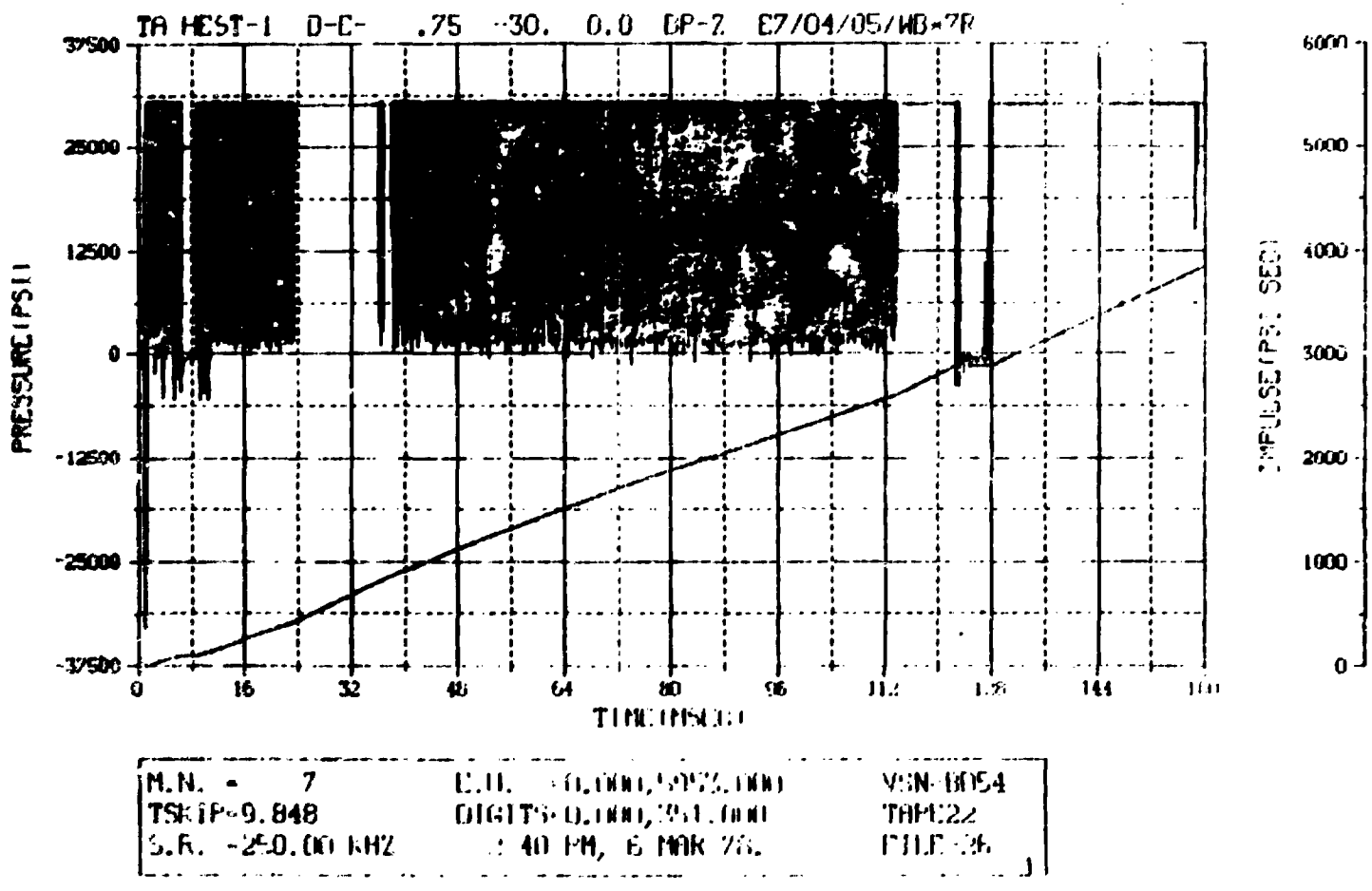
TA HEST-1 D-C- .75 -30. 0.0 DP-Z E7/04/05/WB*7R
PRESSURE(PSI)
37500
25000
12500
0
-12500
-25000
-37500
0
16
32
48
64
80
96
112
128
144
160
TIME(MSEC)
IMPULSE(PSI SEC)
6000
5000
4000
3000
2000
1000
0
M.N. = 7
TSKIP=9.848
S.R. -250.00 KHZ
E.U. =0.000,5953.000
DIGITS=0.000,351.000
40 PM, 6 MAR 78.
VSN=B054
TAPE22
FILE=26

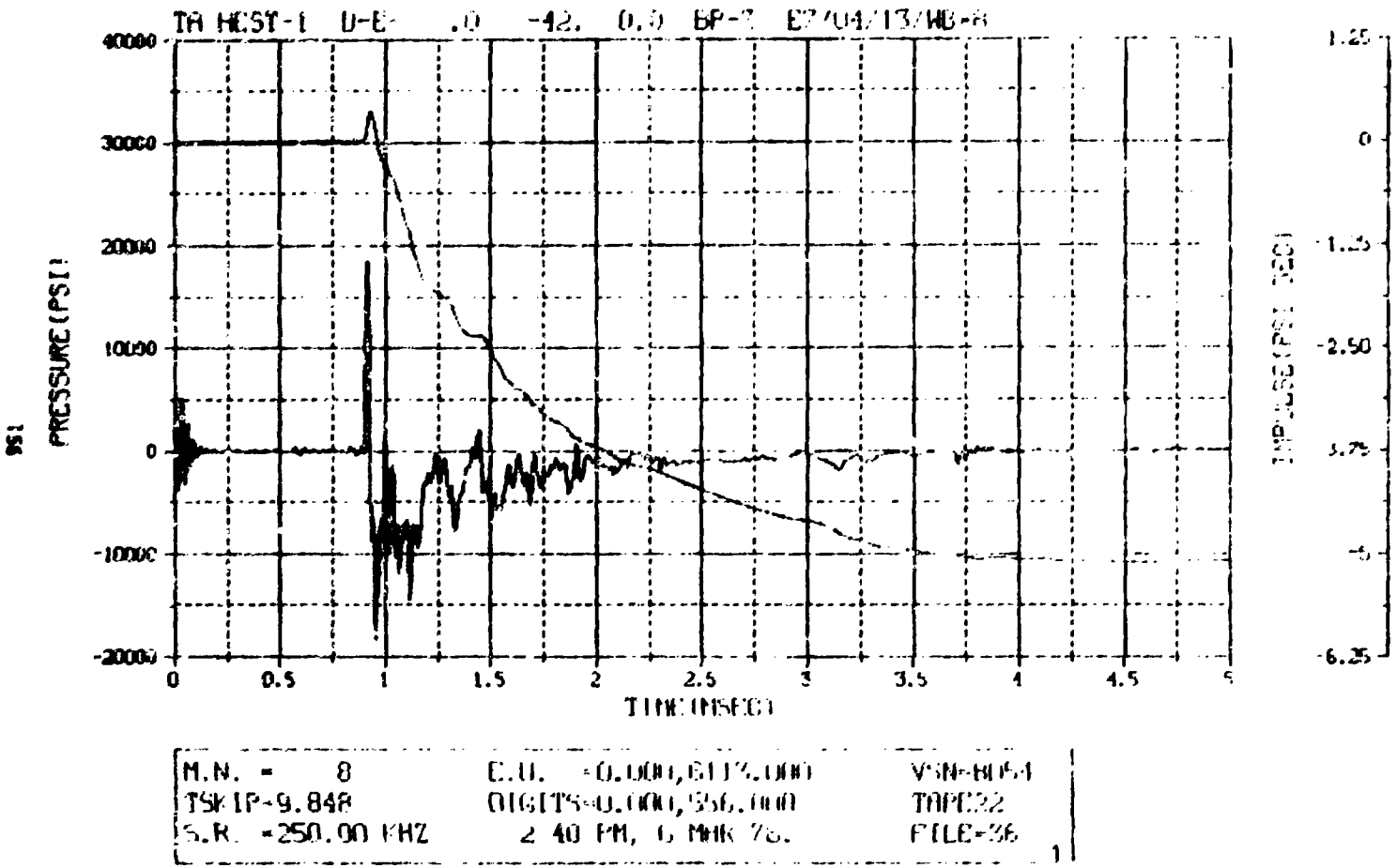
TR MCST-1 U-E- .0 -42. 0.0 BP-? E?/04/13/MB-6
40000
30000
20000
10000
0
-10000
-20000
PSI
PRESSURE(PSI)
0
0.5
1
1.5
2
2.5
3
3.5
4
4.5
TIME(MSEC)
1.25
0
-1.25
-2.50
-3.75
-5
-6.25
M.N. = 8
C.U. =0.000,6113.000
VSN=8054
TSKIP=9.848
DIGITS=0.000,256.000
TAPE:22
S.R. =250.00 KHZ
2 40 PM, 6 MAR 78.
FILE=36

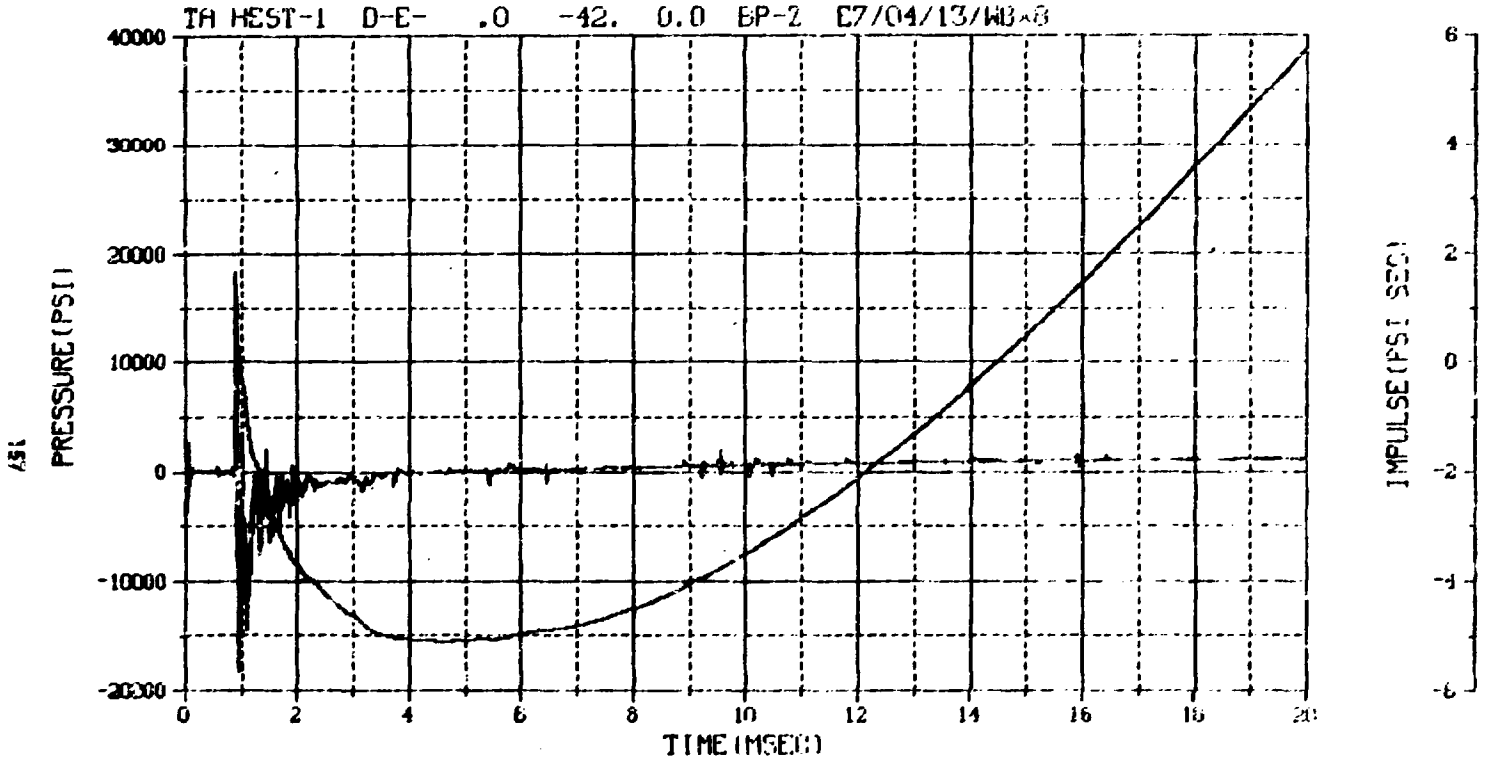

M.N. = 8	E.U. =0.000,611%.000	VSN=BD54
TSKIP=9.848	DIGITS=0.000,556.000	TAPE22
S.R. =250.00 KHZ	2 40 PM, 6 MAR 78.	FILE=36

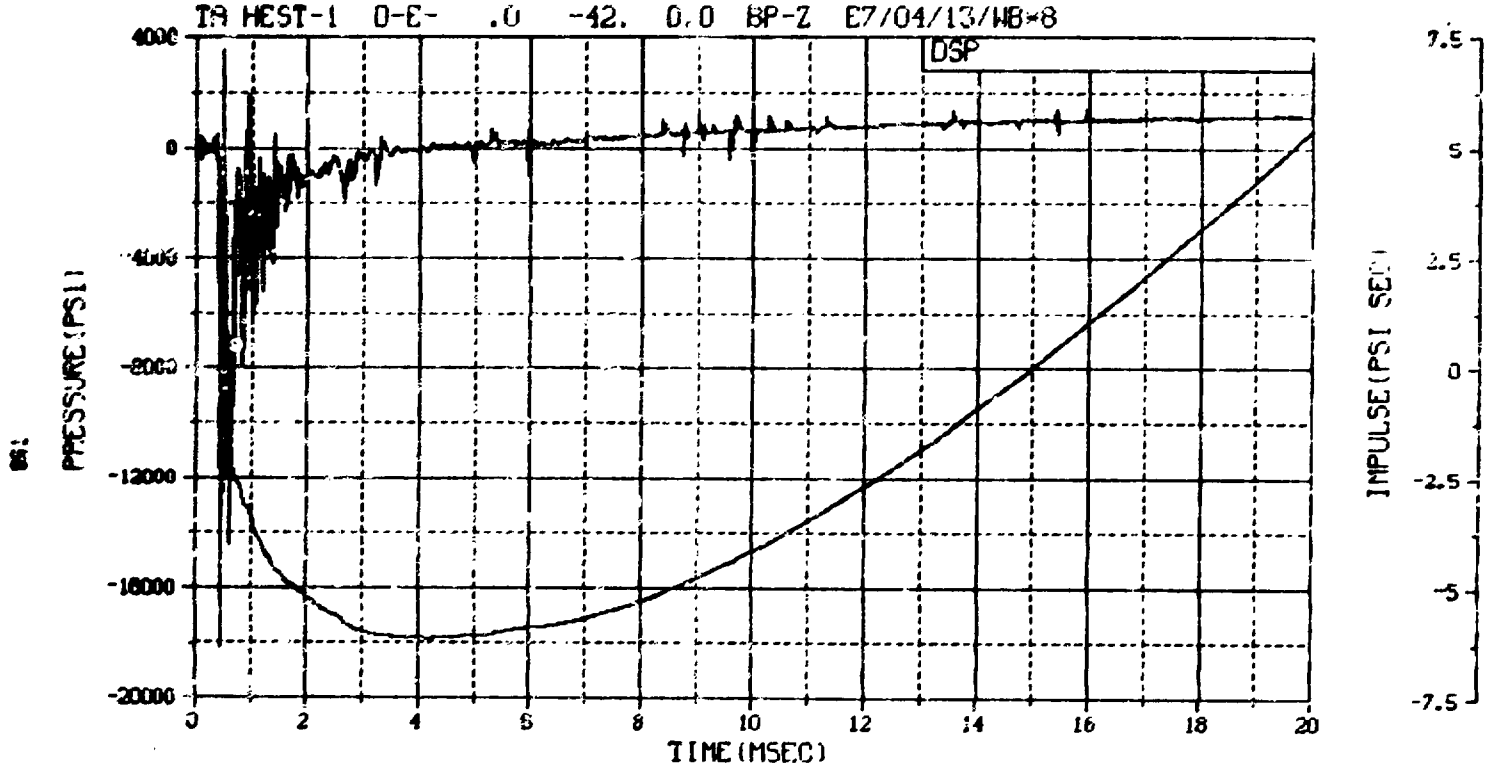

M.N. =80008	E.U. =0.000,6113.000	VSN=
TSKIP=10.350	DIGITS=0.000,556.000	TAPE26
S.R. =125.00 KHZ	3 49 PM,11 APR 78.	FILE=15

1

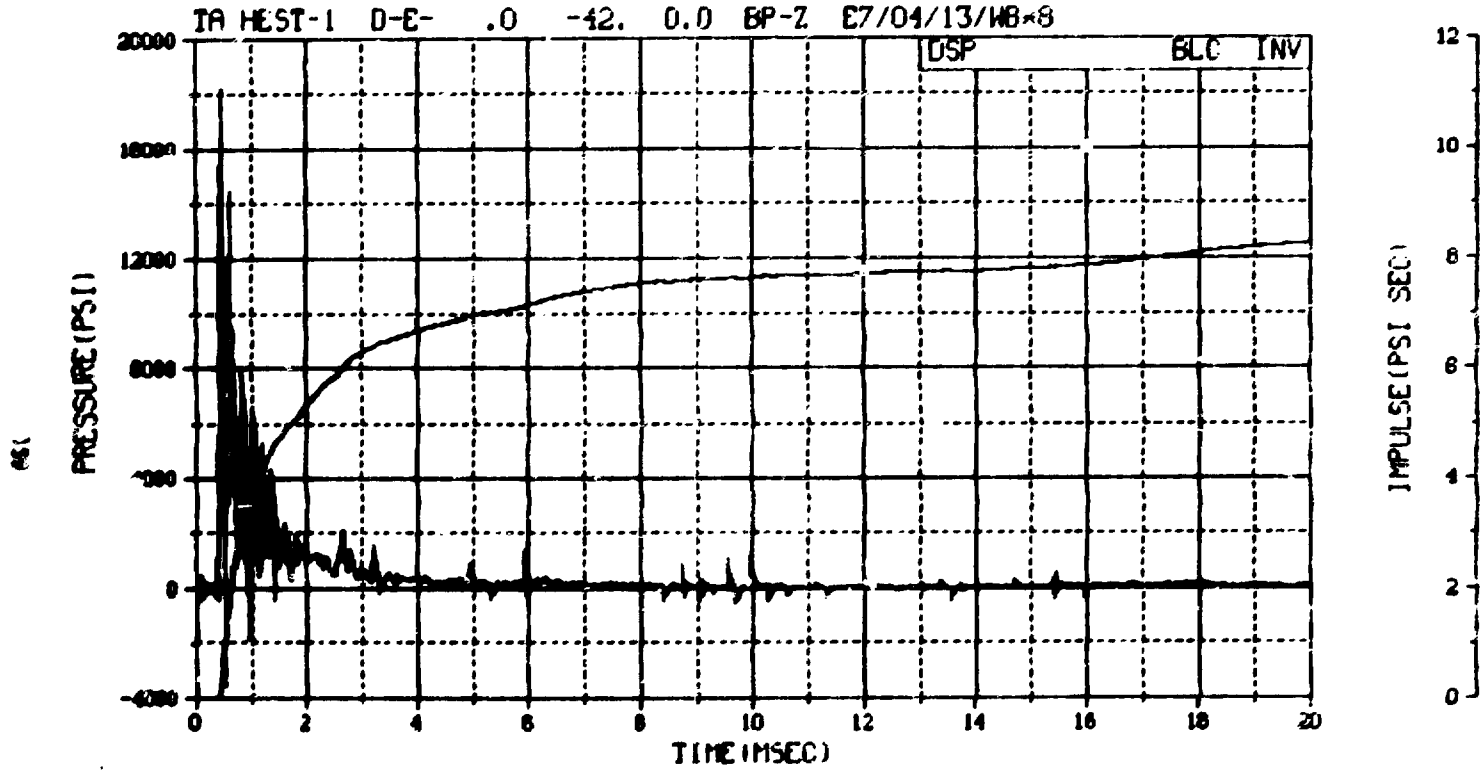

.N. -90008	E.U. -0.000,6113.000	VSN- DI39
TSK(P-10.350	DIGITS-0.000,556.000	TAPE26
S.R. -125.00 KHZ	3 49 PM, 11 APR 78.	FILE-~~WB~~ 1

167

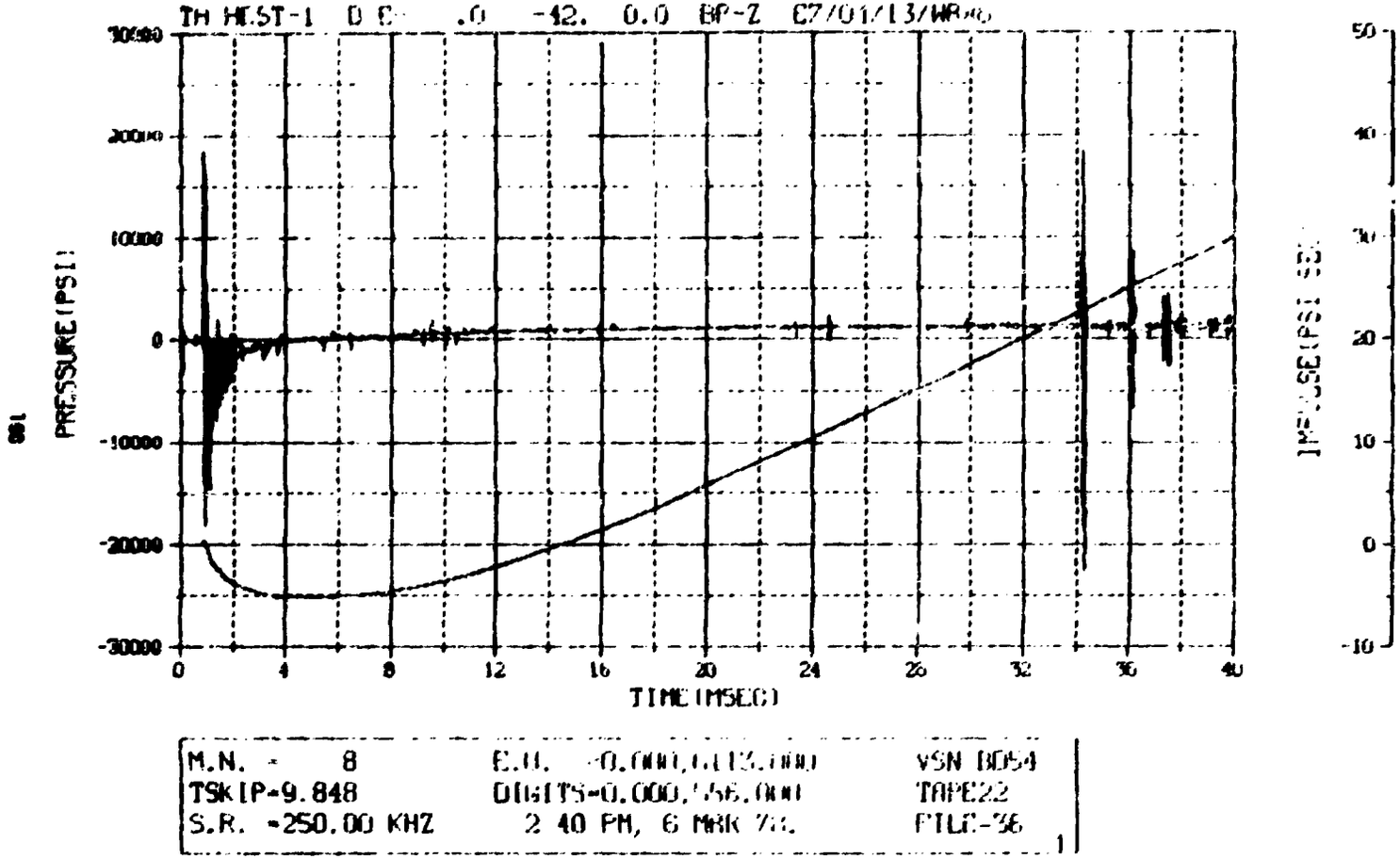

M.N. = 8	E.U. -0.000,0.113.000	VSN 8054
TSK IP-9.848	DIGITS-0.000,256.000	TAPE22
S.R. =250.00 KHZ	2 40 PM, 6 MAR 73.	FILE-36

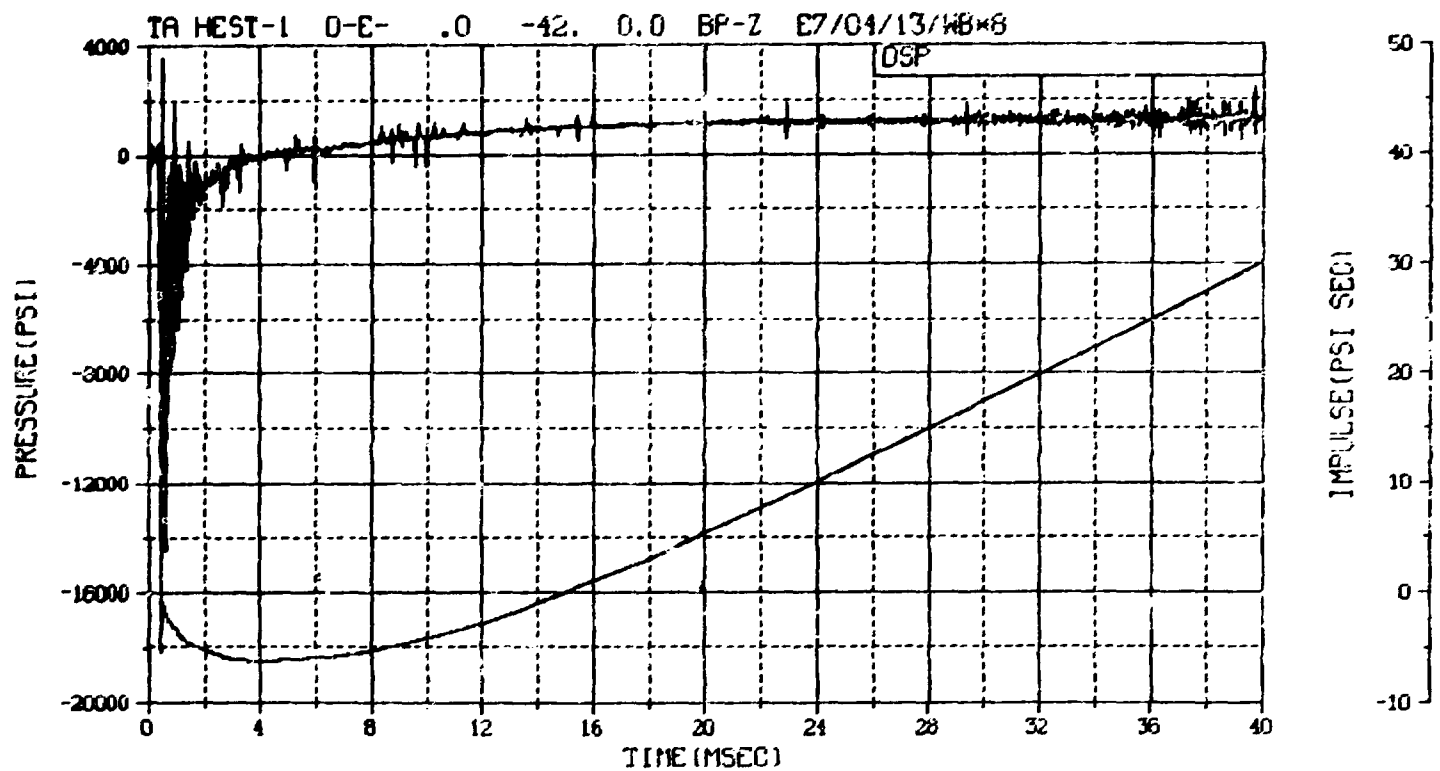
TA HEST-1 0-E- .0 -42. 0.0 BP-Z E7/04/13/WB×8
OSP
PRESSURE(PSI)
IMPULSE(PSI SEC)
TIME(MSEC)
4000
0
-4000
-8000
-12000
-16000
-20000
50
40
30
20
10
0
-10
0
4
8
12
16
20
24
28
32
36
40
M.N. -80008
E.U. -0.000,6113.000
VSN-
TSK(P-10.350
DIGITS-0.000,556.000
TAPE26
S.R. -125.00 KHZ
3 49 PM,11 APR 78.
FILE-15

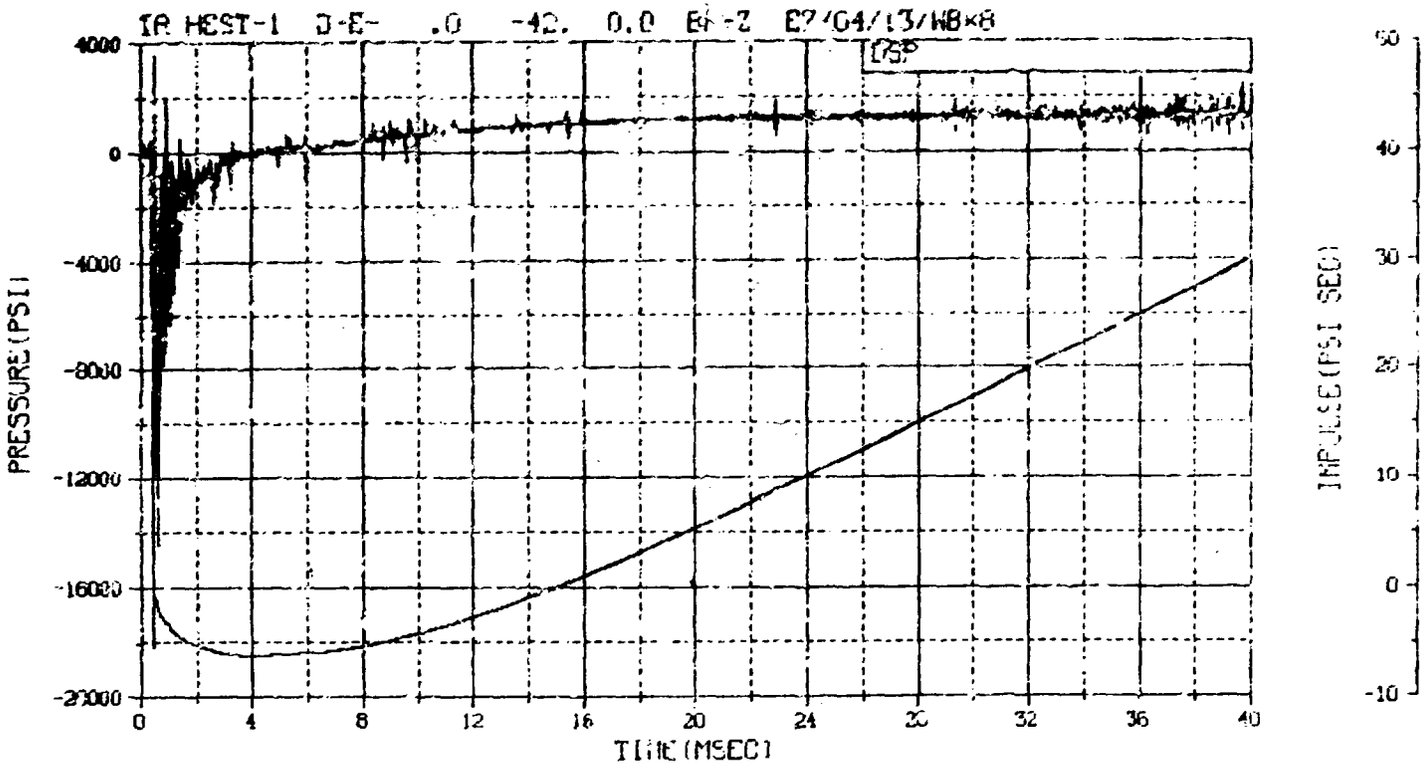

M.N. =80008	E.U. =0.000,6113.000	VSN=
TSKIP=10.350	DIGITS=0.000,556.000	TAPE26
S.R. =125.00 KHZ	3 49 PM, 11 APR 78.	FILE=15

191

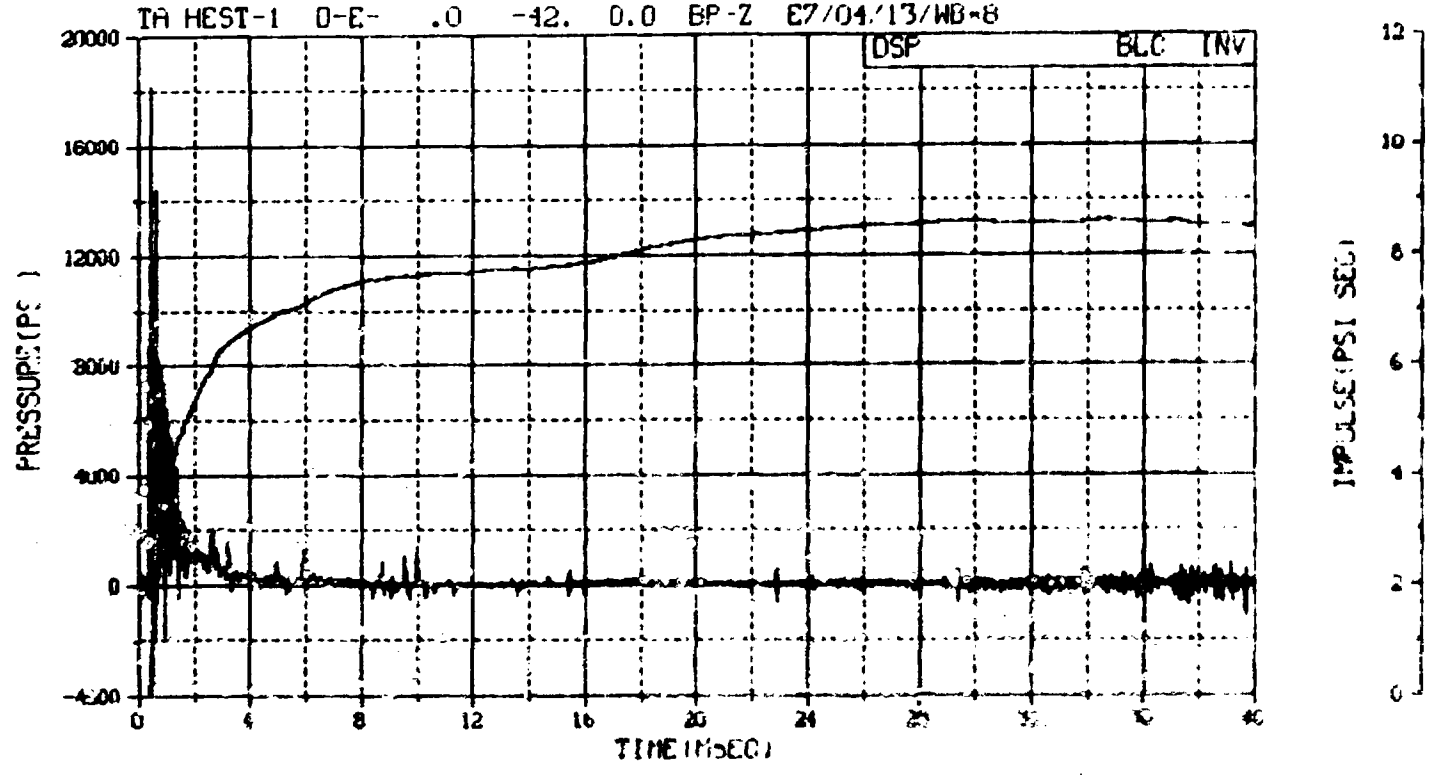
TA HEST-1 0-E- .0 -42. 0.0 BP-Z E7/04/13/WB=8
DSP BLC INV
20000
16000
12000
8000
4000
0
-4000
0
4
8
12
16
20
24
28
32
36
40
TIME(MSEC)
12
10
8
6
4
2
0
M.N. =90008
ISK:P=10.350
S.R. =125.00 KHZ
E.U. =0.000,6113.500
DIGITS=0.000,556.900
3 43 PM,11 APR 78.
VSR=
TAPE=6
FILE=16

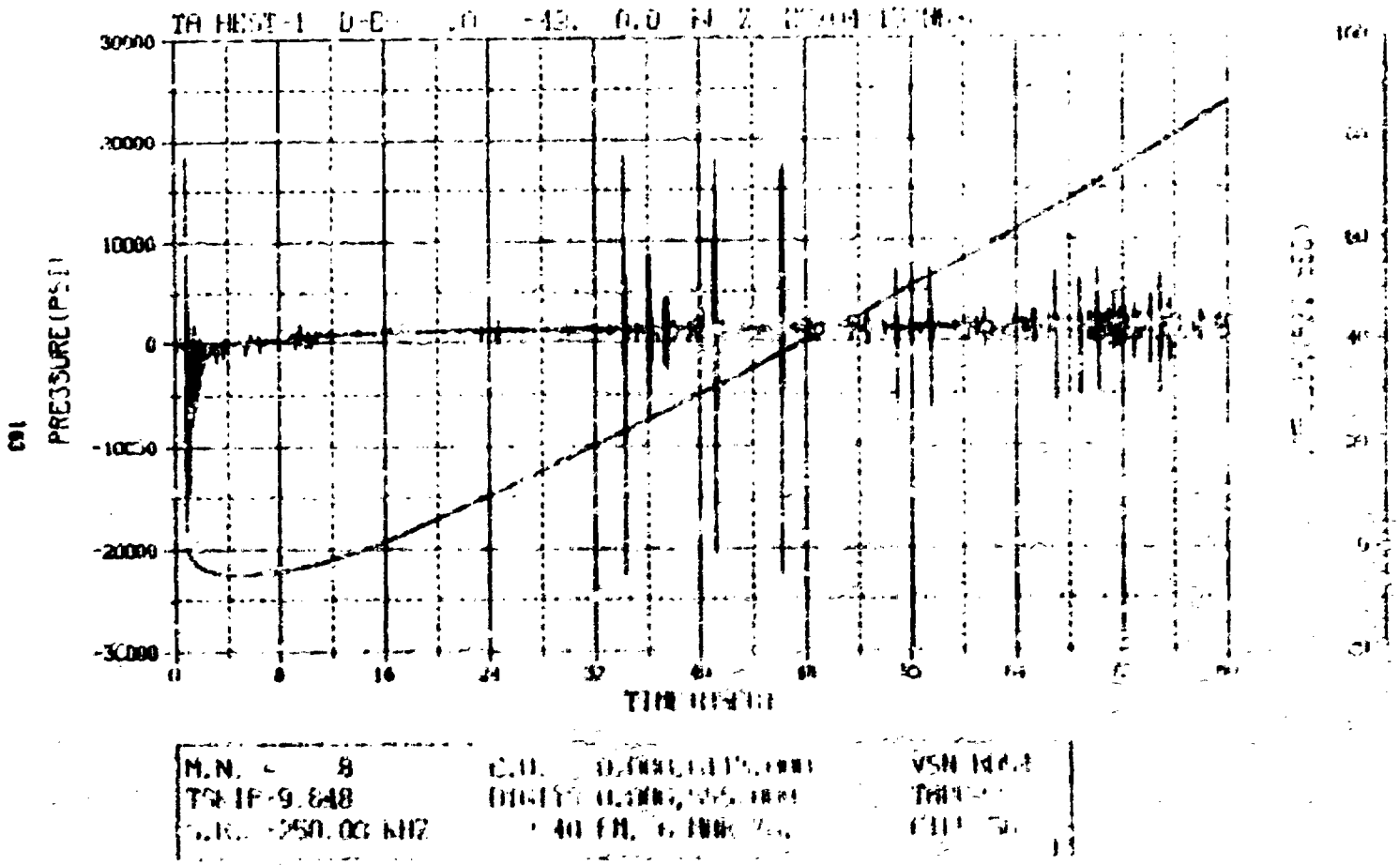

30000
20000
10000
0
-10000
-20000
-30000
PRESSURE (PSI)
0
8
16
24
32
40
48
56
64
72
80
TIME (MSEC)
M.N. = 8
TSKIP=9.848
S.R. =250.00 KHZ
VSN

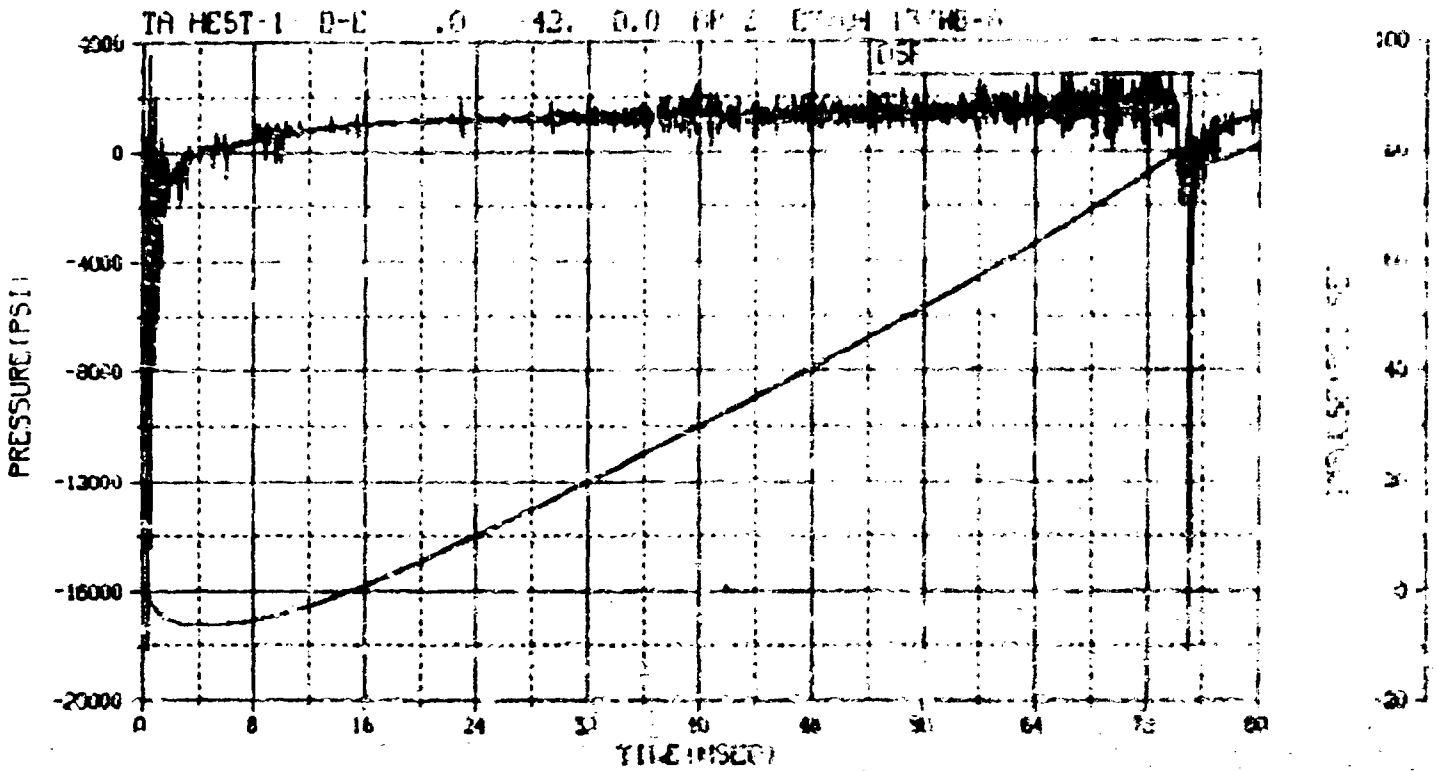
PRESSURE (PSI)
TIME (MSEC)
0
8
16
24
32
40
48
56
64
72
80
-20000
-16000
-12000
-8000
-4000
0
2000

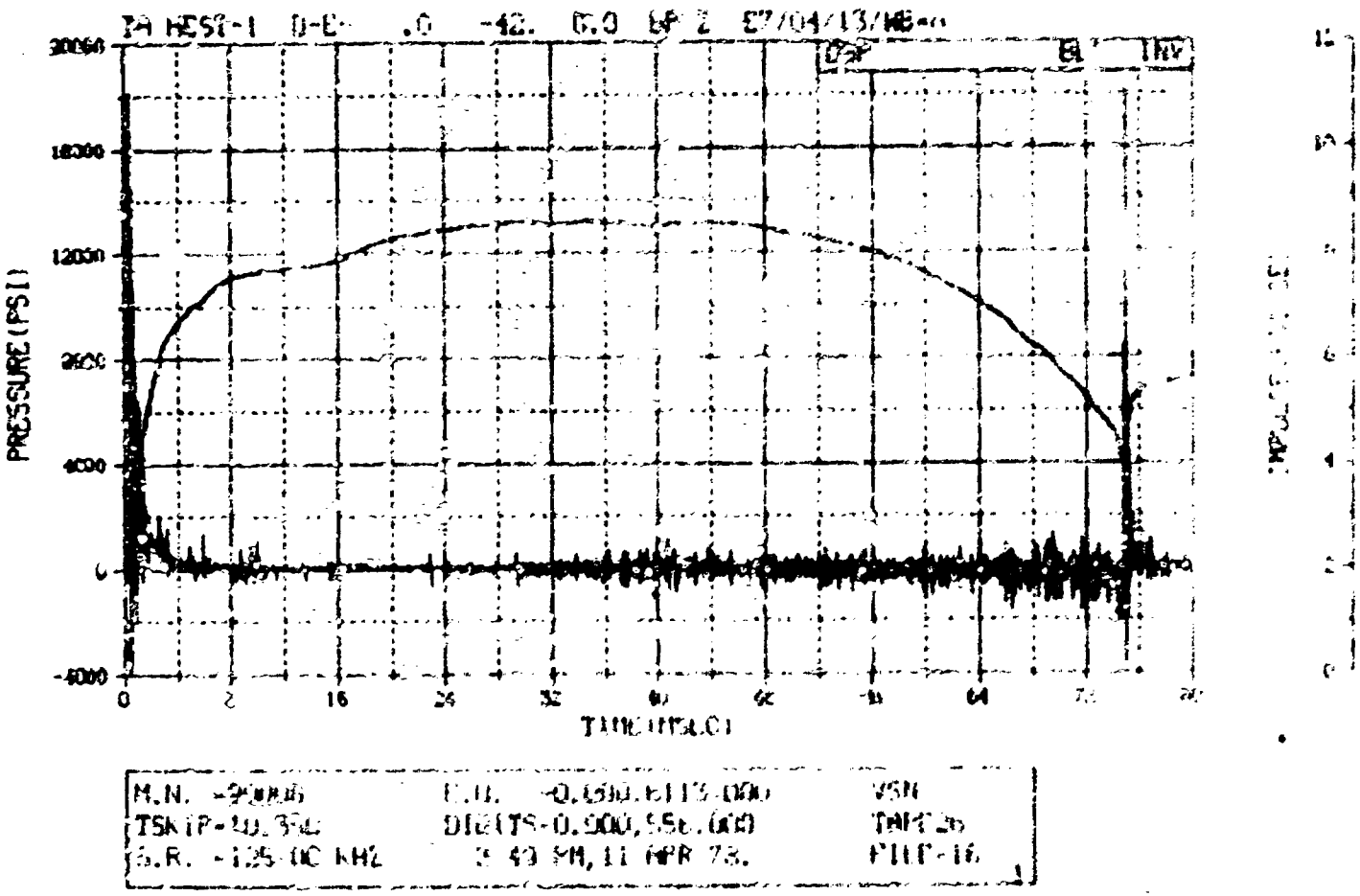
PRESSURE (PSI)
20000
16000
12000
8000
4000
0
-4000
0
8
16
24
32
40
48
56
64
72
80

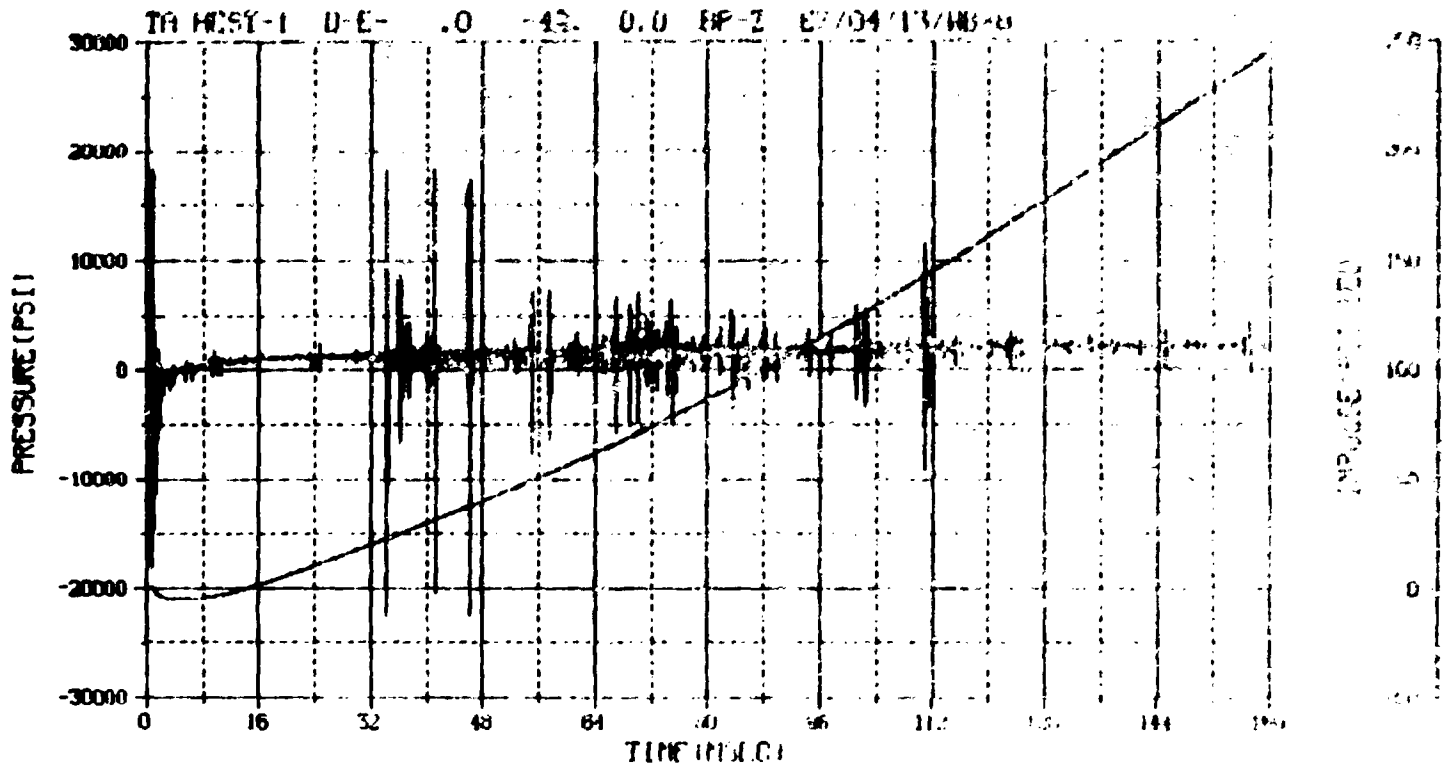

M.N. = 8	E.U. =0.000,[illegible]	VSN [illegible]
TSKIP=9.848	DIGITS=0.000,[illegible]	TAPE[illegible]
S.R. =250.00 KHZ	2 40 PM, [illegible]	FILE [illegible]

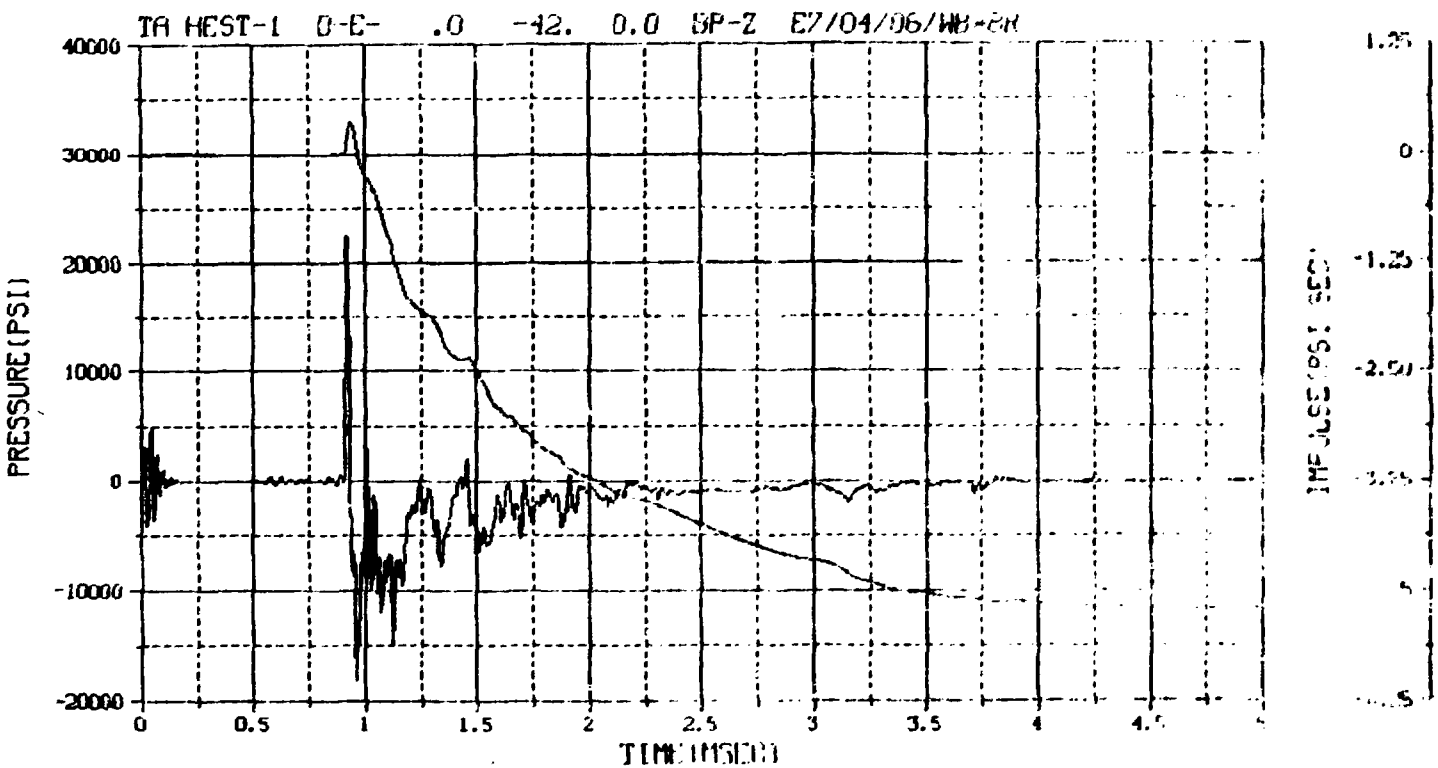
TA HEST-1 0-E- .0 -42. 0.0 GP-Z E7/04/06/WB-2R
PRESSURE(PSI)
TIME(MSEC)
40000
30000
20000
10000
0
-10000
-20000
0
0.5
1
1.5
2
2.5
3
3.5
4
1.25
0
-1.25
-2.5
M.N. = 8
TSKIP=9.848
S.R. =250.00 KHZ
2 40 PM, 6 MAR 96

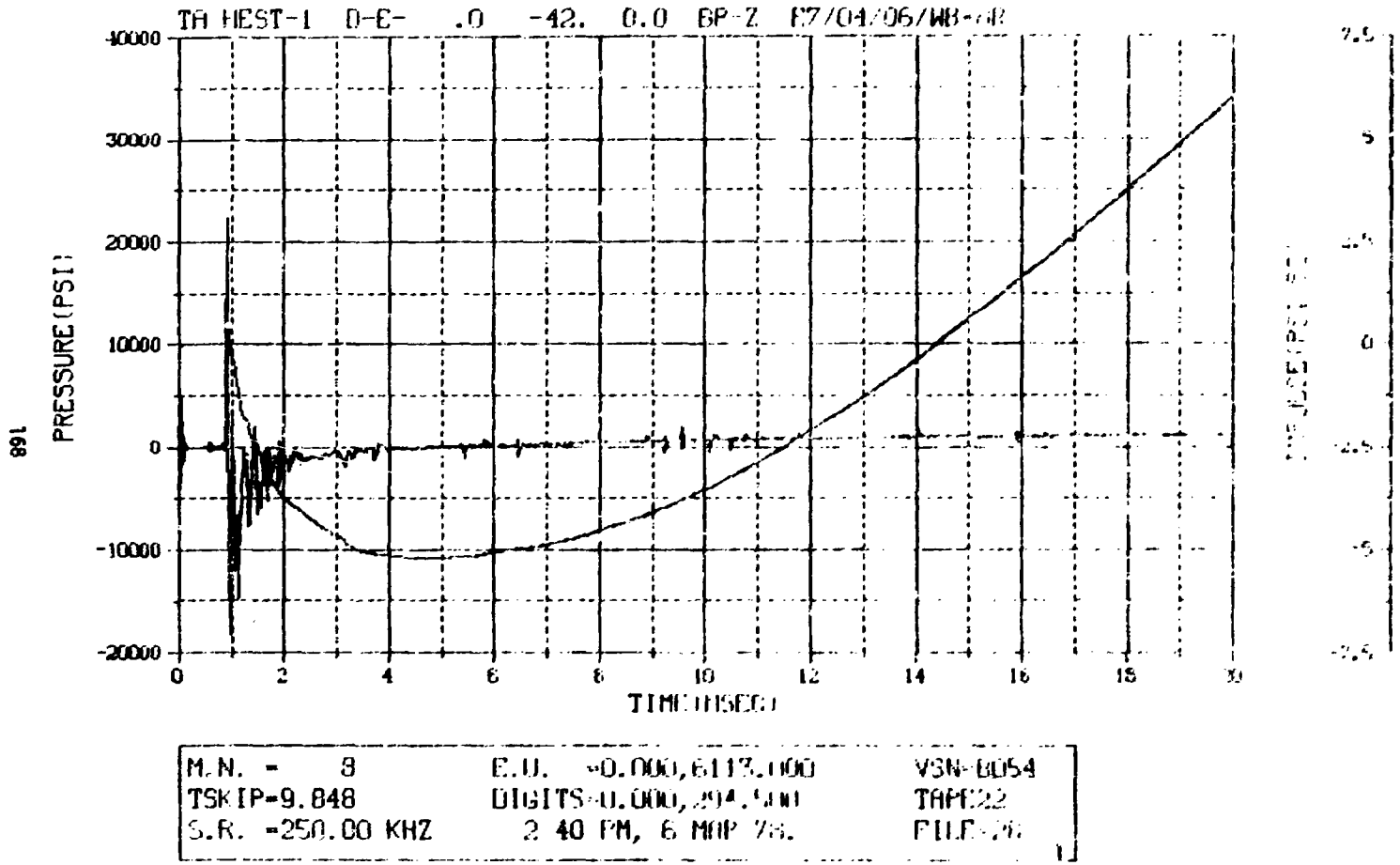
TA HEST-1 0-E- .0 -42. 0.0 BP-Z
PRESSURE(PSI)
40000
30000
20000
10000
0
-10000
-20000
0
2
4
6
8
10
12
14
16
18
20
M.N. = 8
TSKIP=9.848
S.R. =250.00 KHZ
E.U. =0.000,6113.000
DIGITS=0.000,
2 40 PM, 6 MAR 78.
VSN=0054
TAPE=22

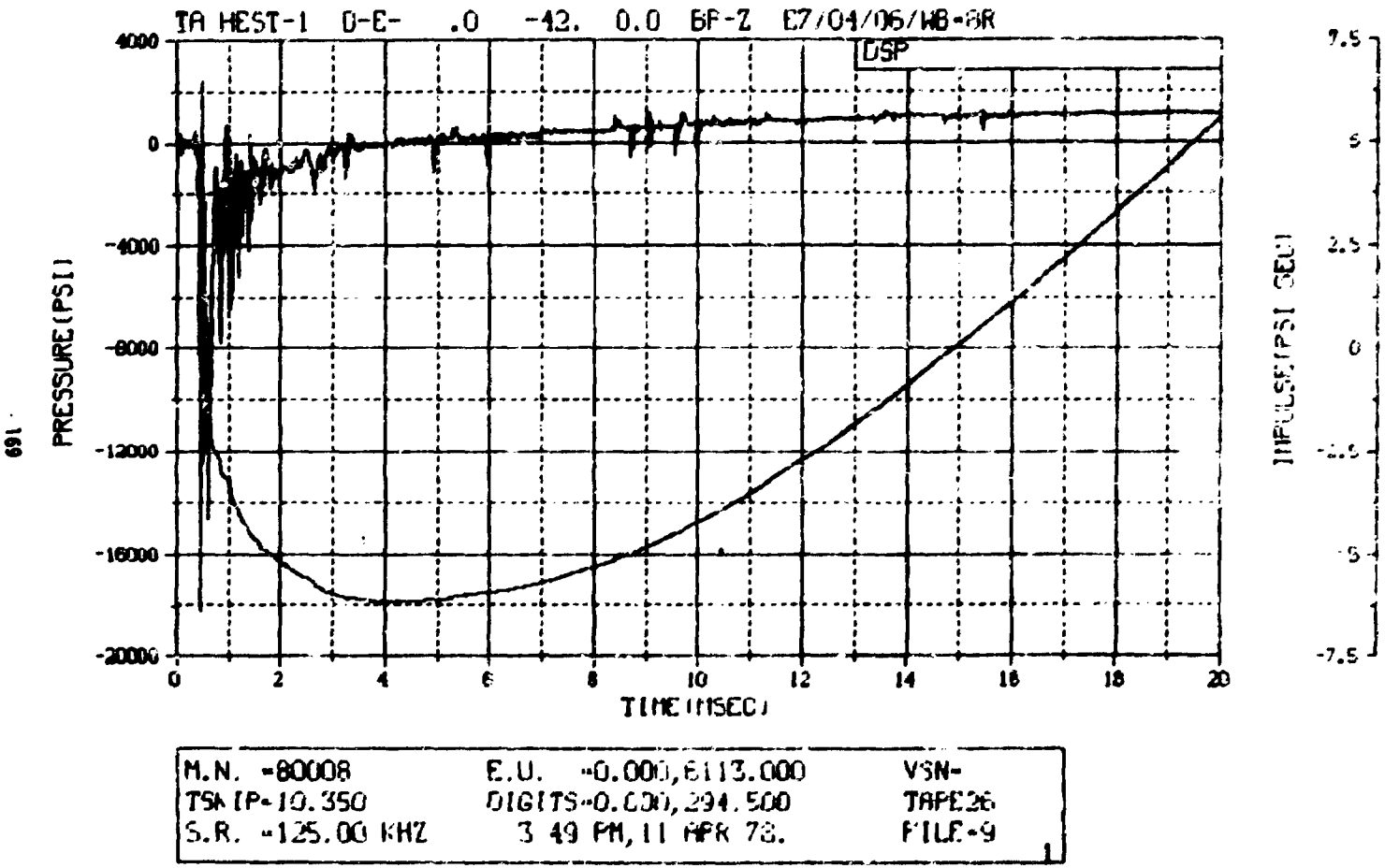
TA HEST-1 0-E- .0 -42. 0.0 BF-Z E7/04/06/HB-BR
DSP
PRESSURE(PSI)
IMPULSE(PSI SEC)
TIME(MSEC)
4000
0
-4000
-8000
-12000
-16000
-20000
7.5
5
2.5
0
-2.5
-5
-7.5
0
2
4
6
8
10
12
14
16
18
20
M.N. =80008
E.U. =0.000,8113.000
VSN=
TSAMP=10.350
DIGITS=0.000,294.500
TAPE26
S.R. =125.00 KHZ
3 49 PM, 11 APR 78.
FILE=9

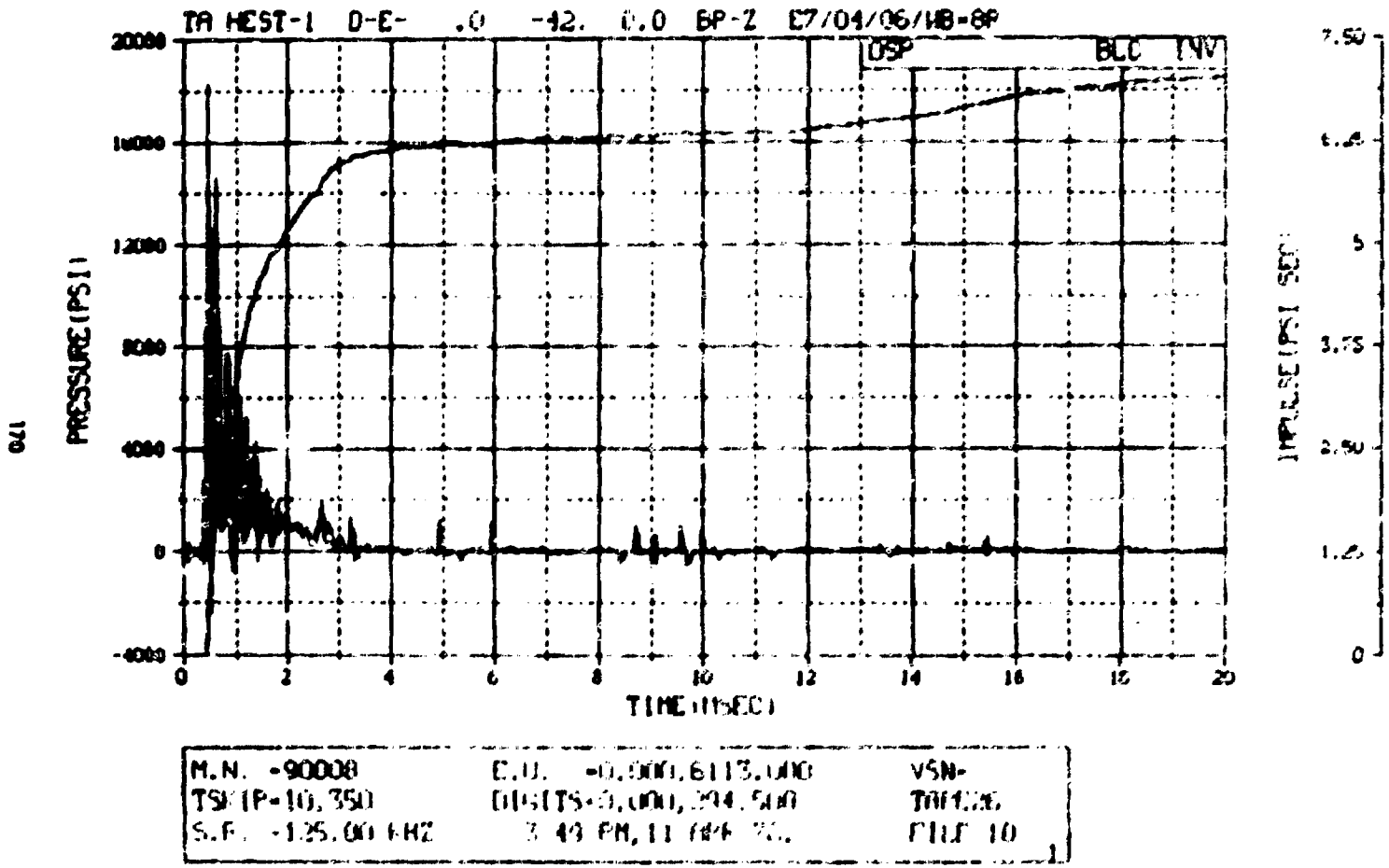
TA HEST-1 D-E- .0 -42. 0.0 BP-Z E7/04/06/WB-8P
OSP
BLC
INV
PRESSURE(PSI)
IMPULSE(PSI SEC)
TIME(MSEC)
M.N. -90008
TSKIP-10,350
S.F. -125.00 KHZ
E.U. -0.000,6113.000
DIGITS-0.000,294.500
3 49 PM, 11 APR 76
VSN-
FILE 10

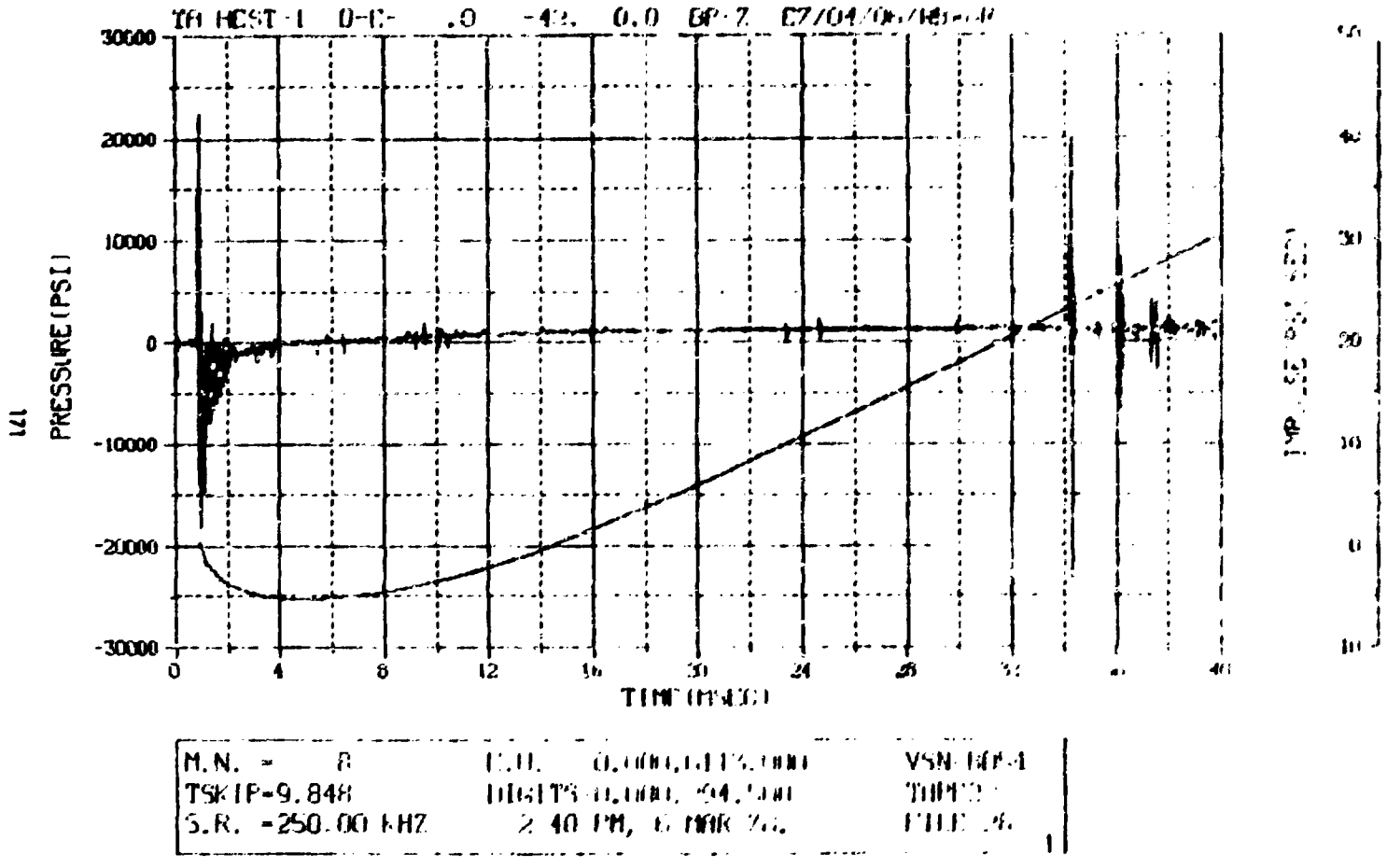
TR HCST-1 0-C- .0 -42. 0.0 BP-7
30000
20000
10000
0
-10000
-20000
-30000
PRESSURE(PSI)
0
4
8
12
16
20
24
28
32
36
40
TIME(HOUR)
M.N. = 8
TSKIP=9.848
S.R. =250.00 KHZ
2 40 PM,

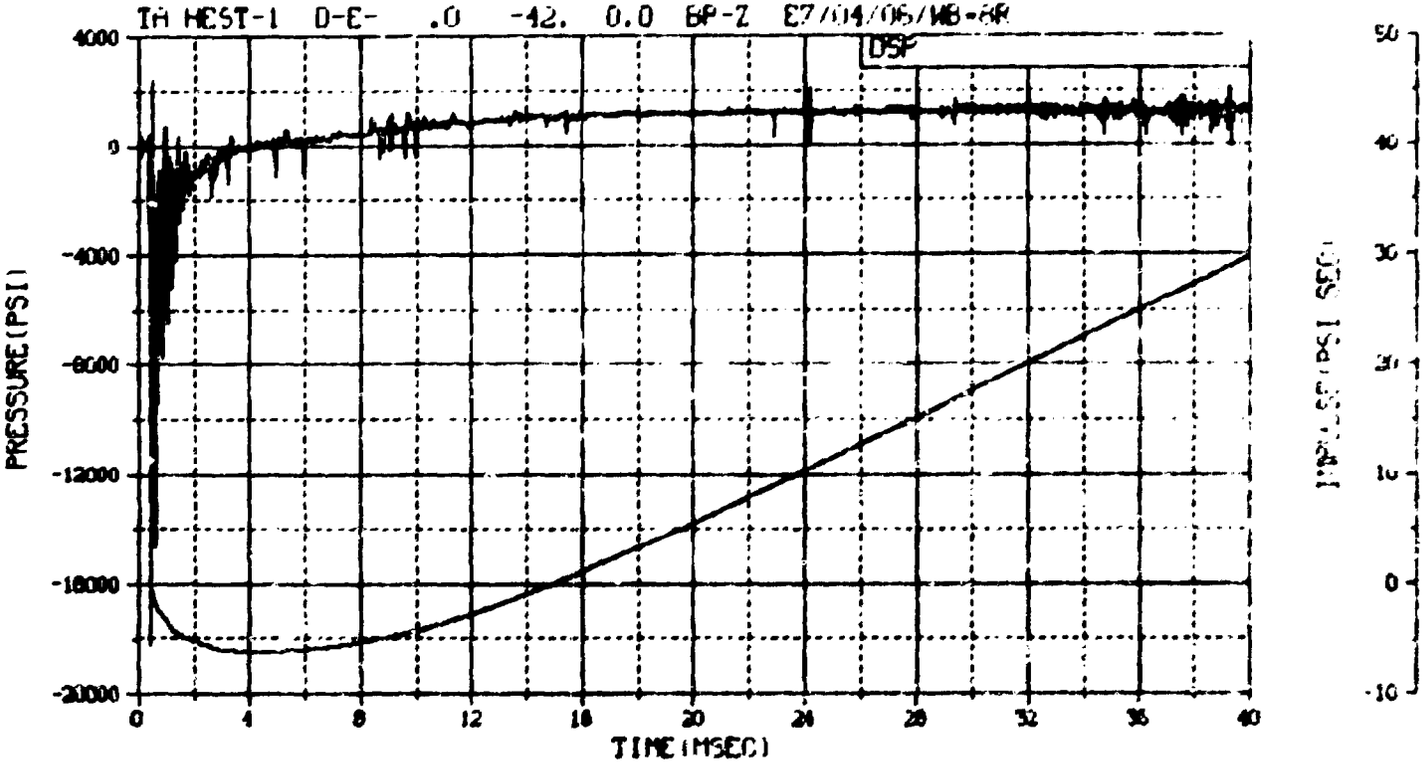

M.N. -80006	E.U. -0.000,6113.000	VSN-
TSKIP=10.350	DIGITS=0.000,294.500	TAPE26
S.R. =125.00 KHZ	3 49 PM, 11 APR 78.	FILE=9

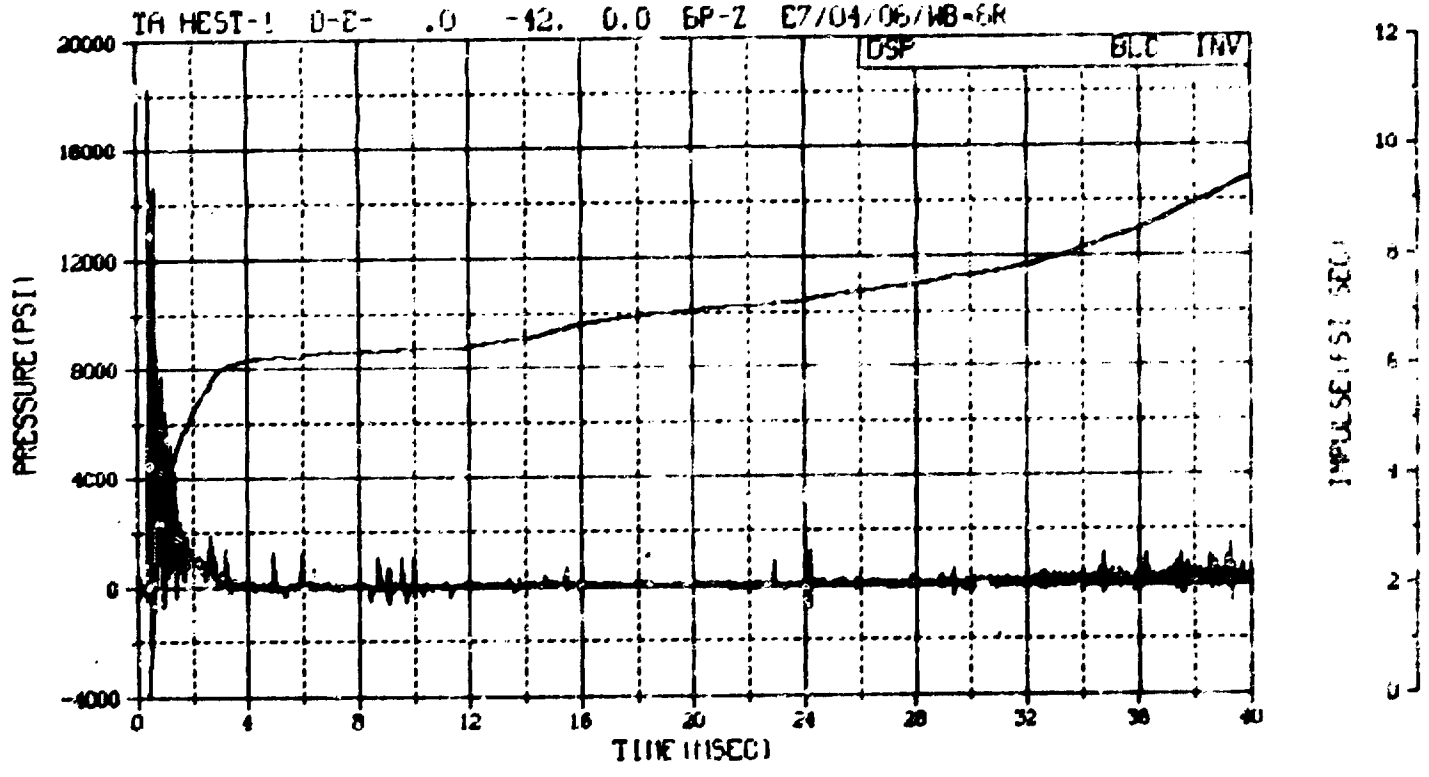

M.N. =90008	E.U. =0.000,6113.000	VSN=
TSKIP=10.350	DIGITS=0.000,294.500	TAPE36
S.R. =125.00 KHZ	3 49 PM,11 APR 78.	FILE=10

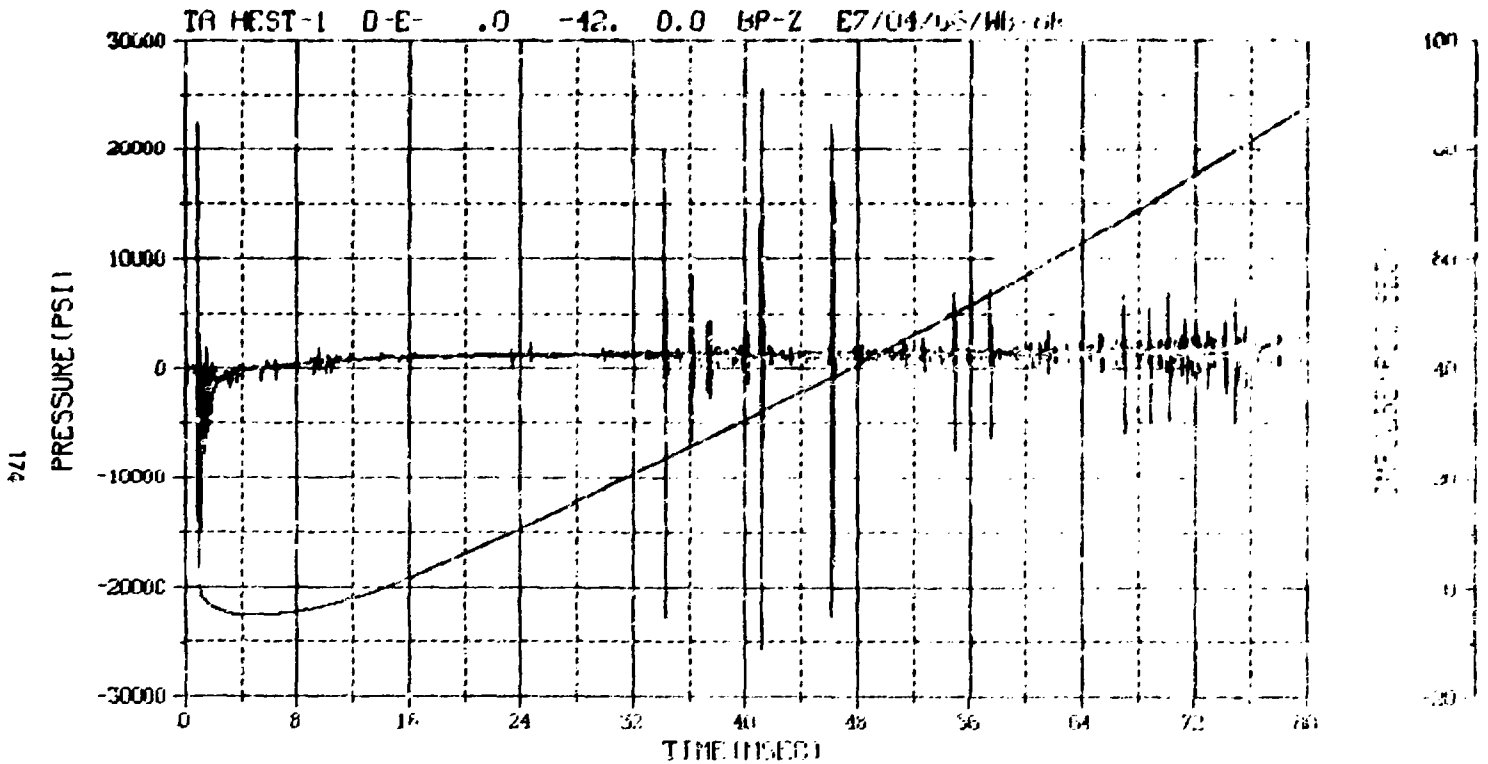

M.N. = 8	E.U. =0.000,6113.000	VSN=8054
TSKIP=9.848	DIGITS=0.000,294.500	TAPE=22
S.R. =250.00 KHZ	2 40 PM, 6 MAR 76.	FILE=28

1

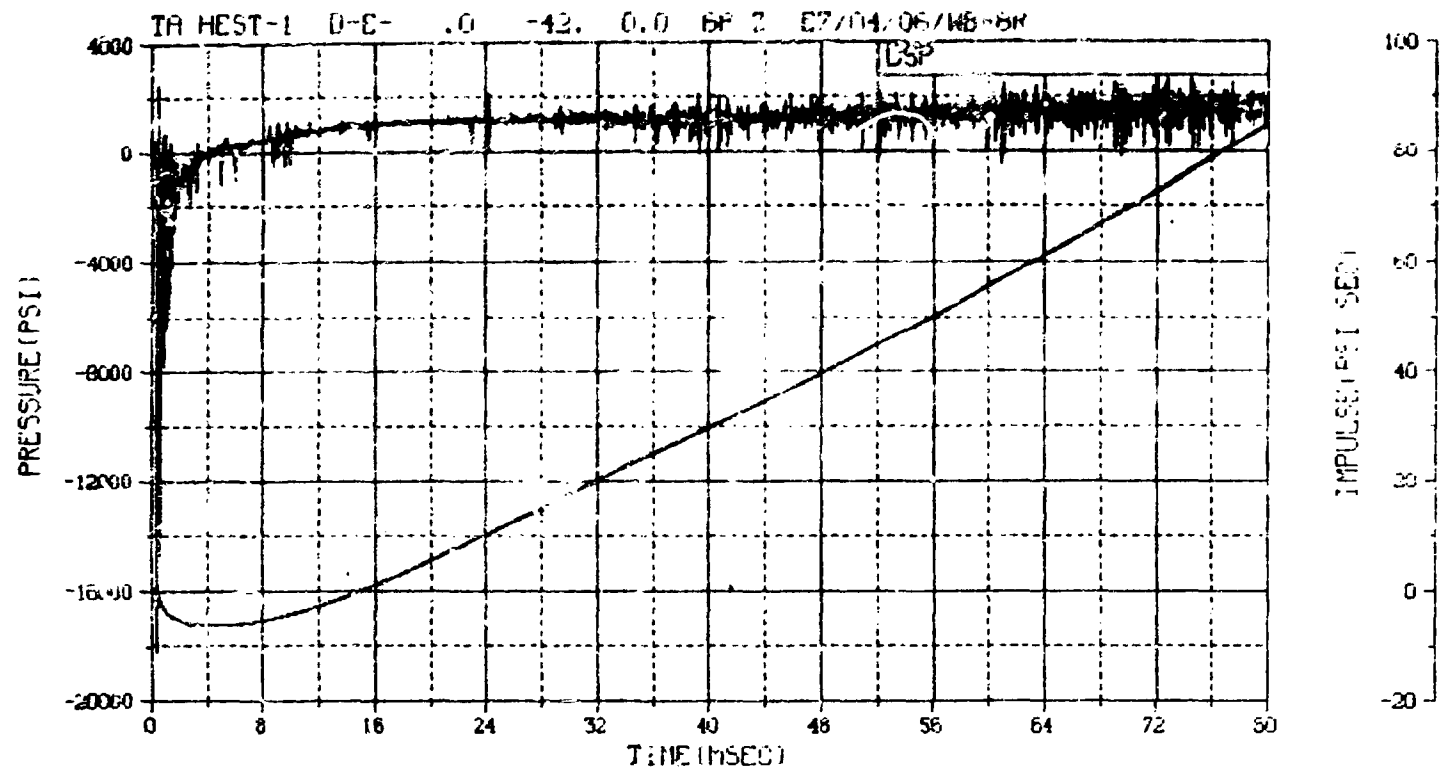

M.N. =80008	E.U. =0.000,6113.000	VSN=
TSKIP=10.350	DIGITS=0.000,294.500	TAPE26
S.R. =125.00 KHZ	3 49 PM,11 APR 78.	FILE=9

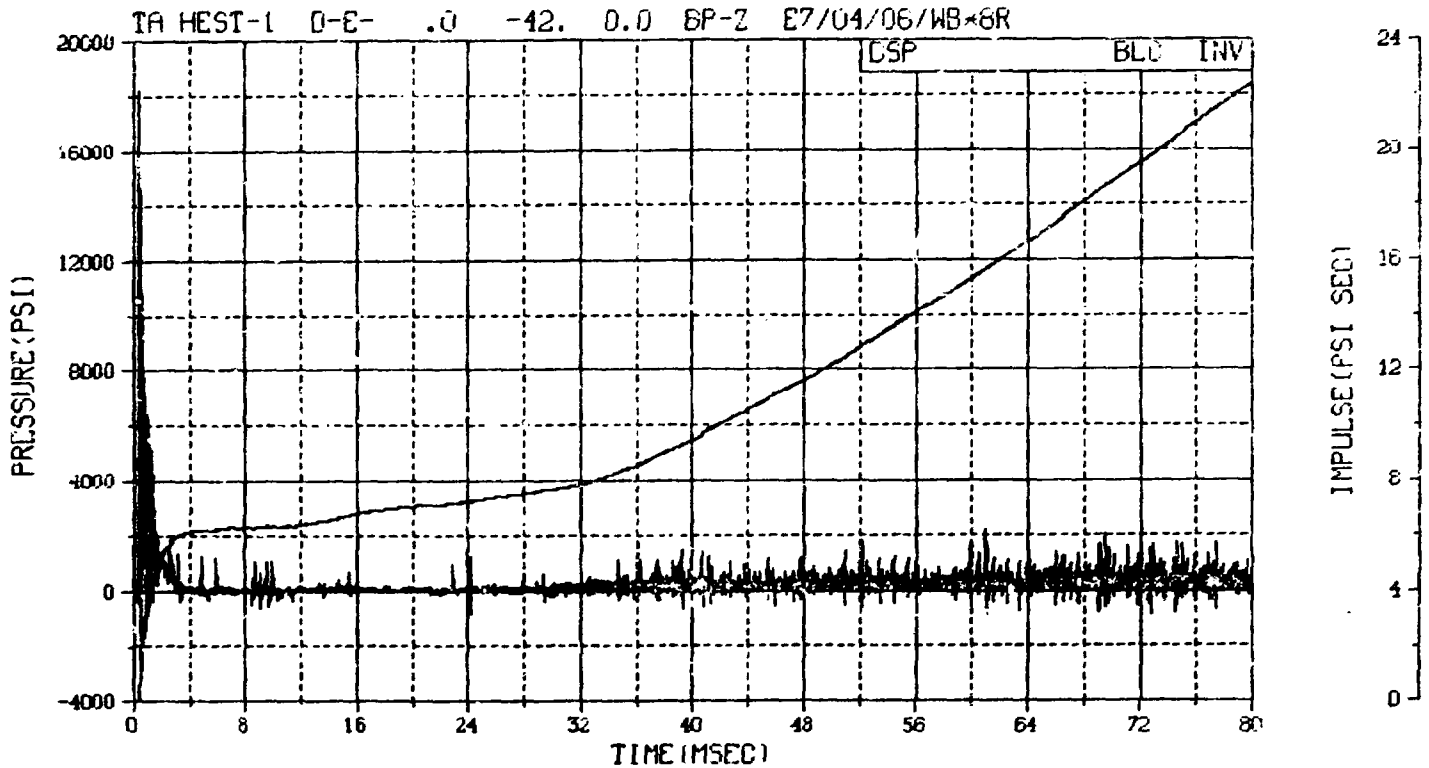

M.N. =90008	E.U. =0.000,8113.000	VSN=
TSKIP=10.350	DIGITS=0.000,294.500	TAPE26
S.R. =125.00 KHZ	3 49 PM,11 APR 78.	FILE=10

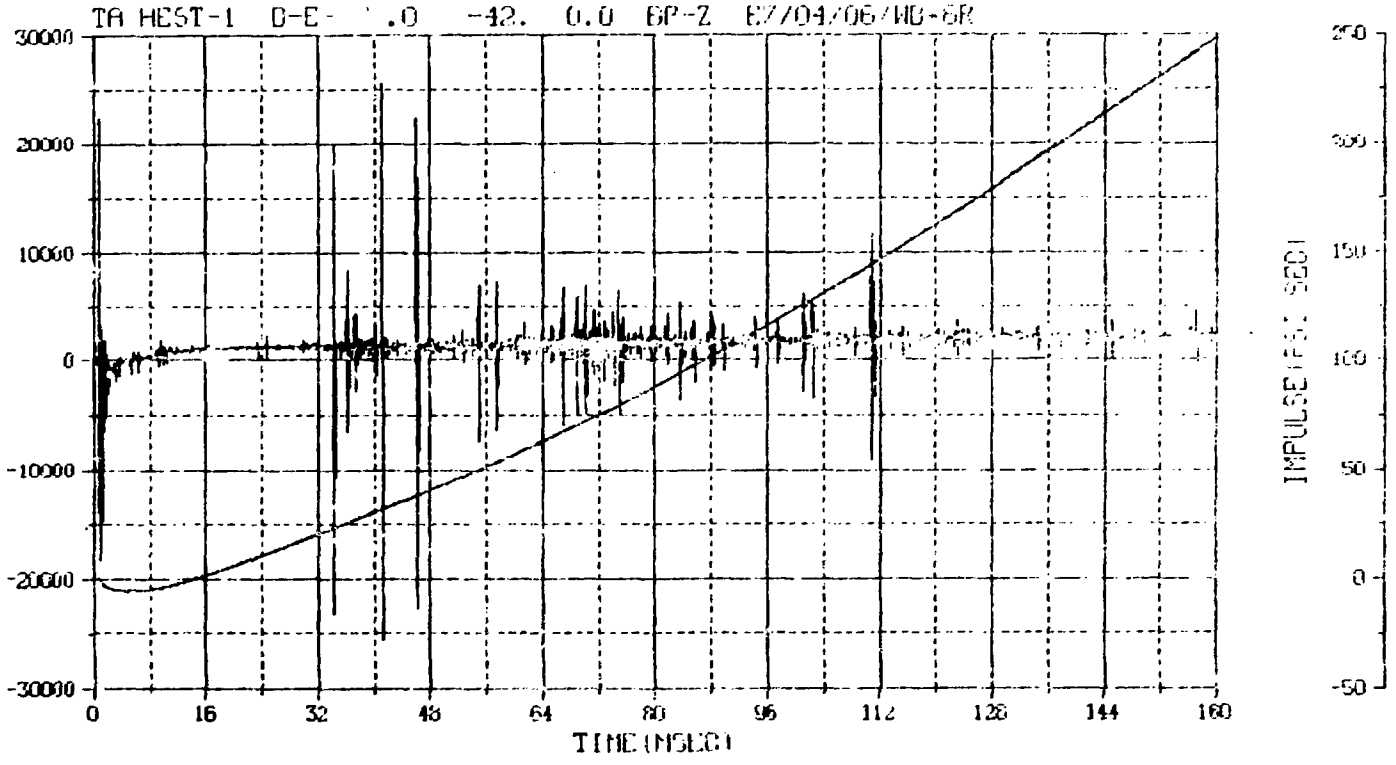

M.N. = 8	E.U. =0.000,6113.000	VSN=BD54
TSKIP=9.848	DIGITS=0.000,294.500	TAPE22
S.R. =250.00 KHZ	2:40 PM, 6 MAR 87	FILE=28

1